

**Molecular Genetics of Alopecia Areata in
Dundee Experimental Bald Rats and in Humans**

Inaugural-Dissertation

zur

Erlangung des Doktorgrades
der Mathematisch-Naturwissenschaftlichen Fakultät
der Universität zu Köln

vorgelegt von

Jennifer Kristina Kuhn

aus Heilbronn

Köln

2011

Berichterstatter:

(Gutachter)

Prof. Dr. Peter Nürnberg

Prof. Dr. Angelika A. Nögel

Tag der mündlichen Prüfung:

28. Juni 2011

Table of Contents

A	Introduction	1
1	Introduction to Skin and Hair	1
1.1	The Skin	1
1.2	The Hair	3
1.3	The Hair Growth Cycle	6
2	Alopecia Areata	7
2.1	History	7
2.2	The Hair Growth Cycle in Alopecia	9
2.3	Clinical Features and Diagnostics	9
2.4	Pathology	10
2.5	Treatment	12
3	Dundee Experimental Bald Rats	13
3.1	History	13
3.2	Characterization	13
B	Objectives of this Doctoral Thesis	15
C	Materials and Methods	17
1.	Materials	17
1.1	Rat Samples	17
1.2	Human Samples	17
1.3	Kits	18
1.4	Chemicals	18
1.5	Machines and Robots	19
2.	Methods on DNA-Level	21
2.1	DNA-Isolation and Quality Control	21
a)	DNA-Isolation from Rat Liver	21
b)	DNA-Isolation from Human Blood	22
c)	Quality Control of isolated DNA	24
2.2	PCR and Gelelectrophoresis	25
2.3	Sequencing	26
a)	Sanger Sequencing	26

b)	Next Generation Sequencing (NGS) using Illumina Genome Analyzer IIx	27
c)	Pyrosequencing	27
2.4	Microsatellite Analysis	28
2.5	High Resolution Melting (HRM) Curve Analysis	29
2.6	Taqman	33
2.7	SNPstream	33
2.8	Affymetrix Genome-Wide Human SNP Array 6.0 and GeneChip Human Mapping 500K Array	36
3.	Methods on RNA-Level	37
3.1	RNA-Isolation and Quality Control	37
a)	RNA-Isolation from Rat and Human Tissues	37
b)	RNA-Isolation from Rat Fibroblasts	37
c)	Quality Control of isolated RNA	38
3.2	Quantitative Real Time PCR (qRT - PCR)	38
3.3	Whole-Transcript Expression Analysis using Affymetrix Rat Gene 1.0 ST Array	40
3.4	Ingenuity Pathways Analysis (IPA)	40
4.	Methods on Protein-Level	41
4.1	Histology	41
a)	Fixation, Paraffin Embedding and Sectioning	41
b)	Haematoxylin - Eosin (HE) Staining	41
c)	Immunohistochemical (IHC) Staining	42
d)	DAPI Staining	43
5.	Methods for Cell Culture	44
5.1	Cell Culture Media	44
5.2	Isolation and Culture of Rat Fibroblasts	45
5.3	Isolation and Culture of Rat Keratinocytes	46
D	Results - Rat Samples	47
<hr/>		
1.	Short summary of the study design and the obtained results	47
2.	Saturation Mapping of Chromosome 19 with Microsatellites	48
3.	Exon Sequencing of Candidate Genes	51
4.	Next Generation Sequencing of the Candidate Region	53
5.	Expression Analyzes	56
5.1	Affymetrix Rat Gene 1.0 ST Array	56

5.2	Inguinity Pathways Analysis (IPA)	57
5.3	Quantitative Real Time PCR (qRT - PCR)	59
5.4	Comparison of qRT-PCR data with Affymetrix RatGeneChip data	64
6.	Histology	67
6.1	HE-Staining	67
6.2	Immunohistochemical (IHC) Staining	68
E	Results - Human Samples	70
<hr/>		
1.	Short summary of the study design and the obtained results	70
2.	Fine mapping of the candidate region on chromosome 19	71
2.1	Association Analyzes (CaCo, TDT)	72
2.2	Linkage Analyzes (ASP, FAM)	73
3.	Mutation screening in Candidate Genes ZNF567 and ZNF568	76
4.	Whole Genome Association and Linkage Analyzes with larger sample set	77
4.1	Association Analyzes (CaCo, TDT)	77
4.2	Linkage Analyzes (FAM)	82
5.	Histology	87
5.1	HE - Staining	87
5.2	Immunohistochemical (IHC) Staining	87
F	Discussion	90
<hr/>		
1.	Expression Analyzes	90
2.	Histological Analyzes	98
3.	Genetic Analyzes	103
G	Abstract	109
<hr/>		
H	Zusammenfassung	111
<hr/>		
I	Danksagung	113
<hr/>		
J	List of Literature	114
<hr/>		
K	Appendix	122
<hr/>		
1	Primer Sequences	122
2	Detailed Expression Analysis Data from Rat Samples	136
3	Detailed Association and Linkage Analysis Data from Human Samples	142
	Erklärung I	155
	Lebenslauf	156

A Introduction

1 Introduction to Skin and Hair

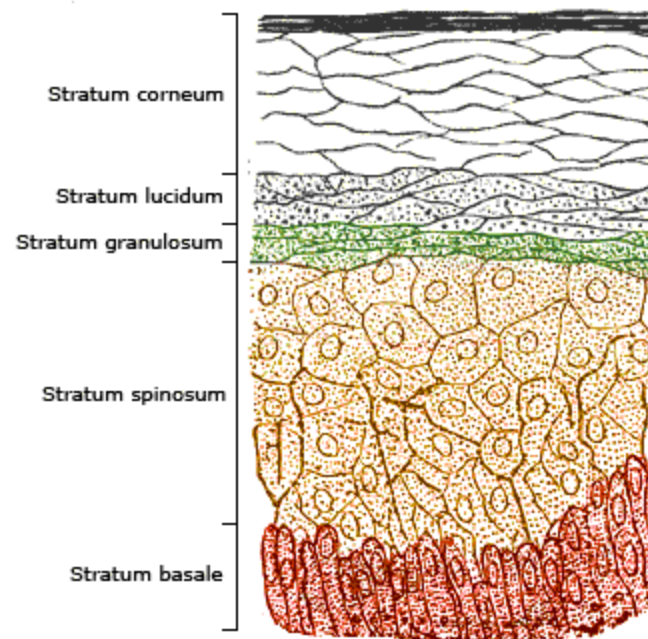
1.1 The Skin

The skin is one of the largest organs of a body and makes up for at least 6 percent of an individual's total weight. It consists of two layers, which are called epidermis and dermis.

The epidermis is the outermost layer of the skin and consists primarily of Merkel cells, keratinocytes, melanocytes, and Langerhans cells. Cells in the deepest layers are nourished by diffusion from blood capillaries beneath the epidermis since the epidermis itself doesn't contain blood vessels. Beginning with the innermost layer the epidermis can be further divided into stratum basale, stratum spinosum, stratum granulosum, stratum lucidum (only in palms of hands and bottoms of feet), and stratum corneum (figure 1).

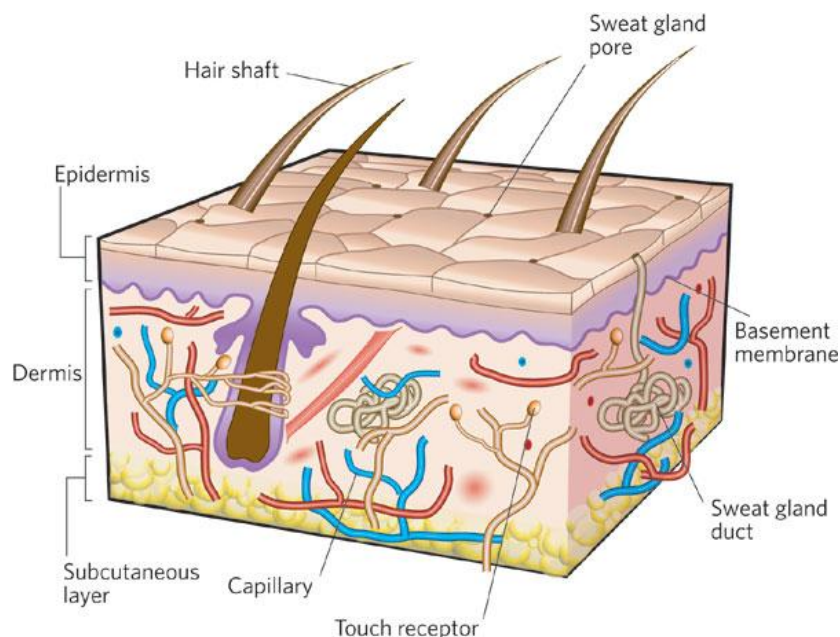
At the stratum basale new cells are formed, which migrate up the strata changing shape and composition as they die due to the isolation from their blood source. The cytoplasm is released and replaced with keratin. When they reach the stratum corneum, which consists of about 15-350 layers of dead cells, they finally slough off (desquamation). This process takes place within about 27 days and is called keratinization (Matoltsy 1958, Flesch 1958, Achten 1956).

Figure 1: Skin layers of human epidermis
(From <http://en.wikipedia.org/wiki/File:Skinlayers.png>)



The dermis is structurally divided into the papillary region, which is adjacent to the epidermis and is composed of loose areolar connective tissue, strengthening the connection between the two layers of skin, and the reticular region, which is much thicker and is composed of irregular connective tissue (collagenous, elastic, and reticular fibers, ensuring strength, extensibility, and elasticity to the dermis), hair roots, sebaceous glands, sweat glands, receptors, and blood vessels (figure 2).

Figure 2: The structure of human skin. (From MacNeil S. Progress and opportunities for tissue-engineered skin. *Nature* 2007; 445, 874-880)



The skin is attached to the underlying bone and muscle, as well as supplied with blood vessels and nerves via the hypodermis. It consists of loose connective tissue and elastin. The most important functions of skin include flexible physical support and covering for underlying tissues, maintenance of a constant temperature through its extensive blood supply and sweat glands, removal of waste materials as salts and water via the skin's sweat glands, photochemical production of vitamin D, sensing pressure, texture, temperature, and pain through the extensive network of sensory receptors, protection against the excesses of ultraviolet light through melanin pigments, prevention of desiccation of the inner organs as well as prevention of absorption of unwanted and potentially dangerous chemicals via the epidermis, and finally protection against the entry of opportunistic pathogenic organisms (Proksch 2008, Madison 2003, Stücker 2002).

1.2 The Hair

The hair follicle, as an appendage to the skin, is of great importance to many of the skins properties. Its main function is the protection against heat loss by trapping air adjacent to the skin, providing an invisible, insulating layer. Hair fibers help to protect the epidermis from minor abrasions and from ultraviolet light. Specialized hair such as eyebrows and eyelashes protect the eyes by channeling or sweeping away fluids, dust, and debris whereas nasal hair keeps air borne foreign particles from entering the lungs. Hair can also provide indications of sexual development through the onset of beard and pubic hair development and it may also play a role in attracting mates as an indicator of the general health and vitality of an individual based on color, distribution, and quality of the hair (Bubenik 2003, Sabah 1974,Robins 2002, Stenn 2001).

An adult human being has about 5 million hair follicles spread across the body with about 1 million on the head of which 100.000 cover the scalp. Only the palms of the hands and soles of the feet are skin regions devoid of hair follicles. The hair follicle can be recognized as a separate entity within the skin with formation and maintenance based on interaction between dermal and epidermal components. Keratin proteins are the primary components of hair fibers.

The mature anagen hair follicle can be vertically divided into the upper follicle (infundibulum and isthmus), middle follicle (bulge), and lower follicle (suprabulbar and bulbar areas). Only the lower follicles regenerate with every new hair follicle cycle whereas the other compartments are permanent.

The infundibulum describes the region between the epidermis and the opening of the sebaceous gland duct. Since its epithelium is continuous with the epidermis its cells can regenerate the epidermis and replenish it after wounding or injury. The inner cavity usually contains the hair shaft, keratin material, and natural oil produced by sebaceous glands (figure 3 D).

The isthmus reaches from the opening of the sebaceous gland duct to the insertion of the arrector pili muscle. Across from the insertion site of the arrector pili muscle is located the bulge region. It is believed that hair follicle stem cells are located within this area. It is often difficult to identify in adult anagen hair follicles, but becomes prominent in the resting phase.

Beneath the isthmus starts the suprabulbar area and stretches down to the bulb. This region consists of (outermost to innermost) the dermal sheath, outer root sheath, inner root sheath, and hair shaft, which give a description of the horizontal compartments of hair.

This is where the inner root sheath layers Henle's layer, Huxley's layer and the cuticle completely keratinize and become impossible to differentiate from one another.

The dermal sheath envelops the epithelial components of the hair follicle and consists of the connective tissue sheath and the hyaline or vitreous membrane. This membrane is continuous with the interfollicular basement membrane and is most prominent around the outer root sheath at the bulb in anagen follicles. During catagen, it thickens in the lower portion of the follicle and then disintegrates.

The outer root sheath is continuous with the epidermis and forms a non-keratinizing region at the periphery of the follicle (figure 3 A, B, C). It reaches down to the tip of the bulb, around which it consists of greatly flattened cells in two layers. It contains vacuoles, golgi complexes, smooth and rough endoplasmic reticulum, mitochondria and other cell organelles as well as lots of glycogen in the lower part of the follicle. Since glycogen is an energy source for protein synthesis during hair growth, the presence of glycogen in the outer root sheath suggests an energy-consuming activity in these cells.

The inner root sheath stretches down from the isthmus to the base of the bulb. The lower part shows large eosinophilic cytoplasmic inclusions called trichohyaline granules. Trichohyaline as well as keratin fibers are produced in the cells of the inner root sheath. Three cell lineages can be distinguished within this sheath, depending on structure, patterns of keratinization, and incorporation of trichohyaline. Outermost is located the Henle's layer (figure 3 A, B, C) that is only one cell layer thick. This layer is the first to develop trichohyaline granules and the first to cornify. It is followed by the Huxley's layer (figure 3 A, B, C) which is two to four cell layers thick and cornifies above Henle's layer at the region known as Adamson's fringe. The innermost cuticle (figure 3 B) is again one cell layer thick and develops only a few trichohyaline granules. It keratinizes below the Adamson's fringe. The cells overlap one another with their free edges oriented towards the deep portion of the follicle. They are in opposition to the cells of cuticle of the hair shaft that are oriented upwards, thereby anchoring the hair shaft in place. The fully cornified inner root sheath therefore anchors and directs the growth of the emerging hair shaft. The inner root sheath breaks down at the level of the sebaceous gland to leave only the hair cortex and surrounding cuticle to protrude above the epidermis.

Above the scalp can be seen the hair shaft (figure 3 B), which reaches down to the bulb and consists mainly of dead cells. It is composed of the cuticle, the cortex, and the medulla (outermost to innermost). The cuticle consists of a single cell layer and lacks trichohyaline granules (in contrast to cells of the inner root sheath) as well as melanin (in contrast to cells destined to become the cortex). The main portion of the hair shaft is made up of the cortex which gives hair its elasticity and curl. It is packed with keratin strands, lying along

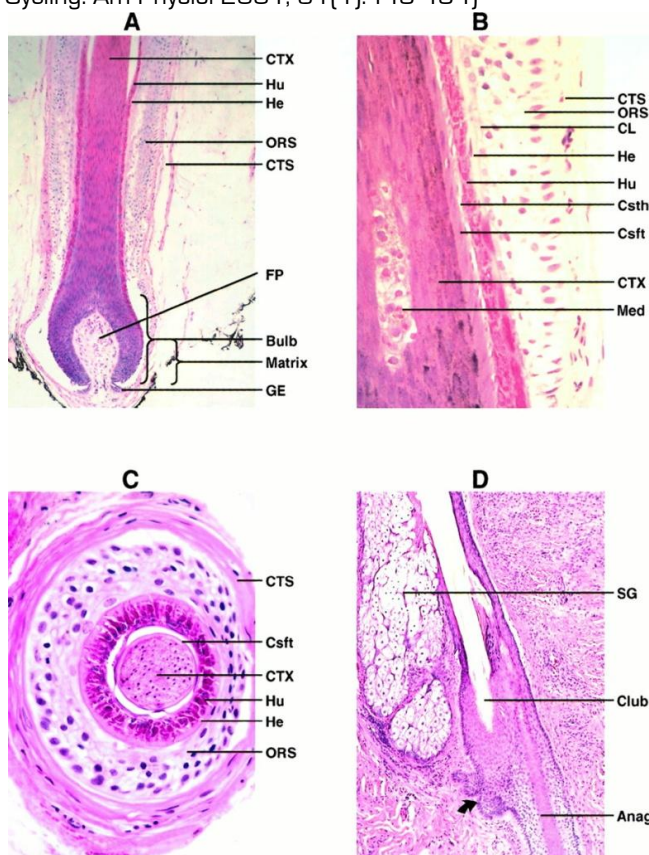
the length of the hair and also contains granules of melanin. The medulla is the central hollow core that can be seen in most of the terminal hairs.

The lowest part of the hair follicle is the bulb (figure 3 A). It surrounds the dermal papilla and contains the matrix cells, which is a group of living, actively proliferating cells that differentiate and become keratinized to form the hair cortex and surrounding hair cuticle of the hair shaft at the center of which is situated the medulla [in terminal hairs]. The rate of matrix cell proliferation is one of the highest in the body. As the cells grow and develop, they steadily push the previously formed ones upwards. When they reach the upper part of the bulb they begin to rearrange themselves into six cylindrical layers, one inside the other. The inner 3 cell layers turn out as the actual hair whereas the outer 3 cell layers become the inner root sheath.

The dermal papilla (figure 3 A) is a pear shaped region of the hair follicle that directs and dictates the embryonic generation of hair follicles. It consists of fibroblasts, collagen bundles, stroma, nerve fibers, and a single capillary loop and is continuous with the dermal sheath.

[Christiano 2010, Reynolds 1996, Jahoda 1994, Sperling 1991, Price 1985, Malkinson 1978, Braun-Falco 1966].

Figure 3: Follicular histomorphology: human skin. (From Stenn KS and Paus R. Controls of Hair Follicle Cycling. *Am Physiol* 2001; 81(1):449-494)

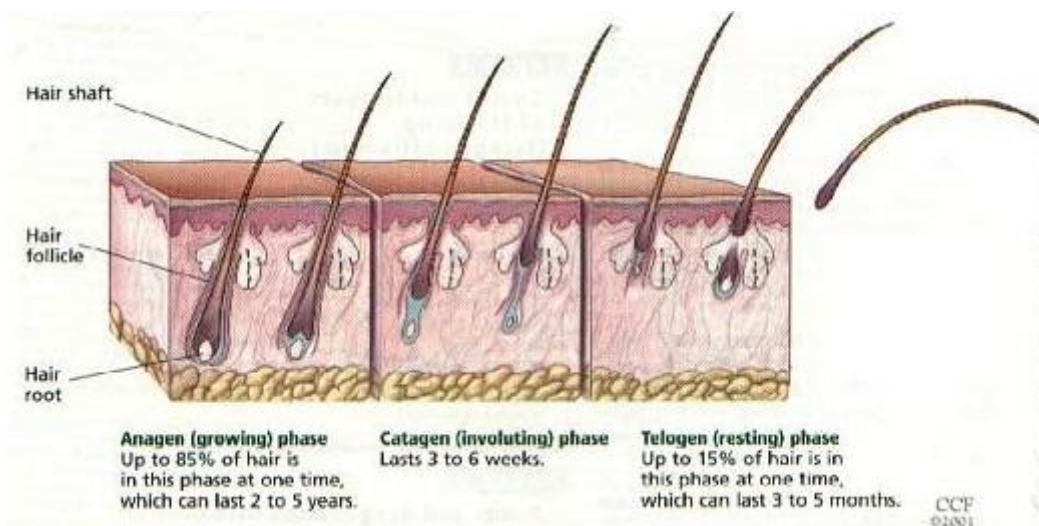


The defined lineages are the outer root sheath (ORS), the companion layer (CL), the internal root sheath Henle's layer (He), internal root sheath Huxley's layer (Hu), the cuticle of the internal root sheath (Csth), the cuticle of the hair shaft (Cstf), the cortex of the shaft (CTX), and the medulla of the shaft (Med). *A*: vertical section of proximal anagen follicle. *B*: vertical section of proximal anagen follicle. *C*: cross section of proximal anagen follicle. *D*: telogen shaft with anagen follicle below. Note the secondary hair germ epithelium at the base of the telogen follicle (arrow). CTS, connective tissue sheath; SG, sebaceous gland; Club, telogen shaft base; Anag, proximal anagen follicle; FP, follicular papilla; GE, germinative epithelium.

1.3 The Hair Growth Cycle

Healthy hair growth in each hair follicle consists of three phases and occurs in a cycle (figure 4) [Van Scott 1968]. Hair fiber is actively produced in the anagen phase. Hair follicle cells are dividing rapidly, adding to the hair shaft leading to a hair growth of about 1 cm every 28 days. It is genetically determined how long the hair follicle stays in the anagen phase. Scalp hair stays in this active phase of growth for two to six years. This is followed by the catagen phase which lasts for about two to three weeks while a club hair is formed (the outer root sheath shrinks and becomes attached to the hair shaft and cuts off the hair from its blood supply and from the cells that produce new hair fibers). This period signals the end of the active growth of a hair. The final telogen phase consists of a so-called resting state. About 10% to 15% of all hairs at any given time are in this phase. It lasts for about 3 months for scalp hairs and much longer for eyebrows, eyelashes, arm or leg hairs.

Figure 4 Hair Growth Cycle. (From Bergfeld WF & Mulinari-Brenner F. Shedding: a common cause of hair loss. *Cleve Clin J Med* 2001; 68(3):256-261)



2 Alopecia Areata

2.1 History

Two forms of alopecia characteristics were first described by Cornelius Celsus in 30 A.D (Robinson 1883). One form he described as a complete baldness occurring in people of all ages and the other form he called “ophiasis” due to a snake-like winding way the bald region spreads across the skin, which he suggested occurs only in children. In Sauvages publication “Nosologica Medica” in 1760 (Lyons, France) the actual term “alopecia areata” was used for the first time.

The cause of alopecia areata was considerably debated with the beginning of the 1800's. One hypothesis suggested a parasitic infection (Gruby 1843, Radcliffe-Crocker 1903) because of the infection-like expansion of lesions and because of the apparent epidemics that were reported to occur in orphanages, schools, and other institutions where lots of people live together in close spaces (Bowen 1899, Colcott Fox 1913, Davis 1914). However, an infective organism could never be isolated from alopecia areata patients and transfers by inoculation have failed (Sabouraud 1896, Ormsby 1948, Ikeda 1967).

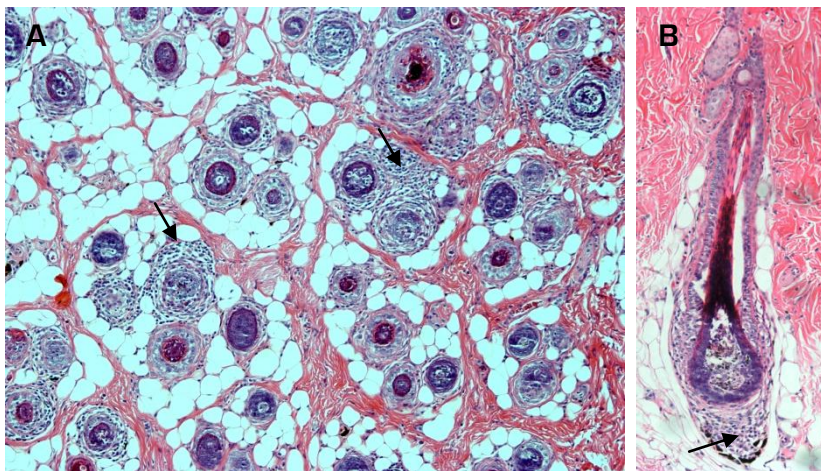
Another hypothesis based on a nervous disorder (Von Barenstrung 1858). This was supported by the frequency of observed emotional or physical stress and trauma in the onset stage of alopecia areata (Sequeira 1913, Kingsbury 1909). It was believed that emotional stress and physical damage adversely affect hair follicles via the nervous system. Joseph (1886) tried to proof this by cutting nerves in the necks of cats and thereby induced patchy hair loss but later it was suggested that the cats scratched themselves and therefore lost hair.

The neuropathic hypothesis was put forward by Jacquet (1902). He suggested a nerve irritation that may occur through defective and diseased teeth as a source of initiation of alopecia areata. This was confirmed by Decelle (1909), although Bailly (1910) showed that dental disease occurred equally frequent in people without alopecia areata. Kinnear (1939) suggested eye strain as a cause of alopecia areata.

A hormone dysfunction due to disorders of the endocrine gland was believed to be the cause with the start of the twentieth century (Sabouraud 1913) and another hypothesis developed at that time based on toxic agents (Adamson 1912) which was supported by the sudden remission and relapse of alopecia areata and its simultaneous action over the body. In addition, hair loss with the expression of exclamation point mark hairs – a diagnostic feature of alopecia areata (Roxburgh 1950) - could be induced by the injection of thallium acetate, which is a rat poison (Adamson 1912, Dixon 1927, Ormsby 1948).

Even though it was already shown in 1891 by Giovannini that alopecia areata affected hair follicles were invaded by inflammatory cells, the now widely believed hypothesis of an inflammatory autoimmune disease did not become popular until the 1950s. The first to discuss this view was Rothman, referring to a paper by Van Scott (1958). This hypothesis suggests that the patient's immune system attacks tissue from its own organism and is supported by histological findings of "swarm of bees"-like perifollicular and intrafollicular inflammatory infiltrate around the hair follicle bulbs (see figure 5 as an example in rat skin).

Figure 5: Histological 'swarm of bees' like perifollicular inflammatory infiltrate around the hair follicle bulbs (black arrows) in rat skin. A Horizontal cut B Vertical cut.



However, attacks of the immune system usually result in the complete destruction of the targeted tissue. In the case of alopecia areata the hair follicles are just disrupted and prohibited from producing hair. Therefore it has been suggested that the immune system is directed not against the hair follicle tissue itself but against a controlling hair growth promoter mechanism (Price 1991). By immune cells and hair follicles produced cytokines are also discussed to adversely affect the hair follicle (Goldsmith 1991). Another theory is based on an existing antigen that is exposed just shortly at the initiation of alopecia areata that eventually leads to an imbalance in the immune system.

Still, alopecia areata is nowadays defined as a non-scarring, inflammatory, hair loss disease that may affect men and women of all ages. Activating factors of the disease as well as the mechanisms of its development are still not fully understood. Though the disease is not life threatening, the psychological devastation of hair loss in an image orientated society is enormous.

2.2 The Hair Growth Cycle in Alopecia

The hair growth cycle of alopecia areata patients lacks the catagen phase completely or enters it just shortly and rapidly proceeds to the telogen phase. Follicles that produce poor aberrant hair fibers due to the continued activity of the disease are described as being in a dystrophic anagen state (figure 5 B shows an example in rat skin). From some researchers it is believed that the hair follicles continue indefinitely to oscillate between rapid cycles of dystrophic anagen and telogen phases (Van Scott 1958, Messenger 1986). Others instead believe that many of the follicles are eventually arrested in telogen phase (Swanson 1981), which is the most popular current hypothesis. This would mean the hair follicles would not express as many antigens and so antigenic stimulation of the immune cells would be reduced or removed. The immune cells would then disperse until the hair follicle reverted back to its active anagen state when the immune cells would return (McDonagh 1994, Messenger 1986). By running through this repeated cycle of events, or by remaining in telogen, the hair follicle could avoid the worst of the tissue destruction. More than one of the above mentioned mechanisms may be involved.

2.3 Clinical Features and Diagnosis

Alopecia areata is usually seen with a single or several patches of hair loss about one to two centimeters in diameter on the scalp. Other parts of the body may be affected as well. The patches may expand in size, even leading to a complete loss of scalp hair (alopecia totalis) or a complete loss of all scalp and body hair (alopecia universalis). Usually, extensive hair loss develops gradually over time. But some individuals experience simultaneous hair loss all over the scalp and/or body leading to alopecia totalis or universalis in just a few weeks.

Shed hair fibers can sometimes be used to diagnose alopecia areata. With scanning electron microscopy hair fibers are seen at the edge of an expanding bald patch as intact at the oldest part of the hair (furthest away from the scalp) whereas if you look at the newer part of the hair (close to the scalp) it can look aberrant. An increase of irregularity can be observed in the shape of the hair fiber. Deposits of unordered keratins are involved as well as constrictions. The cuticle might be missing and longitudinal cracks along the length of the hair might be observed. The constituent keratins are the same but seem to be abnormally assembled. This irregular construction of the hair leads to fracturing of the hair leaving back a stumpy, one to two millimeter long hair fiber also known as exclamation mark hair, often seen in expanding patches of alopecia areata. This abnormal hair formation may occur in other conditions as well and is therefore by itself not enough for a

save diagnosis of alopecia areata. Less severely damaged hairs may continue in anagen phase but produce dystrophic hairs as described earlier. Unpigmented or white hairs are less affected than pigmented hairs. In addition, some patients may experience sporadic or permanent changes in hair color during, or after, an episode of hair loss. There might also be times of spontaneous hair re-growth involved as well as aberrant nail formation (Muller 1963, Baran 1984). Nail dystrophy varies from a diffuse, fine pitting to severe alteration in a few cases (Gollinck 1990). Brittle nails, longitudinal ridging, spotting of the lunulae (half-moon resemblance at the base of the fingernail), onycholysis (loosening or separation of a fingernail or toenail from its nail bed), onychomadesis (complete shedding of a fingernail or toenail), and koilonychias (concavity of the outer surface of the nail) have been reported. These nail abnormalities can precede, follow or occur simultaneously with hair loss. There is no conclusive diagnostic test available so far leaving the dermatologist to deduce alopecia areata by an elimination process of other hair loss causes. Sometimes hair pull tests are conducted at the margins of the bald patches or small biopsies of the skin taken to check for focal inflammation of the hair follicles under a microscope.

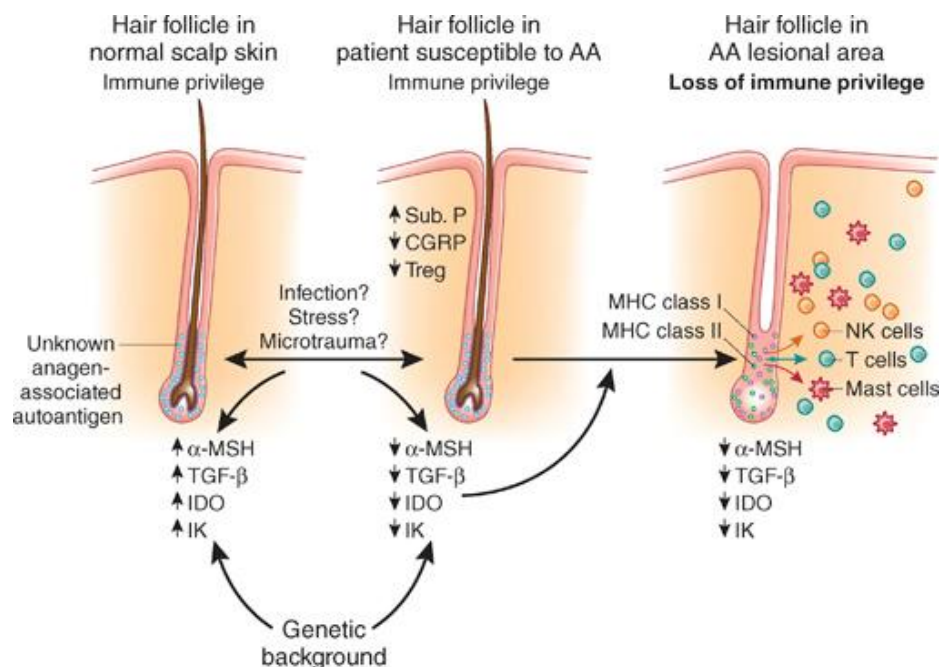
2.4 Pathology

The pathogenesis of alopecia areata is still unknown, but evidence points to a substantial role of genetic factors, nonspecific immune- and organ-specific autoimmune reactions, as well as environmental triggers (Madani 2000, Norris 2004, McElwee 1999, Kalish 2003). The genetic component of the disease is supported by the accumulated occurrence in families (Duvic 2001). Between 10% and 42% of alopecia areata patients report a family history, with higher incidences in patients with an early onset of hair loss and in identical twins (Shellow 1992, Scerri 1992). Especially the HLA-region was found to be involved in several genetic studies (Pethukova 2010, Madani 2000, Colombe 1995, de Andrade 1999), which supports the theory of loss of immune-privilege in hair follicles (Paus 1997, Paus 2003). Hair follicles usually do not express MHC class I and II molecules (Paus 1997, Christoph 2000, Westgate 1991, Paus 1994). There are only few Langerhans cells located around and within hair follicles, and they have functional impairment because they do not express MHC class II molecules, which normally play a role in antigen presentation. Furthermore, immunosuppressive cytokines are expressed prominently by the follicular epithelium (Teraki 1996). These cytokines are believed to maintain the immune privilege of the hair follicles and to induce peripheral tolerance (Gilhar 2007, Gilhar 2010).

In the acute progressive state of alopecia areata granulomatous inflammation and lymphocytic infiltrates have been observed within the hair follicle and around late anagen hairs (Messenger 1986) (figure 6). The inflammatory cell infiltrate mostly consists of

activated T lymphocytes, with the presence of CD4, CD8, and Langerhans' cells [Todes-Taylor 1984, Perret 1984, Ranki 1984, Gollinck 1990]. It can also be observed above the hair follicle bulb and may also invade follicular streamers. It is generally not observed in the bulge area and the region where the arrector pili muscle inserts into the hair follicle. Also the region where hair follicle stem cells are situated is usually not affected and might explain why follicles are not destroyed in alopecia areata. Via stem cell proliferation the damage to the hair follicles can be repaired if the stem cells are still intact. In long term chronic alopecia areata a slow decrease of inflammation activity and fewer lymphocytes, macrophages, and Langerhan's cells can be observed, but is still more than is usual in healthy skin.

Figure 6: Pathogenic model of alopecia areata. [From Gilhar A Collapse of Immune Privilege in Alopecia Areata: Coincidental or Substantial? J Invest Dermatol 2010; 130:2535-37]



The normal hair follicle represents a site of immune privilege (IP). The guardians of IP include immune-suppressive cytokines such as α melanocyte stimulating hormone (α MSH), transforming growth factor- β (TGF- β), IK, indoleamine 2,3-dioxygenase (IDO), and IL-10. Patients with a specific genetic background are susceptible to developing alopecia areata (AA), most probably by downregulation of this immunosuppressive environment. It has been suggested that events such as stress, infection, or microtrauma might lead to downregulation of immunosuppressive cytokines. This downregulation enables the accumulation of natural killer (NK) cells around hair follicles. Furthermore, stress or other trauma may also alter the production of neuropeptides, including substance P (SP) and calcitonin gene-related peptide (CGRP). SP may upregulate the production of nerve growth factor, which in turn induces accumulation of mast cells around hair follicles. SP causes degranulation of mast cells, leading to a release of large amounts of TNF- α , which is known to inhibit hair growth. Furthermore, SP induces accumulation of CD8⁺ cells and induces these cells to produce large amounts of IFN- γ . IFN- γ , produced by the activated CD8⁺ cells and the NK cells, induces expression of major histocompatibility complex (MHC) class I molecules in the lower part of the follicular epithelium, resulting in presentation of follicular autoantigens to the CD8⁺ cells and loss of IP. IFN- γ also may induce MHC class II molecule expression by the follicular epithelium, leading to a second wave of CD4⁺ cells that may bolster CD8⁺ activity via released cytokines. Treg, regulatory T cell.

Some studies have also shown the presence of mast cells in addition to the lymphocytic infiltrate [Cetin 2009], whereas others have shown evidence of eosinophils in all stages of alopecia areata within the fibrous tracts and the peribulbar infiltrate [Müller 2011, Elston 1997]. At the apex of the dermal papilla pigment incontinence may be seen, and some of the pigment may be retained in follicular streamers [Lew 2009].

Necrosis, apoptosis, and dark cell transformation have been reported as well as a circumscribed cystic change in the supra-bulbar region above the dermal papilla as patterns of hair follicle cellular degeneration in acute alopecia areata [Philpott 1996, Hoffmann 1999, Bodemer 2000].

Most of the observed nail changes have been shown to be related to changes within the proximal matrix via light and electron microscopy.

2.5 Treatment

Even after many years of hair loss potentially everyone is capable of re-growing hair, due to the before mentioned fact that hair follicle stem cells are not affected. Since the underlying cause of the disease is still not known only symptoms can be treated but no cure is available. There is no strong evidence that the long term course of alopecia areata can be altered by drug induced remissions or therapies. Therefore treatment may promote hair re-growth but treatment has to be permanent to have a longtime hair growth promoting effect.

The most popular drugs to treat patchy hair loss are corticosteroids as they are known to strongly inhibit the activation of T lymphocytes. Another treatment option is PUVA, a phototherapy that involves taking psoralen (P) two hours before exposure to long-wave ultraviolet light (UVA). 40 to 80 treatments may initiate hair re-growth, whereas a complete re-growth may take up to two years. Contact sensitizers like squaric acid dibutylester (SADBE) or diphenylcyclopropanone (DCP) might also be used as treatment in Europe or Canada, but are not FDA approved in the USA. Weekly treatments are necessary for complete hair re-growth and there might be side effects experienced like a mild eczematous reaction and enlargement of retroauricular lymph nodes.

3 Dundee Experimental Bald Rats (DEBR)

3.1 History

In the 1970s Druckrey crossed BD I rats with rats of the BD VIII strain and generated the BD IX strain by subsequently selecting brother-sister pairs for agouti coat color and dark, pigmented eyes (Druckrey 1971). Some of these rats were transferred around 1977 to the Medical Research Council Laboratory of Animal Health (LAH) center in Carshalton, Surrey, England. There, a spontaneous mutation occurred leading to the alopecia areata phenotype. Because of exceptionally poor fecundity two BD IX rats were crossed with two wistar rats. The DEBR descendants of this cross were derived from full-sibling matings and were transferred in 1984 to the University of Dundee, Scotland (Michie 1991, Oliver 1991). After that the strain moved to the University of Marburg in Germany and was supervised by Dr. Kevin J. McElwee (2004) before it was finally moved to the University of Cologne, CCG (dermatogenetics group), Germany in 2006. Since then the strain is supervised by Dr. Hans Christian Hennies. The original colonies have all passed away, so that the brown hooded substrain in Cologne is the only available colony in the world.

3.2 Characterization

There are no documentations about the current inbred generation of the DEBR colony. McElwee reported in 2003 an inbred generation of F38 in the ancestors of the current colony. Considering a further full sib pair mating of three times per year the inbred generation should be somewhere around F62 by the end of 2010. This high inbreeding status ensures a high homogeneity but fecundity in these animals is again very critical. The animals can only be successfully mated within the ages 3 to 5 months. The main problem seems to be the small size of and the low milk production in the mother animals so that the offspring animals soon start to dehydrate and are eventually killed and eaten by the mother animals. This problem could be partially solved by additional feeding of the mother animals and their offspring with a mix of curd cheese, smashed banana and honey. Since the animal husbandry capacity is not given for another crossing with Wistar or PVG rats, 318 DEBR embryos were cryoconserved at Harlan Laboratories Ltd, Füllinsdorf, Switzerland, to ensure the safety of the colony for future use.

DEBR rats develop a full coat of hair within two weeks of birth. Starting with the age of 3 to 4 months the rats start to lose their whiskers and beginning patchy hair loss can be observed on the head (figure 7 A) and on the tail, extending rapidly over the shoulders around the age of 5 to 6 months (figure 7 B). At the age of 6 to 8 months hair loss also

affects the flanks (figure 7 C) and extends within a few weeks over the whole body (figure 7 D), including the throat and stomach. With the age of 1 year most animals are naked except for a few patches of hair left around the tailhead, at the feet and above the backbone in some animals. There are no non-affected animals in the colony and since 2008 only one histologically affected animal (full pelage coat but infiltrate around anagen hair follicles) was observed. Females and males are affected alike, but hair loss starts in general in males about 1 to 2 months later as in females. In some females a change of brown coat color to grey could be observed after giving birth (figure 8).

Figure 7: Progression of alopecia areata in DEBR rats. A) Beginning of hair loss behind ears, around eyes and nose as well as loss of whiskers. B) Hair loss patches get bigger and extend over the shoulders. C) Additional hair loss at the flanks. D) Severe hair loss on the whole body.

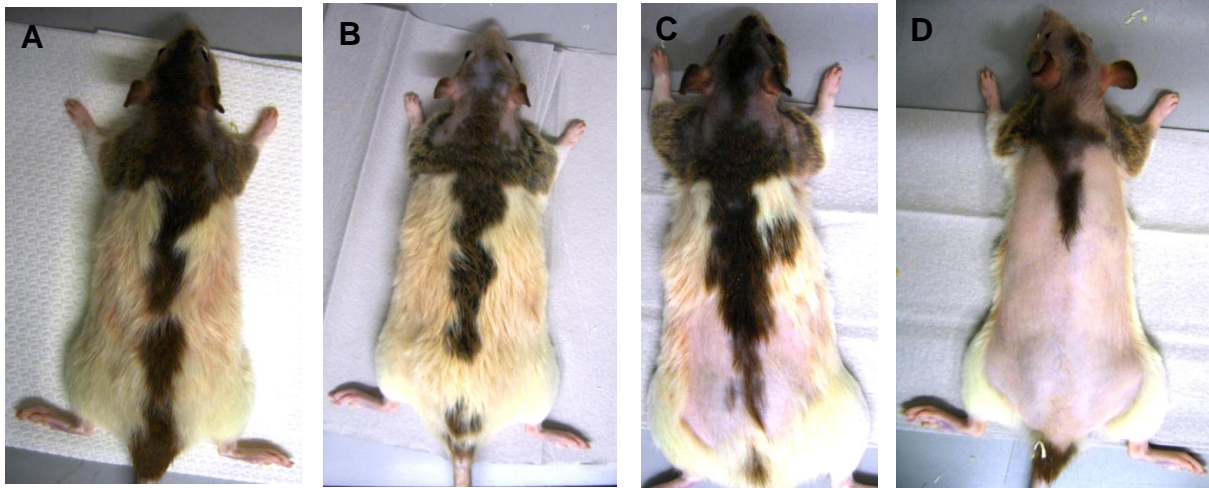


Figure 8: Young female DEBR rat with a scant hair coat and a change in coat color.



B Objectives of this Doctoral Thesis

As an animal model of Alopecia areata the rat strain Dundee Experimental Bald Rat (DEBR) was used. Prior to this study an intercross of DEBR with PVG rats gave an F2 population of 320 female animals with which a whole genome scan for linkage with 176 microsatellite markers was performed at the CCG (dermatogenetics group), Cologne. This analysis resulted in one highly significant locus on chromosome 19 with a lod score of 20 amongst others with much lower lod scores.

Based on these results the aim of this study will be to characterize the genetic basis of Alopecia areata in the rat model. This will be accomplished as follows:

- a) Saturation mapping will be performed with further microsatellite markers on chromosome 19 to identify a candidate region by haplotype analysis.
- b) Candidate genes will then be screened for mutations by sequencing and, if necessary, by next generation sequencing to identify the genetic basis of alopecia in the rodent model.
- c) In another approach a whole-transcript expression analysis will be performed with the Affymetrix Rat Gene 1.0ST Array and data will be processed with the softwares provided by Ingenuity Pathways Analysis to identify more candidate genes and possible pathways involved in the pathogenesis of alopecia areata (AA).
- d) Expression of candidate genes will then be validated and refined with quantitative real time PCR using the LC480 system and
- e) proteins of candidate genes will be immunohistologically stained in skin punch biopsies and, if necessary, in other organs to give further insights into the pathogenesis of AA in the rodent model.

In addition to the rodent model of AA human DNA from single patients and also from families with at least one AA affected person are available for this work. Prior to this study a whole genome scan for association and linkage with the Affymetrix Mapping 500K Array was performed at the CCG (dermatogenetics group) that resulted in one highly significant linked locus on chromosome 19.

Based on these results the aim of this study will be to characterize the genetic basis of Alopecia areata in humans. This will be accomplished as follows:

- a) Fine mapping of the candidate region on chromosome 19 with SNPstream, Taqman, and Pyrosequencing analysis will be conducted and
- b) association as well as linkage analysis will be performed with the obtained data to define candidate genes which will then be screened for mutations with high resolution melting curve analysis combined with sequencing.
- c) In addition more samples will be collected for whole genome genotyping with Affymetrix Genome-Wide Human SNP Array 6.0. The data obtained with these samples together with the data that was obtained earlier will be analyzed again for association and linkage.
- d) Immunohistological stainings will also be done in human skin punch biopsies to validate the findings in the rodent model and to proof the importance of the DEB rat strain as an adequate model for the human disease.

C Materials and Methods

1 Materials

1.1 Rat Samples

119 rats of the strain Dundee Experimental Bald Rat (DEBR) were used as well as 2 Sprague Dawley (SD), 6 Wistar (Wi) and 3 PVG rats. The DEB rats were cared for under the supervision of Dr. Kevin McElwee, University of Marburg before they were brought to the CCG (dermatogenetics group), Cologne, in 2006.

Of all animals skin and liver samples were collected. In addition to skin and liver, stomach, kidney, pancreas, small intestine, bladder, sexual organs, diaphragm, muscle, lung and heart were taken from all control rats and most of the DEBs.

Samples for DNA and protein isolation were frozen immediately at -80°C, samples for RNA isolation were kept in RNA-Later overnight at 4°C and then stored for later use at -80°C, samples for fibroblast and keratinocyte isolation were stored in transportation medium and skin samples for histological analyzes were stored in 10% neutral buffered formaldehyde.

In addition the DNA of 320 female F2 DEBs was analyzed for genetic variations. These animals were obtained prior to this work by cross-breeding DEBs with PVG/OlaHsd rats. 129 F2 animals showed overt hair loss whereas 63 animals only showed a histological phenotype (full pelage coat but infiltrate around anagen hair follicles). 128 of the F2 animals were not affected by alopecia areata.

1.2 Human Samples

Blood samples from alopecia areata patients and if possible from their family members were collected by Dr. med Hella Blech (CCG and private practice of dermatology, Rödental) under the supervision of Dr. Hans Christian Hennies, CCG (dermatogenetics group), Cologne. All participating persons gave their written consent to take part in this study and a standardized questionnaire that was developed by Dr. Rolf Hoffmann (Dermaticum, Practice for Dermatology, Freiburg) was filled out, giving background information about ancestry, further known diseases, and especially about the severity of hair loss in AA patients. In this study, the phenotype of AA patients is therefore categorized in five defined stages of severity by extent of hair loss and by localization of hair loss on the scalp and/or on other body parts, In total 1071 samples, including 199 parents with one affected child, 80 affected sib-pair families and 110 single patients were analyzed. In addition to the blood

samples skin punch biopsies from one patient with alopecia areata and one patient with alopecia universalis were collected.

352 control DNAs with european background provided by the University of Essen were used for SNPstream analysis and 2534 control DNAs from the biobank KORA, which is organized by the Helmholtz Center in Munich, Germany, (project number: K26/11) and POPGEN, which is organized by the UKSH in Kiel, Germany, (project number: BSP+SPC/110217/83) were used for whole genome linkage and association analysis.

1.3 Kits

QIAamp DNA Blood Maxi Kit	Qiagen GmbH
Dneasy Blood & Tissue Kit	Qiagen GmbH
EXPRESS One-Step SYBR GreenER Universal	Invitrogen GmbH
KGM Gold Bullet Kit	Lonza Sales AG
LC480 HRM Master	Roche Diagnostics GmbH
RNase-Free DNAs Set (50)	Qiagen GmbH
Rneasy Midi Kit	Qiagen GmbH
Zonula Adherens Sampler Kit	BD Transduction Laboratories

1.4 Chemicals

Aceton	Carl Roth GmbH+Co.KG
Albumin	Sigma-Aldrich Chemie GmbH
Alexa Fluor 488 Goat anti-mouse IgG	Invitrogen GmbH
Aseptisol	Bode Chemie GmbH
Baccilol	VWR International GmbH
Betaisodonna	Mundipharma GmbH
DAPI	VWR International GmbH
Dimethylsulfoxid (DMSO)	Merck KGaA
Dispase II	Roche Diagnostics GmbH
DMEM	Invitrogen GmbH
Dnase I (Rnase-free)	Invitrogen GmbH
Eosin G	Carl Roth GmbH+Co.KG
Essigsäure	Merck KGaA
Ethanol (unvergällt)	Merck KGaA
Ethanol (vergällt)	Merck KGaA
Ethylendiaminteraessigsäure (EDTA)	Carl Roth GmbH+Co.KG
Formalin	Sigma-Aldrich Chemie GmbH
Formamid	Merck KGaA
Fungizone	Invitrogen GmbH
Gentamicin (50mg/ml)	Invitrogen GmbH
Hämalaunlösung nach Mayer	Carl Roth GmbH+Co.KG
Isopropanol	Carl Roth GmbH+Co.KG
Methanol	Carl Roth GmbH+Co.KG

Methanol (ultareinst.)	Carl Roth GmbH+Co.KG
Natriumchlorid	Carl Roth GmbH+Co.KG
PBS 1x	Invitrogen GmbH
Phenol	Carl Roth GmbH+Co.KG
Polyvinylalkohol-Einschlussmittel	Sigma-Aldrich Chemie GmbH
ProFreeze-CDM	Lonza Sales AG
Proteinase K	Qiagen GmbH
Qiazol Lysis Reagent	Qiagen GmbH
RNA Later	Qiagen GmbH
Rnase A	Qiagen GmbH
Roti-Histofix	Carl Roth GmbH+Co.KG
SDS	Carl Roth GmbH+Co.KG
Sodium Pyruvate MEM	Invitrogen GmbH
Trichlormethan/Chloroform	Carl Roth GmbH+Co.KG
Tris(hydroxymethyl)-Aminomethan (TRIS)	Carl Roth GmbH+Co.KG
Triton X100	Carl Roth GmbH+Co.KG
Trypsin, 0,05% mit 0,53 mM EDTA	Invitrogen GmbH
Tween20	Carl Roth GmbH+Co.KG
Ultra Pure Distilled Water	Invitrogen GmbH
Water, distilled	Invitrogen GmbH
Xylol, Isomere	Merck KGaA
β -Mercapto-Ethanol	Merck KGaA

1.5 Machines and Robots

2100 Bioanalyzer	Agilent Technologies GmbH
3730 DNA Analyzer	Applied Biosystems GmbH
7900HT	Applied Biosystems GmbH
Alphalmager	Alpha Innotec GmbH
Axiovert40CFL	Zeiss
B12 function line	Thermo Fisher Scientific, Inc.
BBD6220	Thermo Fisher Scientific, Inc.
Biomek FX ^P	Beckman Coulter GmbH
Biotage PSQ HS96A	Biotage GmbH
Biowizard Xtra Golden Line	Kojair Tech Oj
BVC21NT	vaccubrand GmbH + Co.KG
Centrifuge 5810R	Eppendorf AG
CTR6500	Leica Microsystems GmbH
DM6000B	Leica Microsystems GmbH
Galaxy MiniStar	VWR International GmbH
GeneAmp 9700	Applied Biosystems GmbH
Genome Analyzer Ix	Illumina, Inc.
GenomeLab SNPstream	Beckman Coulter GmbH
Heraeus BIOFUGE fresco	Thermo Fisher Scientific, Inc.
HI 1210	Leica Microsystems GmbH
Horizon 11-14	Life Technologies GmbH

Leica ASP200S	Leica Microsystems GmbH
Leica EG 1150H	Leica Microsystems GmbH
LEICA RM2255	Leica Microsystems GmbH
LightCycler480	Roche Diagnostics GmbH
Megafuge 1.0R	Thermo Fisher Scientific, Inc.
Microlab STAR	Hamilton Messtechnik GmbH
MiniSpin plus	Eppendorf AG
Mixer UZUSIO VTX-3000L	LMS Consult GmbH + Co.KG
MR3001K	Heidolph Instruments GmbH + Co.KG
Multifuge X1R	Thermo Fisher Scientific, Inc.
NanoDrop 8000	peqlab Biotechnologie GmbH
NanoDrop ND-1000	peqlab Biotechnologie GmbH
PSQ HS 96A	Biotage GmbH
Stuart SRT1	VWR International GmbH
Stuart SRT9	VWR International GmbH
TE124S	Sartorius AG
TE1502S	Sartorius AG
Tetrad2	Bio-Rad Laboratories, Inc.
Thermomixer comfort	Eppendorf AG
TiMix	Edmund Bühler GmbH
TLP2824	Zebra Technologies Corporation
VX-75	Systemec
Z2	Beckman Coulter GmbH

2 Methods on DNA-Level

2.1 DNA-Isolation and Photometric Quantification

a) DNA-Isolation from Rat Liver

For the isolation of DNA from rat liver Qiagen DNeasy Blood & Tissue Kit was used.

Qiagen DNeasy Blood & Tissue Kit Protocol:

All centrifugation steps are carried out at room temperature in a microcentrifuge. Vortexing should be performed by pulse-vortexing for 5 – 10 seconds. Make sure that buffers ATL and AL didn't form precipitates upon storage. If necessary, warm to 56°C until the precipitates have fully dissolved. Before using buffers AW1 and AW2 for the first time, ethanol (96-100%) has to be added as indicated on the bottle to obtain a working solution. Preheat a thermomixer to 56°C and equilibrate the sample to room temperature.

- Cut up to 25 mg liver into small pieces, and place in 1.5 ml microcentrifuge tube.
- Add 20 µl proteinase K, mix by vortexing, and incubate at 56°C in a thermomixer until completely lysed.
- Add 4 µl RNase A (100mg/ml), mix by vortexing, and incubate for 2 min at room temperature.
- Vortex for 15 seconds, add 200 µl buffer AL to the sample, and mix thoroughly by vortexing. Then add 200 µl ethanol (96-100%) and mix again thoroughly.
- Pipet the mixture into a DNeasy Mini spin column in a 2 ml collection tube. Centrifuge at 8.000 rpm for 1 min. Discard flow-through and collection tube.
- Place the spin column in a new 2 ml collection tube, add 500 µl buffer AW1, and centrifuge for 1 min at 8.000 rpm. Discard flow-through and collection tube.
- Place the spin column in a new 2 ml collection tube and add 500 µl buffer AW2. Centrifuge for 3 min at 14.000 rpm to dry the DNeasy membrane. Discard flow-through and collection tube.
- Transfer the spin column to a new 1.5 ml or 2 ml microcentrifuge tube and add 200 µl buffer AE for elution. Incubate for 1 min at room temperature. Centrifuge for 1 min at 8.000 rpm. Repeat this step for maximum DNA yield (ranges between 10 - 30 µg) or reload flow-through a second time for maximum DNA concentration.

b) DNA-Isolation from Human Blood

For the isolation of DNA from human blood Qiagens QIAamp DNA Blood Maxi Kit and a manual method by Nukleon were used.

QIAamp DNA Blood Maxi Kit Protocol:

All centrifugation steps are carried out at room temperature in a microcentrifuge capable of running at 5.000 rpm equipped with a swing-out rotor and buckets accommodating 50 ml centrifugation tubes. Make sure that buffer AL didn't form precipitates upon storage. If necessary, warm to 56°C until the precipitates have fully dissolved. Protease stock solution is prepared by adding 5.5 ml distilled water into the vial of lyophilized Protease. Before using buffers AW1 and AW2 for the first time, ethanol [96-100%] has to be added as indicated on the bottle to obtain a working solution. Preheat a water bath to 70°C and equilibrate the samples to room temperature.

- Pipet 500 µl protease into the bottom of a 50 ml centrifuge tube.
- Add 10 ml blood and mix briefly. If sample volume is less than 5 ml, add the appropriate volume of PBS.
- Add 12 ml buffer AL and mix thoroughly by inverting the tubes 15 times, followed by additional vigorous shaking for at least 1 min. Invert multiple tubes simultaneously by clamping them into a rack using another empty rack, grasping both racks, and inverting them together.
- Incubate at 70°C for 10 min.
- Add 10 ml of ethanol [96-100%] to the sample and mix again by vortexing.
- Carefully transfer half of the solution onto the QIAamp Maxi column placed in a 50 ml centrifugation tube. Avoid spilling and do not moisten the rim of the column. Close the cap and centrifuge at 3.000 rpm for 3 min.
- Remove the QIAamp Maxi column, discard the filtrate, and place the column back into the 50 ml centrifugation tube. Load the remainder of the solution onto the column, close the cap, and recentrifuge at 3.000 rpm for 3 min.
- Remove the QIAamp Maxi column, discard the filtrate, and place the column back into the 50 ml centrifugation tube.
- Carefully, without moistening the rim, add 5 ml buffer AW1 to the QIAamp Maxi column. Close the cap and centrifuge at 5.000 rpm for 1 min.
- Carefully, without moistening the rim, add 5 ml of buffer AW2 to the QIAamp Maxi column. Close the cap and centrifuge at 5.000 rpm for 15 min.

- Discard the 50 ml centrifugation tube containing the filtrate, and place the QIAamp Maxi column in a clean 50 ml centrifugation tube.
- Add 1 ml buffer AE, or distilled water, equilibrated to room temperature. Pipet directly onto the membrane of the QIAamp Maxi column and close the cap. Incubate at room temperature for 5 min and centrifuge at 5.000 rpm for 5 min.
- For maximum concentration: Reload the 1 ml of eluate containing the DNA onto the membrane of the QIAamp Maxi column. Close the cap and incubate at room temperature for 5 min. Centrifuge at 5.000 rpm for 5 min.
- For maximum yield: Pipet 1 ml of fresh buffer AE or distilled water, equilibrated to room temperature, onto the membrane of the QIAamp Maxi column. Incubate at room temperature for 5 min and centrifuge at 5.000 rpm for 5 min.

Nukleon Protocol:

All centrifugation steps are carried out at 4°C. Preheat a water bath to 37°C and a thermomixer to 65°C. Equilibrate the samples to room temperature and prepare following solutions:

0,5 mol/L NaEDTA-Solution:

Dilute 46,53 g Na-EDTA in 100 ml distilled water and equilibrate pH to 8 with NaOH. Add distilled water up to 250 ml.

10 % SDS-Solution:

Dilute 10 g SDS in 60 ml distilled water. Fill up to 100 ml with distilled water. Sterile filtrate the solution.

Solution A:

Dilute 1,2114 g Tris in 100 ml and equilibrate pH to 8 with HCl. Add 1,0165 g MgCl₂, 109,536 g Saccharose and 10 ml Triton X. Fill up to 1 Liter with distilled water and autoclave the solution.

Solution B:

Dilute 12,114 g Tris in 100 ml and equilibrate pH to 8 with HCl. Add 2,1915 g NaCl and 30 ml NaEDTA-Solution. Fill up to 225 ml with distilled water and autoclave the solution. Then add 25 ml sterile filtered 10% SDS-Solution.

Solution C:

Dilute 61,22 g Na-perchlorate in 60 ml distilled water. Fill up to 100 ml with distilled water. Autoclave the solution.

- Pipet 500 μ l Protease K (10 mg/ml) into the bottom of a 50 ml centrifuge tube.
- Add blood sample and mix briefly.
- Add 4x the volume of Solution A to each sample and mix gently by inverting the tubes several times. Centrifuge at 2.500 rpm for 5 min.
- Discard flow-through and dry cell pellet by placing the tube bottom-up on a paper towel.
- Add 2 ml Solution B and vortex to dissolve pellet. Transfer solution to a 15 ml tube.
- Add 15 μ l RNase A (50 μ g/ml) and incubate at 37°C for 30 min.
- Add 500 μ l Solution C and invert 15 times.
- Add 2 ml chloroform, invert 15 times, and centrifuge at 2.500 rpm for 5 min.
- Take off supernatant into a new 15 ml tube and repeat chloroform step if the solution is not clear yet. If the solution is clear then add same volume ice cold isopropanol and invert 15 times.
- Pick milky DNA-thread with a glass rod and put in an eppendorf tube filled with 1 ml 70% ethanol. Centrifuge at 13.000 rpm for 15 min. Take off Ethanol and leave pellet to dry.
- Add 270 μ l distilled water and dissolve pellet in a thermomixer at 65°C for 1 hour.
- Add 30 μ l 10x TE-buffer and leave in a thermomixer at 65°C for another 30 min.

c) Quality Control of isolated DNA

To check the concentration and quality of the isolated DNA the absorbance at 280 nm, 260 nm and 230 nm was measured for all samples with NanoDrop2000/8000 (Thermo Scientific). The purity of DNA is determined by the ratio of A_{260}/A_{280} and should be between 1.8 – 2.0. If the ratio value is off there is probably a contamination with proteins, phenol or other substances that absorb strongly at or near 260nm. A secondary measure of nucleic acid purity is given by the ratio of A_{260}/A_{230} and should be between 2.0 – 2.2. If the ratio value is off there is probably a contamination with other substances absorbing 230 nm as for example EDTA, carbohydrates or phenol.

The length of the isolated DNA can be checked by running a 1% agarose gel. After the electrophoresis is done there should be seen a strong, single band. If there is a smear the DNA is degraded.

If a very accurate measurement of yield, purity and length was needed the samples were measured by Bioanalyzer (Agilent Technologies), a microfluidics-based platform.

2.2 PCR and Gelectrophoresis

PCR allows for duplication of specific DNA fragments per cycle. This means that from a single DNA fragment arises $2^{35} = 34$ billion molecules after 35 cycles.

Standard PCR protocol:

12.48 µl	water
1.50 µl	PCR - buffer (10x)
0.3 µl	forward primer (10 µM)
0.3 µl	reverse primer (10 µM)
0.3 µl	dNTPs
0.12 µl	Taq (5 U/µl)
10 ng	DNA, dry

PCR - Settings:

95°C for 1 minute

35 x 95°C for 30 seconds, 60°C (primer dependent) for 45 seconds, 72°C for 30 seconds

72°C for 5 minutes

Hold 4°C

Polarized macromolecules like DNA can be separated in a gel matrix depending on their charge, size, and tertiary structure by an electrical field in gel electrophoresis. The gel matrix works like a sieve where small, highly charged molecules are exposed to a smaller resistance and therefore travel a larger distance in the same time than larger, less charged molecules. Ethidium bromide is added to the gel which intercalates in the DNA and makes it visible in UV light. For sizing the samples a kb-ladder is included in one slot of the gel matrix.

2% agarose gel protocol:

1.6 g agarose

80 ml 1x TBE-buffer

5 µl ethidium bromide

2.3 Sequencing

Sequencing is a method to identify the nucleotide succession in a DNA molecule.

a) Sanger Sequencing

After amplification of a primer specific DNA fragment using PCR and Exo/SAP treatment the product is used for the sequencing reaction. Another amplification step is started, but this time only one primer and not only dNTPs are used but also differently fluorescence labeled ddNTPs. These lead to a chain determination since they don't have a 3'-hydroxy group and inhibit therefore the elongation of the DNA. This leads to amplified DNA fragments with different sizes that can be separated by capillary electrophoresis and detected after excitation by a laser. Sequences were viewed with the program SeqMan which is part of the DNASTAR software package.

Exo/SAP protocol:

8 µl	PCR product
1.625 µl	water
0.3 µl	SAP
0.075 µl	Exo I (20 U/µl)

Exo/SAP - settings:

37 for 25 minutes
72°C for 15 minutes

Sequencing protocol:

5.25 µl	water
2 µl	Exo/SAP product
2 µl	sequencing buffer
0.5 µl	ABI Big Dye version 1.1
0.25 µl	forward or reverse primer (10 µM)

Sequencing settings:

31 x 96°C for 10 seconds, 55°C for 55 seconds, 60°C for 4 minutes
Hold 4°C

b) Next Generation Sequencing (NGS) using Illumina Genome Analyzer IIx

Via a Covaris sonicator 3 µg of genomic DNA was reduced into 50 to 400 base pair fragments. DNA fragments were then subjected to end-repair, phosphorylation and 3'-adenylation. Illumina paired-end adaptors were ligated to the ends. For downstream enrichment templates were size selected by purification on a 2% TAE-agarose gel and excision of fragments 250 +/- 25 base pairs in length. Fifteen rounds of PCR followed to amplify the purified DNA templates. The DNA library fragment lengths were validated on an Agilent Technologies 2100 Bioanalyzer using the Agilent DNA 1000 chip kit. Instead of making thousands of PCRs DNA enrichment can be done using an array based technology. In this case 385,000 unique, overlapping, 60 to 90 nucleotides long probes were designed across the target region of chr19:32.897.608..37.770.047 (RGSC v3.4; m4). For the enrichment step at least 21 µg of DNA per sample have to be provided at a minimum concentration of 200 ng/µl in TE buffer or nuclease-free water. DNA quality must be proven as non-degraded, showing a single, high molecular band (>12kb) on an agarose gel with OD260/280 values at or above 1,8 and OD260/230 values at or above 1,5. The amplified fragments are then hybridized to a Roche NimbleGen Sequence Capture 385K microarray for about 72 hours at 42°C with a Roche NimbleGen Hybridization System 4. Afterwards the array is washed and DNA fragments can be eluted. A PCR-based amplification of the DNA fragments follows. Successful enrichment (at least 10 µg of enriched DNA) is verified by quantitative real-time PCR. The DNA library was then sequenced on a PE flow cell and a 2x50 bp run was conducted using Illumina Genome Analyzer IIx according to the manufacturers' recommendations. The sequencing workflow includes template hybridization, isothermal amplification, linearization, blocking, sequencing primer hybridization, and sequencing-by-synthesis of Read 1. After completion of the first read, the newly sequenced strands are stripped off and the complementary strands are bridge amplified to form clusters. The original templates are then cleaved and removed before the reverse strands undergo sequencing-by-synthesis.

DNA library preparation and data processing and analysis were done by the NGS team of the CCG, Cologne. The design of and hybridization to a customized NimbleGen rat genomic 385K array was done by ATLAS Biolabs GmbH, Berlin. Samples were DNA from a PVG, Wistar, BD IX, affected DEB, histologically affected, and unaffected DEB rat.

c) Pyrosequencing

As a template for pyrosequencing single stranded DNA is used and sequenced by synthesizing the complementary strand base by base. In iterative steps dXTPs are added to the reaction. When the complementary nucleotide is incorporated onto the template by the

polymerase pyrophosphate (PPi) is released. This is quantitatively converted to ATP by sulfurylase in the presence of adenosine 5' phosphosulfate and fuels the luciferase-mediated conversion of luciferin to oxyluciferin. This reaction generates visible light in amounts that are proportional to the amount of ATP and is detected by a camera. Unincorporated nucleotides and ATP are degraded by apyrase, and the reaction starts again with another nucleotide.

Pyrosequencing PCR settings:

95°C for 5 minutes

45 x 95°C for 15 seconds, 62°C for 30 seconds, 72°C for 15 seconds

72°C for 5 minutes

Hold 4°C

Pyrosequencing PCR Protocol:

8.66 µl	water
1.5 µl	PCR - buffer II (10x)
0.24 µl	dNTPs
0.24 µl	biotinylated forward primer (10 µM)
0.24 µl	reverse Primer (10 µM)
0.12 µl	Taq (5 U/µl)
4 µl	DNA

After PCR amplification the product is mixed with 70 µl 3% cepharose solution and left to incubate for five minutes on a shaker. Turn on the vacuum pump of the PyroMark Vacuum Prep Workstation and wash the adaptor in water before aspirating the PCR product. Then place the adaptor for several seconds in 70% ethanol and then in 1 M sodium hydroxide to separate DNA strands. Neutralize several seconds in 1x washing buffer and turn off the pump. Shake off ssDNA in a new plate containing a solution of 11.64 µl AB-buffer with 0.36 µl sequencing primer in each well. Incubate for 2 minutes at 85°C and leave to cool to room temperature before placing the plate in the Biotage PSQ HS96A Pyrosequencer.

2.4 Microsatellite Analysis

Microsatellites are short tandem repeats, mostly located in non-coding DNA regions. A single repeat unit's length is usually restricted between 2 to 7 bases whereas the number of repeat units can be highly variable and can therefore be used as markers to establish

linkage groups in crosses and to map genetically identified mutations to chromosomal positions.

Microsatellite PCR Protocol:

8,32 µl water
 1 µl PCR - buffer (10x)
 0.2 µl fluorescence labeled forward primer (10 µM)
 0.2 µl reverse primer (10 µM)
 0.2 µl dNTPs
 0.08 µl Taq (5 U/µl)
 6 ng DNA, dry

Microsatellite PCR settings:

94°C for 3 minutes
 3 x 94°C for 30 seconds, 61°C for 45 seconds, 72°C for 1 minute
 3 x 94°C for 30 seconds, 59°C for 45 seconds, 72°C for 1 minute
 3 x 94°C for 30 seconds, 57°C for 45 seconds, 72°C for 1 minute
 3 x 94°C for 30 seconds, 55°C for 45 seconds, 72°C for 1 minute
 72°C for 10 minutes
 Hold 4°C

Mix 6.3 µl formamide with 0.7 µl Rox500 standard per sample and add 3µl diluted PCR product. The dilution factor has to be optimized and is usually between 1:50 and 1:200. The fragments can then be resolved by capillary electrophoresis. The number of repeat units can be determined using for example GeneMapper software.

2.5 High Resolution Melting (HRM) Curve Analysis

High resolution melting curve analysis was performed using Roche's High Resolution Melting Master (see table 1 for protocol) and Light Cycler 480 system.

Table 1: 10-µl reaction with 20 ng dry DNA

x mM MgCl ₂	1,0	1,5	2,0	2,5	3,0	3,5
Mastermix 2x	5,0	5,0	5,0	5,0	5,0	5,0
Primer F	0,2	0,2	0,2	0,2	0,2	0,2
Primer R	0,2	0,2	0,2	0,2	0,2	0,2
MgCl ₂	0,4	0,6	0,8	1,0	1,2	1,4
ddH ₂ O	4,2	4,0	3,8	3,6	3,4	3,2
<i>Target in ng, dry</i>	<i>20,0</i>	<i>20,0</i>	<i>20,0</i>	<i>20,0</i>	<i>20,0</i>	<i>20,0</i>

This method is used for detection of sequence variants among several samples. In a first step primer specific DNA fragments are amplified in a PCR reaction. After each cycle a single measure of fluorescence activity is made so that the formation of amplicon during PCR can be monitored real time. The amplification step is followed by high resolution melting. The samples are heated from 60 to 95°C and fluorescence is measured continuously (table 2).

The fluorescence dye used in this kit is ResoLight, which is a fluorescence dye that intercalates in double stranded DNA and is more sensitive than SYBR Green. It is excited by light with a wavelength between 450 and 500 nm. The emission maximum is at 503 nm.

Table 2: PCR Parameters for HRM

Setup				
Detection Format			SYBR Green I	
Programs				
Program Name	Cycles		Analysis Mode	
Preincubation	1		None	
Amplification	45		Quantification	
High Resolution Melting	1		Melting Curves	
Cooling	1		None	
Temperature Targets				
Target (°C)	Acquisition Mode	Hold (mm:ss)	Ramp Rate (°C/s)	Acquisitions (per °C)
Preincubation				
95	None	10:00	4.4	-
Amplification				
95	None	00:10	4.4	-
primer dependent	None	00:10	2.2	-
72	Single	00:20	4.4	-
High Resolution Melting				
95	None	01:00	4.4	-
40	None	01:00	2.2	-
60	None	00:01	1	-
95	Continuous	-	-	25
Cooling				
40	None	00:10	4.4	-

For best results the amplified DNA-fragments should not be longer than 500 base pairs because the sensitivity of variant detection will decrease. In addition, for each primer the conditions of PCR have to be optimized by adjusting the MgCl₂ concentration, the annealing temperature, and the number of cycles.

Melting curve analysis verifies the specificity of the amplification reaction by showing a single melting peak at the same temperature for all samples (figure 9). Depending on the melting curve shapes (figures 10 and 12) gene scanning software can then distinguish between up to 6 different genotypes (see figures 11 and 13).

Figure 9: Melting curve analysis for fragment ZNF568_e7.9.

First negative derivative of the sample fluorescence versus temperature showing one melting peak for all samples. This indicates a pure, homogenous amplification of a single PCR product.

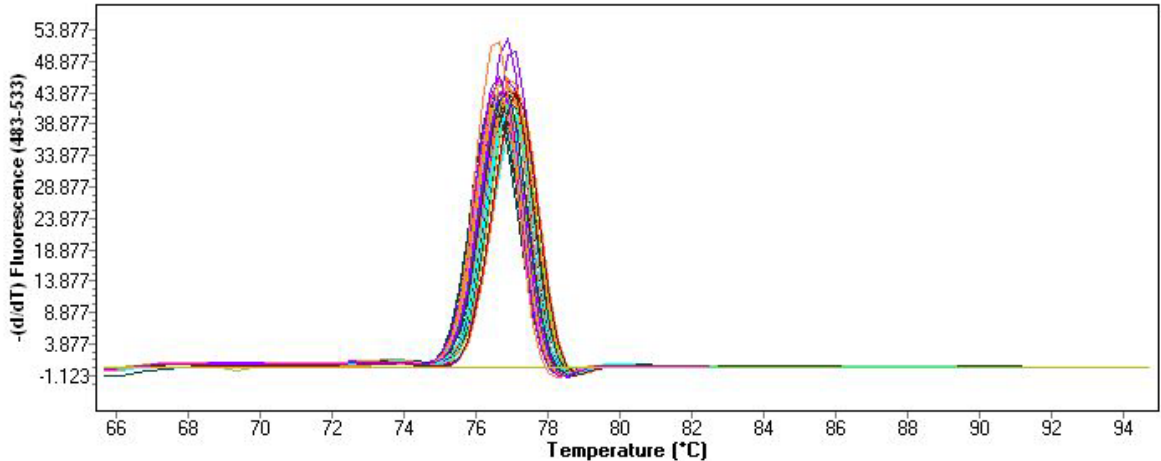


Figure 10: Normalized and temperature shifted melting curve data for fragment ZNF568_e7.9.

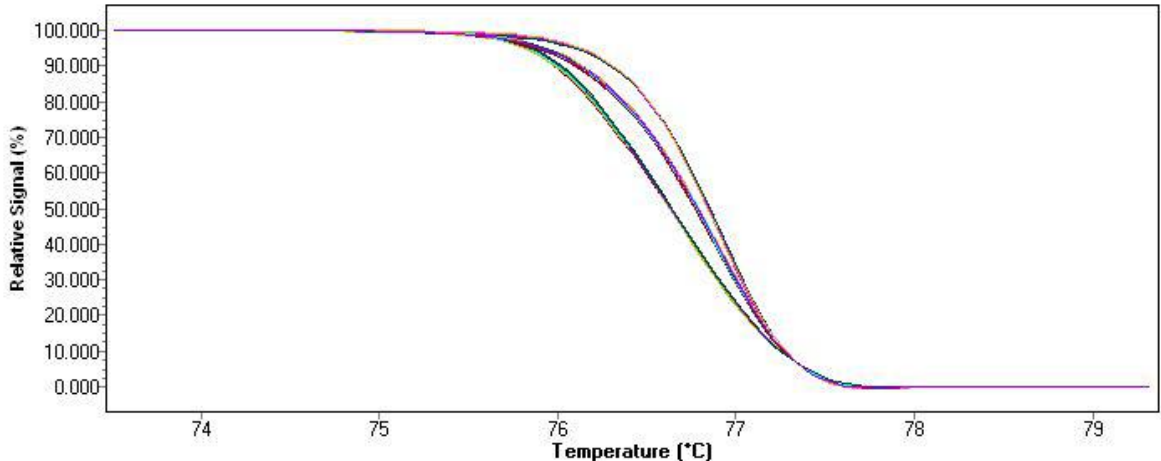


Figure 11: Normalized and temperature shifted difference plot for fragment ZNF568_e7.9.
Samples are divided in 3 genotypes.

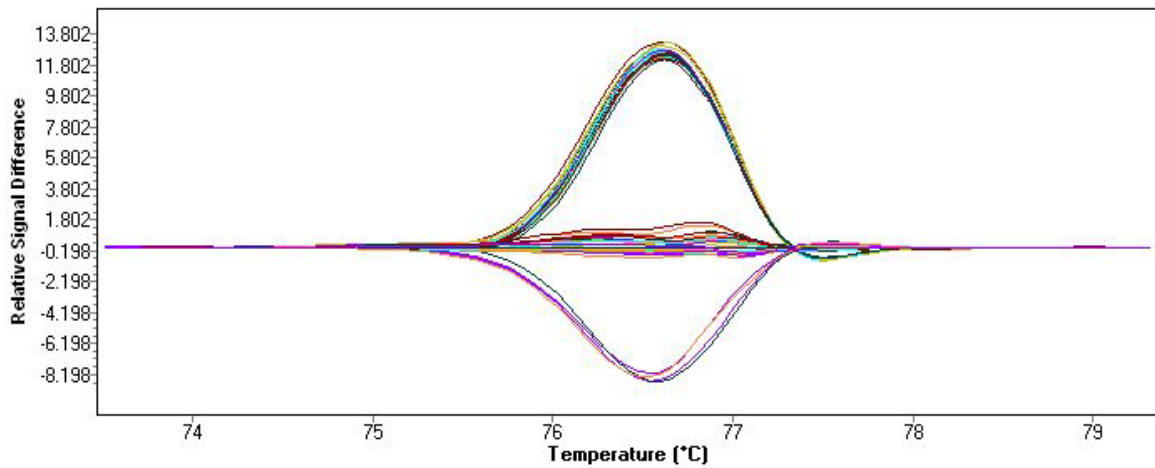


Figure 12: Normalized and temperature shifted melting curve data for fragment ZNF568_e7.2.

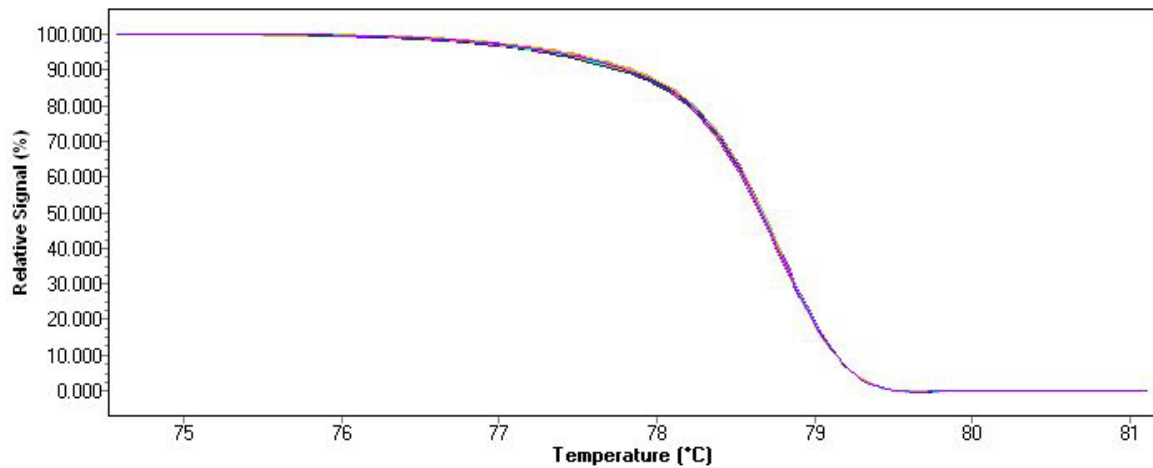
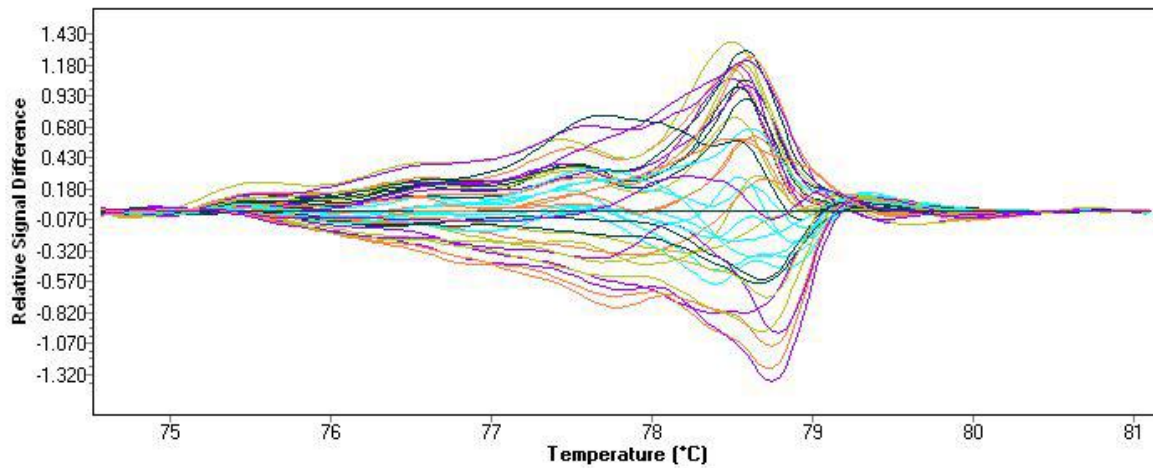


Figure 13: Normalized and temperature shifted difference plot for fragment ZNF568_e7.2.
All samples have the same genotype.



2.6 Taqman

SNP genotyping with Taqman assays works with two MGB (minor groove binding) probes which are labeled with either VIC or 6FAM fluorescent dye at the 5' end. This allows genotyping of the two possible variant alleles at the SNP site in a DNA target sequence. Probes anneal to the complementary template during PCR and are cleaved by the polymerase in the amplification step. This separates the nonfluorescent quencher at the 3' end of the probe from the reporter dyes, so that the fluorescence of the probe dyes is no longer suppressed and can be detected.

3 µl reaction with 10 ng DNA protocol:

1,5 µl	2x PCR-Mastermix
0,075 µl	40x Taqman Genotyping Assay
1,425 µl	ddH ₂ O
10 ng	dry DNA

PCR parameters:

95°C for 10 minutes
40 x 92°C for 15 seconds and 60°C for 1 minute
Hold 4°C

2.7 SNPstream

SNP genotyping with SNPstream allows for detecting 48 SNPs in 384 samples in each run. In a first step primers are designed with the online software of Beckman&Coulter (www.autoprimer.com) and pooled as needed. PCR amplification follows. Then the products are purified with SBE Clean-Up, split on two plates, mixed with tagged sequencing primers, and TAMRA- or BODIPY- fluorescein labeled nucleotide terminator extension mixes. The products can then be spatially resolved by hybridization to the complementary oligonucleotide tag on a SNPware Tag Array. Assay results are finally read by direct two - color fluorescence on SNPstream Array Imager.

Primerpool preparation for 96 PCR-Primers:

Primer stocks are concentrated at 250 µM.

A 1:100 dilution is needed to get a 2,5 µM concentration.

Pipet 10 µl of each Primer in a tube and add 40 µl ddH₂O to reach a final volume of 1000 µl.

SNPware Primer Panel 1 (S-TCAG) preparation:

Primer stocks are concentrated at 250 μ M.

A 1:50 dilution is needed to get a 5 μ M concentration.

Pipet 10 μ l of all S-TCAG Primers in a tube and add ddH₂O to reach a final volume of 500 μ l.

SNPware Primer Panel 2 (S-CGAT) preparation:

Primer stocks are concentrated at 250 μ M.

A 1:50 dilution is needed to get a 5 μ M concentration.

Pipet 10 μ l of all S-CGAT Primers in a tube and add ddH₂O to reach a final volume of 500 μ l.

5 μ l 48plex reaction with 8 ng DNA protocol:

0,1 μ l	TaqGold
0,045 μ l	dNTPs (2,5 mM each)
1 μ l	MgCl ₂ (25 mM)
0,1 μ l	Primerpool (2,5 μ M each)
0,5 μ l	10x PCR-Buffer II
3,255 μ l	ddH ₂ O
8 ng	dry DNA

PCR parameters:

94°C for 1 minute

40 x 94°C for 30 seconds, 55°C for 30 seconds and 72°C for 1 minute

Hold 4°C

SBE Clean-Up protocol for a 384 well plate:

50 μ l SBE Clean-Up Reagent

1.200 μ l SBE Clean-Up Diluent

Mix thoroughly and add 3 μ l to each well onto the 5 μ l of PCR product.

Seal PCR plates and spin briefly.

SBE Clean-Up parameters:

37°C for 30 minutes

96°C for 10 minutes

Hold 4°C

After SBE Clean-Up transfer 4 µl of each well to a new 384 well plate. One of the plates will then be used for the S-TCAG primer extension reaction, whereas the other plate will be used for the S-CGAT primer extension reaction.

3,5 µl S-TCAG primer extension reaction protocol for a 384 well plate:

2.116 µl	ddH ₂ O
2.658 µl	Extension Mix Diluent
63 µl	TC Extension Mix
63 µl	AG Extension Mix
21 µl	SNPware Primer Panel 1
15 µl	DNA Polymerase

Add 3,5 µl to each well onto one of the SBE Clean-Up plates.

3,5 µl S-CGAT primer extension reaction protocol for a 384 well plate:

2.116 µl	ddH ₂ O
2.658 µl	Extension Mix Diluent
63 µl	CG Extension Mix
63 µl	AT Extension Mix
21 µl	SNPware Primer Panel 1
15 µl	DNA Polymerase

Add 3,5 µl to each well onto the second SBE Clean-Up plate.

Universal SBE program:

96°C for 3 minutes
60x 94°C for 20 seconds and 40°C for 11 seconds
Hold 4°C

Preparation of SNPware plates:

30 ml	Wash Buffer I
570 ml	ddH ₂ O

Wash SNPware plate 3 times with 1:20 SNPware Wash Buffer I.

Place SNPware plate face down on a soft tissue in a centrifuge and spin for 2 minutes at 1.500 rpm to dry the plate.

Preparation of Hybridization Solution:

825 ml 2x Hybridization Solution

14,172 ml Hybridization Additive

Add 7 μ l Hybridization Solution into each well of one of the primer extension reaction plates. Mix by pipetting up and down and transfer everything onto the second primer extension reaction plate, so that everything is pooled again. Transfer then 16 μ l from each well to a prewashed SNPware plate. Tap gently at the plate to ensure equal dispersion.

Hybridization protocol:

Incubate the SNPware plate for 2 hours at 42°C with humidity close to 100%.

After hybridization dilute SNPware Wash Buffer II 1:64 and wash the SNPware plate 3 times. Place SNPware plate face down on a soft tissue in a centrifuge and spin for 2 minutes at 1.500 rpm to dry the plate. Load the SNPware plate into the SNPstream Imager to capture the plate image and analyze the data.

2.8 Affymetrix Genome-Wide Human SNP Array 6.0 and GeneChip Human Mapping 500K Array

SNP arrays are a microarray based technology with which a high number of genome wide SNPs can be genotyped for each sample in a short period of time. In this study genotyping was conducted with the Affymetrix Genome-Wide Human SNP Array 6.0 (906,600 SNPs and 946,000 copy number variation probes) and with Affymetrix GeneChip Human Mapping 500K Array (500,000 SNPs). DNA from human blood samples was processed and hybridized according to the manufacturer's instructions by the Affymetrix platform Team of the CCG, Berlin. Data was then processed and analyzed by Dr. Franz Rüschemdorf, Max Delbrück Center for Molecular Medicine, Berlin.

3 Methods on RNA Level

3.1 RNA-Isolation and Quality Control

a) RNA-Isolation from Rat and Human Tissues

- Cut up to 100 mg of tissue into little pieces with a scalpel and put fragments in a tube containing 1 ml of Trizol.
- Homogenize sample and incubate for 5 minutes on ice.
- Centrifuge at maximum speed for 5 minutes at 4°C to pellet debris.
- Transfer supernatant to a new tube, add 0.2 ml chloroform/ml trizol and vortex for 15 seconds.
- Incubate for up to 5 minutes to allow phase separation.
- Centrifuge at maximum speed for 30 minutes at 4°C
- Transfer entire upper, aqueous layer to a new tube, add same volume of 100% ethanol and vortex.
- Centrifuge at maximum speed for 10 minutes at 4°C
- Take off supernatant and wash pellet with 80% ethanol.
- Centrifuge at maximum speed for 10 minutes at 4°C
- Take off supernatant, dry pellet and resuspend in 100 µl RNase free water.

b) RNA-Isolation from Rat Fibroblasts

For the isolation of RNA from rat fibroblasts Qiagen's RNeasy Midi Kit was used.

RNeasy Midi Kit Protocol:

Do not use more than $3-4 \times 10^7$ cells per RNeasy midi column to avoid overloading and clogging the column. Add 10 µl beta-mercaptoethanol per 1 ml buffer RLT needed and add 100% of ethanol as indicated on the bottle before using buffer RPE for the first time. All steps, including centrifugation, are performed at room temperature.

- Resuspend the cell pellet in 4 ml RLT buffer and homogenize cells using a conventional rotor-stator homogenizer for at least 45 seconds at maximum speed until the sample is uniformly homogeneous.
- Add 1 volume of 70% ethanol to the lysate, and mix thoroughly by shaking vigorously.
- Apply the sample, including any precipitate that may have formed, to an RNeasy midi column placed in a 15 ml centrifuge tube. Centrifuge at 3.000 – 5.000 g for 5 minutes. Discard the flow-through.

- Add 2 ml buffer RW1 to the column and centrifuge at 3.000 – 5.000 g for 5 minutes. Discard the flow-through.
- Add 20 µl DNase I stock solution to 140 µl buffer RDD. Mix by gently flicking the tube, and centrifuge briefly to collect residual liquid from the sides of the tube.
- Pipet the DNase I incubation mix directly onto the RNeasy silica-gel membrane, and place on the benchtop for 15 minutes at room temperature.
- Pipet 2 ml buffer RW1 into the column, and place on the benchtop for 5 minutes. Centrifuge at 3.000 – 5.000 g for 5 minutes. Discard the flow-through.
- Add 2.5 ml buffer RPE to the column and centrifuge at 3.000 – 5.000 g for 2 minutes. Discard flow-through.
- Add another 2.5 ml buffer RPE to the column and centrifuge at 3.000 – 5.000 g for 5 minutes. Remove the RNeasy column from the centrifuge tube carefully so the column does not contact the flow-through as this will result in carryover of ethanol.
- Transfer the column to a new 15 ml collection tube. Pipet 150 µl RNase-free water directly onto the RNeasy silica-gel membrane. Let it stand for 1 minute, and then centrifuge for 3 minutes at 3.000 – 5.000 g.
- Repeat the elution step as described with a second volume of RNase-free water.

c) Quality Control of isolated RNA

To check the concentration and quality of the isolated RNA the absorbance at 280 nm, 260 nm and 230 nm was measured for all samples with NanoDrop2000/8000 (Thermo Scientific). The purity of RNA is determined by the ratio of A_{260}/A_{280} and should be between 1.9 – 2.1. If the ratio value is off there is probably a contamination with proteins, phenol or other substances that absorb strongly at or near 260nm. A secondary measure of nucleic acid purity is given by the ratio of A_{260}/A_{230} and should be above 1.8. If the ratio value is off there is probably a contamination with other substances absorbing 230 nm as for example EDTA, carbohydrates or phenol.

If a very accurate measurement of yield and purity was needed the samples were measured with the Bioanalyzer (Agilent Technologies), a microfluidics-based platform.

3.2 Quantitative Real Time PCR (qRT - PCR)

qRT-PCR was performed using Invitrogen's EXPRESS One-Step SYBR GreenER Kit and Roche's Light Cycler 480 system.

In a first step the RNA has to be transcribed to cDNA followed by primer specific amplification and a melting curve analysis [table 3]. The melting curve is used to check that all samples have amplified the exact same fragment, so there is no variation that would

influence expression value calculations. For relative quantification samples as well as controls have to be analyzed for the candidate gene and for a housekeeping gene. After amplification the software will calculate expression levels by comparing the samples to the controls and normalizing the values with the comparison of the housekeeping gene samples to the housekeeping gene controls [formula 1].

Table 3: PCR Parameters for qRT-PCR

Setup				
Detection Format			SYBR Green I	
Programs				
Program Name	Cycles		Analysis Mode	
cDNA Synthesis	1		None	
Pre Incubation	1		None	
Amplification	45		Quantification	
Melting Curve	1		Melting Curves	
Cooling	1		None	
Temperature Targets				
Target [°C]	Acquisition Mode	Hold (mm:ss)	Ramp Rate [°C/s]	Acquisitions (per °C)
cDNA synthesis				
55	None	05:00	4.4	-
Preincubation				
95	None	02:00	4.4	-
Amplification				
95	None	00:10	4.4	-
primer dependent	None	00:30	2.2	-
72	Single	00:06	4.4	-
Melting Curve				
95	None	00:05	4.4	-
60	None	01:00	2.2	-
97	Continuous	-	0.11	5
Cooling				
40	None	00:10	1.5	-

Formula 1: Normalization of expression values

$$\text{Normalized Ratio} = \left(\frac{\text{conc. target}}{\text{conc. reference}} \right)_{\text{sample}} : \left(\frac{\text{conc. target}}{\text{conc. reference}} \right)_{\text{calibrator}}$$

20- μ l reaction with 10 ng RNA protocol:

- 10 μ l EXPRESS SYBR GreenER qPCR SuperMix Universal
- 0.4 μ l 10 μ M Primer F (200 nM final)
- 0.4 μ l 10 μ M Primer R (200 nM final)
- 0.5 μ l EXPRESS SuperScript Mix for One-Step SYBR GreenER
- 3.7 μ l RNase free water
- 5 μ l Template RNA (2 ng/ μ l)

3.3 Whole-Transcript Expression Analysis using Affymetrix Rat Gene 1.0 ST Array

The Affymetrix Rat Gene 1.0 ST Array is a single-labeled high-density oligonucleotide expression array offering whole-transcript coverage with the representation of 27,342 well-characterized genes by approximately 26 probes spread across the full length of the gene. RNA from 6 DEB and Wistar rat skins and 3 DEB and Wistar heart samples were processed and hybridized according to the manufacturer's instructions by the Affymetrix platform team of the CCG, Berlin. Data was then processed and analyzed by Dr. Peter Frommolt, CCG, Cologne.

3.4 Ingenuity Pathways Analysis

With Ingenuity Pathways Analysis software expression data from the Affymetrix Rat Gene 1.0 ST Array was further analyzed. The whole set of expression data as well as the expression data of chromosome 19 genes within the candidate region 19:32.986.041..36.535.127 only were downloaded and checked for promising protein networks, pathways and genes. The software integrates data from a variety of experimental platforms and allows an easy search of scientific literature. Dynamic pathway models can be built and complex experimental data can be quickly analyzed to give key insights into relationships, mechanisms, functions, and pathways of relevance.

4 Methods on Protein Level

4.1 Histology

a) Fixation, Paraffin Embedding and Sectioning

Skin samples were punched with a 6 mm punch biopsy and heart was horizontally sliced in the middle. The punches and slices were then put in a cell safe capsule. Each cell safe capsule was placed in a processing cassette and fixation was performed with the tissue processor LEICA ASP200S with a protocol shown in table 4.

Table 4: Fixation protocol

Step	Time	Reagent	Step	Time	Reagent
1	2 hours	Formalin	7	1 hour	100% Ethanol
2	1,5 hours	Formalin	8	1,5 hours	Xylol
3	1,5 hours	70% Ethanol	9	1,5 hours	Xylol
4	1,5 hours	80% Ethanol	10	1,5 hours	Histowax (62°C)
5	1 hour	100% Ethanol	11	1,5 hours	Histowax (62°C)
6	1 hour	100% Ethanol	12	1,5 hours	Histowax (62°C)

After fixation samples were kept in the paraffin station LEICA EG1150H preheated to 65°C until further processing. Skin samples were then halved with a scalpel and put in a stainless steel base mold with the cutting edge on the downside. Heart samples were also put in steel base molds. The processing cassette was put on top and the mold filled with 65°C warm paraffin. The molds were left to cool on a cold plate until the paraffin block could be easily retrieved.

5 µm thin sections were cut with the fully automated rotary microtome LEICA RM2255 and put in a water bath with 37°C from where the sections could be easily transferred to coated slides. The slides were left to dry on a heating plate with 37°C for one hour and then transferred to an incubator with 37°C overnight.

b) Haematoxylin - Eosin (HE) Staining

Haematoxylin is extracted from the bark of the logwood tree and stains cell nuclei blue. As a counterstain Eosin is used, which is a fluorescent red dye staining cytoplasm, collagen, muscle fibers and blood cells.

Place slides in a slide holder and deparaffinize sections in a glass chamber filled with xylol for 15-20 minutes. Wipe off excess xylol on a paper towel and rehydrate sections two times in 100% ethanol, two times in 80% ethanol, two times in 30% ethanol, and two times in deionized water for three minutes each. Then place slides in a glass chamber filled

with haematoxin solution for three to five minutes, rinse with deionized water and develop stain under tap water for 10-15 minutes. Rinse again with deionized water, then incubate slides in eosin G-solution (add 1 drop of acidic acid per 100 ml eosin G-solution) for three minutes and rinse before dehydrating samples by placing the slides in water, two times in 30% ethanol, two times in 80% ethanol, 100% ethanol, and finally in xylol for three minutes each. Mount slides and view under a microscope.

c) Immunohistochemical Staining

Before the actual staining an antigene retrieval step has to be performed due to the formation of methylene bridges during fixation, which cross-link proteins and mask antigenic sites. Therefore Tris-EDTA buffer is brought to the boil in a microwave, Take out of the microwave and incubate deparaffinized and rehydrated sections for one hour. Wash two times in TBST buffer and incubate in blocking solution for two hours. Wipe around the sections with soft tissue paper and apply primary antibody diluted as shown in table 5 in antibody dilution solution. Incubate overnight at 4°C. Wash sections two times in TBST buffer, apply secondary antibody Alexa Fluor Goat anti_mouse 488 (yellow fluorescence, dilution factor 1:400), and incubate for one hour at room temperature. Wash three times in TBST buffer and continue with DAPI staining.

Tris-EDTA buffer (10mM Tris Base, 1mM EDTA Solution, 0,05% Tween 20, pH 9.0):

1.21 g	Tris
0.37 g	EDTA
1000 ml	distilled water
0.5 ml	Tween 20

TBST buffer (20mM Tris.HCl, pH 7.4, 150 mM NaCl, 0.04% Tween 20):

100 ml	Tris.HCl
40 g	NaCl
4900 ml	distilled water
0.9 ml	Tween 20

Blocking solution (10% FCS, 1% BSA):

50 ml	FCS
5 g	BSA
450 ml	PBS

Antibody dilution solution [1% BSA, 0.025% Triton X-100]:

5 g	BSA
500 ml	PBS
125 µl	Triton X-100

Table 5: Dilution factors for primary antibodies

Primary Antibody	Isotype	Dilution Factor
VE-Cadherin/Cadherin 5	IgG1	1:500
E-Cadherin/Cadherin 1	IgG2a	1:5000
M-Cadherin/Cadherin 15	IgG2a	1:250
N-Cadherin/Cadherin 2	IgG1	1:2500
P-Cadherin/Cadherin 3	IgG1	1:250
R-Cadherin/Cadherin 4	IgG1	1:500
Alpha-Catenin	IgG1	1:250
Beta-Catenin	IgG1	1:500
Gamma-Catenin/Plakoglobin/Jup	IgG2a	1:2000
Desmoglein	IgG1	1:1000
P120 Catenin	IgG1	1:1000

d) DAPI Staining

DAPI (4',6-diamidino-2-phenylindole) is used for nuclear and chromosome counterstaining. It is excited at 345 nm and emits blue fluorescence at 458 nm upon binding to AT regions of DNA.

Incubate slides for 3 minutes in DAPI solution (10 µg/ml). Wash thoroughly five times in TBST, mount coverslips and leave overnight at 4-8°C to dry before viewing.

5 Methods for Cell Culture

5.1 Cell Culture Media

All Media must be prepared under a cell culture hood in a sterile environment.

Transportation medium for tissue samples:

10 ml	FCS
2 ml	Fungizone (250 µg/ml)
1 ml	Penicillin/Streptomycin (10.000 IU/ml)
200 µl	Gentamycin (50 mg/ml)
Add. 100 ml	DMEM (without L-Glutamine/Sodium Pyruvate)

Washing solution:

500 ml	PBS
30 ml	Fungizone (250 µg/ml)
20 ml	Penicillin/Streptomycin (10.000 IU/ml)
4 ml	Gentamycin (50 mg/ml)

HEK-Medium for rat fibroblasts:

430 ml	MEM with NEAA (without L-Glutamine/Sodium Pyruvate)
50 ml	FCS
10 ml	Sodium Pyruvate (100 mM)
5 ml	Glutamine (200 mM)
5 ml	Penicillin/Streptomycin (10.000 IU/ml)

KGM-Gold Keratinocyte Growth Medium BulletKit (Lonza):

500 ml	KGM-Gold Basal Medium
+	Bovine Pitutary Extract
+	hEGF
+	Insulin
+	Hydrocortisone
+	GA-1000 (Gentamicin, Amphotericin-B)
+	Epinephrine
+	Transferrin

5.2 Isolation and Culture of Rat Fibroblasts

For all steps sterile working under a cell culture hood is necessary. Use only sterile instruments and consumables.

Take out skin samples of the transportation medium with forceps, place in 50 ml tube filled with 30 ml washing solution, and shake vigorously. Repeat this step two times with fresh washing solution. Then put the skin sample in Betaisodona for 30 seconds and shake vigorously. Wash again three to five times with washing solution until all Betaisodona is washed off. Cut off as much dermis as possible with scissors and place pieces on a culture dish. The rest of the skin will be used for isolation of keratinocytes. Leave dermis pieces to dry for several minutes, so that the samples stick to the dish when medium is added. Carefully add HEK-Medium until the sample pieces are completely covered. Place in an incubator with 37°C, 95% air humidity and 5% CO₂. Medium has to be changed every three to four days.

After several days the fibroblasts will start to grow out of the tissue pieces. As soon as the cells are confluent they can be harvested by taking off all medium and putting on 5 ml Trypsin-EDTA per dish for three minutes. Prod gently, add 5 ml HEK-Medium to stop the trypsinization reaction followed by a centrifugation step with 1.200 rpm for five minutes. Take off all medium and resuspend in 9 ml fresh HEK-Medium. Plate cells in three T225 cell culture bottles and add 50 ml HEK-Medium. Keep the cells in an incubator with 37°C, 95% air humidity and 5% CO₂. Medium has to be changed every three to four days.

When the cells are confluent again take off medium, trypsinize with 10 ml Trypsin-EDTA for 5 minutes, stop reaction with 10 ml HEK-Medium and centrifuge with 1.200 rpm for five minutes. Take off all medium and resuspend two pellets in 3.6 ml FCS with 10% DMSO each. Take six cryoconservation tubes, put 1.2 ml of resuspended cells in each and freeze in a nitrogen tank for later cell culture. The third pellet was stored for RNA-isolation at -20°C.

5.3 Isolation and Culture of Rat Keratinocytes

Place skin with the epidermis on the downside in a new cell culture dish and add 20 ml dispase II (1.5 U/ml). Keep overnight at 4-8°C. The next day the epidermis can be separated from the dermis using forceps. The dermis can be cut in smaller pieces and used for isolation of fibroblasts as described in chapter 5.1. Put the epidermis in 10 ml Trypsin-EDTA and heat for 30 minutes at 37°C in a water bath shaking vigorously with a magnetic stir bar. Stop trypsinization reaction by adding 10 ml Trypsin-Inhibitor (0.5 mg/ml) and filter through a 70 µm cell filter to get rid of debris and undigested particles. Centrifuge cell suspension at 1.400 rpm for 10 minutes. Take off supernatant and resuspend pellet in 9 ml KGM-Gold medium. Put 3 ml of resuspended cells in each T225 cell bottle, add 50 ml KGM-Gold Medium and keep in an incubator with 37°C, 95% air humidity and 5% CO₂. The next day the medium has to be changed. Afterwards medium has to be changed every second day.

Once the cells are confluent up to 60% they need to be trypsinized using 10 ml Trypsin-EDTA for 8 to 10 minutes. Stop reaction with same amount of trypsin inhibitor and centrifuge at 1.400 rpm for 10 minutes. Take off supernatant and resuspend two of the three pellets in 3.6 ml Keratinocyte Freezing Medium each. Store in nitrogen tank for later cell culture. The third pellet was stored at -20°C for RNA isolation.

D Results – Rat Samples

1. Short Summary of the study design and the obtained results

For reasons of clarity and better interpretation of the results a short summary of the study design and the obtained results will be given at this point. Results are demonstrated in detail within the next chapters and partially in the Appendix.

Former results of a whole genome scan linkage analysis in 320 F2 females with 176 microsatellite markers pointed to a highly significant locus on chromosome 19 with a non parametric lod score of 20. This analysis was conducted by the dermatogenetic group at the CCG, Cologne. In a first step, saturation mapping was performed in this study with 13 more microsatellite markers. Haplotype analysis of the affected and non-affected F2 animals led to a candidate region of about 3.5 Mb. Most genes within that region were exon-sequenced but no mutation as a potential cause for the disease could be identified. In a next step the whole candidate region was therefore sequenced again by next generation sequencing but as before, no immediate mutation could be detected as a potential cause for the disease.

In another approach to find candidate genes expression analysis was performed using the Affymetrix Rat Gene 1.0ST Array. Highest fold changes were obtained for keratin genes and other genes involved in skin, hair, and nail structure as well as several immunologically relevant genes. Functional analysis and Network Explorer analysis as tools of the Ingenuity Pathway Analysis revealed an indication for the importance of cadherins for the expression data obtained from genes within the candidate region. Therefore expression levels of some candidate genes, including keratins, cadherins, desmogleins, and catenins were validated and refined by quantitative real time PCR. In addition immunohistological stainings were made for proteins involved in adherens junctions and desmosomes showing abnormalities for the catenin plakoglobin.

2 Saturation mapping of Chromosome 19 with Microsatellites

Former results of a whole genome scan linkage analysis in 320 F2 females with 176 microsatellite markers pointed to a highly significant locus on chromosome 19 with a non parametric lod score of 20. This analysis was conducted by the dermatogenetic group at the CCG, Cologne. In a first step, saturation mapping was performed in this study with 13 more microsatellite markers followed by haplotype analysis on 129 affected and 128 unaffected F2 females. The criteria for selection of the candidate region flanking markers were arbitrarily set assuming that markers in the candidate interval have the highest frequency of DEBR alleles in affected animals as compared to unaffecteds.

In affected animals flanking markers were therefore set where at least two animals are heterozygous for the DEBR and the PVG allele framing a region of homozygous DEBR alleles. The results of the 6 most informative haplotypes are given in table 6 for the affected F2 animals showing animal 127 homozygous with the DEBR allele beginning with marker D19Rat33. Since no other of the affected F2 animals showed homozygosity with the DEBR allele at this marker and also not for the next two markers, these were not accepted as flanking markers for the candidate region. Marker D19Rat46 is the first upstream marker that is homozygous for the DEBR allele in more than one affected F2 animal and therefore marker D19Rat118 is accepted as the upstream flanking marker of the candidate region. The same method resulted in the downstream flanking marker RM24C19N53 framing a 3,5 Mb large region [19:32986041..36535127] where all but one of the 129 affected F2 animals are homozygous for the DEBR allele.

In unaffected animals flanking markers were set where at least two animals are homozygous for the DEBR allele framing a region of heterozygosity. Therefore marker D19Rat91 was accepted as the upstream and RM22C19N47 as the downstream flanking marker. The results of the 6 most informative haplotypes are given in table 7 for the unaffected F2 animals. These results support the underlying hypothesis of higher DEBR allele frequency within the candidate region in affected animals since there are no unaffected animals found homozygous for the DEBR allele within the candidate region.

In the next step exons of candidate genes from this defined region were sequenced to look for possible mutations that might cause alopecia areata.

Table 6: Positions of microsatellite markers and their allele sizes for the 6 most informative haplotypes of affected F2 animals. Blue = DEBR allele, green = PVG allele, x = missing data.

Position	Marker	affected F2 animals											
		5		49		127		100		124		57	
55447056	D19Rat60	7	7	6	7	6	7	6	6	6	6	6	6
47444682	D19Rat7	149	149	137	149	137	149	137	137	137	137	137	137
46282836	D19Rat70	169	169	163	169	163	169	x	x	x	x	163	163
45668882	D19Rat88	221	221	205	221	205	221	205	205	205	205	205	205
45090802	D19Mit7	107	107	99	107	99	107	99	99	99	99	99	99
45001545	D19Rat66	14	14	8	14	8	14	8	8	8	8	8	8
44186608	D19Rat90	227	227	196	227	196	227	196	196	196	196	196	196
42862032	D19Rat9	9	9	7	9	7	9	7	7	7	7	7	7
40725526	D19Rat117	201	201	197	201	197	201	197	197	197	197	197	197
40062222	D19Rat35	8	8	17	8	17	8	17	17	17	17	17	17
39448152	D19Arb2	349	349	357	349	357	349	357	357	357	357	357	357
38910730	D19Rat72	151	143	x	x	151	143	151	151	x	x	x	x
38295381	D19Rat24	165	172	165	172	165	172	165	165	165	165	x	x
37769951	D19Rat91	80	89	80	89	80	89	80	80	80	80	x	x
37324190	D19Rat33	204	224	204	224	204	204	204	204	204	204	x	x
36614365	D19Rat22	128	132	128	132	128	128	128	128	x	x	128	128
36535127	D19Rat118	242	238	242	238	x	x	242	242	242	242	242	242
36472017	D19Rat46	7	18	7	7	7	7	7	7	7	7	7	7
36405081	D19Rat23	173	170	173	173	173	173	173	173	173	173	173	173
34910174	D19Rat53	x	x	116	116	116	116	116	124	116	116	116	116
34781500	RM20C19N6	x	x	227	227	227	227	227	229	227	227	227	227
32986041	RM24C19N53	261	261	261	261	261	261	261	257	261	257	261	257
32795927	RM22C19N47	309	309	309	309	309	309	309	311	309	311	309	311
32388800	RM22C19N8	207	207	207	207	207	207	207	203	207	203	207	203
31926069	RM25C19N3	236	236	236	236	236	236	236	222	236	222	236	222
29575651	D19Rat30	16	16	16	16	16	16	16	7	16	7	16	7
29207613	D19Rat110	8	8	8	8	8	8	8	11	11	11	8	11
27497109	D19Rat12a	7	7	7	7	7	7	7	8	8	8	7	8
2265038	D19Rat34	6	6	6	6	6	6	x	x	7	7	7	7
15426254	D19Rat15	6	6	6	6	6	6	6	12	12	12	12	12
11311216	D19Rat81	8	8	8	8	8	8	8	11	11	11	11	11
7316493	D19Rat98	109	109	109	109	109	109	x	x	111	111	111	111

Table 7: Positions of microsatellite markers and their allele sizes for the 6 most informative haplotypes of not affected F2 animals. Blue = DEBR allele, green = PVG allele, x = missing data.

Position	Marker	not affected F2 animals											
		248		619		256		580		574		601	
55447056	D19Rat60	6	6	6	6	6	6	6	7	6	7	6	7
47444682	D19Rat7	137	137	137	137	137	137	137	149	137	149	x	x
46282836	D19Rat70	163	163	163	163	163	163	163	169	163	169	x	x
45668882	D19Rat88	205	205	205	205	205	205	205	221	205	221	205	221
45090802	D19Mit7	99	99	99	99	99	99	99	107	99	107	99	107
45001545	D19Rat66	8	8	8	8	8	8	8	14	8	14	8	14
44186608	D19Rat90	196	196	196	196	196	196	x	x	x	x	x	x
42862032	D19Rat9	7	7	7	7	7	7	7	9	7	9	7	9
40725526	D19Rat117	197	197	197	197	197	197	197	201	197	201	197	201
40062222	D19Rat35	17	17	17	17	17	17	17	8	17	8	17	8
39448152	D19Arb2	357	357	357	357	357	357	357	349	357	349	357	349
38910730	D19Rat72	151	151	151	151	151	151	x	x	x	x	x	x
38295381	D19Rat24	165	165	165	165	165	172	165	172	165	172	165	172
37769951	D19Rat91	80	80	80	80	80	89	80	89	80	89	80	89
37324190	D19Rat33	204	224	204	224	204	224	x	x	x	x	x	x
36614365	D19Rat22	128	132	128	132	128	132	x	x	x	x	128	132
36535127	D19Rat118	242	238	242	238	242	238	242	238	242	238	242	238
36472017	D19Rat46	7	18	x	x	7	18	7	18	7	18	7	18
36405081	D19Rat23	173	170	173	170	173	170	173	170	x	x	173	170
34910174	D19Rat53	116	124	116	124	116	124	116	124	116	124	116	124
34781500	RM20C19N6	x	x	227	229	227	229	227	229	227	229	227	229
32986041	RM24C19N53	261	257	261	257	261	257	261	257	261	257	261	261
32795927	RM22C19N47	x	x	309	311	x	x	309	311	309	309	309	309
32388800	RM22C19N8	207	203	207	203	207	203	207	207	207	207	207	207
31926069	RM25C19N3	236	222	236	222	236	222	236	236	236	236	236	236
29575651	D19Rat30	16	7	16	7	16	7	16	16	16	16	16	16
29207613	D19Rat110	8	11	8	11	8	11	8	8	8	8	8	8
27497109	D19Rat12a	7	8	7	8	7	8	7	7	16	16	7	7
2265038	D19Rat34	6	7	6	7	6	7	6	6	16	16	6	6
15426254	D19Rat15	6	12	6	12	6	12	6	6	6	6	6	6
11311216	D19Rat81	8	11	8	11	8	11	8	8	8	8	8	8
7316493	D19Rat98	111	111	109	111	109	111	109	109	109	109	109	109

3 Exon Sequencing of Candidate Genes

After saturation mapping of chromosome 19 a candidate region of 3.5 Mb in size was detected between markers D19Rat118 and RM24C19N53. In the next step exons of candidate genes within this region were sequenced and screened for mutations.

Following genes have been exon sequenced (in alphabetical order): Acd, Agrp, Atp6v0d1, Cdh1, Cdh3, Cenpt, Ctcf, Ctrl, Ddx28, Dpep2, Dpep3, Dus2l, Edc4, Fam65a, Gfod2, Hsd11b2, Kctd19, Lcat, Lin10, Lypla3, Nfatc3, Nol3, Ntf2, Pard6a, Prmt7, Pskh1, Psmb10, Ranbp10, Rbm35b, RGD1307357, RGD1561415, Slc7a6, Slc7a6os, Slc9a5, Slc12a4, Smpd3, Thap11, Tradd, Tsnaix1 and Zfp90. All variations found are given in table 8. A mutation as a potential cause for hair loss in alopecia areata could not be identified since all found amino acid changes can also be detected in other species without an association to hair loss and intronic variations could not be ascribed to known splice sites.

Therefore the region was sequenced in toto by genomic sequencing in the next step.

Table 8: Variations found by sanger sequencing

Gene	Variation f	Position	Gene	Variation	Position
Acd	g.2503A>C	Intron	Kctd19	g.10G>A	Gly4Ser
Agp	g.258delG	Intron	Kctd19	g.15587G>A	Exon 3
Agp	g.252T>G	Intron	Kctd19	g.1721T>C	Intron
Agp	g.251_252insT	Intron	Kctd19	g.18853C>G	Ser282Cys
Agp	g.859_860insG	3'UTR	Kctd19	g.20330A>G	Met402Val
Atp6vOd1	g.37476T>C	Intron	Kctd19	25797A>G	Intron
Atp6vOd1	g.43805T>C	3'UTR	Lcat	g.851_852insCG	Intron
RGD1307357	g.1621C>G	Ala125Gly	Lcat	g.1351delT	Intron
RGD1307357	g.1782_1786del CGTGT	Intron	Lin10	g.15172G>A	Intron
RGD1307357	g.4037T>C	Intron	Lypla3	g.4627T>A	Intron
RGD1307357	g.4159T>C	Tyr317His	Nol3	g.902C>A	3'UTR
RGD1307357	g.4280T>C	3'UTR	Nol3	g.782_811del	Glu193_Pro202del
Cdh3	g.20354G>T	Intron	Ntf2	g.16841T>C	Intron
Cdh3	g.23205G>A	3'UTR	Pard6a	g.837T>C	Intron
Cenpt	g.4285G>A	Val290Met	Pard6a	g.1560T>A	Leu311His
Cenpt	g.4343A>G	Intron	Pard6a	g.1840T>C	3'UTR
Cenpt	g.4409G>C	Intron	Pskh1	g.12459T>C	Exon 2
Cenpt	g.6153C>T	Intron	Pskh1	g.31521A>G	Exon 3
Ctcf	g.718T>A	Exon 1	Psmb10	g.85C>T	5'UTR
Ctcf	g.19452A>G	3'UTR	Psmb10	g.1145T>C	Intron
Ddx28	g.442A>G	Ile148Val	Psmb10	g.2283C>T	Intron
Dpep2	g.9T>C	5'UTR	Ranbp10	g.48822A>G	Intron
Dpep2	g.97G>T	Intron	Ranbp10	g.57607_57608insTC CTTCCT	3'UTR
Dpep2	g.99_102delTGGG	Intron	Slc9a5	g.78878A>G	Intron
Dpep2	g.2902G>A	Exon 7	Slc9a5	g.15760T>C	Exon 16
Dpep2	g.6176T>C	Exon 11	Slc9a5	g.18439C>G	Exon 17
Dpep3	g.1986C>A	Intron	Slc12a4	g.18675G>A	Exon 18
Dpep3	g.5659G>A	Intron	Slc12a4	g.21384A>G	3'UTR
Edc4	g.3616T>C	Exon 2	Slc12a4	g.21745G>A	3'UTR
Edc4	g.7244T>C	Exon 13	Thap11	g.559_560insACAACA	Gln114_Gln115insGlnGln
Edc4	g.9947T>C	Exon 23	Thap11	g.82778G>A	3'UTR
Edc4	g.10289A>G	Exon 24	Tsnaxip1	g.13269C>T	Intron
Fam65a	g.4496A>G	Intron	Tsnaxip1	g.13792A>C	Intron
Fam65a	g.4554C>T	Intron	Tsnaxip1	g.14640T>C	Intron
Fam65a	g.5213C>G	Intron	Tsnaxip1	g.15332C>T	Intron
Fam65a	g.5362T>C	Cys906Arg	Tsnaxip1	g.15881G>C	Intron
Hsd11b2	g.4668A>T	Thr388Ser	Tsnaxip1	g.16912G>C	Val536Ile

4 Next Generation Sequencing of the Candidate Region

Exon sequencing of most of the genes within the defined candidate region did not lead to any mutations that might cause alopecia. Therefore the whole candidate region was sequenced again by next generation sequencing (NGS).

The candidate region (19:32986041..36535127) was sequenced by NGS in one BDIX, one PVG, and one Wistar rat as control sequences as well as in one unaffected DEB rat (DEB722), one histologically affected DEB rat (DEB807), and one severely affected DEB rat (DEB806). Target enrichment was accomplished in combination with Roche NimbleGen hybridization System 4 which resulted in 70.1% sequence capture of the target region. In total, 117 variations with a coverage of at least 30 were found that were specific for the affected DEB806 rat and not found in any of the other samples and not in the official reference sequence rn4. No non-synonymous coding variation specific for DEB806 only could be detected. 337 variations with a coverage of at least 30 are specific for the histologically affected DEB807 and 91 variations with a coverage of at least 30, including one non-synonymous variation in the pseudogene RGD1562390 (Pro764Thr), are specific for DEB806 and DEB807 together. Detailed results are given in table 9.

Table 9: Variations found by NGS analysis specific for affected DEB806 only, histologically affected DEB807 only, and DEB806 in common with DEB807 only. First number states all variations found, second number states all variations found with a coverage of at least 30.

Variation Type	Specific for DEB 806	Specific for DEB 807	Specific for DEB806 and DEB807
Intergenic	230/87	534/304	75/73
Intronic	47/29	57/32	20/16
Non-synonymous coding	0/0	0/0	1/1
Synonymous coding	1/1	0/0	0/0
UTR	2/0	1/1	1/1
Total	280/117	592/337	97/91

In addition, NGS data was compared to the findings of the Sanger sequencing data. Some variations found by Sanger sequencing could not be verified in the NGS analysis (marked with an x in table 10). All other detected variations could also be found in other samples than the affected DEB806 (table 10). A mutation as a potential cause for hair loss in alopecia areata could still not be identified.

Table 10: Comparison of variations found by sanger sequencing with NGS data

Gene	Ensembl ID	Variation	Position	NGS-Data: variation found in
Acd	ENSRNOG00000038973	g.2503A>C	Intron	BDIX, DEB722, DEB806, DEB807
Agrp	ENSRNOG00000039001	g.258delG	Intron	x
Agrp	ENSRNOG00000039001	g.252T>G	Intron	DEB807
Agrp	ENSRNOG00000039001	g.251_252insT	Intron	DEB807
Agrp	ENSRNOG00000039001	g.859_860insG	3'UTR	x
Atp6vOd1	ENSRNOG00000017235	g.37476T>C	Intron	BDIX, DEB722, DEB806, DEB807
Atp6vOd1	ENSRNOG00000017235	g.43805T>C	3'UTR	BDIX, DEB806, DEB807
RGD1307357	ENSRNOG00000024364	g.1621C>G	Ala125Gly	x
RGD1307357	ENSRNOG00000024364	g.1782_1786delCG TGT	Intron	x
RGD1307357	ENSRNOG00000024364	g.4037T>C	Intron	x
RGD1307357	ENSRNOG00000024364	g.4159T>C	Tyr317His	x
RGD1307357	ENSRNOG00000024364	g.4280T>C	3'UTR	x
Cdh3	ENSRNOG00000020129	g.20354G>T	Intron	DEB722, PVG
Cdh3	ENSRNOG00000020129	g.23205G>A	3'UTR	x
Cenpt	ENSRNOG00000024178	g.4285G>A	Val290Met	BDIX, DEB722, DEB806, DEB807
Cenpt	ENSRNOG00000024178	g.4343A>G	Intron	BDIX, DEB722, DEB806, DEB807
Cenpt	ENSRNOG00000024178	g.4409G>C	Intron	BDIX, DEB722, DEB806, DEB807
Cenpt	ENSRNOG00000024178	g.6153C>T	Intron	BDIX, DEB722, DEB806, DEB807
Ctcf	ENSRNOG00000017674	g.718T>A	Exon 1	BDIX, DEB722, DEB806, DEB807
Ctcf	ENSRNOG00000017674	g.19452A>G	3'UTR	BDIX, DEB722, DEB806, DEB807
Ddx28	ENSRNOG00000019817	g.442A>G	Ile148Val	BDIX, DEB722, DEB806, DEB807
Dpep2	ENSRNOG00000023303	g.9T>C	5'UTR	x
Dpep2	ENSRNOG00000023303	g.97G>T	Intron	DEB806, DEB807
Dpep2	ENSRNOG00000023303	g.99_102delTGGG	Intron	x
Dpep2	ENSRNOG00000023303	g.2902G>A	Exon 7	BDIX, DEB722, DEB806, DEB807
Dpep2	ENSRNOG00000023303	g.6176T>C	Exon 11	BDIX, DEB722, DEB806, DEB807
Dpep3	ENSRNOG00000019757	g.1986C>A	Intron	BDIX, DEB722, DEB806, DEB807
Dpep3	ENSRNOG00000019757	g.5659G>A	Intron	x
Edc4	ENSRNOG00000024025	g.3616T>C	Exon 2	x
Edc4	ENSRNOG00000024025	g.7244T>C	Exon 13	x
Edc4	ENSRNOG00000024025	g.9947T>C	Exon 23	x
Edc4	ENSRNOG00000024025	g.10289A>G	Exon 24	x
Fam65a	ENSRNOG00000017604	g.4496A>G	Intron	x
Fam65a	ENSRNOG00000017604	g.4554C>T	Intron	x
Fam65a	ENSRNOG00000017604	g.5213C>G	Intron	x
Fam65a	ENSRNOG00000017604	g.5362T>C	Cys906Arg	x
Hsd11b2	ENSRNOG00000017084	g.4668A>T	Thr388Ser	BDIX, DEB722, DEB806, DEB807
Kctd19	ENSRNOG00000016760	g.10G>A	Gly4Ser	BDIX, DEB722, DEB806, DEB807
Kctd19	ENSRNOG00000016760	g.15587G>A	Exon 3	BDIX, DEB722, DEB806, DEB807
Kctd19	ENSRNOG00000016760	g.1721T>C	Intron	BDIX, DEB722, DEB806, DEB807
Kctd19	ENSRNOG00000016760	g.18853C>G	Ser282Cys	BDIX, DEB722, DEB806, DEB807
Kctd19	ENSRNOG00000016760	g.20330A>G	Met402Val	BDIX, DEB722, DEB806, DEB807
Kctd19	ENSRNOG00000016760	25797A>G	Intron	BDIX, DEB722, DEB806, DEB807

Gene	Ensembl ID	Variation	Position	NGS-Data: variation found in
Lcat	ENSRNOG000000019573	g.851_852insCG	Intron	x
Lcat	ENSRNOG000000019573	g.1351delT	Intron	x
Lin10	ENSRNOG000000014668	g.15172G>A	Intron	x
Lypla3	ENSRNOG000000019859	g.4627T>A	Intron	x
Nol3	ENSRNOG000000015588	g.902C>A	3'UTR	BDIX, DEB722, DEB806, DEB807
Nol3	ENSRNOG000000015588	g.782_811del	Glu193_Pro202del	x
Ntf2	ENSRNOG000000018945	g.16841T>C	Intron	x
Pard6a	ENSRNOG000000017746	g.837T>C	Intron	x
Pard6a	ENSRNOG000000017746	g.1560T>A	Leu311His	x
Pard6a	ENSRNOG000000017746	g.1840T>C	3'UTR	x
Pskh1	ENSRNOG000000019290	g.12459T>C	Exon 2	BDIX, DEB722, DEB806, DEB807
Pskh1	ENSRNOG000000019290	g.31521A>G	Exon 3	BDIX, DEB722, DEB806, DEB807
Psemb10	ENSRNOG000000019494	g.85C>T	5'UTR	BDIX, DEB722, DEB806, DEB807
Psemb10	ENSRNOG000000019494	g.1145T>C	Intron	BDIX, DEB722, DEB806, DEB807
Psemb10	ENSRNOG000000019494	g.2283C>T	Intron	BDIX, DEB722, DEB806, DEB807
Ranbp10	ENSRNOG000000018000	g.48822A>G	Intron	BDIX, DEB722, DEB806, DEB807
Ranbp10	ENSRNOG000000018000	g.57607_57608insTCCTTCCT	3'UTR	x
Slc9a5	ENSRNOG000000028844	g.78878A>G	Intron	BDIX, DEB722, DEB806, DEB807
Slc9a5	ENSRNOG000000028844	g.15760T>C	Exon 16	BDIX, DEB722, DEB806, DEB807
Slc9a5	ENSRNOG000000028844	g.18439C>G	Exon 17	BDIX, DEB722, DEB806, DEB807
Slc12a4	ENSRNOG000000019657	g.18675G>A	Exon 18	x
Slc12a4	ENSRNOG000000019657	g.21384A>G	3'UTR	x
Slc12a4	ENSRNOG000000019657	g.21745G>A	3'UTR	x
Thap11	ENSRNOG000000000257	g.559_560insACAA CA	Gln114_Gln115ins sGlnGln	x
Thap11	ENSRNOG000000000257	g.82778G>A	3'UTR	x
Tsnaxip1	ENSRNOG000000018954	g.13269C>T	Intron	x
Tsnaxip1	ENSRNOG000000018954	g.13792A>C	Intron	x
Tsnaxip1	ENSRNOG000000018954	g.14640T>C	Intron	x
Tsnaxip1	ENSRNOG000000018954	g.15332C>T	Intron	x
Tsnaxip1	ENSRNOG000000018954	g.15881G>C	Intron	x
Tsnaxip1	ENSRNOG000000018954	g.16912G>C	Val536Ile	x

5 Expression Analyzes

5.1 Affymetrix Rat Gene 1.0 ST Array

In addition to the direct search of candidate genes by genetic analyzes another approach was directed through the analysis of expression data. Therefore expression analysis was performed using the Affymetrix Rat Gene 1.0ST Arrays for 6 skin and 3 heart samples from affected DEBR rats as well as from Wistar rats as controls.

The 50 most upregulated genes in skin expression have fold changes ranging between 1,3055 and 1,6866 [see table 11 in the appendix]. 10 of the 50 genes are key components in skin, hair, and nail structure including 3 keratin genes under the top 4 upregulated genes. 21 of the 50 genes are involved in immunological pathways.

The 50 most downregulated genes in skin expression have fold changes ranging between 0,5822 and 0,7606, including 6 genes (5 casein genes and Lalba) involved in milk production [see table 12 in the appendix].

Skin expression data of the candidate region Chr19:32.986.041..36.535.127, which includes 72 genes, resulted in fold changes ranging between 0.9274 at the lowest and 1.1515 at the highest [see table 13 in the Appendix].

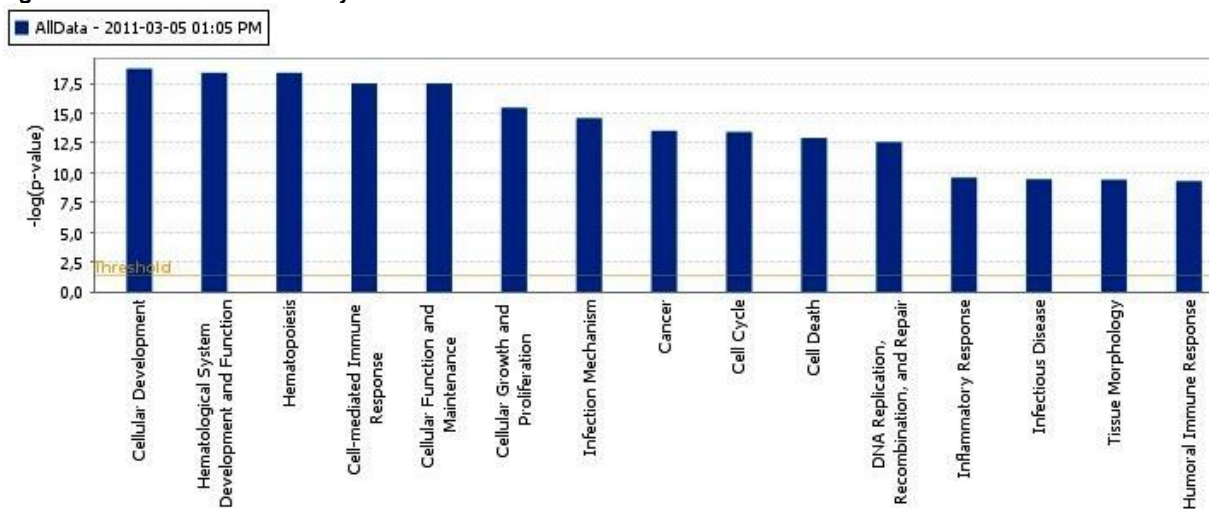
The 50 most up- and downregulated genes in heart expression have fold changes ranging between 1.2244 and 1.4408 for the upregulated genes and between 0.6622 and 0.8528 for the downregulated genes respectively. 13 of the 50 most upregulated genes are involved in immunological pathways [see table 14 in the Appendix].

Heart expression data of the candidate region resulted in fold changes ranging between 0.9160 at the lowest and 1.1527 at the highest [see table 15 in the Appendix].

5.2 Ingenuity Pathways Analysis (IPA)

Functional analysis of the whole expression data set with IPA revealed significant associations to biological functions like cellular development (p-value $1,90E-19$ - $2,21E-04$, including 1071 genes), hematological system development and function (p-value $4,19E-19$ - $2,39E-04$, including 1032 genes), and hematopoiesis (p-value $4,19E-19$ - $1,31E-04$, including 553 genes) amongst others (figure 14). The p-values are calculated using the right-tailed Fisher Exact Test, considering for a given function the number of functional analysis molecules that participate in that function and the total number of molecules that are known to be associated with that function in the Ingenuity Knowledge Database.

Figure 14: IPA functional analysis of the whole data set.

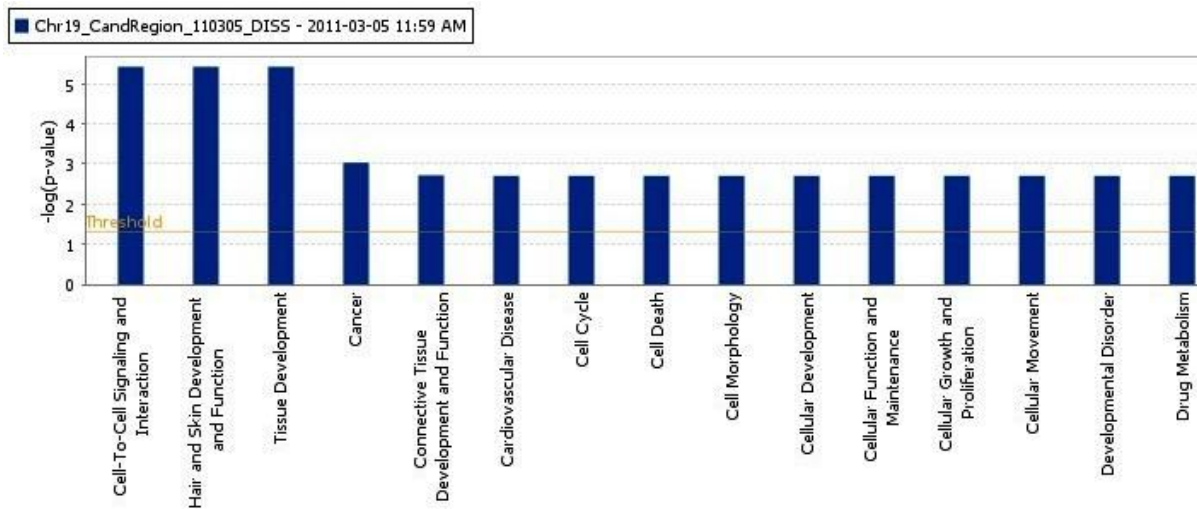


© 2000-2011 Ingenuity Systems, Inc. All rights reserved.

Functional analysis of the expression data set from the candidate region on chromosome 19 with IPA revealed significant associations to biological functions like cell-to-cell signaling and interaction (p-value $3,78E-06$ - $3,71E-02$, 5 genes), hair and skin development and function (p-value $3,78E-06$ - $3,14E-02$, 3 genes), and tissue development (p-value $3,78E-06$ - $4,10E-02$, 4 genes) amongst others (figure 15).

In addition to the functional analysis of the expression data set from the candidate region the IPA tool Network Explorer was used to visualize molecular relationships (figure 16). Molecules colored in red indicate an upregulation of expression values, grey colored molecules did not show any significant up- or downregulation, and white colored molecules were not included in the uploaded data set but were added from the Ingenuity Knowledge Base to specifically connect two or more smaller networks by merging them into a larger one.

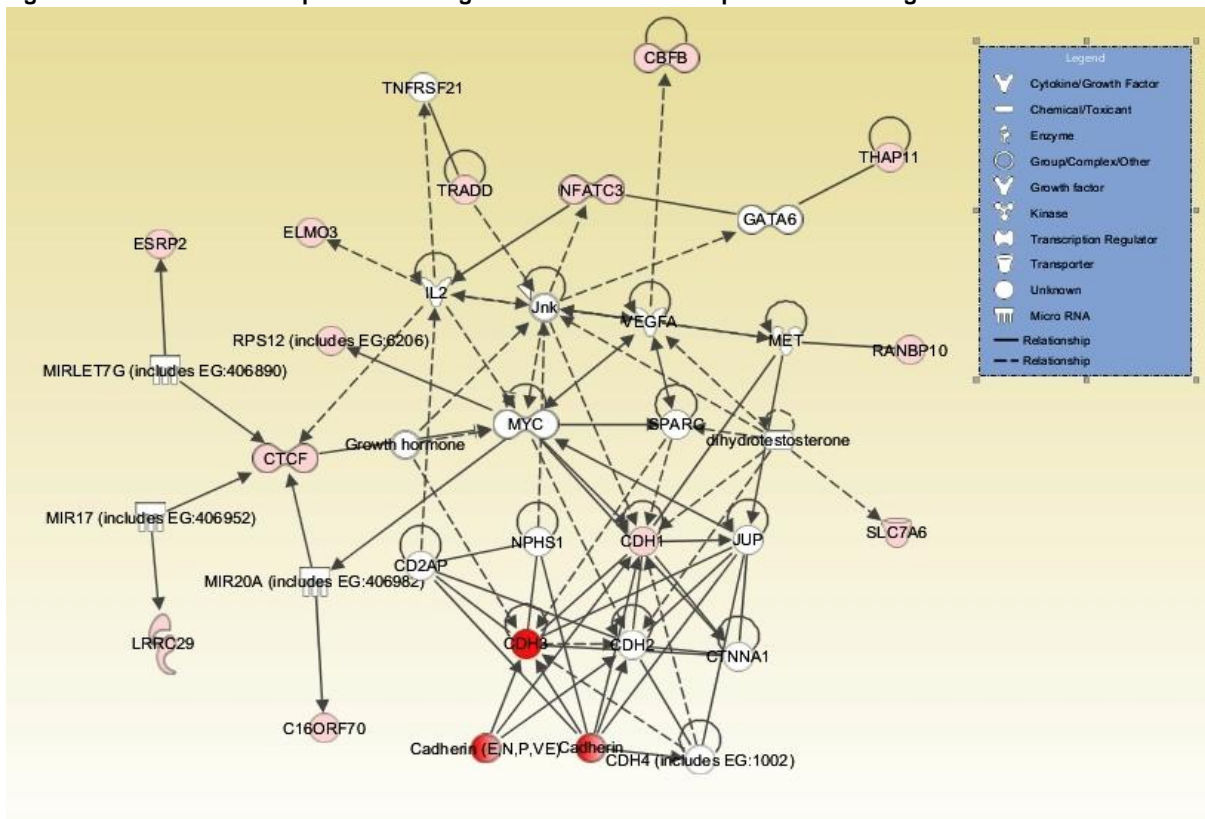
Figure 15: IPA bio functions for candidate region data set.



© 2000-2011 Ingenuity Systems, Inc. All rights reserved.

Figure 16 shows a significant network including 35 genes with the associated functions of cell-to-cell signaling and interaction (p-value 6,57E-09 – 6,98E-03, 15 genes), connective tissue development and function (p-value 6,57E-09 – 2,25E-02, 11 genes), and tissue development (p-value 6,57E-09 – 6,98E-03, 15 genes). In this network, especially cadherin genes seem to be of importance.

Figure 16: IPA network explorer showing molecular relationships of candidate genes.



© 2000-2011 Ingenuity Systems, Inc. All rights reserved.

5.3 Quantitative Real Time – PCR (qRT-PCR)

The expression of the 4 keratin genes Krt25, 26, 27, and 73 found most upregulated in the chip based expression analysis as well as selective cadherins, catenins and desmogleins were validated and refined by qRT-PCR using the LightCycler 480 System (Roche). For each analysis RNA from 6 affected DEBs as well as 6 Wistar or 6 BD IX rats respectively as controls were used. Expressions were normalized with 6 housekeeping genes (Actin beta, Tbp, Ywhaz, Rps18, Mrp2, and Prdx2).

The left hand side of figure 17 shows the mean skin expression value for keratin 27 in each sample. There are big differences in the expression levels of keratin 27 between the 6 samples with the lowest fold change of about 185 in sample DEB800 and the highest fold change of about 660 in sample DEB811. The average keratin 27 expression in the 6 samples is shown on the right hand side in figure 17 with a fold change of approximately 411. Therefore keratin 27 is significantly upregulated in the DEB sample set.

Figure 17: Keratin 27 expression in 6 DEBR skins in comparison to 6 Wistar skins

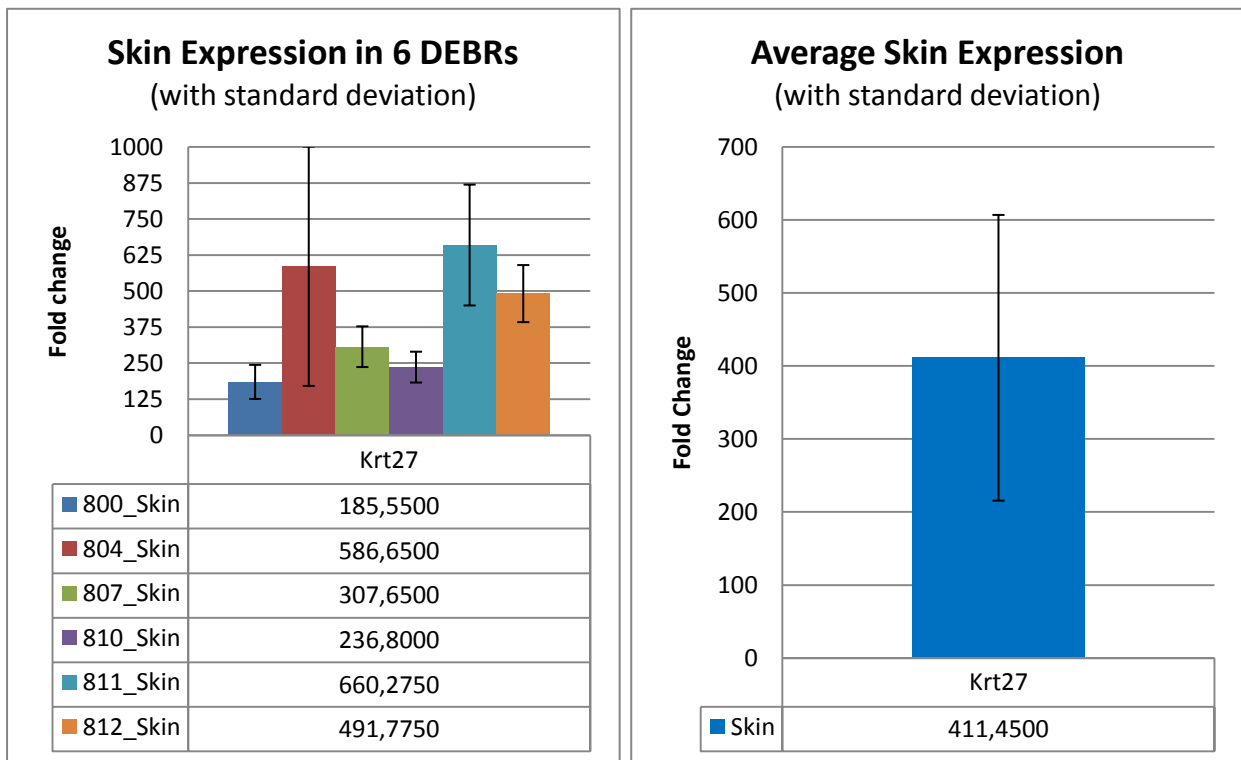


Figure 18 shows skin expression values for keratins 25, 26, and 73. Fold changes for keratin 25 vary between 47 in DEB810 and 204 in DEB811. Fold changes of keratin 26 vary between 9 in DEB810 and 80 in DEB804. Fold changes of keratin 73 vary between 25 in DEB810 and 114 in DEB811. The average fold change in keratin 25 is 118, in

keratin 26 it is 31, and in keratin 73 it is 68. All three keratins are therefore upregulated in the DEB sample set.

Figure 18: Keratin expressions in 6 DEBR skins in comparison to 6 Wistar skins

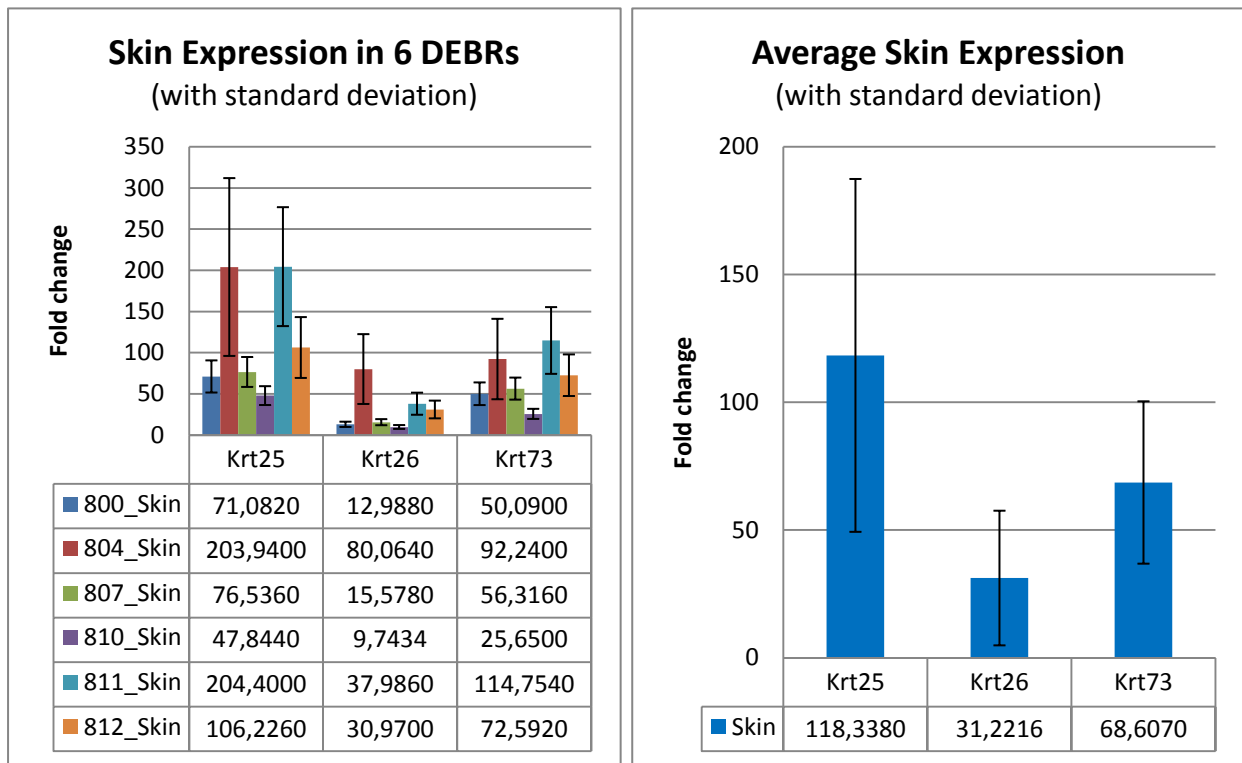


Figure 19 shows skin expression values for the genes catenin alpha 1 [Ctnna1], catenin beta 1 [Ctnnb1], catenin delta 1 [Ctnnd1], catenin gamma [Jup], desmoglein 1 beta [Dsg1b], desmoglein 2 [Dsg2], desmoglein 3 [Dsg3], cadherin 1 [Cdh1], cadherin 2 [Cdh2], cadherin 3 [Cdh3], cadherin 4 [Cdh4], and cadherin 15 [Cdh15]. Expression in all catenins, Dsg3, and all cadherins except Cdh15 is not significantly altered. Dsg1b shows a slight decrease of expression in 4 of the samples with fold changes ranging between 0,54 in DEB806 and 0,77 in DEB809. DEB835 doesn't show any altered expression in comparison to the control samples whereas DEB807 shows an overexpression in Dsg1b with a fold change of 7.34. All samples, except for DEB807, show an underexpression in Dsg2 with fold changes ranging between 0.16 in DEB810 and 0.50 in DEB809. Sample DEB807 is normally expressed with a fold change of 1.14. All samples, except for DEB810, show an underexpression in Cdh15 with fold changes ranging between 0.21 in DEB809 and 0.64 in DEB807. Sample DEB810 is slightly overexpressed with a fold change of 2.69.

Figure 19: Candidate gene expressions in 6 DEBR skins in comparison to 6 BDIX skins

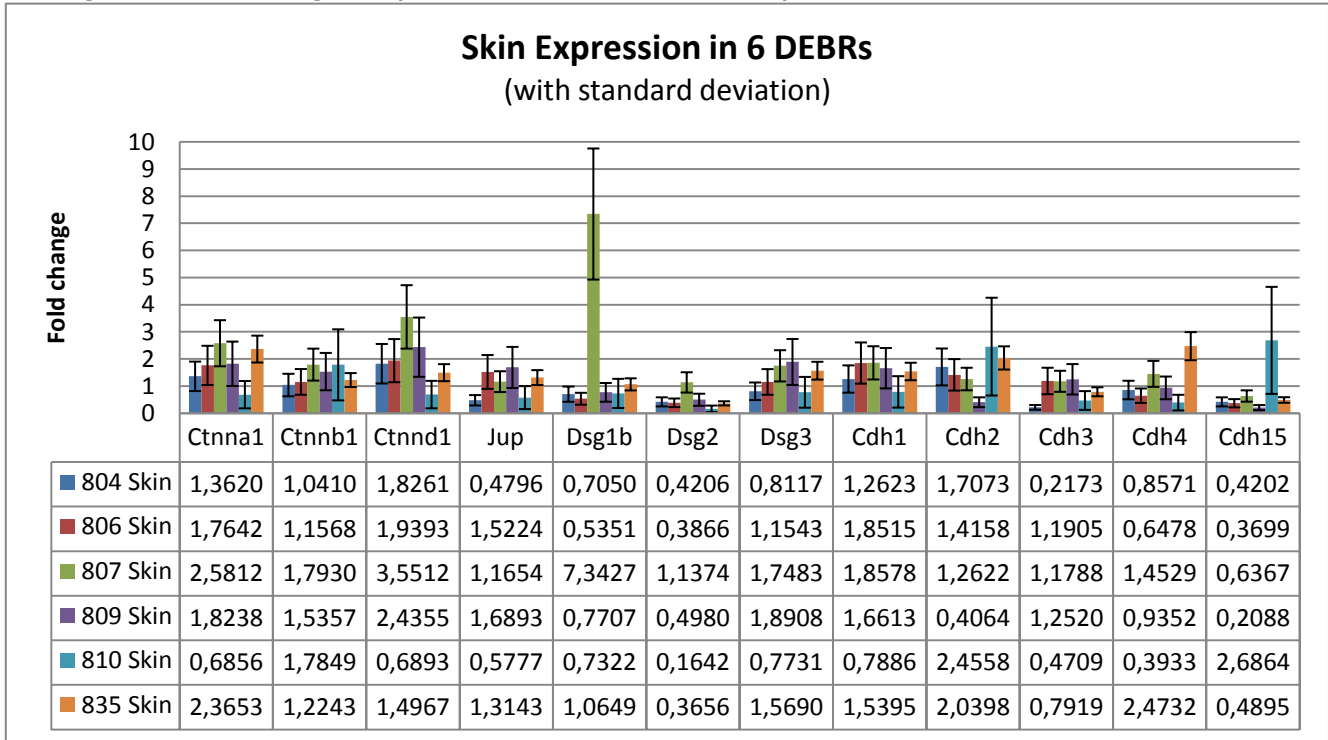


Figure 20 shows the expression values for Desmoglein 4 (Dsg4) in skin samples. Individual expression is very different between the samples with fold changes ranging between 0.75 in DEB810 and 33 in DEB809. Therefore the average fold change of Dsg4 in the skin samples is 13.05, pointing to a general overexpression.

Figure 20: Dsg4 expression in 6 DEBR skins in comparison to 6 BDIX skins

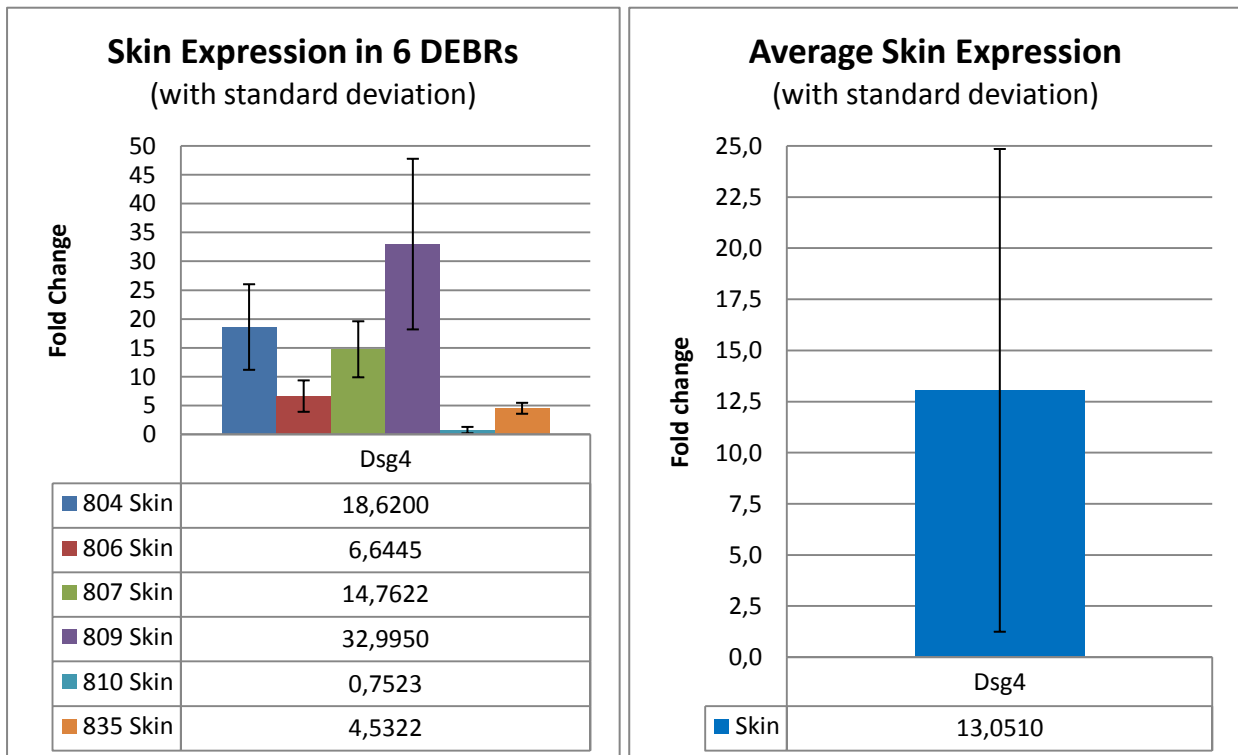
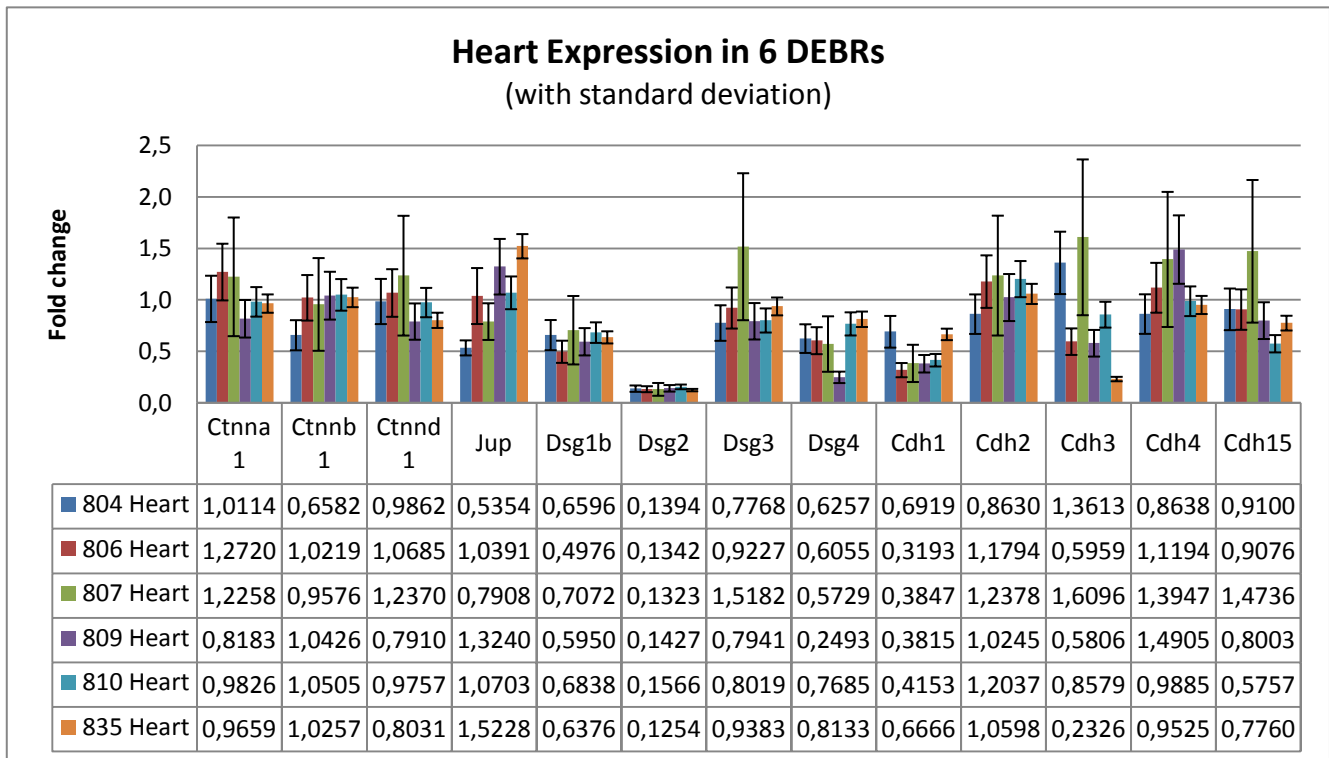


Figure 21 shows heart expression values for the same genes as in figure 19 plus Desmoglein 4 [Dsg4]. The expression value variation between individuals in heart samples is a lot lower than in skin samples. Expression in all catenins, Dsg3, and all cadherins except

Figure 21: Candidate gene expressions in 6 DEBR hearts in comparison to 6 BDIX hearts

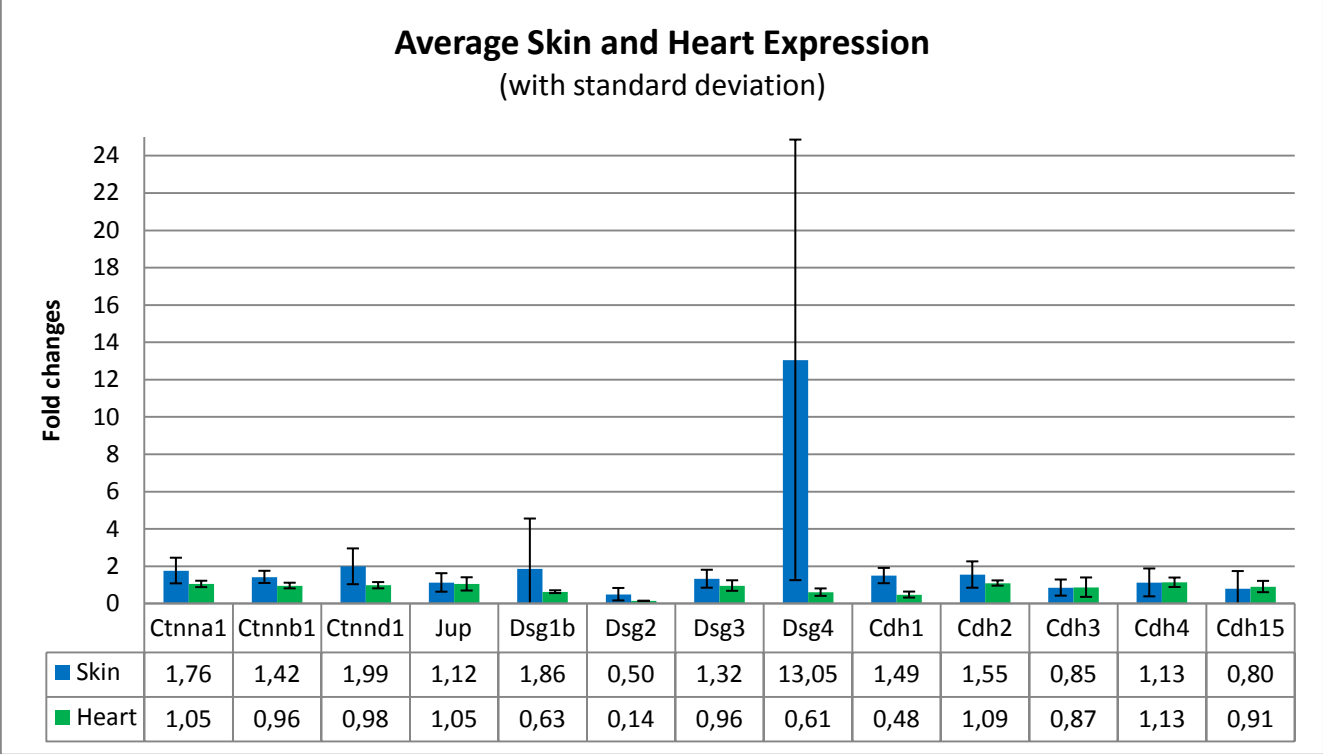


Cdh1 is not altered. Downregulation can be seen in Dsg1b with the fold changes ranging between 0.50 in DEB806 and 0.71 in DEB807, in Dsg2 with the fold changes ranging between 0.13 in DEB835 and 0.16 in DEB810, and in Cdh1 with fold changes ranging between 0.32 in DEB806 and 0.69 in DEB804. Dsg 4 is downregulated in sample DEB809 with a fold change of 0.25. In all other samples it is slightly downregulated with fold changes ranging between 0.57 in DEB807 and 0.81 in DEB835.

Figure 22 shows a comparison of the average gene expression values in the skin and heart samples for all analyzed genes. In all catenin genes expression is a little higher in skin samples compared to heart samples. The average Dsg1b skin expression is higher than in the heart samples because of the very high overexpression in sample DEB807 (see figure 19). Without this sample the average fold change would be about 0.7 and therefore be very close to that in heart with an average fold change of 0.63 pointing to a slight downregulation of the gene in both tissues. Dsg 2 is significantly downregulated in both tissues with an average fold change of 0.14 in heart and 0.5 in skin samples. Dsg3 is normally expressed in both tissues whereas Dsg4 is upregulated in skin samples but

slightly downregulated in heart samples. Cadherin 1 expression is downregulated in heart samples, but not in skin samples. There are no expression changes in cadherin 2 and cadherin 4 compared to the control samples. Cadherins 3 and 15 are slightly downregulated in both skin and heart samples.

Figure 22: Average candidate gene expressions in 6 DEBR skins and hearts in comparison to BDIX



5.4 Comparison of qRT-PCR data with Affymetrix RatGeneChip data

In qRT-PCR analysis Wistar and BDIX samples respectively were used as controls whereas in the chip based analysis Wistar RNA was used as controls.

Figure 23 shows the average fold change values for keratin genes 25, 26, 73, and 27 generated by qRT-PCR using the LightCycler480 (LC480) system from Roche and the RatGeneChip microarray (GeneChip) from Affymetrix in the skin samples. The expression values generated with qRT-PCR show a strong overexpression of all genes. In comparison the expression values of the GeneChip show just a slight overexpression for all genes.

Figure 23: Comparison of expression values generated by qRT-PCR and by RatGeneChip microarray

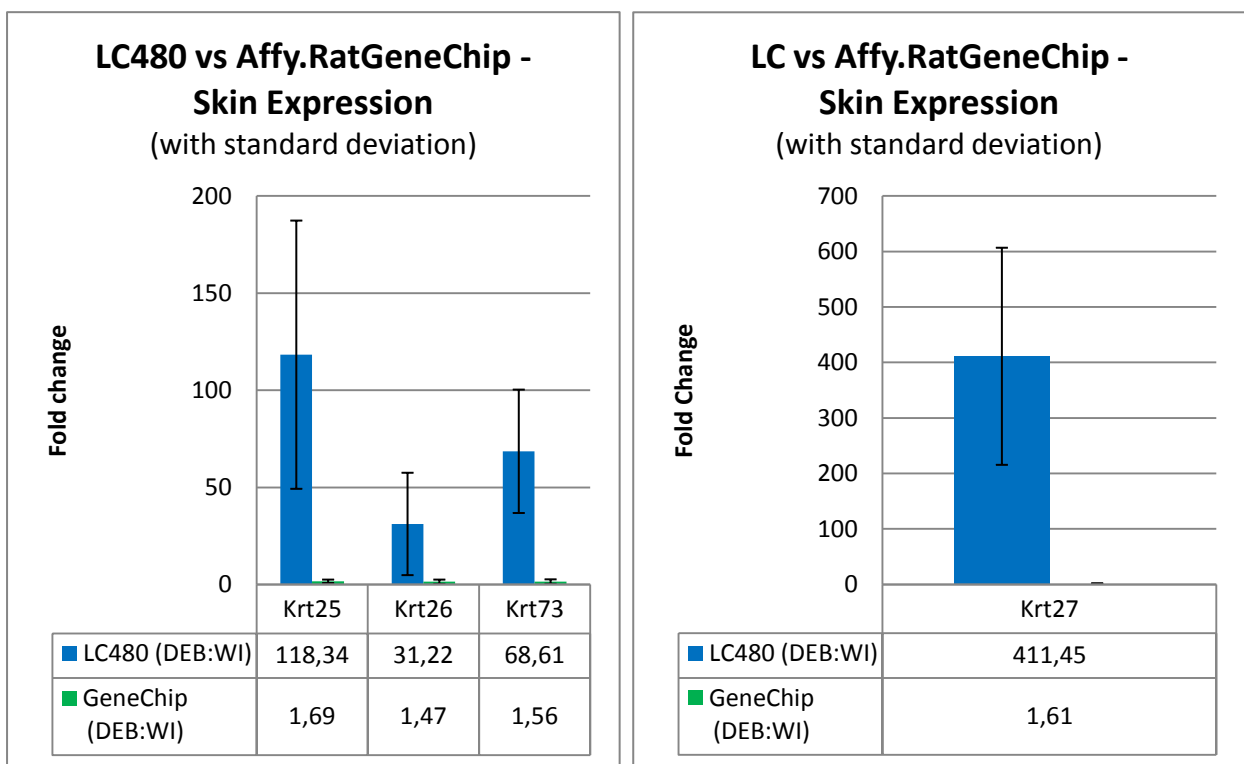


Figure 24 and 25 show the average fold change values for desmoglein genes 1b, 2, 3, and 4 as well as cadherin genes 1, 2, 3, and 15 generated by qRT-PCR using the LightCycler480 (LC480) system from Roche and the RatGeneChip microarray (GeneChip) from Affymetrix in the skin samples. The expression values generated with the RatGeneChip don't show any expression changes except for a slight upregulation in Dsg4 with a fold change of 1.32. In comparison the expression values generated by qRT-PCR show a significant upregulation in Dsg4, a slight upregulation in Dsg1b, a slight downregulation in cadherins 3 and 15, and a stronger downregulation in Dsg2. All other genes are commonly expressed.

Figure 24: Comparison of expression values generated by qRT-PCR and expression chips

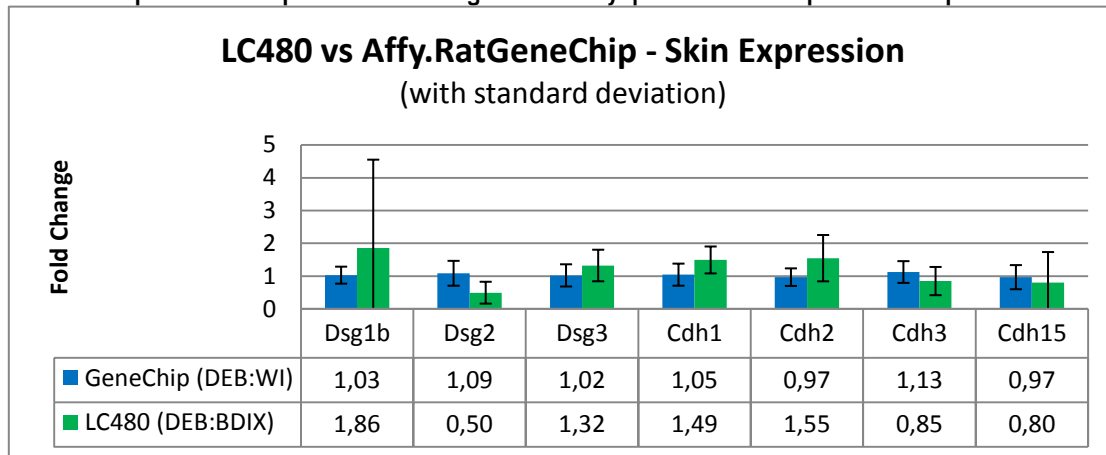


Figure 25: Comparison of expression values generated by qRT-PCR and expression chips

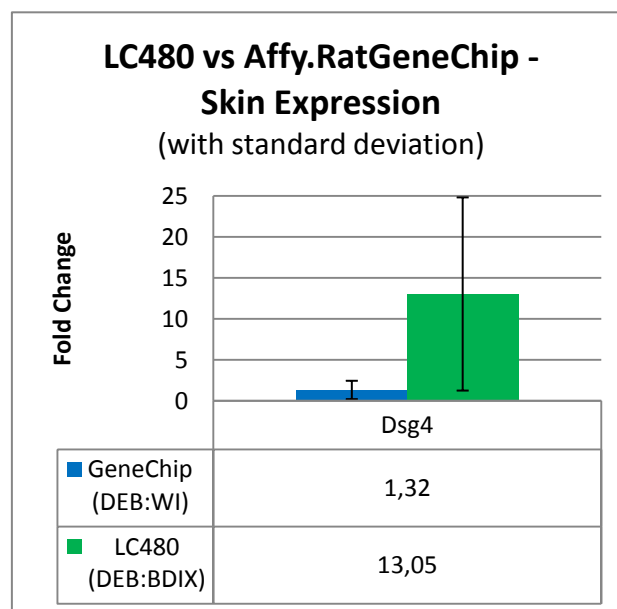


Figure 26 shows the average fold change values for catenin genes a1, b1, d1, and Jup generated by qRT-PCR using the LightCycler480 (LC480) system from Roche and the RatGeneChip microarray (GeneChip) from Affymetrix in the skin samples. The expression values generated with qRT-PCR show a slight overexpression in Ctnna1 and Ctnnd1,. All other genes show normal expression. In comparison the expression values of the GeneChip show normal fold changes in all genes.

Figure 27 shows the average fold change values for catenin genes a1, b1, d1, and Jup, as well as for desmogleins 1b, 2, 3, and 4, and cadherins 1, 2, 3, and 15 generated by qRT-PCR using the LightCycler480 (LC480) system from Roche and the RatGeneChip microarray (GeneChip) from Affymetrix in the heart samples. The expression values generated with the GeneChip show normal fold changes in all genes. In qRT-PCR analysis

the expression of Dsg2 and Cdh1 is downregulated. Genes Dsg1b and Dsg 4 are slightly downregulated. All other genes show normal expression.

Figure 26: Comparison of expression values generated by qRT-PCR and expression chips

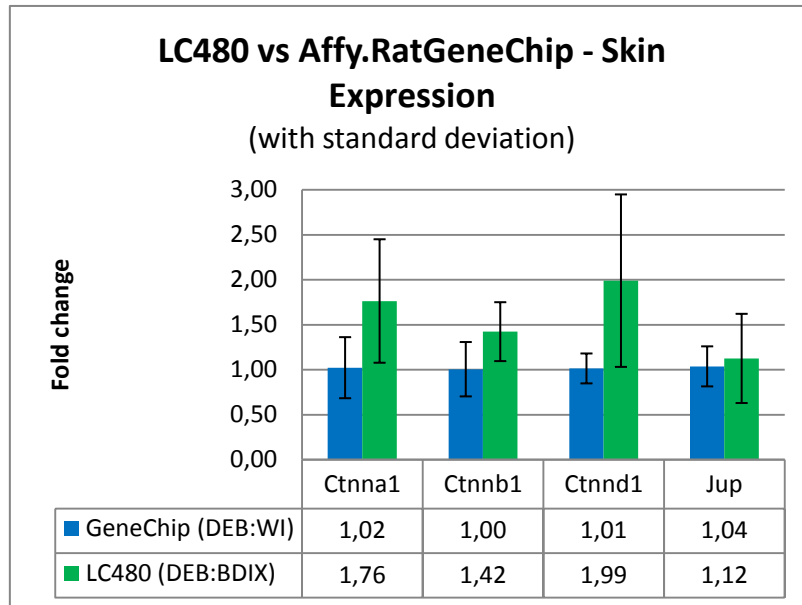
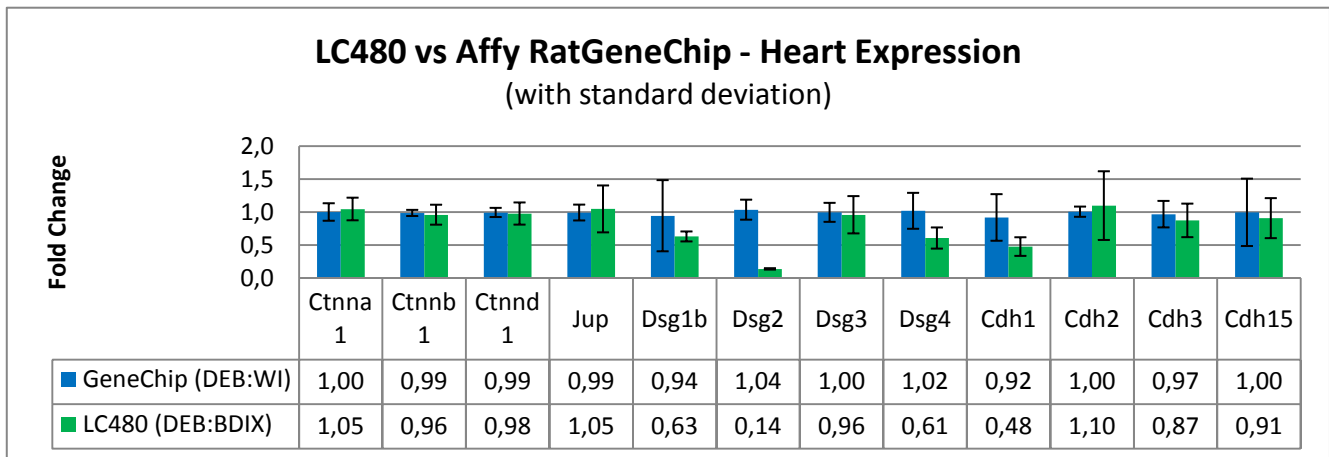


Figure 27: Comparison of expression values generated by qRT-PCR and expression chips



6 Histology

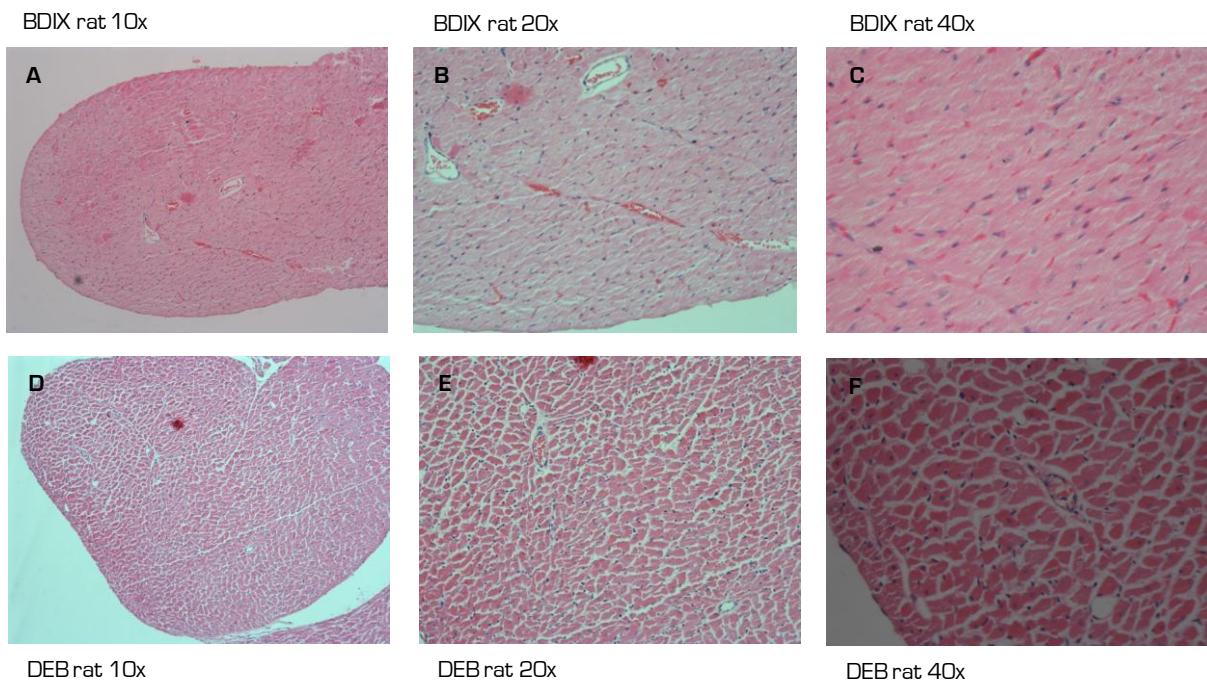
6.1 HE - Staining

From all rats skin sections were made and HE-stained to check for signs of inflammation and the structure and ratio of anagen, catagen, and telogen hairs to confirm the diagnosis of alopecia areata.

In addition to skin heart sections were HE-stained for some rats. Figure 28 shows in the top row (figure 28 A-C) HE-stained heart sections showing the papillary muscle of BDIX rats which are used as controls. The bottom row (figure 28 D-F) shows the same magnifications in heart sections from DEB rats with severe hair loss. Large gaps can be seen between the cells in the DEBR heart that are not present in the BDIX heart.

Figure 28 HE staining of the papillary muscle in rat heart sections.

A-C) wildtype heart sections from a BDIX rat D-F) heart sections from a DEB rat with severe hair loss
A+D) 10x magnification B+E) 20x magnification C+F) 40x magnification.

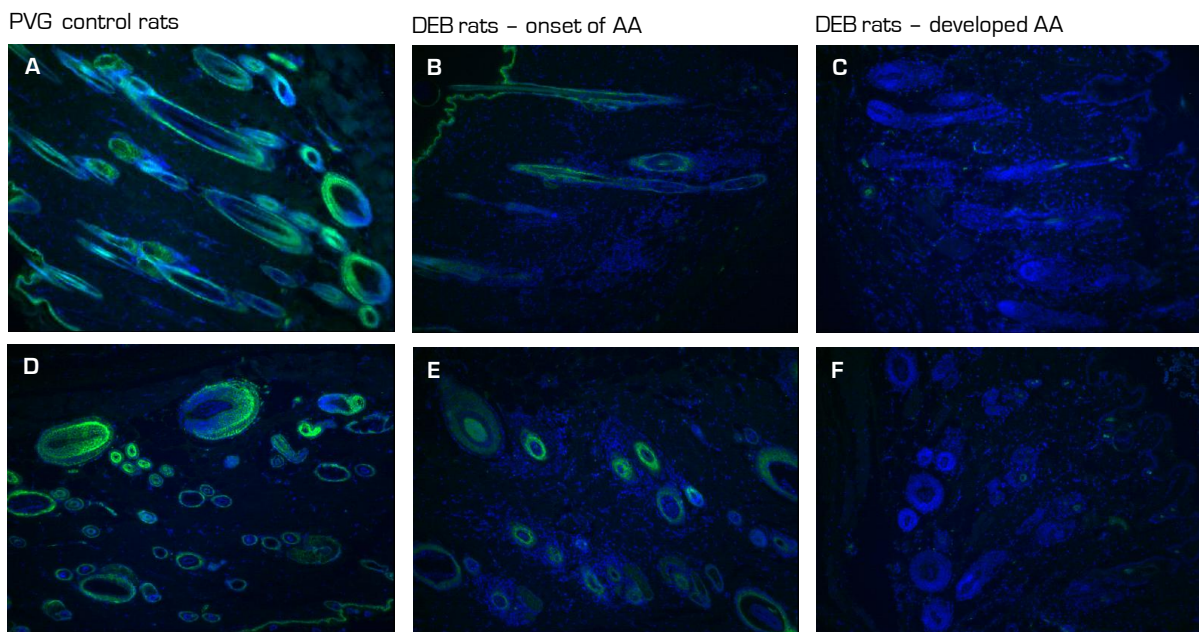


6.2 Immunohistochemical Staining

Since the Network Explorer analysis with the Ingenuity Pathways Analysis software pointed to an important role of cadherins in the data set the Zonula Adherens Sampler Kit was bought allowing immunohistochemical (IHC) stainings of cadherins 1, 2, 3, 4, 5, 15, catenins alpha, beta, gamma (also known as plakoglobin), p120, and desmoglein 1. No differences could be observed in the DEB rat skins and hearts in comparison to the PVG rat control skins and hearts in all IHC stainings but catenin gamma. As is shown in figure 29 the hair follicles as well as the epidermis show a strong staining of catenin gamma (figure 29 A+D) in PVG wildtype skins. The fluorescence intensity decreases slightly with the onset of AA in DEB rat skin (figure 29 B+E) and is no longer detectable at all in skin sections from DEB rats with developed AA.

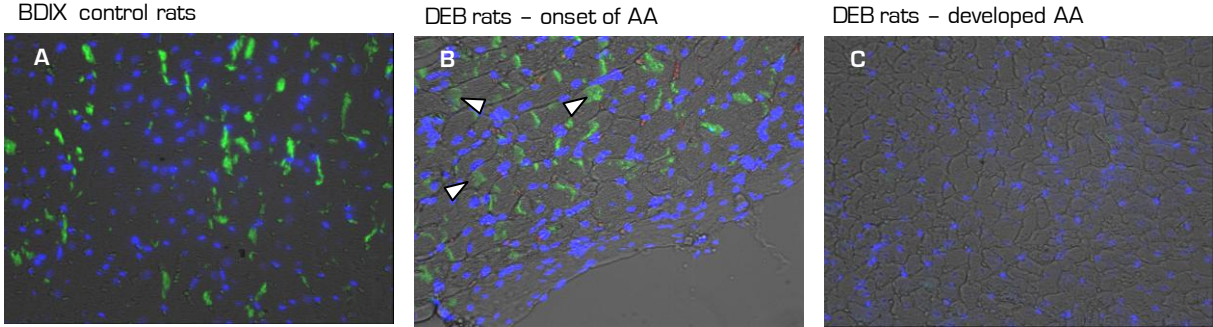
Figure 29: IHC staining of catenin gamma (yellow) and DAPI (blue) in rat skin.

10x magnification A-C) vertical sections D-F) horizontal sections A+D) wildtype skin sections from a PVG rat B+E) skin sections of a DEB rat with beginning hair loss C+D) skin sections of a DEB rat with severe hair loss



The same phenomenon can be seen in heart sections (figure 30). In addition, strong catenin gamma staining in heart sections of BDIX rats with 40x magnification show that catenin gamma is concentrated in a dense line between two adjoining cells. This is also observed in DEB rats with an onset of AA but additionally some cells show diffuse localization of catenin gamma within the cell. These cells then do not show a defined line of catenin gamma between two adjoining cells (figure 30 A, B). In case of developed AA catenin gamma can no longer be detected (figure 30 C).

Figure 30: IHC staining of catenin gamma (yellow) and DAPI (blue) in rat heart. 40x magnification
White arrows in B show diffuse localization of catenin gamma within cells that have lost the focused localization between two adjoining cells.



E Results – Human Samples

1. Short Summary of the study design and the obtained results

For reasons of clarity and better interpretation of the results a short summary of the study design and the obtained results will be given at this point. Results are demonstrated in detail within the next chapters and partially in the Appendix.

Former results of a whole genome scan linkage analysis with 253.487 SNP markers of the Affymetrix GeneChip Human Mapping 500K Array in 112 families, including 411 individuals, pointed to a significant locus on chromosome 19 with a non parametric lod score of 5 for a peak at 42.4 Mb (Build 36.3) and 4 for a second peak at 40.7 Mb (Build 36.3). This analysis was conducted by the dermatogenetic group at the CCG, Cologne. In a first step, fine mapping with SNP markers was performed in this study using SNPstream, Taqman, and Pyrosequencing. Association analysis of the data did not lead to significant results. Linkage Analysis, however, resulted in significant non parametric lod scores of 4.7 for a peak at 42.1 Mb (Build 36.3) and 3.7 for a second peak at 41.9 Mb (Build 36.3). Nearest genes to the SNPs with the highest lod scores were the zinc finger genes 567 as well as 568. These genes were therefore screened for mutations using high resolution melting curve analysis together with sequencing but all variations found are known as SNPs.

In addition, more samples were collected and genotyped using the Affymetrix Genome-Wide Human SNP Array 6.0. This allowed for case control (CaCo) analysis with 357 cases, transmission disequilibrium test (TDT) with 259 families and family based linkage (FAM) analysis with 259 families, including 855 individuals. Associations could be detected for two regions each on chromosome 5 and 6 (including the HLA region) as well as a region on chromosome 16 in a dominant model of CaCo. P-values obtained in the TDT analysis did not exceed the significance threshold. FAM analysis revealed significant regions on chromosomes 10 and 19 with non parametric lod scores as high as 4 and 6 respectively.

Finally, immunohistological stainings were made for proteins involved in adherens junctions and desmosomes showing abnormalities for the catenin plakoglobin, cadherin 3 and 15.

2 Fine mapping of the Candidate Region on Chromosome 19

A former linkage analysis with 112 families, including 411 individuals, that was performed at the CCG (dermatogenetics group) pointed to a significant region on chromosome 19. This region, which includes 60 genes and is about 10.6 Mb in size, was therefore fine mapped in this study using SNPstream analysis. Some SNPs that failed were genotyped again with either Taqman analysis or Pyrosequencing. Table 16 shows the analyzed SNPs and their genomic location (GRCH37) on chromosome 19.

Table 16: Genotyped SNPs and their genomic positions on chromosome 19.

SNP	Position (GRCH37)	SNP	Position (GRCH37)	SNP	Position (GRCH37)
rs11672876	30.231.605	rs2301617	36.041.707	rs472226	37.458.213
rs583121	34.718.558	rs17776451	36.043.949	rs475026	37.458.517
rs2290652	35.174.708	rs2733743	36.050.469	rs17639910	37.466.629
rs12110	35.660.008	rs2285421	36.168.414	rs1667354	37.481.651
rs541169	35.718.520	rs231233	36.270.639	rs7246473	37.533.839
rs12975589	35.839.230	rs437168	36.333.919	rs8102196	37.581.704
rs8107905	35.921.197	rs2285424	36.498.673	rs1533736	37.654.476
rs409093	35.940.748	rs1008328	36.594.936	rs11084878	37.667.969
rs926026	35.966.924	rs3108186	37.184.470	rs12459637	37.689.498
rs11880530	35.968.644	rs1830031	37.202.749	rs320890	37.703.600
rs8102875	35.969.289	rs826986	37.237.210	rs172786	37.712.484
rs8113518	35.976.659	rs1673082	37.240.641	rs2460950	37.752.739
rs6510490	35.976.809	rs1227820	37.257.017	rs1530500	37.823.311
rs7976	35.977.799	rs2245366	37.263.834	rs3745765	37.853.735
rs17638216	35.977.958	rs8107274	37.284.893	rs10422527	37.893.968
rs2293690	35.978.077	rs11670106	37.296.831	rs12461941	37.984.150
rs10407971	35.978.964	rs1148399	37.328.805	rs8109103	37.993.611
rs11880364	35.988.294	rs1144540	37.330.113	rs12977460	38.023.771
rs2293693	35.989.472	rs1035441	37.353.291	rs1038084	38.030.182
rs4254439	35.997.862	rs10403306	37.374.779	rs10500277	38.056.902
rs7245699	35.998.991	rs543518	37.385.711	rs4803277	38.072.427
rs7254211	36.003.221	rs7250197	37.388.970	rs17245425	38.074.094
rs4806163	36.003.606	rs16971772	37.394.406	rs2927743	38.131.834
rs1108552	36.011.495	rs547483	37.440.865	rs35153242	38.151.242
rs2106446	36.011.584	rs496730	37.450.939	rs2909109	38.168.855
rs17705633	36.015.152	rs569371	37.453.497	rs17246792	38.183.762
rs12151182	36.023.232	rs474017	37.453.619	rs241941	38.307.516
rs17705657	36.024.242	rs565721	37.455.331	rs1469698	38.993.056
rs11882238	36.030.898	rs7251087	37.455.403	rs8103362	39.759.691
rs2239945	36.032.960	rs519551	37.455.448	rs759120	40.357.183
rs7599	36.037.890	rs7254717	37.456.902	rs744389	40.904.102

2.1 Association Analyzes (CaCo; TDT)

Case control (CaCo) genetic association analysis was conducted with the software PLINK. 760 individuals were included with 407 cases and 353 controls. 131 individuals were male and 629 individuals were female. The data set was checked for mendelian errors and unlikely genotypes prior to case control analysis. Therefore a total of 51 genotypes were deleted. Table 17 (see Appendix) shows the calculated p – values for each SNP in a dominant and a recessive model of the case control study. The significance threshold is not reached by any SNP in either model. Figures 31 and 32 show the results as a scatter plot.

Figure 31: Scatter plot for case control analysis with a recessive model using PLINK.
Positions in Build36.3

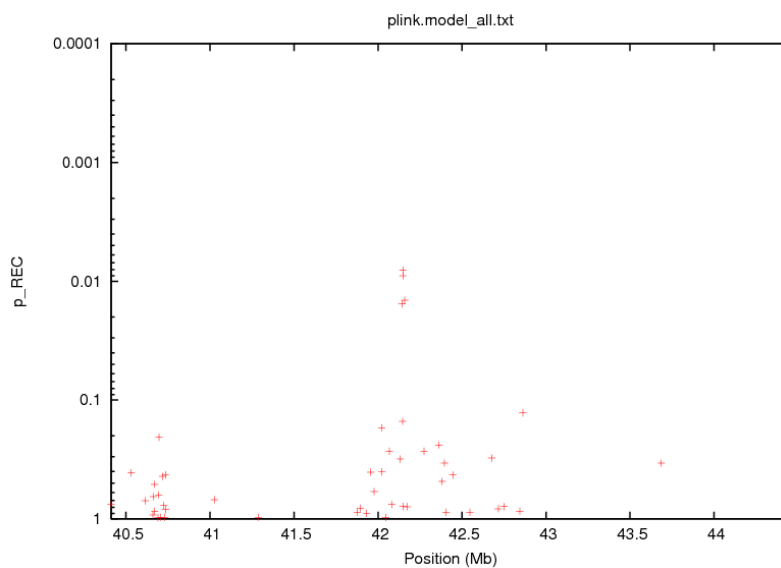
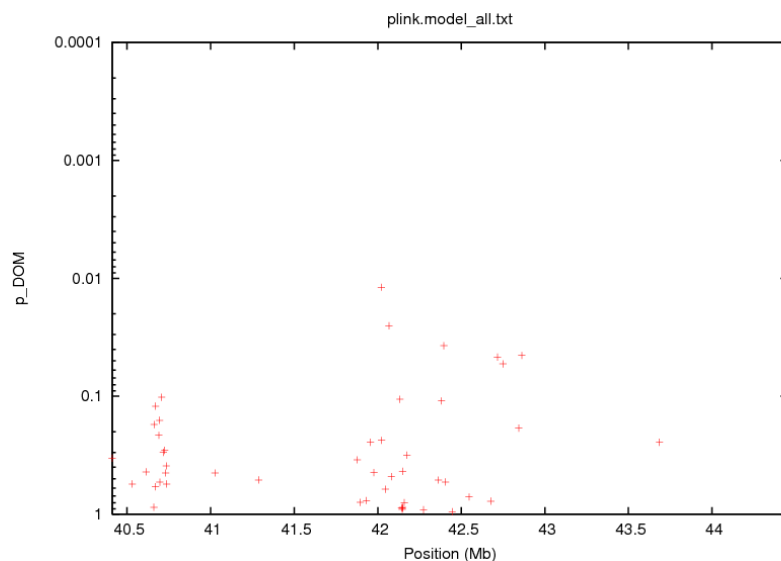


Figure 32: Scatter plot for case control analysis with a dominant model using PLINK.
Positions in Build36.3



Transmission Disequilibrium Test (TDT) analysis was performed with the software PLINK. 199 families were included. The data set was checked for mendelian errors and unlikely genotypes prior to TDT analysis. Therefore a total of 89 genotypes were deleted. Table 18 (see Appendix) shows the calculated p – values for each SNP of which neither one reached significance.

2.2 Linkage Analyzes (ASP; FAM)

An Affected Sib Pair (ASP) linkage analysis was performed with the software MERLIN for 77 families including 320 individuals. The data set was checked for mendelian errors and unlikely genotypes prior to linkage analysis. Therefore a total of 130 genotypes were deleted. Table 19 (see Appendix) shows the calculated npLOD and HLOD values for each SNP.

Figures 33 and 34 show the results graphically in a plot. There are two separate regions with SNPs that exceed the significance threshold of 2.6. The first region is defined by SNPs rs3108186 and rs1830031 with the highest HLOD score for SNP rs1830031 of 2.886 and the highest npLOD score of 3.240. This first region includes the gene ZNF567 only. The second region is defined by SNPs rs10403306 and rs2460950 with the highest HLOD score for SNP rs496730 of 2.971 and the highest npLOD score of 3.510. This second region includes 9 genes. 6 of them are zinc finger proteins with ZNF568 lying closest to the SNP with the highest LOD scores.

Figure 33: Plot of $-\log(p\text{-value})$ in a parametric ASP linkage analysis using MERLIN.

Positions in Build36.3. Disease allele with frequency of 0.01. Penetrances are 0.00, 0.8, 0.8 for wildtype homozygotes, heterozygote carriers and risk allele homozygotes, respectively

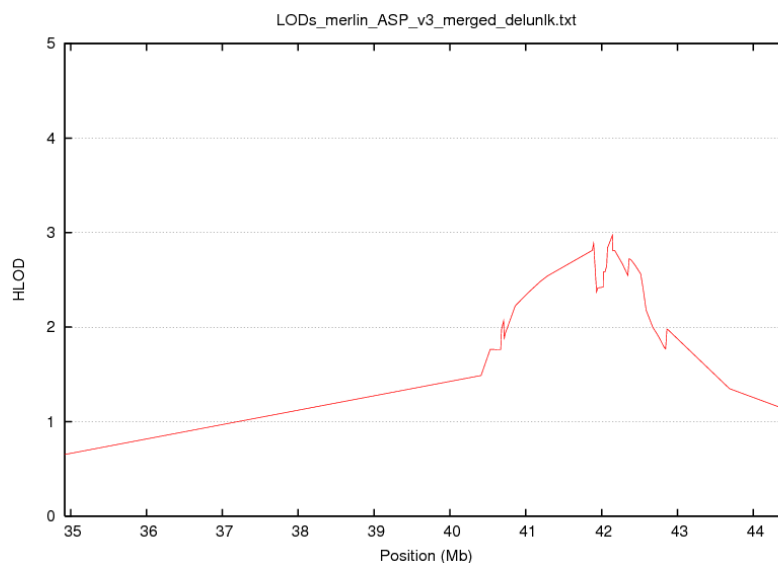
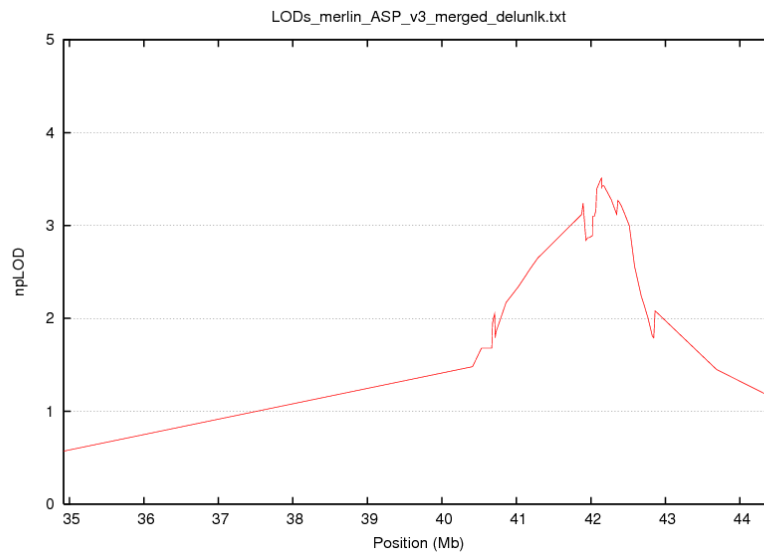


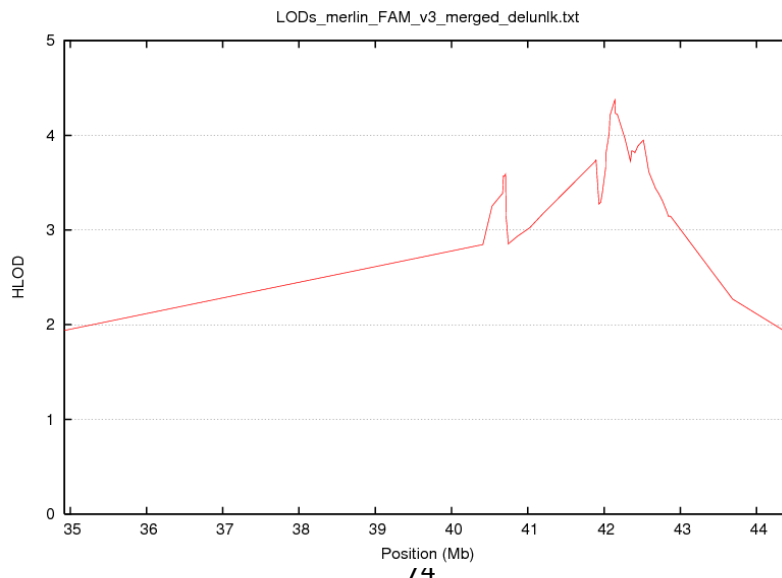
Figure 34: Plot of $-\log(p\text{-value})$ in a non-parametric ASP linkage analysis using MERLIN.
Positions in Build36.3



A family based linkage analysis (FAM) was performed with the software MERLIN for 301 families including 1131 individuals. The data set was checked for mendelian errors and unlikely genotypes prior to linkage analysis. Therefore a total of 144 genotypes were deleted. Table 20 (see Appendix) shows the calculated npLOD and HLOD values for each SNP.

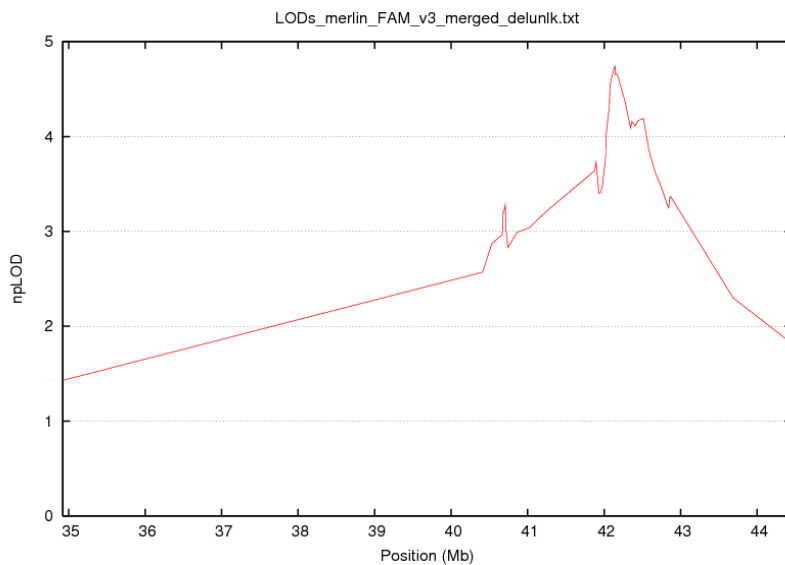
Figures 35 and 36 show the results graphically in a plot. There are two separate regions with SNPs that exceed the significance threshold of 3.6. The first region is defined by SNPs rs3108186 and rs1830031 with the highest HLOD score of 3.739 and the highest

Figure 35: Plot of $-\log(p\text{-value})$ in a family based parametric linkage analysis using MERLIN.
Positions in Build36.3. Disease allele with frequency of 0.01. Penetrances are 0.00, 0.8, 0.8 for wildtype homozygotes, heterozygote carriers and risk allele homozygotes, respectively



npLOD score of 3.730 for SNP rs1830031. This first region includes the gene ZNF567 only. The second region is defined by SNPs rs1144540 and rs10422527 with the highest HLOD score of 4.374 and the highest npLOD score of 4.740 for SNP rs496730. This second region includes 14 genes. 8 of them are zinc finger proteins with ZNF568 lying closest to the SNP with the highest LOD scores.

Figure 36: Plot of $-\log(p\text{-value})$ in a family based non-parametric linkage analysis using MERLIN.
Positions in Build36.3



3 Mutation Screening in Candidate Genes ZNF567 and ZNF568

Fine mapping of chromosome 19 with SNP markers resulted in two closely neighboring regions with significant lod scores. The SNP markers with the highest lod score in these regions are either in or next to the genes ZNF567 and ZNF568 respectively. Therefore these genes were scanned for mutations with high resolution melting curve analysis using the LightCycler480 system from Roche. 46 samples from the most affected family members of affected sib pair families were used as well as CEPH control DNA and one negative control. Table 21 shows the number of genotypes found for each amplicon. Two samples of each genotype group were then sequenced to check for variations. If there were more than 6 genotype groups all samples were sequenced. No mutations were found since all differing genotype groups were due to known SNP variants. In future experiments this region will be sequenced again by NGS.

Table 21: Number of genotypes found by HRM curve analysis in genes ZNF567 and ZNF568

PCR amplicon	Number of detected genotypes	PCR amplicon	Number of detected genotypes	PCR amplicon	Number of detected genotypes
ZNF567_e1F	2	ZNF568_e6F	5	ZNF568_e8.1F	>6
ZNF567_e2-3F	5	ZNF568_e7.1F	2	ZNF568_e8.2F	6
ZNF567_e4F	1	ZNF568_e7.2F	1	ZNF568_e8.2_2F	>6
ZNF567_e5.1F	4	ZNF568_e7.3F	4	ZNF568_e9F	2
ZNF567_e5.2F	5	ZNF568_e7.4F	3	ZNF568_e10F	>6
ZNF567_e5.3R	2	ZNF568_e7.5F	4	ZNF568_e11F	5
ZNF567_e5.4F	2	ZNF568_e7.6F	6	ZNF568_e12_2F	1
ZNF567_e5.5F	1	ZNF568_e7.7F	1	ZNF568_e13_2F	4
ZNF567_e5.6F	1	ZNF568_e7.8R	2	ZNF568_e14F	4
ZNF568_e1F	2	ZNF568_e7.9F	3	ZNF568_e15.1F	1
ZNF568_e2F	1	ZNF568_e7.10F	6	ZNF568_e15.2F	>6
ZNF568_e3R	1	ZNF568_e7.11_2F	>6	ZNF568_e15.3F	5
ZNF568_e4F	1	ZNF568_e7.12_2F	2	ZNF568_e15.4F	5
ZNF568_e5F	1	ZNF568_e7.13F	3		

4 Whole Genome Association and Linkage Data Analyzes with a Larger Sample Set

4.1 Association Analyzes (CaCo; TDT)

Case control [CaCo] genetic association analysis including 258.673 SNPs was conducted with the software PLINK. 2891 individuals were included with 357 cases and 2534 controls. The data set was checked for mendelian errors and unlikely genotypes prior to case control analysis. Therefore a total of 88069 genotypes were deleted. There were no significant results using a recessive model. Figure 37 shows the results of a dominant model in a manhattan plot, pointing to significant regions on chromosomes 5, 6, and 16.

Figure 37: Manhattan plot for case control analysis with a dominant model using PLINK.
Positions in Build36.3

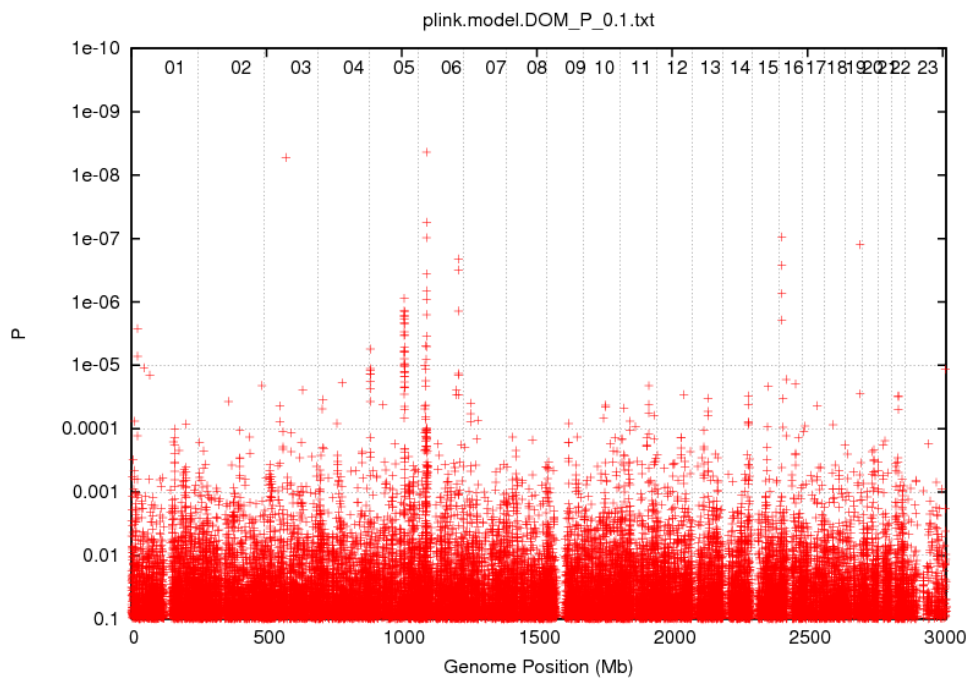


Figure 38 shows a scatter plot for the case control analysis using a dominant model on chromosome 5 pointing to 2 significant clusters exceeding the significance threshold of $1e-06$. The first region is defined by SNPs rs10512779 and rs4473739 with the lowest p-value of $5.55e-6$ for SNP rs7720820. This first region includes the gene ADAMTS16 only. The second region is defined by SNPs rs6596007 and rs12653237 with the lowest p-value of $8.76e-7$ for SNP rs27421. This second region includes 7 genes [CDC42SE2, LOC100505941, RAPGEF6, FNIP1, ACTBP4, LOC100505572, LOC728637]. Tables 22 and 23 [see Appendix] show the significant cluster regions in detail with the according SNPs and their p-values.

Figure 38: Scatter plot for case control analysis with a dominant model using PLINK for chr 5 only. Positions in Build36.3

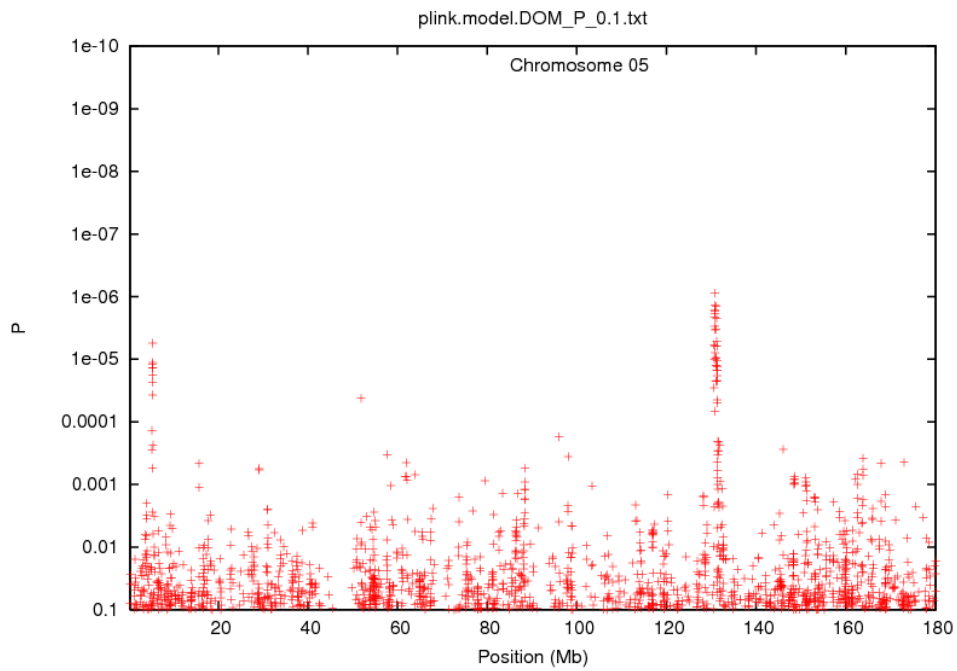
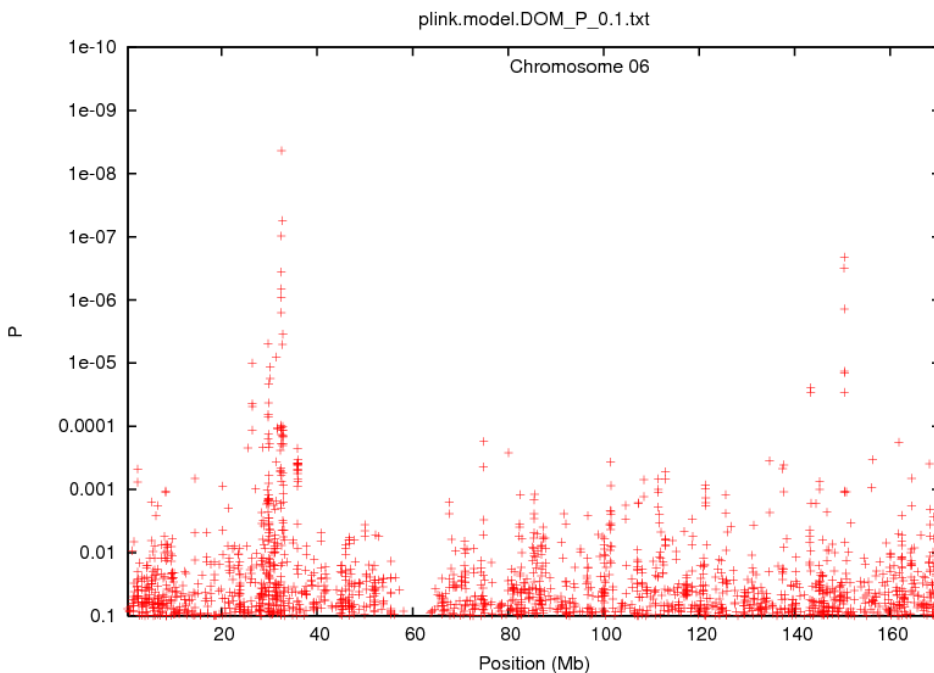


Figure 39 shows a scatter plot for the case control analysis on chromosome 6 pointing to 3 significant SNP clusters exceeding the significance threshold of $1e-06$. The first region is defined by SNPs rs123367 and rs2523405 with the lowest p-value of $4.87e-06$ for SNP rs29228. This first region includes 5 genes (HLA-F, ZFP57, MOG, and 2 pseudogenes).

Figure 39: Scatter plot for case control analysis with a dominant model using PLINK for chr 6 only. Positions in Build36.3



The second region is defined by SNPs rs3135363 and rs3892710 with the lowest p-value of 4.34e-09 for SNP rs9268856. This second region includes 7 genes. All of these genes are part of the HLA complex. The third region is defined by SNPs rs6557200 and rs2181923 with the lowest p-value of 3.14e-07 for SNP rs5017316. This region includes 5 genes (ULBP1, LOC646024, RAET1L, LOC100131886, and 1 pseudogene). Tables 24, 25 and 26 (see Appendix) show the significant cluster regions in detail with the according SNPs and their p-values.

Figure 40 shows a scatter plot for the case control analysis on chromosome 16 pointing to one significant SNP clusters exceeding the significance threshold of 1e-06. This region is defined by SNPs rs6498146 and rs9746695 with the lowest p-value of 7.40e-07 for SNP rs3893660. This first region includes 1 pseudo gene and CLEC16A. Table 27 (see Appendix) shows the significant cluster regions in detail with the according SNPs and their p-values.

Figure 40: Scatter plot for case control analysis with a dominant model using PLINK for chr 16 only.
Positions in Build36.3

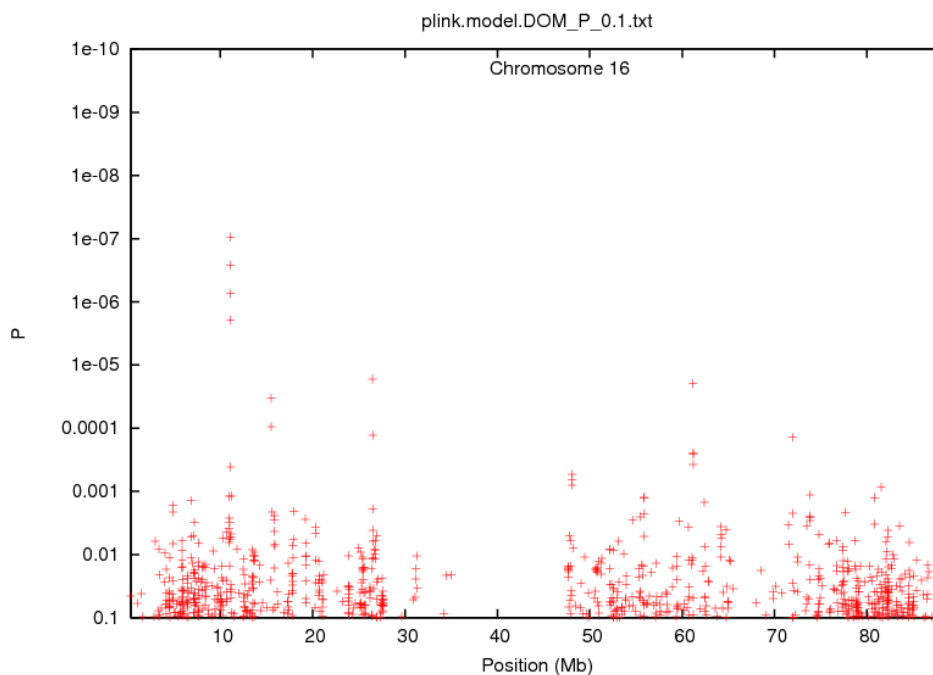


Figure 41 shows the results of a trend model in a manhattan plot, pointing to significant clusters on chromosomes 5 and 6 reaching p-values lower than 1e-06.

Figure 42 shows a scatter plot for the case control analysis on chromosome 5 pointing to 2 significant clusters exceeding the significance threshold of 1e-06. The first region is

Figure 41: Manhattan plot for case control analysis with a trend model using PLINK.
Positions in Build36.3

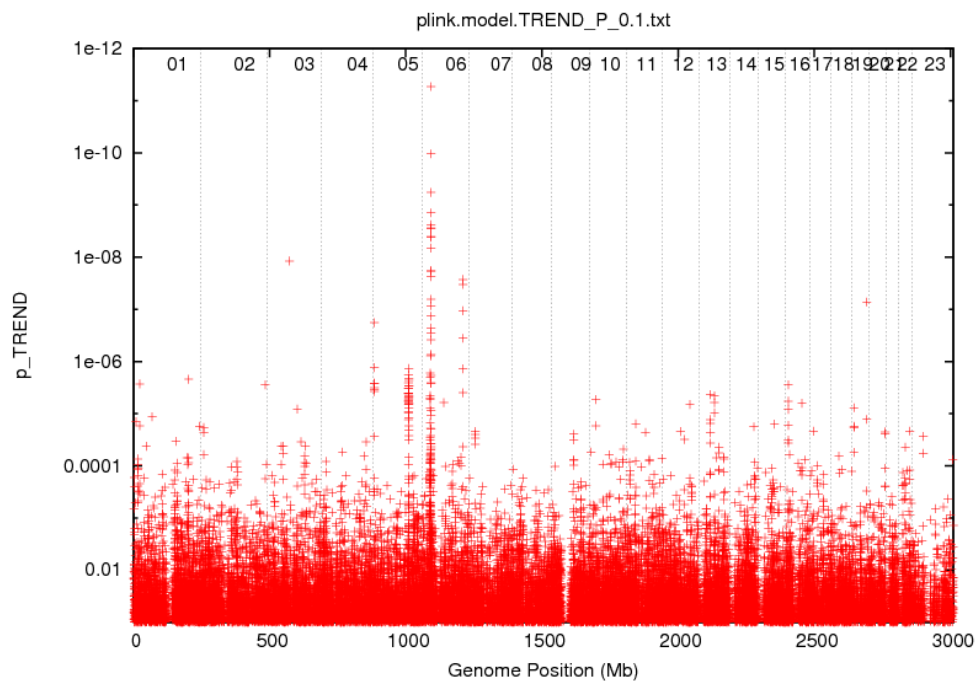
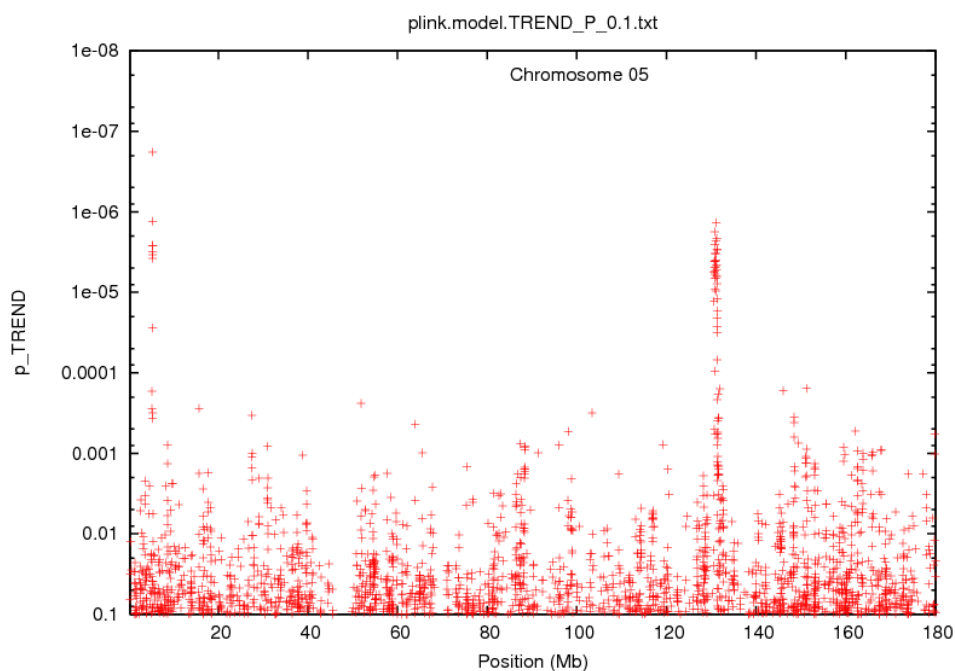


Figure 42: Scatter plot for case control analysis with a trend model using PLINK for chr 5 only.
Positions in Build36.3

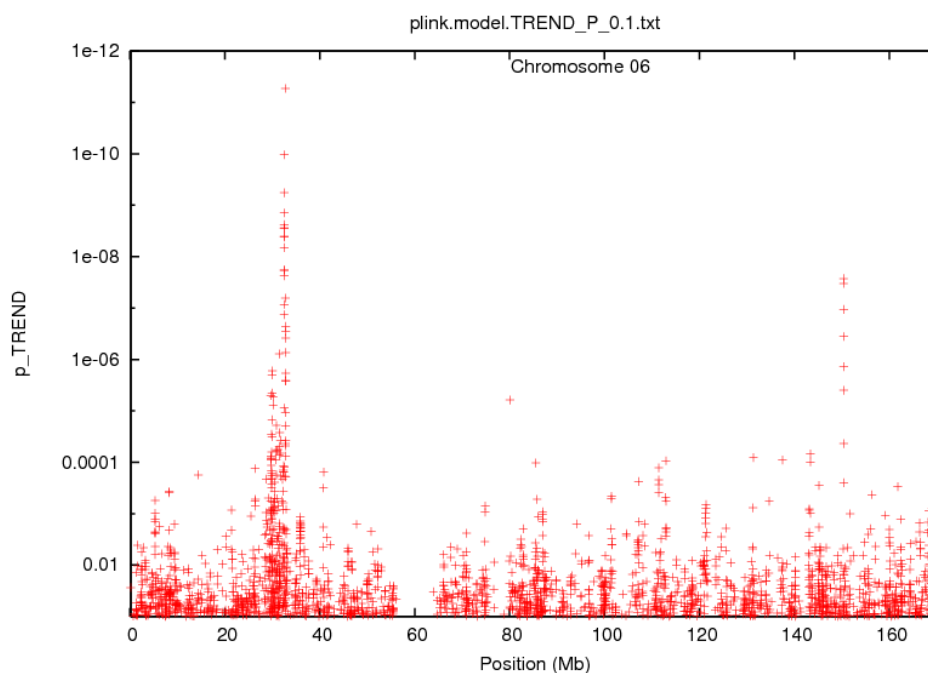


defined by SNPs rs2913657 and rs4473739 with the lowest p-value of $1.81e-7$ for SNP rs7720820. This first region includes the gene ADAMTS16 only. The second region is defined by SNPs rs17165964 and rs253943 with the lowest p-value of $6.59e-6$ for SNP

rs11242095. This second region includes 9 genes. Tables 28 and 29 (see Appendix) show the significant cluster regions in detail with the according SNPs and their p-values.

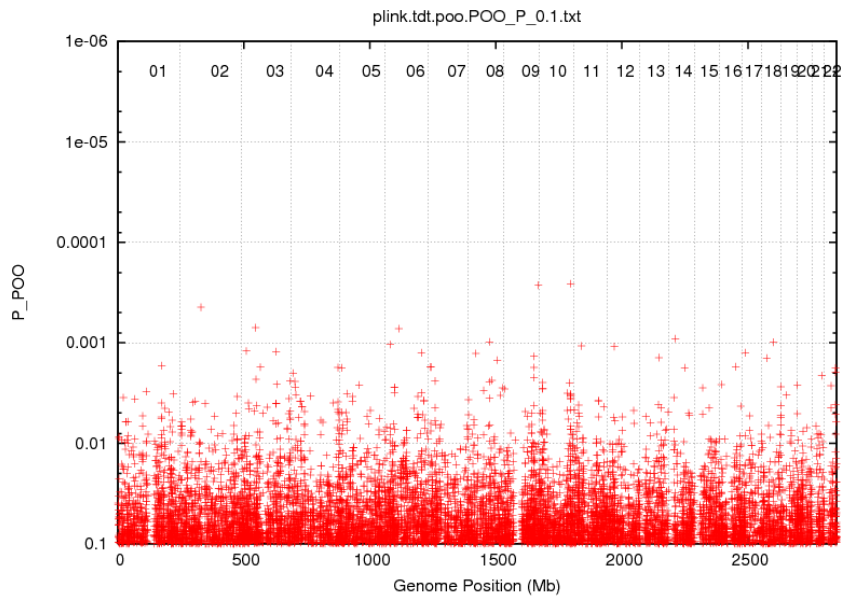
Figure 43 shows a scatter plot for the case control analysis on chromosome 6 pointing to 3 significant SNP clusters exceeding the significance threshold of $1e-06$. The first region is defined by SNPs rs1611699 and rs2517595 with the lowest p-value of $7.69e-06$ for SNP rs1264702. This first region includes 35 genes of which most belong to the HLA complex. The second region is defined by SNPs rs9268429 and rs9296044 with the lowest p-value of $5.35e-12$ for SNP rs9469220. This second region includes 10 genes. All of these genes are part of the HLA complex. The third region is defined by SNPs rs4870174 and rs11155699 with the lowest p-value of $3.31e-8$ for SNP rs5017316. This third region includes 5 genes of which 3 are pseudogenes. Tables 30, 31 and 32 (see Appendix) show the significant cluster regions in detail with the according SNPs and their p-values.

Figure 43: Scatter plot for case control analysis with a trend model using PLINK for chr 6 only.
Positions in Build36.3



A Transmission Disequilibrium Test (TDT) was performed for 259 families with the software PLINK. The data set was checked for mendelian errors and unlikely genotypes prior to TDT analysis. Therefore a total of 88069 genotypes were deleted. Figure 44 shows the results in a manhattan plot. No SNP clusters reached the significance threshold.

Figure 44: Manhattan plot for a transmission disequilibrium test using **PLINK.**
Positions in Build36.3



4.2 Linkage Analyzes (FAM)

A family based linkage analysis (FAM) with a set of 271.150 SNPs was performed with the software MERLIN for 259 families including 855 individuals. The data set was checked for mendelian errors and unlikely genotypes prior to linkage analysis. Therefore a total of 88.069 genotypes were deleted. Figure 45 shows the results in a plot, pointing to significant clusters on chromosomes 10 and 19 reaching npLOD scores of 3.6 or higher.

Figure 45: Plot of npLOD scores in a family based non parametric linkage analysis with 271.150 SNPs using **MERLIN.** Positions in Build36.3

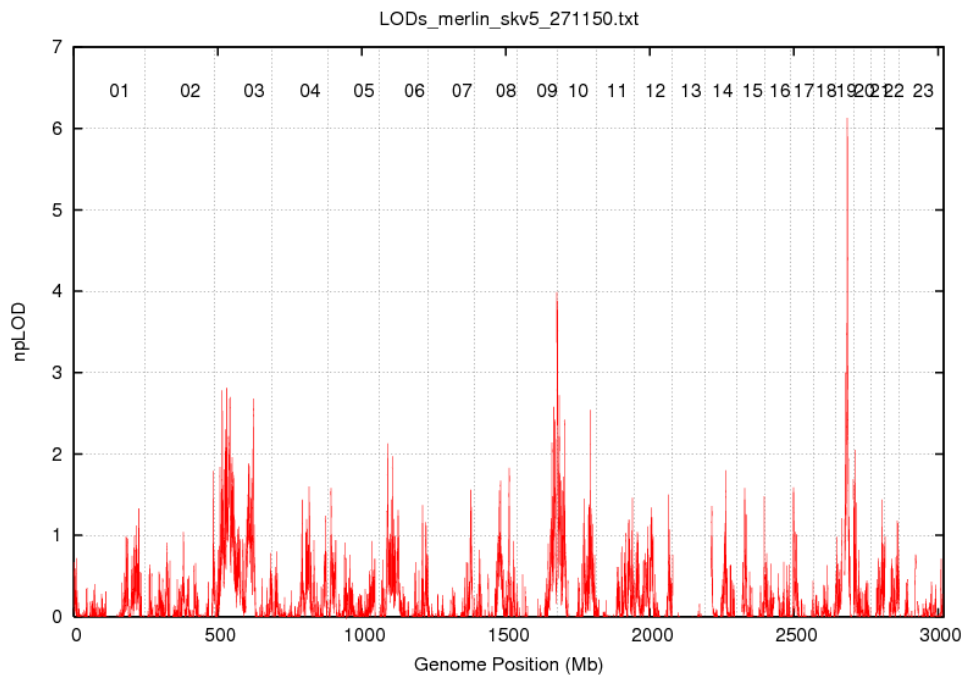


Figure 46 shows a plot of Chr10 for the family based linkage analysis with 271.150 SNPs pointing to 3 significant SNP clusters exceeding the significance threshold of 3.6. The first region is defined by SNPs rs12246970 and rs17136375 with the highest npLOD score of 3.99 for SNPs rs1539231, rs11252693, and rs2096134. This first region includes 3 genes (DIP2C, LOC642278, C10orf108). The second region is defined by SNPs rs17294166 and rs11250965 with the highest npLOD score of 3.77 for SNPs rs7082514, rs11250838, rs4077784, rs9919410, rs10794793, and rs10794794. There are no genes located within this region. The third region is defined by SNPs rs10751884 and rs1909690 with the highest npLOD score of 3.88 for SNPs rs2065683, rs2184413, rs2065685, and rs11251502. There are no genes within this region. Tables 33, 34, and 35 (see Appendix) show the calculated npLOD values for each SNP in the 3 clustered regions.

Figure 46: Plot of npLOD scores in a family based non parametric linkage analysis for chromosome 10 only using MERLIN. Positions in Build36.3

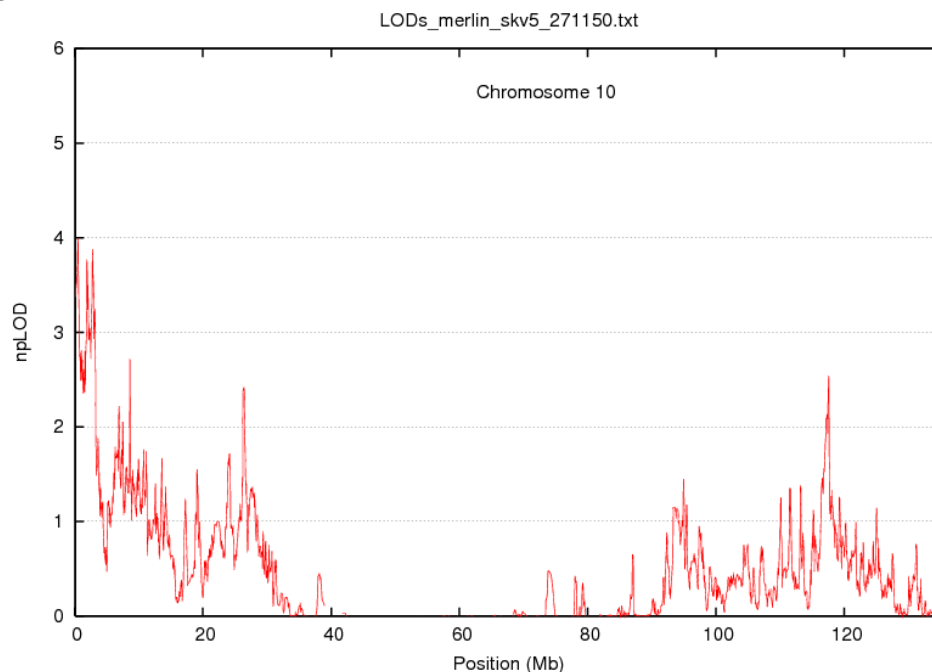
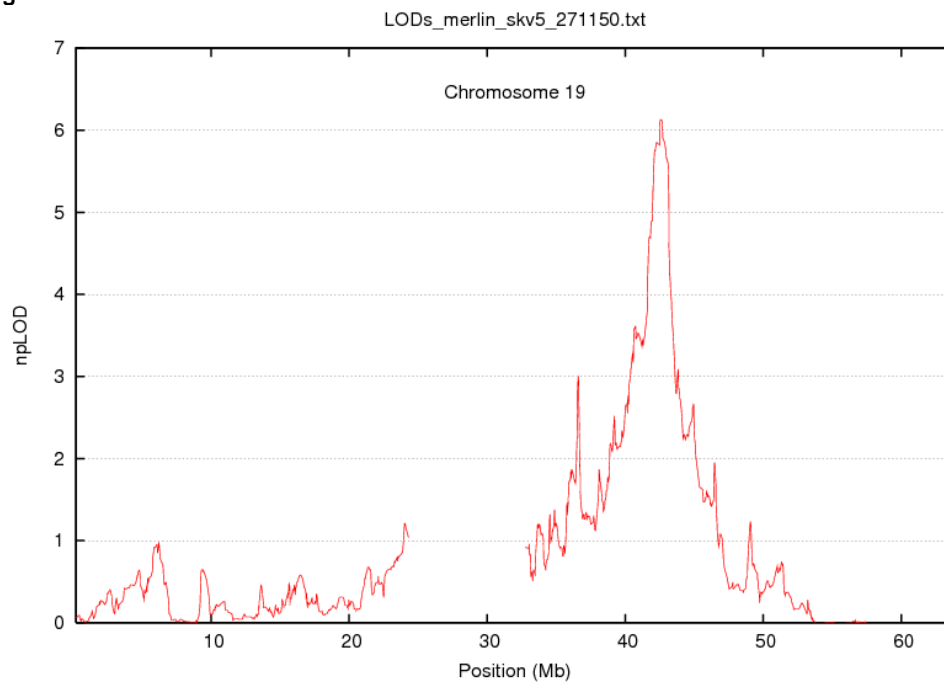


Figure 47 shows a plot of chromosome 19 for the family based linkage analysis with 271.150 SNPs pointing to 1 significant SNP cluster exceeding the significance threshold of 3.6. The region is defined by SNPs rs2432055 and rs41465446 with the highest npLOD score of 6.13 for SNPs rs713256 and rs256733. This region contains 48 genes, including 27 zinc finger genes. The highest npLOD score is found within gene ZNF527. Table 36 (see Appendix) shows the calculated npLOD values for each SNP in the clustered region.

Figure 47: Plot of npLOD scores in a family based non parametric linkage analysis for chromosome 19 only using MERLIN. Positions in Build36.3



A family based linkage analysis (FAM) with a set of 62,990 SNPs was performed with the software MERLIN for 259 families including 855 individuals. The data set was checked for mendelian errors and unlikely genotypes prior to linkage analysis. Therefore a total of 88,069 genotypes were deleted. Figure 48 shows the results in a plot, pointing to a significant cluster on chromosomes 19 reaching an npLOD score of 4.15.

Figure 48: Plot of npLOD scores in a family based non parametric linkage analysis with 62,990 SNPs using MERLIN. Positions in Build36.3

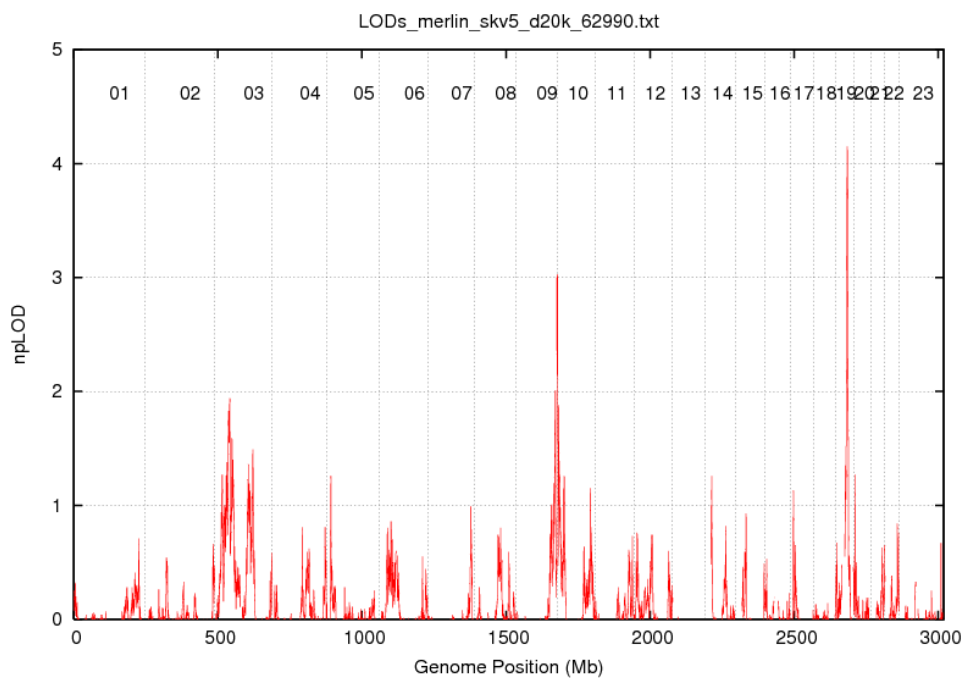
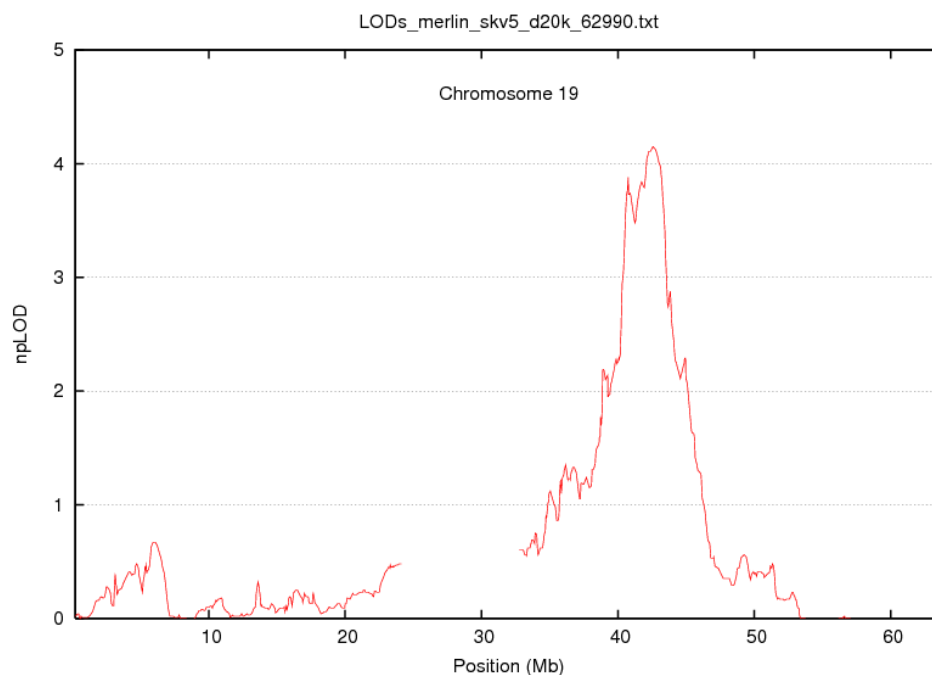


Figure 49 shows a plot of Chr19 for the family based linkage analysis with 62,990 SNPs pointing to 1 significant SNP cluster exceeding the significance threshold of 3.6. The region is defined by SNPs rs16970276 and rs2278431 with the highest npLOD score of 4.15 for SNP rs256733. This region contains 93 genes, including KRTDAP, DMKN, and SBSN and 30 zinc finger genes. The highest npLOD score is found within gene ZNF527. Table 37 (see Appendix) shows the calculated npLOD values for each SNP in the clustered region.

Figure 49: Plot of npLOD scores in a family based non parametric linkage analysis for chromosome 19 only using MERLIN. Positions in Build36.3



A family based linkage analysis (FAM) with a set of 83,371 SNPs was performed with the software MERLIN for 259 families including 855 individuals. The data set was checked for mendelian errors and unlikely genotypes prior to linkage analysis. Therefore a total of 35,601 genotypes were deleted. Figure 50 shows the results in a plot, pointing to a significant cluster on chromosomes 19 reaching an npLOD score of 3.87.

Figure 51 shows a plot of Chr19 for the family based linkage analysis with 83,371 SNPs pointing to 1 significant SNP cluster exceeding the significance threshold of 3.6. The region is defined by SNPs rs16970293 and rs12462868 with the highest npLOD score of 3.87 for SNP rs2239945. This region contains 31 genes, including KRTDAP, DMKN, and SBSN. The highest npLOD score is found within gene GAPDHS. Table 38 (see Appendix) shows the calculated npLOD values for each SNP in the clustered region.

Figure 50: Plot of npLOD scores in a family based non parametric linkage analysis with 83.371 SNPs using MERLIN. Positions in Build36.3

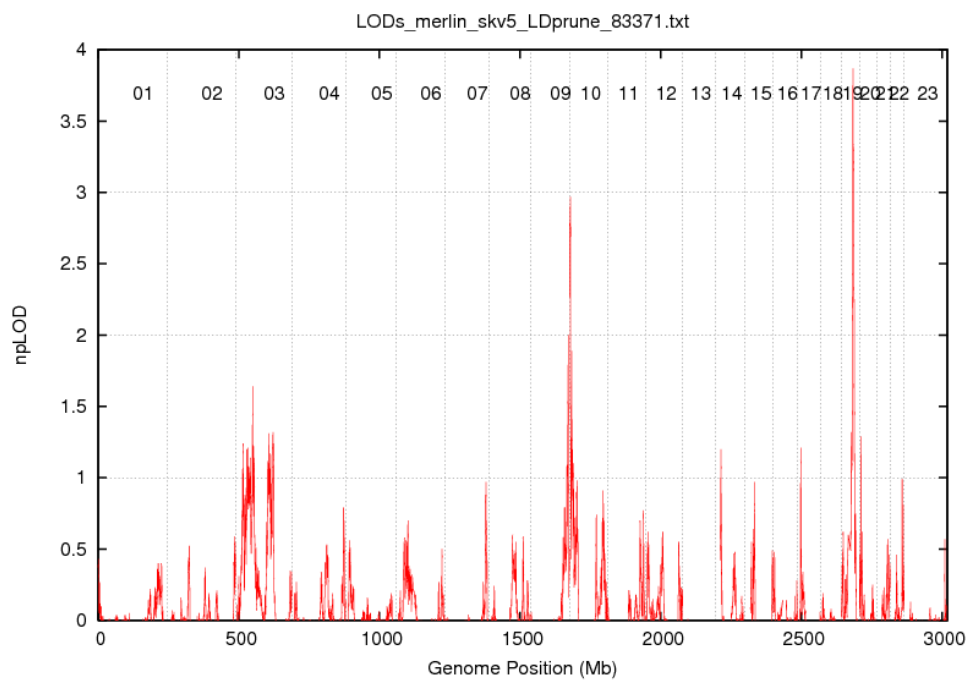
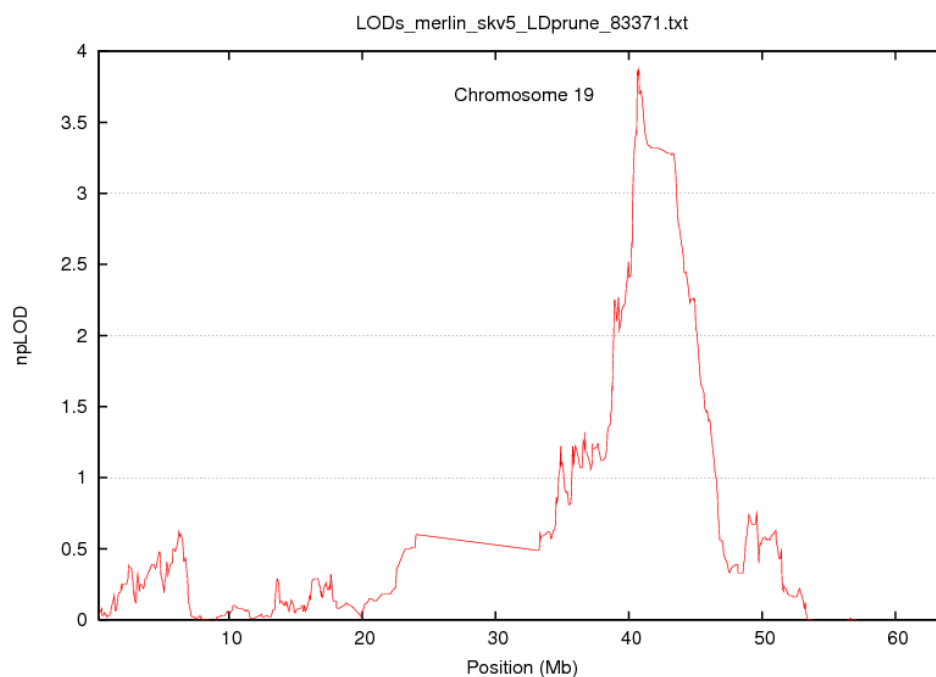


Figure 51: Plot of npLOD scores in a family based non parametric linkage analysis for chromosome 19 only using MERLIN. Positions in Build36.3



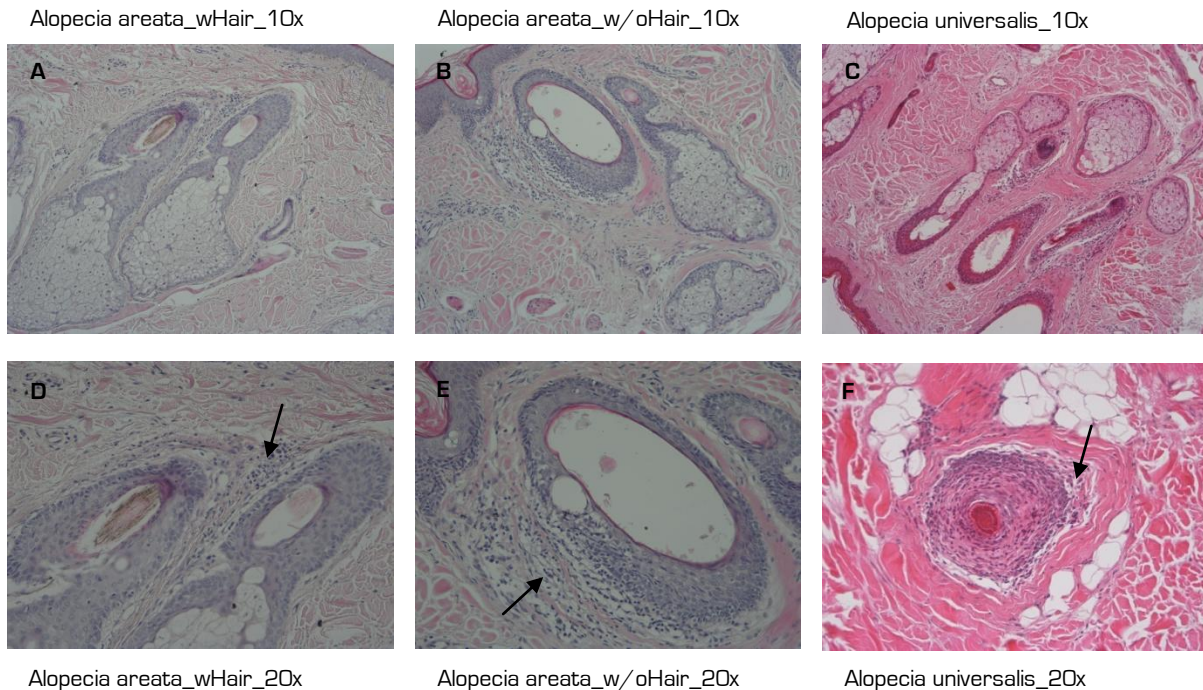
3 Histology

3.1 HE - Staining

Perifollicular inflammatory infiltrate was evident in all 3 HE - stained samples (figure 52).

Figure 52: HE staining in human skin sections.

A-C) 10x magnification D-F) 20x magnification A+D) skin from an alopecia areata patient, taken from a spot on the head where hair was still growing B+E) skin from the same alopecia areata patient but taken from the center of a hairless patch C+F) skin from an alopecia universalis patient.



3.2 Immunohistochemical Staining

Immunohistochemical (IHC) stainings of cadherins 1, 2, 3, 15, catenins alpha, beta, gamma, p120, and desmoglein 1 were done in human skin samples. Differences between the samples could be observed in the catenin gamma, cadherin 15, and cadherin 3 stainings only.

As is shown in figure 53 the hair follicles show a strong staining of catenin gamma in an alopecia areata skin sample where hair is still growing (figure 53 A+D). The fluorescence intensity decreases slightly in the alopecia areata skin sample from a central area of hair loss (figure 53 B+E) and is no longer detectable in skin sections from an alopecia universalis sample (figure 53 C+F).

Figure 54 shows the IHC staining of cadherin 15 in human skin. There is a strong staining of the epidermis in the alopecia areata skin sample (figure 54 A, B, D, E) whereas there is

only a slight staining of the stratum granulosum evident in the alopecia universalis skin sample (figure 54 C+F).

Figure 53: IHC staining of catenin gamma (yellow) and DAPI (blue) in human skin.

A-C) 10x magnification D-F) 20x magnification A+D) skin from an alopecia areata patient, taken from a spot on the head where hair was still growing B+E) skin from the same alopecia areata patient but taken from the center of a hairless patch C+F) skin from an alopecia universalis patient.

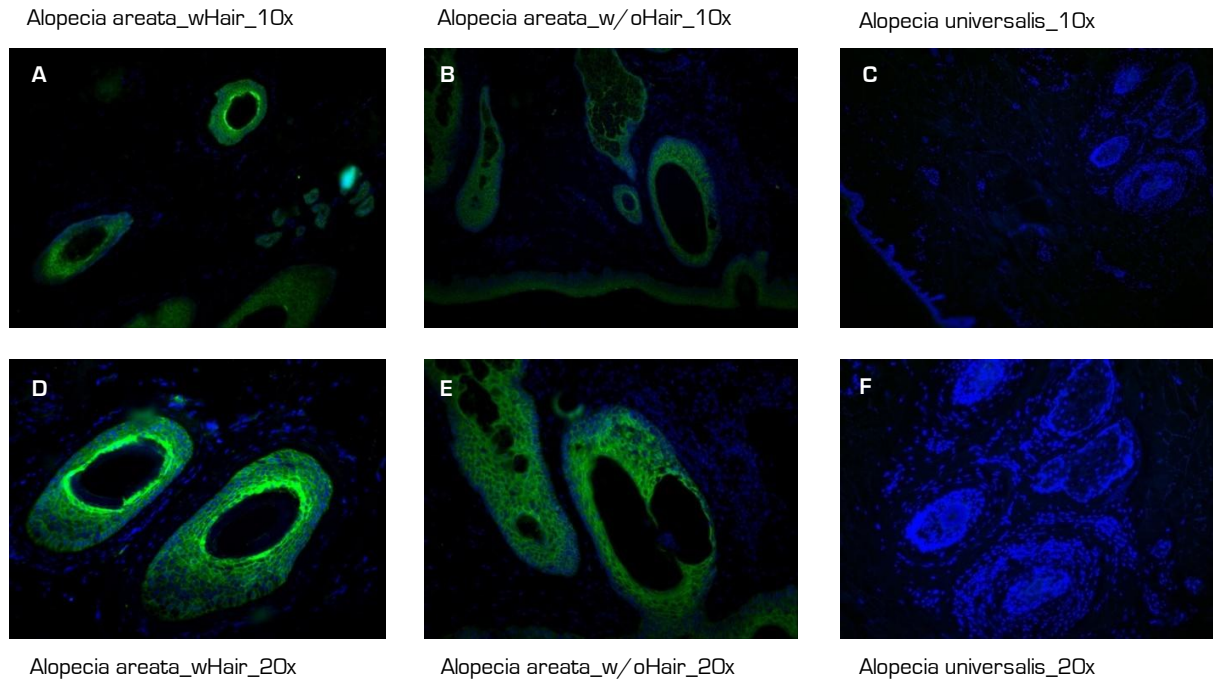


Figure 54: IHC staining of cadherin 15 (yellow) and DAPI (blue) in human skin.

20x magnification A-C) cadherin 15 staining D-F) merged picture with bright light, cadherin 15 and DAPI staining A+D) skin from an alopecia areata patient, taken from a spot on the head where hair was still growing B+E) skin from the same alopecia areata patient but taken from the center of a hairless patch C+F) skin from an alopecia universalis patient.

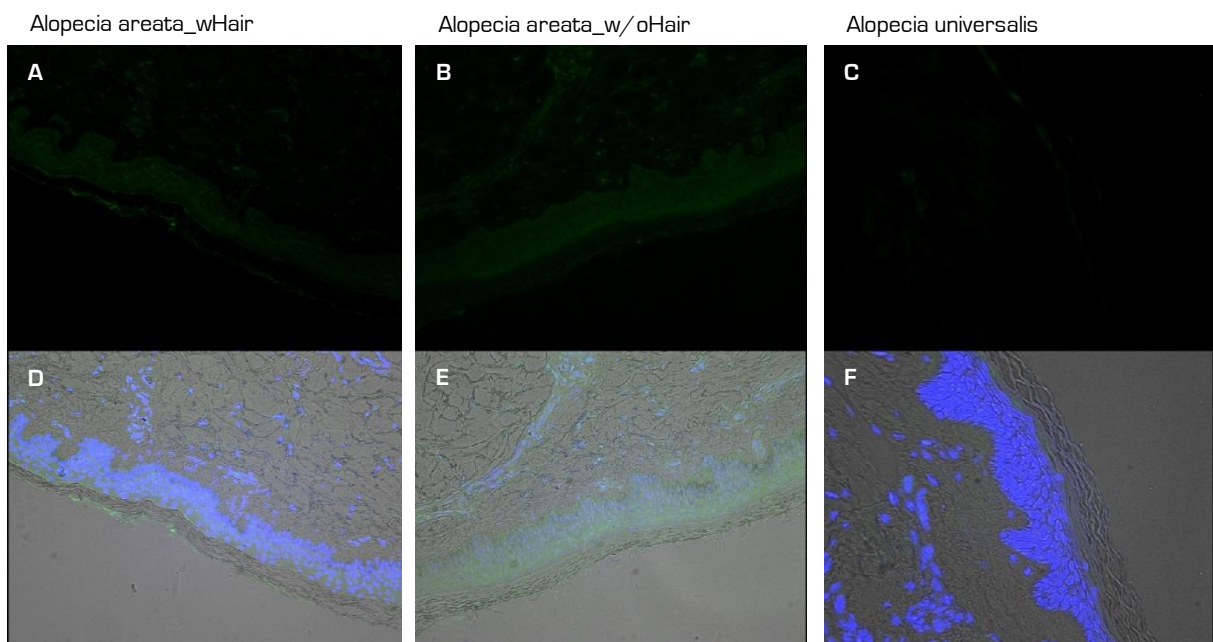
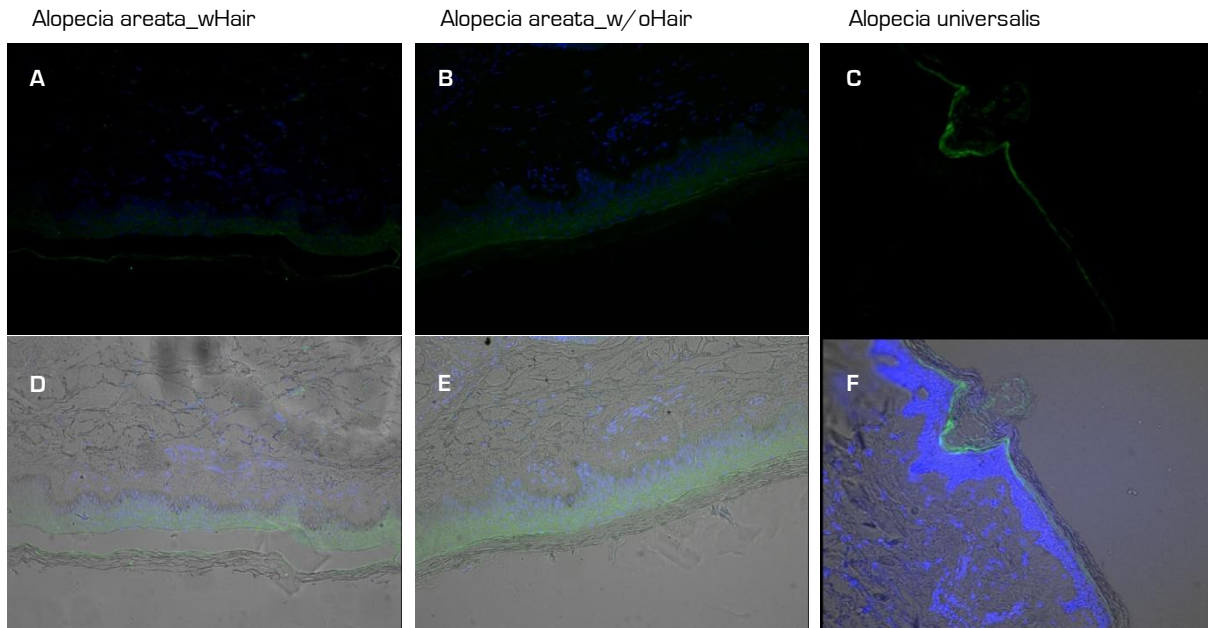


Figure 55 shows the IHC staining of cadherin 3 in human skin. There is a strong staining of the epidermis in the alopecia areata skin sample (figure 55 A, B, D, E) whereas there is only a slight staining of the stratum granulosum evident in the alopecia universalis skin sample (figure 55 C+F).

Figure 55: IHC staining of cadherin 3 (yellow) and DAPI (blue) in human skin.

20x magnification A-B) cadherin 3 and DAPI staining C) cadherin 3 staining D-F) merged picture with bright light, cadherin 3 and DAPI staining A+D) skin from an alopecia areata patient, taken from a spot on the head where hair was still growing B+E) skin from the same alopecia areata patient but taken from the center of a hairless patch C+F) skin from an alopecia universalis patient.



F Discussion

1. Expression Analyzes

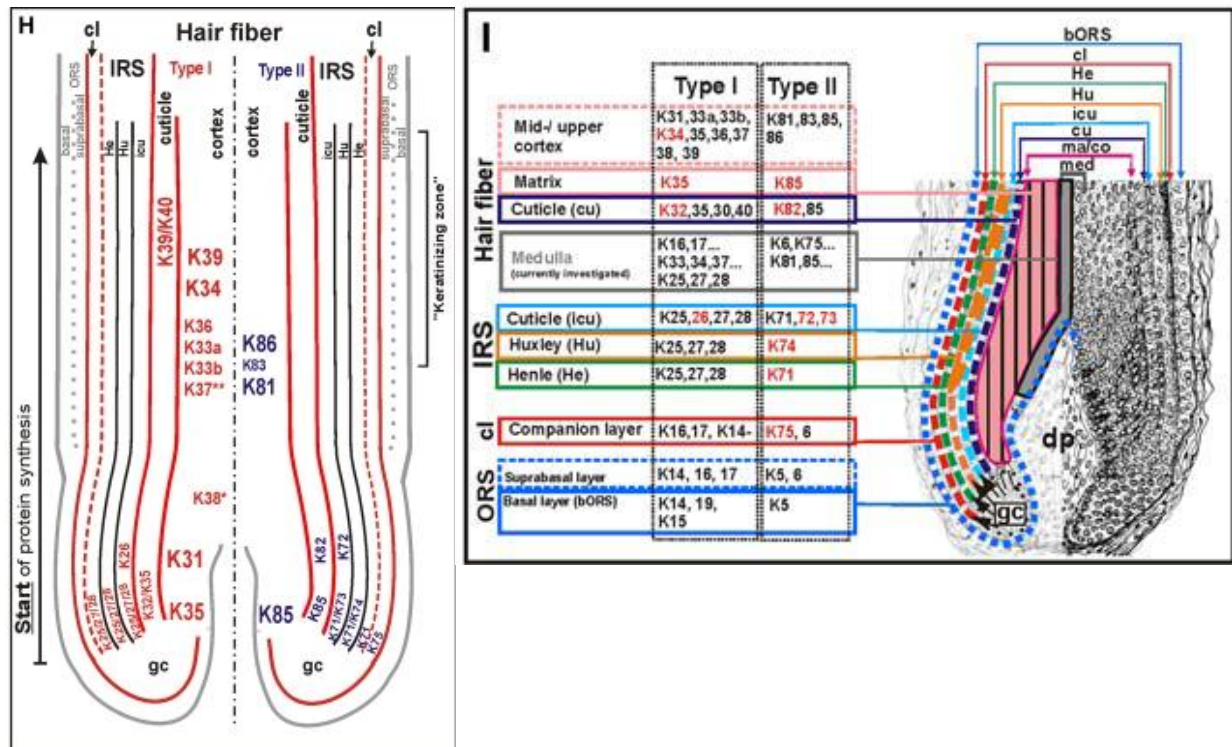
In this study only < 2 fold changes could be detected with the microarray analysis for DEB rat skin and heart samples compared to Wistar rats. The highest obtained fold change in skin was 1.6866 and in heart it was 1.4408. Expression of genes within the candidate region of chromosome 19 only reached fold changes between 0.92 and 1.15 in skin and heart samples. As will be discussed below, differential expression detection and sensitivity is significantly reduced in this expression range. Still, an overall tendency of upregulation in genes affecting the immune system in skin and heart samples could be detected. In addition several genes affecting the skin, hair and nail structure could be found among the top 50 upregulated genes in skin samples, including several keratin genes such as Krt25 (fold change 1.6866), Krt27 (fold change 1.6133), Krt 73 (fold change 1.5567), and Krt26 (fold change 1.4687).

Keratins are the typical intermediate filament proteins of epithelia. They form heterodimers with one type I (“acidic”) and one type II (“basic to neutral”) keratin protein in a α -helical coiled-coil confirmation. These dimers assemble to tetramers, then to octamers and form eventually intermediate filaments (IF). Single keratins deviating from equimolar type I/type II amounts are rapidly degraded [Lu and Lane 1990]. It has been shown that bundled IFs braid the nucleus inside the cell, span through the cytoplasm and are attached to the cytoplasmic plaques of desmosomes which are the typical epithelial cell-cell adherens junctions [Waschke 2008]. Therefore keratins are crucial for the mechanical stability and integrity of epithelial cells and tissues. In addition to this mechanical function of keratins, several regulatory functions have been discovered. Among them are the protection of the placental and trophoblast barrier function [Jaquemar 2003; Hesse 2000], the protection from apoptosis [Caulin 2000, Tong 2006], the protection of the liver against stress and from injury [Zatloukal 2000, Ku 2003], and the regulation of protein synthesis and cell size during wound healing involving intracellular signaling pathways [Kim 2006]. In addition, they may also play a role in epithelial polarity and membrane traffic [Oriolo 2007].

Some epithelial keratins are specifically expressed in and closely restricted to the compartments of the hair follicle inner root sheath. These include type I keratins K25-K28 and type II keratins K71-74 [Langbein 2004, 2006]. Compared to the masses of hair and epidermal keratins these hair follicle keratins are quantitatively under-representated in the tissue. Human hair disorders related to these keratins have not yet been discovered [Moll 2008]. Figure 56 gives an overview of the expression sites of all hair and hair follicle

specific keratins in the human hair follicle. Interestingly, all keratins found with a tendency to overexpression via microarray in this study belong to the inner root sheath specific keratins. As has been stated in the introduction to hair, the cornified inner root sheath anchors and directs the growth of the emerging hair shaft. These findings lead to the assumption of a structural defect as a secondary effect to the basic cause of alopecia.

Figure 56: Summary schemes of the expression of all hair and hair follicle-specific keratins in the human hair follicle. (From Moll R. The human keratins: biology and pathology. Histochem Cell boil 2008; 129:705-733)



Human keratins are clustered at two chromosomal regions. All type I keratins (except KRT18) are found at chromosome site 17q21.2 whereas all type II keratins and KRT18 are found at chromosome site 12q13.13. It has been demonstrated in knock-out experiments and in genetic diseases that mutations in keratin genes often cause more severe defects than the complete loss of a keratin gene whose failure might be compensated by other keratins (Moll 2008). Regulation of keratin gene expression in the skin is mostly found at the transcriptional level (Stellmach 1991). It has been shown, that certain sequences in the 5' upstream region of the genes are involved in regulation processes, as for example AP2-binding sites (Fuchs 1995).

Among the potentially downregulated genes in rat skin several caseins stand out. Caseins are major components of milk. Therefore a downregulation in these proteins might explain why the mother rats do not produce enough milk for their offspring so that they finally

dehydrate and die or get eaten by the mother animal. This problem was overcome by feeding the newborns with curd cheese mixed with mashed bananas as early as possible giving proof that the initial problem of dehydration was due to the lack of milk production in the mother animal and not due to physiological problems in the offspring. There is no reason to believe that this phenomenon is related to AA, though, and is probably an artifact resulting from the extreme homogeneity of the strain after about 63 generations of inbreeding.

For better interpretation of the data it was loaded into the IPA program and functional analysis was performed. This resulted in an obvious association to biological functions like cellular development, hematological system development and function as well as hematopoiesis with p-values as low as 4.19E-19. These findings further emphasize the immunological component in AA pathology. Functional analysis with expression data from the candidate region on chromosome 19 only revealed associations to biological functions as cell-to-cell signaling and interaction, hair and skin development and function, and tissue development with p-values as low as 3.78E-06 indicating an underlying structural defect. One might speculate upon these findings if there is first a structural defect, for example in hair formation, and thereafter the immune system is activated or if the primary cause is an immunological defect attacking hair structures and with that inducing an upregulation in hair and skin structure gene expression. Exploring molecular relationships for genes within the candidate region with the Network Explorer function of IPA produced a network of 35 genes in total pointing again to biological functions like cell-to-cell signaling and interaction, connective tissue development and function as well as tissue development in general with p-values as low as 6.57E-09. Especially cadherin genes stood out as important genes within the network.

Cadherins are a superfamily of about 80 members of single-pass transmembrane proteins involved in Ca^{2+} -dependent homotypic cell adhesion and are characterized by an extracellular, a transmembrane, and an intracellular domain [Tepass 2000]. Depending on their domain composition, genomic organization, and structure cadherin molecules are divided into six subgroups. These are type I (classical), type II, desmosomal, proto-, Flamingo, and FAT-like cadherins [Gooding 2004]. In this context especially type I and desmosomal cadherins are of importance and shall be therefore further described.

With their extracellular domain classical cadherins mediate homotypic as well as heterotypic cell-cell or cell-matrix interactions which are often sufficient to provide Ca^{2+} -dependent adhesion. In addition interactions of the cadherin cytoplasmic tail with the cytoskeleton

significantly increase the strength of cadherin-mediated adhesion [Yap 1997]. This is for example accomplished by building a protein complex of Cadherin 1 (also known as E-cadherin; one of the best characterized cadherins) with catenin beta or catenin gamma and catenin alpha, which in turn links the complex either directly to the actin cytoskeleton or indirectly through alpha-actinin, vinculin, ZO-1, or spectrin [Yamada & Geiger 1997]. Cadherin 1 mediates not only the assembly of adherens junctions, but also affects the formation of desmosomes and tight junctions [Gumbiner 1988, Wheelock & Jensen 1992]. The cytoplasmic domain of cadherin becomes unstructured when unbound to catenin beta [Huber 2001], which is in addition to its function in cadherin-based adhesion an important mediator in the Wnt-signaling pathway [Miller 1999, Peifer 2000] that controls several events in development like differentiation, proliferation, and morphogenesis [Wodarz & Nusse 1998]. The function of cadherins is therefore not limited to linking cells together and forming protein complexes inside the cells, but they also interact in signaling pathways of differentiation, proliferation, and migration [Knudsen 1998]. They do that either by organizing signaling components or by the formation of close cell-cell contact, which affects the signaling mechanisms indirectly [Fagotto & Gumbiner 1996].

Besides desmoplakin, plakoglobin, and plakophilin the desmosomal cadherins desmoglein and desmocollin are major components of desmosomes [Huen 2002]. Desmosomes ensure very strong cell-cell contacts and are crucial to all tissues under constant mechanical stress, such as the skin, myocardium, bladder, and gastrointestinal mucosa [Getsios 2004, Holthofer 2007]. With electron microscopy three distinct areas can be identified which is the extracellular core region (desmoglea), the outer dense plaque (ODP), and the inner dense plaque (IDP) [Kowalczyk 1994, Garrod & Chidgey 2008]. The extracellular domains of the desmogleins and desmocollins mediate cell-cell adhesion, whereas the cytoplasmic tails bind linker proteins, such as plakoglobin and plakophilin, in the ODP region. Desmoplakin associates with both linker proteins and finally attaches to intermediate filaments within the IDP region, tethering the cytoskeletal network to the adhesion complex [Figure 57] [Delva 2009]. Seven desmosomal cadherins (desmoglein 1-4 and desmocollin 1-3) are known at present which are differentially expressed as keratinocytes undergo terminal differentiation [Kottke 2006, Holthofer 2007]. Desmogleins 1 and 4, as well as desmocollin 1 are mainly expressed in the upper layers of the epidermis, whereas desmogleins 2 and 3, as well as desmocollins 2 and 3 are mainly expressed in the lower layers [Figure 58]. Genetic mouse models as well as a number of inherited and acquired human diseases (as for example arrhythmogenic right ventricular cardiomyopathy and pemphigus) implicate that a tight regulation of desmosomal cadherin expression pattern is crucial for correct tissue homeostasis and have therefore important

Figure 57: A structure model of desmosomes. (From Delva E, Tucker DK, Kowalczyk AP. The desmosome. Cold Spring Harb Perspect Biol 2009; 1:a002543)

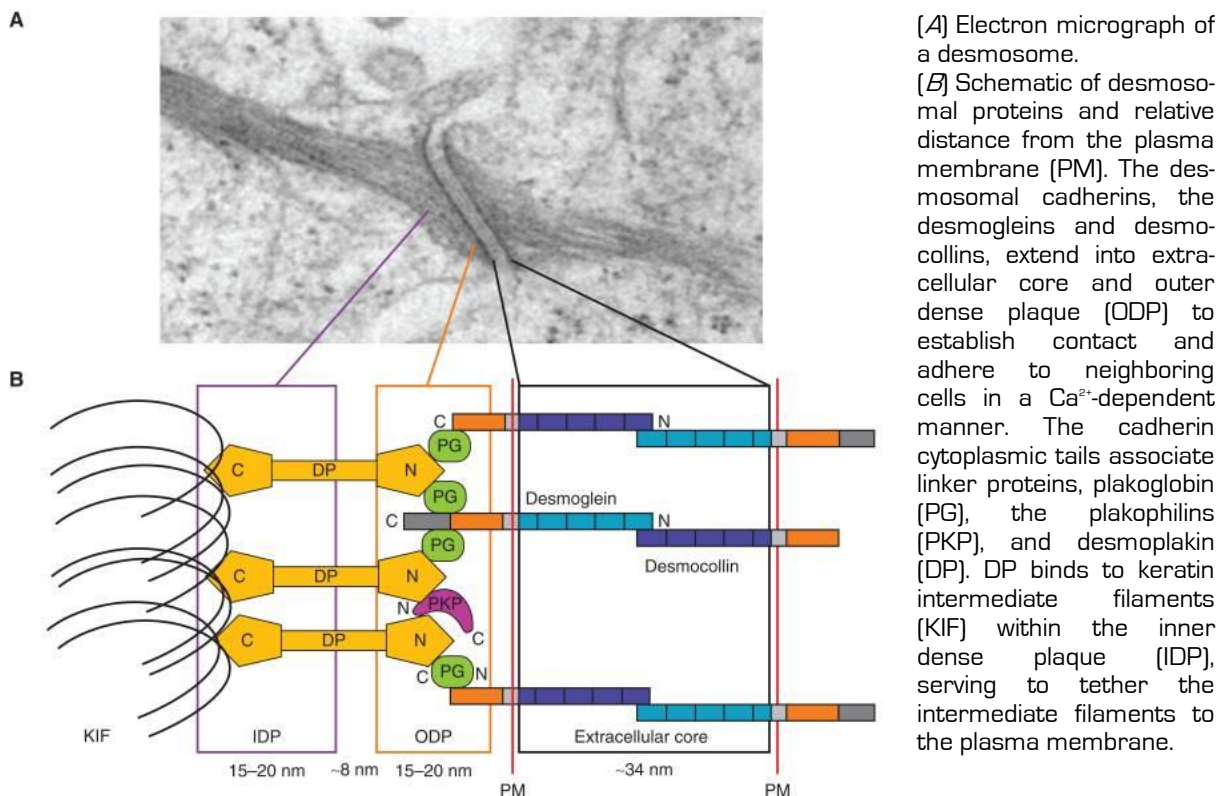
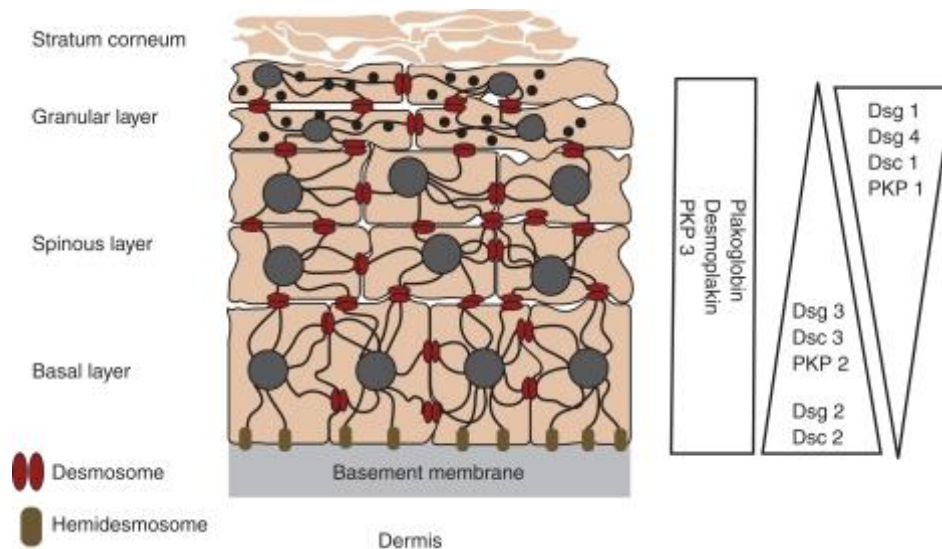


Figure 58: Expression patterns of the desmosomal cadherins in the epidermis. (From Delva E, Tucker DK, Kowalczyk AP. The desmosome. Cold Spring Harb Perspect Biol 2009; 1:a002543)



Expression patterns of the desmosomal cadherins in the epidermis. The epidermis is a stratified epithelium comprised of four distinct layers—the basal layer, spinous layer, granular layer, and the stratum corneum. Keratin filaments are shown connecting to desmosomes at sites of cell-cell contact and to hemidesmosomes at the basement membrane. The relative expression profiles of the various desmosomal cadherins and plaque proteins in the epidermal layers are depicted on the *right*.

functions in epithelial proliferation and differentiation, as well as the strong cell-cell adhesion that is required for tissue integrity (Delva 2009).

DNA microarrays, such as Affymetrix GeneChips, are a powerful and cost-effective tool to analyze expression from thousands of genes simultaneously. But when analyzing and interpreting the data one has to keep in mind, that there are no standard methods available for that, yet, and that therefore fold-changes can vary greatly depending on the algorithms used. More than 50 methodological proposals for processing Affymetrix GeneChip data have been published (Noriega 2009). In addition, a certain level of fold change compression (often two- to tenfold compared to qRT-PCR) has to be expected for microarrays (Conway and Schoolnick 2003). This phenomenon might be due to various technical limitations like limited dynamic range, signal saturations, and cross-hybridizations as well as by certain data-processing/normalization algorithms that aim to reduce variances (Wang 2006). To reduce cross-hybridization effects Affymetrix GeneChips probe pairs consist of a perfect match (PM) sequence and a mismatch (MM), which have one mismatched base pair located at the center of the sequence (Noriega 2009). However, it is also debated on which method is best to integrate PM and MM hybridization signal intensities into an assembled signal for each gene (Irizarry 2006). Further factors causing variation in data analysis are differences in RNA quality or quantity, the microarray manufacturing process, hybridization conditions, and scanning efficiency (Noriega 2009). Wang et al (2006) have shown that microarrays have acceptable sensitivity and accuracy in detecting differential expression, especially for genes with high and medium expression levels and for detecting > 2-fold changes. Therefore microarray performance can be accepted as a reliable exploratory tool for genome-wide gene expression analysis. At low expression levels, however, the overall accuracy of differential expression detection decreases significantly and the detection of small fold changes < 2-fold is relatively poor in sensitivity (Wang 2006).

Because of the limitations of microarrays it is strongly recommended to verify data of the most suggestive genes with qRT-PCR (Ehrenreich 2006). This method does not require post-amplification manipulation, produces quantitative data with an accurate dynamic range of 7 to 8 log of magnitude, and is characterized by single-copy sensitivity (Morrison 1998, Palmer 2003). It has lower coefficients of variation (SYBR Green at 14.2%) than end point assays such as probe hybridization (45.1%) (Schmittgen 2000), it can discriminate between messenger RNAs with almost identical sequences (Wong 2005), and results can be obtained rapidly (Derveaux 2009). Therefore qRT-PCR is referred to as

the “gold standard” for gene expression measurements (Wang 2006, Mackay 2002). On the contrary the limitations of qRT-PCR are not to be underestimated. Due to its very high sensitivity accuracy of the results and reliability of conclusions extremely depend on critical quality issues. First of all RNA purity and integrity have to be assured as well as absence of contaminating DNA. The last issue might be limited by proper DNase treatment after sample extraction and using intron spanning primers in the qRT-PCR reaction (Derveaux 2009). In addition, minor variations in reaction components (Bustin 2002), thermal cycling conditions, enzyme efficiencies, and mispriming events during the early stages of the reaction can lead to differing amounts of amplified products (Wong 2005). PCR inhibitors like transcriptase enzyme carried over from cDNA synthesis or inhibitors originating from the samples and carried over during RNA preparation may affect reaction kinetics (Liss 2002, Lekanne Deprez 2002, Tichopad 2004). Secondary structure of RNA and protein complexes bound to the RNA template may also interfere with cDNA synthesis by causing enzyme pausing, dissociation, or skipping over looped regions (Liss 2002). Furthermore one has to keep in mind that complex *in vivo* tissues, such as skin biopsies, contain several different cell types and composition can vary greatly from sample to sample. This inevitably results in the averaging of the expression of different cell types and the expression profile of a specific cell type may be masked, lost or ascribed to and dismissed as illegitimate transcription because of the bulk of the surrounding cells (Bustin 2002). Finally it has also been reported that significant variations are due to the person performing the experiment (Bustin 2002) and that precision pipeting and pipet calibration are essential for preventing cumulative error (Wong 2005). Even the most careful pipeting technique may have a 1% relative error which will result with a 10-fold dilution in a 1% error in amplification efficiency (Peirson 2003). Another very much discussed aspect of qRT-PCR concerns normalization to internal reference genes (Bustin 2002, Hruz 2011). Reference genes are expected to be stable in their expression and therefore correlate strongly with the total amounts of mRNA present in each sample. It has been repeatedly shown, though, that expression stability is very much tissue dependent and some may also be affected by experimental conditions (Hong Cai 2007). To reduce this effect, it is recommended to use several reference genes for normalization if many target genes are assayed (Vandesompele 2002). The numbers of reference genes used are a trade-off between practical considerations and assay validity within an experimental design (Hong Cai 2007).

To verify the expression data obtained by microarray for the most suggestive keratin, cadherin, catenin and desmoglein genes qRT-PCR analysis was conducted. As expected, due to fold change compression, fold change levels obtained from gene expression analysis

using qRT-PCR were generally higher. This is especially true for the analyzed keratin genes in skin samples, which reached expression levels of approximately 20 to 250fold and desmoglein 4 expression in skin samples with a tenfold higher expression level compared to the array data. In contrast to the array data the qRT-PCR data showed a decrease of desmoglein 2 expression in DEBR skin (fold change 0.5) and heart samples (fold change 0.14), as well as decreased expression levels of cadherin 1 (fold change 0.48), desmoglein 1 (fold change 0.63) and 4 (fold change 0.61) in DEBR heart samples. In addition greater variances in expression levels were detected between samples (especially in skin) leading to higher standard deviations as in the data obtained by microarray analysis. These findings might be ascribed to the higher sensitivity of the qRT-PCR method and to the fact that skin is a complex tissue with varying cell type composition in different samples.

Both, microarrays and qRT-PCR, measure the steady state mRNA levels only. When interpreting the data one has to keep in mind, that these methods give no information about transcription levels, mRNA stability, post-transcriptional regulation, or post-translational modifications. In addition the data obtained is totally uninformative about protein activity and possible mutations that the target gene might harbor. Therefore in some cases it might be necessary to obtain additional insight through immunohistochemical stainings or biochemical assays. (Bustin 2002)

To further clarify the findings from these expression analyzes immunohistological stainings of adherens junction and desmosomal proteins were made to check for protein levels and protein localizations within the cells.

2. Histological Analyzes

Standard HE-stainings were made for the diagnosis of alopecia areata in all rat skin samples. In addition immunohistological stainings were made for cadherins 1 – 5 and 15, desmoglein 1, and catenins alpha, beta, gamma, and p120 in skin samples from DEB and PVG rats. No differences in protein level or localization could be detected between the different rat strains except for catenin gamma which is also known as plakoglobin or junctional plakoglobin (Jup). Protein levels of plakoglobin decreased with continuing hair loss in DEB rat skin cumulating in a complete loss of plakoglobin in severely affected animals.

As mentioned above, plakoglobin is an important linker protein in desmosomes as well as adherens junctions and interacts with several other proteins like desmogleins 1 and 2, desmocollin 1, desmoplakin, cadherin 1, 2, and 3, catenin alpha and beta (Trojanovsky 1994, Hazan 1998, Sacco 1995, Klingelhöfer 2000, Ozawa 1995, Kowalczyk 1997). It is mainly expressed in the skin and the heart with mutations in its gene giving rise to a broad spectrum of phenotypes affecting these two organs (Pigors 2011). It shares high sequence identity (>80%) with catenin beta which can substitute for plakoglobin at many cellular junctions as has been shown in plakoglobin null-mutant mice (Bierkamp 1999). But the affinity of catenin beta to desmogleins is a lot lower suggesting why rather plakoglobin than catenin gamma locates to desmosomes (Choi 2009). Plakoglobin therefore plays a crucial role in normal desmosome plaque assembly. Deletions or loss-of-function give rise to diminished plaques with loss of desmoplakin and intermediate filaments attachment (Acehan 2008). Plakoglobin null-mutant mice usually die between E10.5 and birth, due to fragility of the myocardium (desmosomes are absent, but extended adherens junctions contain desmosomal components) and acantholysis (Bierkamp 1996, Ruiz 1996, Acehan 2008). The few mutant mice offspring that are born show serious epidermal fragility, severe cardiac defects, and early postnatal lethality (Bierkamp 1996). Furthermore evidence has been found that plakoglobin translocation initiates nuclear signaling in epidermis and in myocardium that alter the Wnt/catenin beta signaling pathway (Hu 2003, Garcia-Gras 2006) and it has been shown that plakoglobin overexpression in mouse epidermis decreases keratinocyte proliferation and shortens the anagen phase of the hair cycle (Charpentier 2000).

In humans plakoglobin gene mutations are known to be associated for example with Naxos disease (first described by Protonotarios 1986) which is an autosomal recessive disorder characterized by arrhythmogenic right ventricular cardiomyopathy (ARVC), woolly hair, and palmoplantar keratoderma. The rest function of a truncated form of plakoglobin prevents embryological death, skin fragility and limiting palmoplantar keratoderma to non-

epidermolytic and might be the explanation for the milder phenotype in humans versus mice [Bolling 2009]. Another plakoglobin mutation associated with the disease ARVD12 has been described by Asimaki et al. in 2007 with an autosomal dominant mode of inheritance in a family with non-syndromic ARVC. The patients also showed normal hair and skin growth. Just recently a new plakoglobin homozygous nonsense mutation has been found by Pigors et al. [2011] in a patient with a very severe phenotype. This mutation leads to a complete loss of plakoglobin in the patient's skin. The expression and distribution of desmosomal components is severely affected, only very few abnormal desmosomes are formed and no adhesion structures between keratinocytes are recognizable. This leads to extreme congenital skin fragility with generalized epidermolysis and massive transcutaneous fluid loss causing perinatal death. Cardiac dysfunctions were not observed but might have developed later in life, similar to patients with Naxos disease and ARVD12. In addition qRT-PCR analysis showed reduced expression of direct binding partners of plakoglobin at the transcriptional level in the patient, suggesting regulatory functions of plakoglobin for gene expression of desmosomal cadherins and desmoplakin [Lewis 1997]. Interestingly, the parents of the child were first cousins and one of the other 3 children was affected by alopecia totalis. Further examination of the patient also revealed complete absence of the scalp hair and onycholysis.

Due to the fact, that plakoglobin is not only an important protein in normal skin structure but also in heart tissue immunohistological as well as standard HE-stainings were repeated in DEB rat and BDIX rat heart sections. As observed in skin, no changes in protein level or localization were found between the different rat strains except for plakoglobin. These findings suggest that the mRNA downregulation of cadherin 1, desmoglein 1 and 4 observed with qRT-PCR analysis in DEBR heart samples are either an artifact (for explanations see discussion above) or the generated mRNA is still enough to produce the amount of protein needed in the cells. One has to keep in mind though, that protein quantification is not precise with immunohistochemical staining and small variations in protein levels might not be discerned. Plakoglobin instead, showed normal expression levels of mRNA in both microarray and qRT-PCR analysis. The immunohistochemical stainings, however, showed a prominent decrease in protein level with continuing hair loss in DEB rat skin and heart samples cumulating in a complete loss of plakoglobin in severely affected animals. In addition, DEBR heart sections enlarged with 40x magnification showed some cells with a lost concentrated localization of plakoglobin at cell-cell contact sites. It is found diffusely within the cell instead. Taking into account the expression analysis data one might speculate that plakoglobin is expressed in normal levels and is incorporated in cell-cell

adhesion complexes in a regular manner. With ongoing hair loss plakoglobin seems to lose its binding capacity to the cell-cell adhesion complex and is therefore found diffusely within the cytoplasm of the cell, where it is degraded over time. One of the binding partners of plakoglobin is desmoglein 2 in desmosomes found in heart cells (Bannon 2001, Wahl 2000, Ozawa 1995). As mentioned above, decreased desmoglein 2 mRNA levels in DEBR skin and especially prominent in heart were detected with qRT-PCR. Another binding partner of plakoglobin is the desmosomal cadherin 1 (Knudsen 1992) which also showed downregulated mRNA levels in DEBR heart tissue but was not peculiar in immunohistochemical stainings compared to the control skins. As mentioned before, though, one has to keep in mind that protein quantification is not precise with immunohistochemical staining and small variations in protein levels might not be discerned. However, these findings again support the assumption of a structural defect as a secondary effect to the basic cause of alopecia.

In addition to skin, some heart samples were also HE-stained. These showed no abnormalities in DEB rats with an early onset of hair loss. In DEB rats with a severe phenotype, however, a loss of cell-cell adhesion could be observed in anterior and posterior papillary muscle. It is not clear if this observation is due to the advanced age of the severely affected DEB rats or if this observation is linked with the progressive state of alopecia areata in the rats. Studies of age-related variations in the papillary muscle of rats have been reported previously showing that the density of myocytes, connective-tissue, capillaries, cross-sectional area of myocytes, as well as physical and biochemical characteristics of the papillary muscle are dependent upon age (Maifrino 2009). On the contrary, qRT-PCR analysis showed a decrease in desmoglein 2 at the transcriptional level which functions as a protein besides desmocollin 2 as the extracellular linkers in desmosomes of the myocardium but not in skin where desmogleins 1, 3, 4, desmocollins 1 and 3 as well as corneodesmosin form the extracellular linkage (Maifrino 2009). This might explain why only the heart tissue is affected whereas there is no tissue rupture observed in the skin. In humans, cumulating heart anomalies have not been reported in alopecia patients.

Luckily, it was possible to obtain scalp biopsies from a patient with alopecia areata (one biopsy from an area on the scalp where the hair is still growing normally and one biopsy from the center of a hair loss patch) and a patient with alopecia universalis. These samples were also used for standard HE and immunohistological stainings. HE staining supported the diagnosis of alopecia. The immunohistological staining of plakoglobin showed the same

phenomena in humans as found in the DEBR skin. Plakoglobin is strongly expressed and localized in a dense line at cell-cell adhesion sites in the skin that was obtained from a hairy patch of the scalp in the alopecia areata patient. The fluorescence decreases considerably in the hairless patch of the alopecia areata patient and is finally completely absent in the skin of the alopecia universalis patient. Due to these findings and the functions and importance of plakoglobin in cell-cell adhesion, it would be very interesting to obtain heart biopsies from alopecia patients for immunohistological stainings and expression analysis, even though heart diseases are not common among affecteds. Still, there might be an underlying asymptomatic defect. In addition to plakoglobin, cadherin 3 and 15 also showed abnormalities. Both proteins show an intense staining at the cell-cell adhesion sites in the epidermis and only little staining can be detected within the cytoplasm in the skin biopsy of the alopecia areata patient from a patch where hair is still growing. In the hairless patch of skin the fluorescence intensity decreases at the cell-cell adhesion sites and in addition increases within the cytoplasm of the cells. In the alopecia universalis patient no staining is possible in all but the granular layer of the epidermis.

Cadherin 3, also known as P-cadherin, is one of the major classical cadherins expressed in human epidermis and is localized only at the cell membrane of basal cells in normal epidermis (Hakuno 2001). Hakuno et al. (2001) demonstrated P-cadherin staining in the basal as well as the suprabasal layers similar to the findings in this study in acantholytic lesion of pemphigus vulgaris and pemphigus foliaceus. The upregulation of P-cadherin might be due to altered signaling pathways involved in proliferation and differentiation like the Wnt/catenin beta signaling pathway. Furthermore, P-cadherin is involved in hair follicle morphogenesis (Jamora 2003). Mutations in the gene encoding P-cadherin have been found to cause hypotrichosis with juvenile macular dystrophy (HJMD) as well as ectodermal dysplasia, ectrodactyly and macular dystrophy (EEM) which both are characterized by abnormal hair conditions (Shimomura 2008).

Cadherin 15, also known as M-cadherin, is another member of the classical cadherins and has been described as an important mediator of cell adhesion and complex formation with catenins in myogenic mouse cells (Kuch 1997), especially during skeletal muscle cell differentiation (Donalies 1991). It is also expressed in the brain and cerebellum and mutations in M-cadherin have been shown to cause decreased cell adhesions that might be responsible for causing autosomal dominant mental retardation-3 (MRD3) (Bhalla 2008). However, Hollnagel et al. (2002) hypothesized that M-cadherin is not necessarily required for muscle and cerebellar development since experiments with M-cadherin null-mutant

mice showed an almost complete compensation by N-cadherin. Up to date, M-cadherin has not been described in combination with skin defects.

In conclusion, the findings from the expression analysis in combination with the histological findings point to an important role of desmosomes and adherens junctions in the pathogenesis of alopecia areata. An underlying involvement of signaling pathways, such as the Wnt/catenin beta signaling pathway is probable and should be further analyzed. In addition, electron microscopic analyzes are planned to have a closer look at the structure of desmosomes and adherens junctions in the skin of DEB rats in different phenotype stages. This, in combination with refined expression analysis, should result in a better understanding of the point of time in which plakoglobin loses its binding capacity to the adhesion complex and gives deeper insights into the structural consequences before and after losing the most important linker protein in the desmosomal protein complex.

3. Genetic Analyzes

Prior to this study DEB rats were intercrossed with PVG rats that gave an F2 population with 320 females. A whole genome scan for linkage was performed by the dermatogenetic group of the CCG using 176 microsatellite markers which gave significant results for a locus on chromosome 19 with a highly significant lod score of 20. Therefore this region was mapped with 13 more microsatellite markers and haplotype analysis resulted in a candidate region between 33 and 36.5Mb (rn4). All exons of the most suggestive genes were then sequenced but no mutations could be found that would give clues to the causes of alopecia. Consequently, the candidate region was then sequenced again in toto by Next Generation Sequencing (NGS). 6 DNA samples in total were used for that from 3 control rat strains (Wistar, PVG, and BDIX), 1 unaffected DEB rat, 1 histologically affected DEB rat, and one affected DEB rat. A target sequence capture of 70.2% was reached. To genetically characterize the affected DEB rats the variations specific for the affected DEB rat were identified by deleting all variations found in common with any of the variations found in the other samples. This resulted in 117 specific variations with a base coverage of at least 30 for the affected DEB rat, including 87 intergenic, 29 intronic, and 1 synonymous coding variation. The same procedure resulted in 337 specific variations with a base coverage of at least 30 characterizing the histologically affected DEB rat, including 304 intergenic, 32 intronic, and 1 UTR variation. The affected and the histologically affected DEB rat have 91 variations with a base coverage of at least 30 in common, including one non-synonymous amino acid change (Pro764Thr) in the pseudogene RGD1562390 besides 73 intergenic, 16 intronic, and 1 UTR variation. Additionally, NGS data was compared to the results obtained by Sanger sequencing. Some of the variations found by Sanger sequencing could not be reproduced in the NGS data. Other variations found were also detected in the control rat strains. In conclusion, a mutation as a potential cause for hair loss in alopecia areata could again not be identified. Due to the very high lod score of 20 obtained in linkage analysis and the high number of intergenic variations found in the DEB rats the data should be analyzed again with the aid of bioinformatic software to check for unknown genes in the candidate region and for sequences of regulatory elements such as promoters or enhancers.

Also prior to this study, a genome wide association study (GWAS) has been conducted by the dermatogenetic group of the CCG with human samples pointing to a significant region on chromosome 19. This region was then fine mapped in 1420 samples, including 353 unrelated controls, using SNPstream analysis, pyrosequencing and Taqman analysis in this study. The obtained data was cleaned of mendelian errors and unlikely phenotypes and then

further processed with the softwares PLINK and Merlin. Testing for association with PLINK in a dominant and a recessive model in 407 cases and 353 unrelated controls gave no significant results since all calculated p-values were considerably higher than 0.05. In addition a transmission disequilibrium test (TDT) was performed with the PLINK software using data from 199 trio families which also did not give significant results. With the software package MERLIN an affected sib pair (ASP) linkage analysis was performed for 77 families including 320 individuals resulting in 2 significant loci with lod scores above 2.6. The first region was defined at chr19:41876810..41895089 (Build36.3) with the highest HLOD score for SNP rs1830031 of 2.886 and the highest npLOD score of 3.240. This first region includes the gene ZNF567 only. The second region was defined at chr19:42067119..42445079 (Build36.3) with the highest HLOD score for SNP rs496730 of 2.971 and the highest npLOD score of 3.510. This second region includes 9 genes of which 6 are zinc finger proteins with ZNF568 lying closest to the SNP with the highest lod score. Another analysis performed with MERLIN was a family based linkage analysis showing two significant loci with lod scores above 3.6. The first region was defined at chr19:41876810..41895089 (Build36.3) with the highest HLOD score of 3.739 and the highest npLOD score of 3.730 for SNP rs1830031. This region is therefore identical to the first region found with ASP analysis but with higher lod scores. The second region was defined at chr19:42022453..42586308 (Build36.3) with the highest HLOD score of 4.374 and the highest npLOD score of 4.740 for SNP rs496730. This second region overlaps with the second region found with ASP analysis and gives the highest lod score with the same SNP. This region includes 14 genes of which 8 are zinc finger proteins with ZNF568 lying closest to the SNP with the highest lod score. The zinc finger genes ZNF567 and ZNF568 were then screened for mutations with a combination of high resolution melting curve analysis and sequencing but no mutations could be found. All variations could be accounted for as known SNPs.

Zinc finger proteins are relatively small molecules folding around one or more zinc ions. Depending on their function and the arrangement of their zinc-binding residues more than 20 classes of zinc finger proteins have been identified [Krishna 2003]. About 2% of the proteins encoded by the human genome contain zinc finger domains [Matthews 2002]. The common feature of all zinc finger domains in protein complexes is to mediate interactions with DNA, RNA, other proteins, or lipids [Wolfe 2000, Brown 2005, Mackay 1998, Matthews 2002]. The majority of zinc finger proteins are classified as classical or C2H2 zinc fingers, which ligate zinc with pairs of cysteine and histidine residues and are known for their involvement in transcriptional regulation [Matthews 2002]. ZNF567 and

ZNF568 are examples of classical zinc fingers since both of them are characterized by 15 C₂H₂-type zinc fingers. Nothing has been reported up to date about their specific function but data from the Human Protein Atlas Project show the absence of ZNF567 expression in skin via immunohistological stainings and a low RNA abundance of ZNF568 in skin but no evidence at protein level in the cell line A-431 derived from skin (www.proteinatlas.org).

Additionally, more blood samples of alopecia patients and if possible from their family members were collected and genotyped with the Affymetrix Genome-Wide Human SNP Array 6.0. Together with the aforementioned samples that have already been genotyped with the Affymetrix Human Mapping 500K Array a case control genetic association analysis could be conducted with the software package PLINK including 258.673 SNPs after checking for mendelian errors and unlikely genotypes. Data of 2.891 individuals was used in this analysis including 357 cases and 2534 unrelated controls from the biobank KORA and POPGEN. Under the assumption of a recessive mode of inheritance no significant p-values were reached. The assumption of a dominant mode of inheritance, instead, showed loci on chromosomes 5, 6, and 16 exceeding the significance threshold of 1e-06. Two significant loci were found on chromosome 5. The first region was defined at Chr5:5334408..5361229 (Build36.3) with the lowest p-value of 5.55e-6 for SNP rs7720820 including the gene ADAMTS16 only.

ADAMTS16 is one of 19 members in the disintegrin and metalloproteinase with thrombospondin motifs protein family. Molecules in this family are characterized by several distinct protein modules, including a signal peptide, a propeptide region, a metalloproteinase domain, a disintegrin-like domain, as well as a thrombospondin type 1 motif and a cysteine rich domain [Porter 2005]. Functions of these proteins include the degradation of aggrecan (a large aggregating proteoglycan which is a major structural component of cartilage) at specific loci with ADAMTS5 as the major aggrecanase in cartilage destruction in mice [Glasson 2005], degradation of cartilage oligomeric matrix protein [Dickinson 2003], and collagen biosynthesis [Colige 2002]. ADAMTS16 is highly expressed in fetal lung and kidney as well as adult brain and ovary [Cal 2002] but has not been found expressed in skin. The function of the protein is still unknown but a weak aggrecanase activity has been shown recently in a recombinant truncated form of ADAMTS16 [Zeng 2006] and a full length recombinant ADAMTS16 is capable of cleaving the proteinase inhibitor alpha2-macroglobulin [Gao 2007].

The second region exceeding the significance threshold of 1e-06 found on chromosome 5 was defined at Chr5:130616449..131269677 (Build36.3) with the lowest p-value of

8.76e-7 for SNP rs27421 including 7 genes (CDC42SE2, LOC100505941, RAPGEF6, FNIP1, ACTBP4, LOC100505572, LOC728637).

As an immunologically relevant gene it has been suggested that CDC42SE2 might induce actin filament assembly in the cytoskeleton by acting downstream of CDC42 and that it may play a role in CDC42-mediated F-actin accumulation at the immunological synapse in activated T-cells (Pirone 2000, Ching 2005). It is widely expressed but at higher levels in T lymphocytes (Ching 2005).

Three significant loci were found on chromosome 6. The first region was defined at Chr6:29730199..29803284 (Build36.3) with the lowest p-value of 4.87e-06 for SNP rs29228 including 5 genes (HLA-F, ZFP57, MOG, and 2 pseudogenes). The second region was defined at Chr6:32497626..32790840 (Build36.3) with the lowest p-value of 4.34e-09 for SNP rs9268856 including 7 HLA genes. HLA stands for human leukocyte antigen system and is part of the human major histocompatibility complex (MHC). HLA genes play an important role in the immune system and autoimmunity by presenting antigens to killer T-cells or T-lymphocytes. The third region was defined at Chr6:150314225..150403682 (Build36.3) with the lowest p-value of 3.14e-07 for SNP rs5017316 including 5 genes (ULBP1, LOC646024, RAET1L, LOC100131886, and 1 pseudogene). ULBPs are ligands for the NKG2D receptor and belong to the MHC class I family. They are stress induced molecules that activate multiple signaling pathways in primary natural killer cells, resulting in the production of cytokines and chemokines (Eagle 2007, Sutherland 2002). Petukhova et al. (2010) suggested that ULBP3 is capable of inducing autoimmune destruction in the dermal sheath of the hair follicle in alopecia areata.

The one significant loci on chromosome 16 was found at Chr16:11014208..11115395 (Build36.3) with the lowest p-value of 7.40e-07 for SNP rs3893660 including one pseudogene and CLEC16A. CLEC16A (C-type lectin domain family 15) belongs to the CLEC16A/gop-1 family and is almost exclusively expressed in immune cells, including dendritic cells, B lymphocytes, and natural killer cells (Hakonarson 2007). Polymorphisms in CLEC16A have been associated with an increased risk of multiple sclerosis (Nischwitz 2011) and type 1 diabetes (Zoledziewska 2009) but the function of the protein is basically still unclear.

Calculation under the assumption of a trend model (using the Armitage Trend Test) led to the same significant loci on chromosomes 5 and 6 whereas the locus on chromosome 16 was not found significant. The second region found significant on chromosome 6 including

the HLA cluster reached p-values as low as $5.35e-12$. In addition to case control analysis a TDT was performed using PLINK software but no SNP clusters could be detected that reached the significance threshold. A family based linkage analysis with 259 families including 855 individuals and 271,150 SNPs using the MERLIN software, however, resulted in significant SNP clusters on chromosomes 10 and 19 reaching npLOD scores of at least 3.6. Three significant SNP clusters were detected for chromosome 10 but only the first one at chr10:414200..698293 (Build36.3) with the highest npLOD score of 3.99 includes 3 genes (DIP2C, LOC642278, C10orf108). There are no known genes within the other SNP cluster regions. DIP2 genes encode members of the disco-interacting protein homolog 2 family which share high similarity with a *Drosophila* protein that interacts with the transcription factor disco and are expressed in the nervous system (Tanaka 2010, Mukhopadhyay 2002). DIP2B has been reported to be associated with at least one human neurocognitive disorder (Winnepenninckx 2007). There is no gene information available for the hypothetical gene LOC642278 and C10orf108.

One significant SNP cluster could be detected for chromosome 19 at Chr19:41413208..43454980 (Build 36.3) with the highest npLOD score of 6.13 for SNPs rs713256 and rs256733 within gene ZNF527. This region contains 48 genes, including 27 zinc finger genes. ZNF527 is another example of a classical zinc finger characterized by 12 C2H2-type zinc fingers. It is weakly expressed in epidermal skin cells (www.proteinatlas.org). Its protein function is also unknown but due to its classification an involvement in transcriptional regulation is probable.

Using a defined smaller set of markers (62,990 SNPs) loses the significant locus on chromosome 10 but the npLOD score still reaches 4.15 within the defined region at Chr19:40562188..43398829 (Build36.3) which contains 93 genes, including KRTDAP, DMKN, SBSN, and 30 zinc finger genes. Lowest npLOD scores were obtained for chromosome 19 using a family based linkage analysis with 83,371 SNPs resulting in the highest npLOD score of 3.87 for SNP rs2239945. The SNP cluster reaching npLOD scores above 3.6 is defined at Chr19:40590481..41163676 (Build36.3). This region contains 31 genes, including KRTDAP, DMKN, and SBSN. Again, chromosome 10 did not show significant loci with this analysis.

KRTDAP may act as a soluble regulator of keratinocyte differentiation and is probably important in embryonic skin morphogenesis. In human skin it is exclusively expressed in lamellar granules of granular keratinocytes and in the intracellular space of the stratum

corneum. It has been found upregulated and expressed more widely throughout suprabasal keratinocytes in situ in psoriatic skin [Tsuchida 2004]. DMKN [dermokine] is another protein that may act as a soluble regulator of keratinocyte differentiation that is expressed in the epidermis [Naso 2007]. This gene has been found upregulated in inflammatory diseases and differentially uses promoters and terminators to generate isoforms with specific cellular distributions and domain components [Naso 2007, Toulza 2006]. SBSN [suprabasin] has been found upregulated in differentiating keratinocytes and therefore may play a role in epidermal differentiation [Park 2002].

The findings of the human GWAS in this study for the HLA and ULBP region on chromosome 6 is in accordance with the results of the GWAS analysis conducted by Pethukova et al. [2010] with 1.054 cases and 3.278 controls, which further reinforces the common concept of an autoimmune mechanism as the basis for alopecia. The second region found significant for chromosome 5 containing the gene CDC42SE2 in this study has also been found in the analysis of Pethukova et al. [2010] with the lowest p-value within that region of $7.13e-06$ for rs1295686. Since they set the significance threshold to $1e-07$ this region was only declared near significant in their analysis. Since both analyzes resulted in a tight SNP cluster in this region it can be suggested that an association with alopecia is probable and further emphasizes the immunological character of the disease due to the suggested function of CDC42SE2. The same applies for a region on chromosome 16 which has been found in association with alopecia in our study including the gene CLEC16A which is exclusively expressed in immune cells, but reached only near significance in the analysis by Pethukova et al. with a p-value of $2.75e-5$ for SNP rs12934193.

The family based linkage analyses in this study gives further insight into the multifactorial character of this complex disease. The genes KRTDAP, DMKN, and SBSN found within a significant region on chromosome 19 have been implicated to mediate keratinocyte differentiation. Keratins, as described earlier, are not only the major component of skin and hair fibers, but are also important signal molecules in different pathways. Since keratin expression is regulated on transcription level it is also intriguing that transcription factor genes like zinc fingers and DIP2C were found within significant regions on chromosome 19 and 10 in this study. To further elucidate these new findings a NGS analysis spanning the region of chromosome 19 with the genes KRTDAP, DMKN, SBSN, and the zinc finger cluster will be conducted shortly.

G Abstract

Alopecia areata (AA) [MIM 104000] is a chronic inflammatory, multifactorial disorder of the hair follicles with a strong genetic basis. It is characterized by circular regions of hair loss on the head or also on other parts of the body. The pathogenesis of the AA is still unknown but a tissue-specific autoimmune mechanism has been suggested.

As an animal model of AA the Dundee Experimental Bald Rat (DEBR) was used. An intercross of DEB with PVG rats gave rise to 320 female F2 rats with which a whole genome scan for linkage with microsatellite markers was performed prior to this study that resulted in one highly significant locus on chromosome 19 with a lod score of 20. In this study saturation mapping of this chromosome with more microsatellite markers was conducted which identified a candidate region at 33 to 36.5 Mb (rn4). Exons from most genes within this region were sequenced but mutations could not be detected. The following sequencing of the candidate region in toto by Next Generation Sequencing (NGS) did also not lead to causative mutations but the high number of intergenic variations suggest the existence of unknown genes within that region or there might be a mutation in a regulatory element of a gene as for example in the promoter or enhancer region. This will have to be checked by further bioinformatic analyzes.

In another approach expression analysis was conducted using the Affymetrix GeneChip® Rat Gene 1.0 ST Arrays. This revealed expression differences for various [hair] keratin genes and genes of other structural components, immunoregulatory genes such as chemokines, and H2 genes, the HLA orthologs. Further analysis of the expression data from genes of the candidate region on chromosome 19 with the network explorer tool from Ingenuity Pathways Analysis pointed to an important role of cadherins. Therefore a set of cadherins, catenins, and desmogleins were immunohistochemically stained in skin samples. This experiment showed a decrease in catenin gamma concentration corresponding to the phenotype. In samples of rats with a severe hair loss catenin gamma was no longer detectable at all. These histological findings could also be seen in rat heart samples and in human skin. In addition to catenin gamma, M- and P-cadherin also showed abnormal protein localizations in the epidermis of human skin. The expression results of suggestive genes were then validated and refined in rat skin and partially also in heart samples with qRT-PCR using the LightCycler 480 System. The expression and staining results point to an involvement of the Wnt/catenin beta signaling pathway and a defect in the cell-cell adherent structures in the pathology of alopecia. In the next step immunohistological stainings will be repeated in rat skin of different stages of hair loss and

looked at with electron microscopy, focusing on desmosomes in hair follicles and the epidermis to obtain further insight into the defective structure of cell-cell-adhesion complexes and the point of time of destruction.

A whole-genome scan for linkage with SNP markers was performed with human samples prior to this study showing one significant locus on chromosome 19. Further fine mapping of the locus on chromosome 19 in 301 families (1131 individuals) was performed in this study with SNPstream, Taqman, and Pyrosequencing. Linkage analysis identified a candidate interval in the region between 37 Mb to 38 Mb (GRCH37) including several zinc finger genes. Highest non parametric lod scores were obtained for SNPs in or near the genes ZNF567 and ZNF568. Therefore these genes were screened for mutations with high resolution melting curve analysis and sequencing. No mutations could be found since all detected variations were due to known SNP markers.

In addition more samples were collected and genotyped with Affymetrix Genome-Wide Human SNP Array 6.0 for a SNP based genome-wide association study (GWAS) including 357 cases and 2534 controls. Significantly associated loci were found on chromosomes 5, 6 (including the HLA region), and 16 (CLEC16A). Linkage analysis with 259 families (855 individuals) furthermore resulted in significant regions on chromosomes 10 and 19 (zinc finger region). With a defined set of SNP markers a candidate region at 35,9 Mb to 36,5 Mb (GRCH37) on chromosome 19 could be identified. In the next step the combined region of 35,9 Mb to 38 Mb (GRCH37) will be sequenced in toto by NGS and screened for mutations.

In conclusion, this study shows a strong association of cellular defects in the skin with the disease which will be further addressed in future experiments with the rat model DEBR in the dermatogenetics group at the CCG. In addition to the already known immunoregulatory genes associated with AA, this study also revealed significant linkage results for loci on chromosome 10 and even more so for chromosome 19, including a zinc finger cluster. These results point out anew that several complex mechanisms contribute to the disease susceptibility.

H Zusammenfassung

Alopecia areata (AA) (MIM 104000) ist eine chronisch entzündliche Erkrankung der Haarfollikel mit einer starken genetischen Komponente. Sie ist durch einen kreisrunden Haarverlust am Kopf oder aber auch an anderen Körperstellen charakterisiert. Die Krankheitsentstehung ist nach wie vor unklar, wobei ein gewebespezifischer Autoimmunmechanismus vermutet wird. Als Tiermodell für AA wurde der Rattenstamm Dundee Experimental Bald Rat (DEBR) verwendet.

Aus einer dieser Studie vorangegangenen Kreuzung aus DEB und PVG Ratten gingen 320 weibliche F2-Tiere hervor, die genomweit mit Mikrosatelliten auf Kopplung analysiert wurden, was zu einem hoch signifikanten Locus auf Chromosom 19 mit einem LOD-Score von 20 führte. In dieser Arbeit wurde daher eine Sättigungskartierung für dieses Chromosom mit weiteren Mikrosatellitenmarkern durchgeführt, die eine Kandidatenregion bei 33 bis 36.5 Mb (rn4) identifizierte. Exone der meisten Gene innerhalb dieser Region wurden sequenziert wobei keine Mutationen als potentielle Ursache für Haarausfall identifiziert werden konnten. Die anschließende komplette Sequenzierung der Kandidatenregion mittels Next Generation Sequencing (NGS) offenbarte ebenfalls keine kausativen Mutationen wobei die hohe Anzahl an intergenetischen Varianten das Vorkommen von bisher unbekanntem Genen innerhalb der Kandidatenregion suggerieren oder es könnte sich bei diesen um Mutationen in regulatorischen Elementen wie beispielsweise in Promotor- oder Enhancer-Regionen handeln. Dies muss in weiteren bioinformatischen Analysen geklärt werden.

Ein weiterer Ansatz wurde mit der Expressionsanalyse mittels Affymetrix GeneChip Rat Gene 1.0 ST Arrays verfolgt. Diese ließ Abweichungen in der Expression von verschiedenen (Haar-) Keratingenen, Genen von weiteren strukturellen Komponenten sowie immunregulatorischen Genen wie Chemokine und H2 Gene (Orthologe zu HLA) erkennen. Weitergehende Auswertungen der Expressionsdaten von Genen der Kandidatenregion auf Chromosom 19 mit dem Programm „Network Explorer“ von Ingenuity Pathways Analysis verwiesen auf eine wichtige Rolle von Cadherinen. Daher wurden einige Cadherine, Catenine und Desmogleine immunhistochemisch in Hautproben angefärbt. Dieses Experiment zeigte eine Reduzierung in der Konzentration von Catenin gamma in Übereinstimmung mit dem Phänotyp. In Proben von Ratten mit einem ausgeprägten Haarverlust war Catenin gamma nicht mehr nachweisbar. Zusätzlich zu Catenin gamma zeigte M- und P-Cadherin ebenfalls eine anormale Proteinlokalisierung in der humanen Epidermis der Haut. Die Resultate der Expressionsanalyse von Kandidatengenen wurden schließlich in Rattenhaut und teilweise auch in Herzproben mittels qRT-PCR (Light Cycler 480 System von Roche) validiert und vertieft. Die Ergebnisse der Expressionsanalyse und der Färbungen

weisen auf eine Beteiligung des Wnt/Catenin beta Signalweges und einem Defekt in den Zell-Zell-Verbindungsstrukturen in der Krankheitsentwicklung von Alopezie hin. Im nächsten Schritt werden immunohistochemische Färbungen in Rattenhaut in verschiedenen Stadien von Haarverlust wiederholt und elektronenmikroskopisch untersucht, wobei der Fokus auf Desmosomen der Haarfollikel und der Epidermis liegt, um ein tiefergehendes Verständnis in die strukturellen Defekte der Zell-Zell-Verbindungskomplexe und dem Zeitpunkt der Zerstörung zu bekommen.

Eine genomweite Kopplungsanalyse mit SNP Marker wurde im Vorfeld zu dieser Studie mit humanen Proben durchgeführt, welche auf einen signifikanten Locus auf Chromosom 19 verwies. Im Rahmen dieser Studie wurde eine Feinkartierung dieses Locus auf Chromosom 19 in 301 Familien (1131 Individuen) mittels SNPstream, Taqman und Pyrosequencing durchgeführt. Eine Kopplungsanalyse identifizierte eine Kandidatenregion bei 37 bis 38 Mb [GRCH37], welche mehrere Zinkfinger Gene beinhaltet. Die höchsten nichtparametrischen LOD-Scores wurden für SNPs in oder nahe der Gene ZNF567 und ZNF568 erzielt. Daher wurden diese Gene auf Mutationen mittels Schmelzkurvenanalyse und Sequenzierung untersucht. Es konnten keine Mutationen gefunden werden, da alle aufgetretenen Varianten auf bekannte SNPs zurückzuführen sind. Zusätzlich wurden für eine SNP basierte genomweite Assoziationsstudie (GWAS) mit 357 Fällen und 2534 Kontrollen weitere Proben gesammelt und mit Affymetrix Genome-Wide Human SNP Array 6.0 genotypisiert. Signifikante assoziierte Loci wurden für die Chromosomen 5, 6 (welches die HLA Region beinhaltet) und 16 (CLEC16A) ausfindig gemacht. Außerdem resultierte eine Kopplungsanalyse mit 259 Familien mit 855 Individuen in signifikanten Regionen auf Chromosom 10 und 19 (Zinkfingerregion). Mit einer definierten Auswahl an SNP Marker wurde eine Kandidatenregion bei 35.9 Mb bis 36.5 Mb [GRCH37] auf Chromosom 19 identifiziert. In einem nächsten Schritt soll die kombinierte Region von 35.9 Mb bis 38 Mb in Gänze mit NGS sequenziert und nach Mutationen untersucht werden.

Abschließend weist die vorliegende Studie auf eine starke Assoziation von zellulären Defekten in der Haut mit AA hin, was in weiterführenden Experimenten mit dem Rattenmodell DEBR in der Dermatogenetikgruppe des CCG weitergehend untersucht werden soll. Zusätzlich zu den bereits bekannten immunoregulatorischen Genen, die mit AA assoziiert sind, konnte diese Studie signifikante Kopplungsbefunde für Loci auf Chromosom 10 und besonders Chromosom 19, welcher ein Zinkfingercluster beinhaltet, ausfindig machen. Diese Resultate machen erneut deutlich, dass komplexe Mechanismen zu der Suszeptibilität der Krankheit beitragen.

I Danksagung

An erster Stelle möchte ich aus tiefstem Herzen meinen Eltern danken. Ihr seid einfach spitze und absolut unersetzlich! Vielen Dank für eure Unterstützung und euren Zuspruch.

Mein besonderer Dank gilt ebenso Dr. Mohammad Reza Toliat, der mir während der letzten Jahre ein hervorragender Lehrer und Mentor gewesen ist. Meine Kolleginnen Kerstin Becker, Janine Kurtenbach und Kerstin Wodecki sind Freundinnen geworden und ich werde euch und unser regelmäßiges, gemeinsames Brainstorming genauso wie unsere regelmäßigen CCG Girl's Day Veranstaltungen sehr vermissen. Wir waren sowohl beruflich als auch privat ein tolles Team und unser gemeinsamer Abenteuerurlaub in New York City wird für uns alle ganz bestimmt unvergessen bleiben. Vielen Dank für eure Unterstützung Mädels! Ihr seid eine Bereicherung für mein Leben.

Außerdem möchte ich unbedingt dem ganzen Team vom Barista in der Kyffhäuserstraße in Köln danken. Bei euch haben wir gelacht und geweint, Pläne geschmiedet und die Seele baumeln lassen und haben nebenbei immer den stadtbesten Kaffee und die verführerischste Tiramisu bekommen. Macht weiter so!

Ganz besonders bedanken möchte ich mich auch bei den beiden Alopeziepatienten Andreas K. und Sandra S. Ohne ihre Kopfhautspenden wären viele Einsichten in das Krankheitsbild nicht möglich gewesen und ich hoffe, dass die Ergebnisse meiner Arbeit vielen weiteren Wissenschaftlern Anregungen geben werden weiter zu forschen und letztlich des Rätsels Lösung zu finden.

J List of Literature

- D. Acehan, C. Petzold, I. Gumper, D. D. Sabatini, E. J. Muller, P. Cowin, and D. L. Stokes. Plakoglobin is required for effective intermediate filament anchorage to desmosomes. *J.Invest Dermatol.* 128 (11):2665-2675, 2008.
- G. Achten. [Keratinization of the skin in humans]. *Arch.Belg.Dermatol.Syphiligr.* 12 (2):104-106, 1956.
- H.G. Adamson. Coulstonian lectures on modern views upon the significance of skin. London, *John Bale, Sons and Danielsson Ltd* 1912
- A. Asimaki, P. Syrris, T. Wichter, P. Matthias, J. E. Saffitz, and W. J. McKenna. A novel dominant mutation in plakoglobin causes arrhythmogenic right ventricular cardiomyopathy. *Am.J.Hum.Genet.* 81 (5):964-973, 2007.
- Bailly. L'origine gingivodentaire de la pelade. Lyons, France. 1910
- L. J. Bannon, B. L. Cabrera, M. S. Stack, and K. J. Green. Isoform-specific differences in the size of desmosomal cadherin/catenin complexes. *J.Invest Dermatol.* 117 (5):1302-1306, 2001.
- R. Baran, R.P.R. Dawber. Diseases of the nails and their management. Oxford, *Blackwell Scientific Publications* 1984.
- K. Bhalla, Y. Luo, T. Buchan, M. A. Beachem, G. F. Guzauskas, S. Ladd, S. J. Bratcher, R. J. Schroer, J. Balsamo, B. R. DuPont, J. Lilien, and A. K. Srivastava. Alterations in CDH15 and KIRREL3 in patients with mild to severe intellectual disability. *Am.J.Hum.Genet.* 83 (6):703-713, 2008.
- C. Bierkamp, H. Schwarz, O. Huber, and R. Kemler. Desmosomal localization of beta-catenin in the skin of plakoglobin null-mutant mice. *Development* 126 (2):371-381, 1999.
- C. Bodemer, M. Peuchmaur, S. Fraitag, L. Chatenoud, N. Brousse, and Prost Y. De. Role of cytotoxic T cells in chronic alopecia areata. *J.Invest Dermatol.* 114 (1):112-116, 2000.
- M. C. Bolling and M. F. Jonkman. Skin and heart: une liaison dangereuse. *Exp.Dermatol.* 18 (8):658-668, 2009.
- J.T. Bowen. Two epidemics of alopecia areata in an asylum for girls. *J of Cutaneous and Genito-Urinary Disease* 17:399-404, 1899.
- O. Braun-Falco. [Dynamics of normal and pathological hair growth]. *Arch.Klin.Exp.Dermatol.* 227 (1):419-452, 1966.
- R. S. Brown. Zinc finger proteins: getting a grip on RNA. *Curr.Opin.Struct.Biol.* 15 (1):94-98, 2005.
- G.A. Bubenik. Why do humans get "goosebumps" when they are cold, or under other circumstances? *Scientific American* 2003
- S. A. Bustin. Quantification of mRNA using real-time reverse transcription PCR (RT-PCR): trends and problems. *J.Mol.Endocrinol.* 29 (1):23-39, 2002.
- J. H. Cai, S. Deng, S. W. Kumpf, P. A. Lee, P. Zagouras, A. Ryan, and D. S. Gallagher. Validation of rat reference genes for improved quantitative gene expression analysis using low density arrays. *Biotechniques* 42 (4):503-512, 2007.
- S. Cal, A. J. Obaya, M. Llamazares, C. Garabaya, V. Quesada, and C. Lopez-Otin. Cloning, expression analysis, and structural characterization of seven novel human ADAMTSSs, a family of metalloproteinases with disintegrin and thrombospondin-1 domains. *Gene* 283 (1-2):49-62, 2002.
- C. Caulin, C. F. Ware, T. M. Magin, and R. G. Oshima. Keratin-dependent, epithelial resistance to tumor necrosis factor-induced apoptosis. *J.Cell Biol.* 149 (1):17-22, 2000.
- E. D. Cetin, E. Savk, M. Uslu, M. Eskin, and A. Karul. Investigation of the inflammatory mechanisms in alopecia areata. *Am.J.Dermatopathol.* 31 (1):53-60, 2009.
- E. Charpentier, R. M. Lavker, E. Acquista, and P. Cowin. Plakoglobin suppresses epithelial proliferation and hair growth in vivo. *J.Cell Biol.* 149 (2):503-520, 2000.
- K. H. Ching, A. E. Kisailus, and P. D. Burbelo. The role of SPECs, small Cdc42-binding proteins, in F-actin accumulation at the immunological synapse. *J.Biol.Chem.* 280 (25):23660-23667, 2005.
- H. J. Choi, J. C. Gross, S. Pokutta, and W. I. Weis. Interactions of plakoglobin and beta-catenin with desmosomal cadherins: basis of selective exclusion of alpha- and beta-catenin from desmosomes. *J.Biol.Chem.* 284 (46):31776-31788, 2009.
- T. Christoph, S. Muller-Rover, H. Audring, D. J. Tobin, B. Hermes, G. Cotsarelis, R. Ruckert, and R. Paus. The human hair follicle immune system: cellular composition and immune privilege. *Br.J.Dermatol.* 142 (5):862-873, 2000.
- F.T. Colcott. On a small epidemic of alopecia areata. *Br.J.Dermatol.* 25:51-56 1913.

- A. Colige, I. Vandenberghe, M. Thiry, C. A. Lambert, Beeumen J. Van, S. W. Li, D. J. Prockop, C. M. Lapiere, and B. V. Nusgens. Cloning and characterization of ADAMTS-14, a novel ADAMTS displaying high homology with ADAMTS-2 and ADAMTS-3. *J.Biol.Chem.* 277 (8):5756-5766, 2002.
- B. W. Colombe, V. H. Price, E. L. Khoury, M. R. Garovoy, and C. D. Lou. HLA class II antigen associations help to define two types of alopecia areata. *J.Am.Acad.Dermatol.* 33 [5 Pt 1]:757-764, 1995.
- T. Conway and G. K. Schoolnik. Microarray expression profiling: capturing a genome-wide portrait of the transcriptome. *Mol.Microbiol.* 47 (4):879-889, 2003.
- H. Davis. Epidemic alopecia areata. *Br.J.Dermatol.* 26:207-210 1914.
- Andrade M. de, C. M. Jackow, N. Dahm, M. Hordinsky, J. D. Reveille, and M. Duvic. Alopecia areata in families: association with the HLA locus. *J.Investig.Dermatol.Symp.Proc.* 4 (3):220-223, 1999.
- Decelle. *Bull.et.Mem.Soc.Med.de.Hop.de.Paris* 21:72 1909
- E. Delva, D. K. Tucker, and A. P. Kowalczyk. The desmosome. *Cold Spring Harb.Perspect.Biol.* 1 (2):a002543, 2009.
- S. Derveaux, J. Vandesompele, and J. Hellemans. How to do successful gene expression analysis using real-time PCR. *Methods* 50 (4):227-230, 2010.
- S. C. Dickinson, M. N. Vankemmelbeke, D. J. Buttle, K. Rosenberg, D. Heinegard, and A. P. Hollander. Cleavage of cartilage oligomeric matrix protein (thrombospondin-5) by matrix metalloproteinases and a disintegrin and metalloproteinase with thrombospondin motifs. *Matrix Biol.* 22 (3):267-278, 2003.
- W. E. Dixon. Thallium. *Proc.R.Soc.Med.* 20 (8):1197-1200, 1927.
- M. Donalies, M. Cramer, M. Ringwald, and A. Starzinski-Powitz. Expression of M-cadherin, a member of the cadherin multigene family, correlates with differentiation of skeletal muscle cells. *Proc.Natl.Acad.Sci.U.S.A* 88 (18):8024-8028, 1991.
- H. Druckrey. Genotypes and phenotypes of ten inbred strains of BD-rats. *Arzneimittelforschung.* 21 (8):1274-1278, 1971.
- M. Duvic, A. Nelson, and Andrade M. de. The genetics of alopecia areata. *Clin.Dermatol.* 19 (2):135-139, 2001.
- R. A. Eagle and J. Trowsdale. Promiscuity and the single receptor: NKG2D. *Nat.Rev.Immunol.* 7 (9):737-744, 2007.
- A. Ehrenreich. DNA microarray technology for the microbiologist: an overview. *Appl.Microbiol.Biotechnol.* 73 (2):255-273, 2006.
- D. M. Elston, M. L. McCollough, W. F. Bergfeld, M. O. Liranzo, and M. Heibel. Eosinophils in fibrous tracts and near hair bulbs: a helpful diagnostic feature of alopecia areata. *J.Am.Acad.Dermatol.* 37 (1):101-106, 1997.
- F. Fagotto and B. M. Gumbiner. Cell contact-dependent signaling. *Dev.Biol.* 180 (2):445-454, 1996.
- P. FLESCHE. Chemical data on human epidermal keratinization and differentiation. *J.Invest Dermatol.* 31 (1):63-73, 1958.
- E. Fuchs. Keratins and the skin. *Annu.Rev.Cell Dev.Biol.* 11:123-153, 1995.
- S. Gao, Geyter C. De, K. Kossowska, and H. Zhang. FSH stimulates the expression of the ADAMTS-16 protease in mature human ovarian follicles. *Mol.Hum.Reprod.* 13 (7):465-471, 2007.
- E. Garcia-Gras, R. Lombardi, M. J. Giocondo, J. T. Willerson, M. D. Schneider, D. S. Khoury, and A. J. Marian. Suppression of canonical Wnt/beta-catenin signaling by nuclear plakoglobin recapitulates phenotype of arrhythmic right ventricular cardiomyopathy. *J.Clin.Invest* 116 (7):2012-2021, 2006.
- D. Garrod and M. Chidgey. Desmosome structure, composition and function. *Biochim.Biophys.Acta* 1778 (3):572-587, 2008.
- S. Getsios, A. C. Huen, and K. J. Green. Working out the strength and flexibility of desmosomes. *Nat.Rev.Mol.Cell Biol.* 5 (4):271-281, 2004.
- A. Gilhar, R. Paus, and R. S. Kalish. Lymphocytes, neuropeptides, and genes involved in alopecia areata. *J.Clin.Invest* 117 (8):2019-2027, 2007.
- A. Gilhar. Collapse of immune privilege in alopecia areata: coincidental or substantial? *J.Invest Dermatol.* 130 (11):2535-2537, 2010.
- S. Giovannini. Recherches sur l'histologie pathologique de la pelade. *Annales de Dermatologie et de Syphiligraphie.* 3:923-957 1891

- S. S. Glasson, R. Askew, B. Sheppard, B. Carito, T. Blanchet, H. L. Ma, C. R. Flannery, D. Peluso, K. Kanki, Z. Yang, M. K. Majumdar, and E. A. Morris. Deletion of active ADAMTS5 prevents cartilage degradation in a murine model of osteoarthritis. *Nature* 434 [7033]:644-648, 2005.
- L. A. Goldsmith. Summary of alopecia areata research workshop and future research directions. *J.Invest Dermatol.* 96 (5):98S-100S, 1991.
- H. Gollinck, C.E. Orfanos. Nature et traitement de la pelade – la pelade d'origine dentaire. *Ann.Dermatol.et.de.Syph.* 3:180-190 1902.
- J. M. Gooding, K. L. Yap, and M. Ikura. The cadherin-catenin complex as a focal point of cell adhesion and signalling: new insights from three-dimensional structures. *Bioessays* 26 [5]:497-511, 2004.
- B. Gumbiner. Cadherins: a family of Ca²⁺-dependent adhesion molecules. *Trends Biochem.Sci.* 13 [3]:75-76, 1988.
- H. Hakonarson, S. F. Grant, J. P. Bradfield, L. Marchand, C. E. Kim, J. T. Glessner, R. Grabs, T. Casalunovo, S. P. Taback, E. C. Frackelton, M. L. Lawson, L. J. Robinson, R. Skraban, Y. Lu, R. M. Chiavacci, C. A. Stanley, S. E. Kirsch, E. F. Rappaport, J. S. Orange, D. S. Monos, M. Devoto, H. Q. Qu, and C. Polychronakos. A genome-wide association study identifies KIAA0350 as a type 1 diabetes gene. *Nature* 448 [7153]:591-594, 2007.
- M. Hakuno, M. Akiyama, H. Shimizu, M. J. Wheelock, and T. Nishikawa. Upregulation of P-cadherin expression in the lesional skin of pemphigus, Hailey-Hailey disease and Darier's disease. *J.Cutan.Pathol.* 28 [6]:277-281, 2001.
- R. B. Hazan and L. Norton. The epidermal growth factor receptor modulates the interaction of E-cadherin with the actin cytoskeleton. *J.Biol.Chem.* 273 [15]:9078-9084, 1998.
- M. Hesse, T. Franz, Y. Tamai, M. M. Taketo, and T. M. Magin. Targeted deletion of keratins 18 and 19 leads to trophoblast fragility and early embryonic lethality. *EMBO J.* 19 [19]:5060-5070, 2000.
- R. Hoffmann. The potential role of cytokines and T cells in alopecia areata. *J.Investig.Dermatol.Symp.Proc.* 4 [3]:235-238, 1999.
- A. Hollnagel, C. Grund, W. W. Franke, and H. H. Arnold. The cell adhesion molecule M-cadherin is not essential for muscle development and regeneration. *Mol.Cell Biol.* 22 [13]:4760-4770, 2002.
- B. Holthofer, R. Windoffer, S. Troyanovsky, and R. E. Leube. Structure and function of desmosomes. *Int.Rev.Cytol.* 264:65-163, 2007.
- T. Hruz, M. Wyss, M. Docquier, M. W. Pfaffl, S. Masanetz, L. Borghi, P. Verbrugghe, L. Kalaydjieva, S. Bleuler, O. Laule, P. Descombes, W. Gruissem, and P. Zimmermann. RefGenes: identification of reliable and condition specific reference genes for RT-qPCR data normalization. *BMC.Genomics* 12:156, 2011.
- P. Hu, P. Berkowitz, E. J. O'Keefe, and D. S. Rubenstein. Keratinocyte adherens junctions initiate nuclear signaling by translocation of plakoglobin from the membrane to the nucleus. *J.Invest Dermatol.* 121 [2]:242-251, 2003.
- A. H. Huber and W. I. Weis. The structure of the beta-catenin/E-cadherin complex and the molecular basis of diverse ligand recognition by beta-catenin. *Cell* 105 [3]:391-402, 2001.
- A. C. Huen, J. K. Park, L. M. Godsel, X. Chen, L. J. Bannon, E. V. Amargo, T. Y. Hudson, A. K. Mongiu, I. M. Leigh, D. P. Kelsell, B. M. Gumbiner, and K. J. Green. Intermediate filament-membrane attachments function synergistically with actin-dependent contacts to regulate intercellular adhesive strength. *J.Cell Biol.* 159 [6]:1005-1017, 2002.
- T. Ikeda. Produced alopecia areata based on the focal infection theory and mental motive theory. *Dermatologica* 134 [1]:1-11, 1967.
- R. A. Irizarry, Z. Wu, and H. A. Jaffee. Comparison of Affymetrix GeneChip expression measures. *Bioinformatics.* 22 [7]:789-794, 2006.
- C. A. Jahoda and A. J. Reynolds. Dermal-epidermal interactions. Adult follicle-derived cell populations and hair growth. *Dermatol.Clin.* 14 [4]:573-583, 1996.
- C. Jamora, R. DasGupta, P. Kocieniewski, and E. Fuchs. Links between signal transduction, transcription and adhesion in epithelial bud development. *Nature* 422 [6929]:317-322, 2003.
- D. Jaquemar, S. Kupriyanov, M. Wankell, J. Avis, K. Benirschke, H. Baribault, and R. G. Oshima. Keratin 8 protection of placental barrier function. *J.Cell Biol.* 161 [4]:749-756, 2003.
- I Joseph. Linde 1886-1951. *Conn.State Med.J.* 15 [10]:924, 1951.
- R. S. Kalish and A. Gilhar. Alopecia areata: autoimmunity—the evidence is compelling. *J.Investig.Dermatol.Symp.Proc.* 8 [2]:164-167, 2003.

- S. Kim, P. Wong, and P. A. Coulombe. A keratin cytoskeletal protein regulates protein synthesis and epithelial cell growth. *Nature* 441 (7091):362-365, 2006.
- J.T. Kinnear. Gardiner's handbook of skin diseases. 4th edition. *Edinburgh, E&S Livingstone*. 224-228 1939.
- J. Klingelhofer, R. B. Troyanovsky, O. Y. Laur, and S. Troyanovsky. Amino-terminal domain of classic cadherins determines the specificity of the adhesive interactions. *J.Cell Sci.* 113 (Pt 16):2829-2836, 2000.
- K. A. Knudsen and M. J. Wheelock. Plakoglobin, or an 83-kD homologue distinct from beta-catenin, interacts with E-cadherin and N-cadherin. *J.Cell Biol.* 118 (3):671-679, 1992.
- K. A. Knudsen, C. Frankowski, K. R. Johnson, and M. J. Wheelock. A role for cadherins in cellular signaling and differentiation. *J.Cell Biochem.Suppl* 30-31:168-176, 1998.
- M. D. Kottke, E. Delva, and A. P. Kowalczyk. The desmosome: cell science lessons from human diseases. *J.Cell Sci.* 119 (Pt 5):797-806, 2006.
- A. P. Kowalczyk, T. S. Stappenbeck, D. A. Parry, H. L. Palka, M. L. Virata, E. A. Bornslaeger, L. A. Nilles, and K. J. Green. Structure and function of desmosomal transmembrane core and plaque molecules. *Biophys.Chem.* 50 (1-2):97-112, 1994.
- A. P. Kowalczyk, E. A. Bornslaeger, J. E. Borgwardt, H. L. Palka, A. S. Dhaliwal, C. M. Corcoran, M. F. Denning, and K. J. Green. The amino-terminal domain of desmoplakin binds to plakoglobin and clusters desmosomal cadherin-plakoglobin complexes. *J.Cell Biol.* 139 (3):773-784, 1997.
- S. S. Krishna, I. Majumdar, and N. V. Grishin. Structural classification of zinc fingers: survey and summary. *Nucleic Acids Res.* 31 (2):532-550, 2003.
- N. O. Ku, R. M. Soetikno, and M. B. Omary. Keratin mutation in transgenic mice predisposes to Fas but not TNF-induced apoptosis and massive liver injury. *Hepatology* 37 (5):1006-1014, 2003.
- C. Kuch, D. Winnekendonk, S. Butz, U. Unvericht, R. Kemler, and A. Starzinski-Powitz. M-cadherin-mediated cell adhesion and complex formation with the catenins in myogenic mouse cells. *Exp.Cell Res.* 232 (2):331-338, 1997.
- L. Langbein, H. Spring, M. A. Rogers, S. Praetzel, and J. Schweizer. Hair keratins and hair follicle-specific epithelial keratins. *Methods Cell Biol.* 78:413-451, 2004.
- L. Langbein, M. A. Rogers, S. Praetzel-Wunder, B. Helmke, P. Schirmacher, and J. Schweizer. K25 [K25irs1], K26 [K25irs2], K27 [K25irs3], and K28 [K25irs4] represent the type I inner root sheath keratins of the human hair follicle. *J.Invest Dermatol.* 126 (11):2377-2386, 2006.
- R. H. Lekanne Deprez, A. C. Fijnvandraat, J. M. Ruijter, and A. F. Moorman. Sensitivity and accuracy of quantitative real-time polymerase chain reaction using SYBR green I depends on cDNA synthesis conditions. *Anal.Biochem.* 307 (1):63-69, 2002.
- B. L. Lew, M. K. Shin, and W. Y. Sim. Acute diffuse and total alopecia: A new subtype of alopecia areata with a favorable prognosis. *J.Am.Acad.Dermatol.* 60 (1):85-93, 2009.
- J. E. Lewis, J. K. Wahl, III, K. M. Sass, P. J. Jensen, K. R. Johnson, and M. J. Wheelock. Cross-talk between adherens junctions and desmosomes depends on plakoglobin. *J.Cell Biol.* 136 (4):919-934, 1997.
- B. Liss. Improved quantitative real-time RT-PCR for expression profiling of individual cells. *Nucleic Acids Res.* 30 (17):e89, 2002.
- X. Lu and E. B. Lane. Retrovirus-mediated transgenic keratin expression in cultured fibroblasts: specific domain functions in keratin stabilization and filament formation. *Cell* 62 (4):681-696, 1990.
- I. M. Mackay, K. E. Arden, and A. Nitsche. Real-time PCR in virology. *Nucleic Acids Res.* 30 (6):1292-1305, 2002.
- J. P. Mackay and M. Crossley. Zinc fingers are sticking together. *Trends Biochem.Sci.* 23 (1):1-4, 1998.
- S. Madani and J. Shapiro. Alopecia areata update. *J.Am.Acad.Dermatol.* 42 (4):549-566, 2000.
- K. C. Madison. Barrier function of the skin: "la raison d'etre" of the epidermis. *J.Invest Dermatol.* 121 (2):231-241, 2003.
- L. B. Maifirino, R. C. Araujo, C. C. Faccini, E. A. Liberti, E. F. Gama, A. A. Ribeiro, and R. R. Souza. Effect of exercise training on aging-induced changes in rat papillary muscle. *Arq Bras.Cardiol.* 92 (5):356-7, 387, 2009.
- F. D. Malkinson and J. T. Keane. Hair matrix cell kinetics: a selective review. *Int.J.Dermatol.* 17 (7):536-551, 1978.
- A. G. MATOLTSY. Keratinization of embryonic skin. *J.Invest Dermatol.* 31 (6):343-346, 1958.

- J. M. Matthews and M. Sunde. Zinc fingers—folds for many occasions. *IUBMB Life* 54 (6):351-355, 2002.
- A. J. McDonagh and A. G. Messenger. Alopecia areata. *Clin.Dermatol.* 19 (2):141-147, 2001.
- K.. J. McElwee. Spontaneous Rat Model of Alopecia Areata in Dundee Experimental Bald Rat (DEBR). In: Animal Models of Human Inflammatory Skin Diseases by L. S. Chan. Boca Raton, Fla, *CRC Press*, 2004.
- K. J. McElwee, D. J. Tobin, J. C. Bystry, L. E. King, Jr., and J. P. Sundberg. Alopecia areata: an autoimmune disease? *Exp.Dermatol.* 8 (5):371-379, 1999.
- K. J. McElwee, P. Freyschmidt-Paul, J. P. Sundberg, and R. Hoffmann. The pathogenesis of alopecia areata in rodent models. *J.Investig.Dermatol.Symp.Proc.* 8 (1):6-11, 2003.
- A. G. Messenger, D. N. Slater, and S. S. Bleehen. Alopecia areata: alterations in the hair growth cycle and correlation with the follicular pathology. *Br.J.Dermatol.* 114 (3):337-347, 1986.
- H. J. Michie, C. A. Jahoda, R. F. Oliver, and B. E. Johnson. The DEBR rat: an animal model of human alopecia areata. *Br.J.Dermatol.* 125 (2):94-100, 1991.
- J. R. Miller, A. M. Hocking, J. D. Brown, and R. T. Moon. Mechanism and function of signal transduction by the Wnt/beta-catenin and Wnt/Ca²⁺ pathways. *Oncogene* 18 (55):7860-7872, 1999.
- R. Moll, M. Divo, and L. Langbein. The human keratins: biology and pathology. *Histochem.Cell Biol.* 129 (6):705-733, 2008.
- T. B. Morrison, J. J. Weis, and C. T. Wittwer. Quantification of low-copy transcripts by continuous SYBR Green I monitoring during amplification. *Biotechniques* 24 (6):954-8, 960, 962, 1998.
- M. Mukhopadhyay, P. Pelka, D. DeSousa, B. Kablar, A. Schindler, M. A. Rudnicki, and A. R. Campos. Cloning, genomic organization and expression pattern of a novel Drosophila gene, the disco-interacting protein 2 (dip2), and its murine homolog. *Gene* 293 (1-2):59-65, 2002.
- C. S. Muller and L. El Shabrawi-Caelen. 'Follicular Swiss cheese' pattern—another histopathologic clue to alopecia areata. *J.Cutan.Pathol.* 38 (2):185-189, 2011.
- E. Muller, R. Caldelari, Bruin A. De, D. Baumann, C. Bierkamp, V. Balmer, V, and M. M. Suter. Pathogenesis in pemphigus vulgaris: A central role for the armadillo protein plakoglobin. *J.Invest Dermatol.* 115 (2):332, 2000.
- S. A. MULLER and R. K. WINKELMANN. ALOPECIA AREATA. AN EVALUATION OF 736 PATIENTS. *Arch.Dermatol.* 88:290-297, 1963.
- M. F. Naso, B. Liang, C. C. Huang, X. Y. Song, L. Shahied-Arruda, S. M. Belkowski, M. R. D'Andrea, D. A. Polkovitch, D. R. Lawrence, D. E. Griswold, R. W. Sweet, and B. Y. Amegadzie. Dermokine: an extensively differentially spliced gene expressed in epithelial cells. *J.Invest Dermatol.* 127 (7):1622-1631, 2007.
- S. Nischwitz, S. Cepok, A. Kroner, C. Wolf, M. Knop, F. Muller-Sarnowski, H. Pfister, P. Rieckmann, B. Hemmer, M. Ising, M. Uhr, T. Bettecken, F. Holsboer, B. Muller-Myhsok, and F. Weber. More CLEC16A gene variants associated with multiple sclerosis. *Acta Neurol.Scand.* 123 (6):400-406, 2011.
- N. C. Noriega, S. G. Kohama, and H. F. Urbanski. Gene expression profiling in the rhesus macaque: methodology, annotation and data interpretation. *Methods* 49 (1):42-49, 2009.
- D. Norris. Alopecia areata: current state of knowledge. *J.Am.Acad.Dermatol.* 51 (1 Suppl):S16-S17, 2004.
- R. F. Oliver, C. A. Jahoda, K. A. Horne, H. J. Michie, T. Poulton, and B. E. Johnson. The DEBR rat model for alopecia areata. *J.Invest Dermatol.* 96 (5):97S, 1991.
- A. S. Oriolo, F. A. Wald, V. P. Ramsauer, and P. J. Salas. Intermediate filaments: a role in epithelial polarity. *Exp.Cell Res.* 313 (10):2255-2264, 2007.
- O.S. Ormsby, H. Montgomery. Diseases of the skin. 7th edition. London. *Henry Kimpton.* 1365-1375 1948.
- M. Ozawa, H. Terada, and C. Pedraza. The fourth armadillo repeat of plakoglobin (gamma-catenin) is required for its high affinity binding to the cytoplasmic domains of E-cadherin and desmosomal cadherin Dsg2, and the tumor suppressor APC protein. *J.Biochem.* 118 (5):1077-1082, 1995.
- S. Palmer, A. P. Wiegand, F. Maldarelli, H. Bazmi, J. M. Mican, M. Polis, R. L. Dewar, A. Planta, S. Liu, J. A. Metcalf, J. W. Mellors, and J. M. Coffin. New real-time reverse transcriptase-initiated PCR assay with single-copy sensitivity for human immunodeficiency virus type 1 RNA in plasma. *J.Clin.Microbiol.* 41 (10):4531-4536, 2003.
- G. T. Park, S. E. Lim, S. I. Jang, and M. I. Morasso. Suprabasin, a novel epidermal differentiation marker and potential cornified envelope precursor. *J.Biol.Chem.* 277 (47):45195-45202, 2002.

- R. Paus, S. Eichmüller, U. Hofmann, B. M. Czarnetzki, and P. Robinson. Expression of classical and non-classical MHC class I antigens in murine hair follicles. *Br.J.Dermatol.* 131 (2):177-183, 1994.
- R. Paus. Immunology of the hair follicle in: Bos JD, ed. The skin immune system. Boca Raton, FL: CRC Press. 377 1997.
- R. Paus, N. Ito, M. Takigawa, and T. Ito. The hair follicle and immune privilege. *J.Investig.Dermatol.Symp.Proc.* 8 (2):188-194, 2003.
- M. Peifer and P. Polakis. Wnt signaling in oncogenesis and embryogenesis—a look outside the nucleus. *Science* 287 (5458):1606-1609, 2000.
- S. N. Peirson, J. N. Butler, and R. G. Foster. Experimental validation of novel and conventional approaches to quantitative real-time PCR data analysis. *Nucleic Acids Res.* 31 (14):e73, 2003.
- C. Perret, L. Wiesner-Menzel, and R. Happle. Immunohistochemical analysis of T-cell subsets in the peribulbar and intrabulbar infiltrates of alopecia areata. *Acta Derm.Venereol.* 64 (1):26-30, 1984.
- L. Petukhova, M. Duvic, M. Hordinsky, D. Norris, V. Price, Y. Shimomura, H. Kim, P. Singh, A. Lee, W. V. Chen, K. C. Meyer, R. Paus, C. A. Jahoda, C. I. Amos, P. K. Gregersen, and A. M. Christiano. Genome-wide association study in alopecia areata implicates both innate and adaptive immunity. *Nature* 466 (7302):113-117, 2010.
- M. P. Philpott, D. A. Sanders, J. Bowen, and T. Kealey. Effects of interleukins, colony-stimulating factor and tumour necrosis factor on human hair follicle growth in vitro: a possible role for interleukin-1 and tumour necrosis factor-alpha in alopecia areata. *Br.J.Dermatol.* 135 (6):942-948, 1996.
- M. Pigors, D. Kiritsi, S. Krumpelmann, N. Wagner, Y. He, M. Podda, J. Kohlhase, I. Hausser, L. Bruckner-Tuderman, and C. Has. Lack of plakoglobin leads to lethal congenital epidermolysis bullosa: a novel clinico-genetic entity. *Hum.Mol.Genet.* 20 (9):1811-1819, 2011.
- D. M. Pirone, S. Fukuhara, J. S. Gutkind, and P. D. Burbelo. SPECS, small binding proteins for Cdc42. *J.Biol.Chem.* 275 (30):22650-22656, 2000.
- S. Porter, P. N. Span, F. C. Sweep, V. C. Tjan-Heijnen, C. J. Pennington, T. X. Pedersen, M. Johnsen, L. R. Lund, J. Romer, and D. R. Edwards. ADAMTS8 and ADAMTS15 expression predicts survival in human breast carcinoma. *Int.J.Cancer* 118 (5):1241-1247, 2006.
- M. L. Price and W. A. Griffiths. Normal body hair—a review. *Clin.Exp.Dermatol.* 10 (2):87-97, 1985.
- V. H. Price. Alopecia areata: clinical aspects. *J.Invest Dermatol.* 96 (5):68S, 1991.
- E. Proksch, J. M. Brandner, and J. M. Jensen. The skin: an indispensable barrier. *Exp.Dermatol.* 17 (12):1063-1072, 2008.
- N. Protonotarios, A. Tsatsopoulou, P. Patsourakos, D. Alexopoulos, P. Gezerlis, S. Simitsis, and G. Scampardonis. Cardiac abnormalities in familial palmoplantar keratosis. *Br.Heart J.* 56 (4):321-326, 1986.
- A. Ranki, U. Kianto, L. Kanerva, E. Tolvanen, and E. Johansson. Immunohistochemical and electron microscopic characterization of the cellular infiltrate in alopecia [areata, totalis, and universalis]. *J.Invest Dermatol.* 83 (1):7-11, 1984.
- A. J. Reynolds and C. A. Jahoda. Hair follicle stem cells: characteristics and possible significance. *Skin Pharmacol.* 7 (1-2):16-19, 1994.
- C.R. Robins. Chemical and Physical Behavior of Human Hair. New York. *Springer Verlag.* 2002.
- T. Robinson. Baldness and Greyness, Their Etiology, Pathology and Treatment. 2nd edition. London. *Kimpton.* 1883.
- P. Ruiz, V. Brinkmann, B. Ledermann, M. Behrend, C. Grund, C. Thalhammer, F. Vogel, C. Birchmeier, U. Gunthert, W. W. Franke, and W. Birchmeier. Targeted mutation of plakoglobin in mice reveals essential functions of desmosomes in the embryonic heart. *J.Cell Biol.* 135 (1):215-225, 1996.
- A.C. Roxburgh. Common skin diseases. 9th edition. London. *HK Lewis & Co. LTD.* 406-412, 1950.
- N. H. Sabah. Controlled stimulation of hair follicle receptors. *J.Appl.Physiol* 36 (2):256-257, 1974.
- R. Sabouraud. Sur les origines de la pelade. *Annales de Dermatologie et Syphiligraphie.* 3:253-277, 1896.
- R. Sabouraud. Nouvelles recherches sur l'étiologie de la pelade [pelade et ménopause]. *Annales de Dermatologie et Syphiligraphie.* 5:88-97, 1913.
- P. A. Sacco, T. M. McGranahan, M. J. Wheelock, and K. R. Johnson. Identification of plakoglobin domains required for association with N-cadherin and alpha-catenin. *J.Biol.Chem.* 270 (34):20201-20206, 1995.

Sauvages. Nosologica Medica. Lyons. 1760

L. Scerri and J. L. Pace. Identical twins with identical alopecia areata. *J.Am.Acad.Dermatol.* 27 (5 Pt 1):766-767, 1992.

R. J. Schaffer, E. N. Friel, E. J. Souleyre, K. Bolitho, K. Thodey, S. Ledger, J. H. Bowen, J. H. Ma, B. Nain, D. Cohen, A. P. Gleave, R. N. Crowhurst, B. J. Janssen, J. L. Yao, and R. D. Newcomb. A genomics approach reveals that aroma production in apple is controlled by ethylene predominantly at the final step in each biosynthetic pathway. *Plant Physiol* 144 (4):1899-1912, 2007.

T. D. Schmittgen, B. A. Zakrajsek, A. G. Mills, V. Gorn, M. J. Singer, and M. W. Reed. Quantitative reverse transcription-polymerase chain reaction to study mRNA decay: comparison of endpoint and real-time methods. *Anal.Biochem.* 285 (2):194-204, 2000.

Sequeira. Trans XVII Int Cong Med. London. 13:142, 1913.

W. V. Shellow, J. E. Edwards, and J. Y. Koo. Profile of alopecia areata: a questionnaire analysis of patient and family. *Int.J.Dermatol.* 31 (3):186-189, 1992.

Y. Shimomura, M. Wajid, L. Shapiro, and A. M. Christiano. P-cadherin is a p63 target gene with a crucial role in the developing human limb bud and hair follicle. *Development* 135 (4):743-753, 2008.

Y. Shimomura and A. M. Christiano. Biology and genetics of hair. *Annu.Rev.Genomics Hum.Genet.* 11:109-132, 2010.

L. C. Sperling. Hair anatomy for the clinician. *J.Am.Acad.Dermatol.* 25 (1 Pt 1):1-17, 1991.

V. Stellmach, A. Leask, and E. Fuchs. Retinoid-mediated transcriptional regulation of keratin genes in human epidermal and squamous cell carcinoma cells. *Proc.Natl.Acad.Sci.U.S.A* 88 (11):4582-4586, 1991.

K. S. Stenn and R. Paus. Controls of hair follicle cycling. *Physiol Rev.* 81 (1):449-494, 2001.

M. Stucker, A. Struk, P. Altmeyer, M. Herde, H. Baumgartl, and D. W. Lubbers. The cutaneous uptake of atmospheric oxygen contributes significantly to the oxygen supply of human dermis and epidermis. *J.Physiol* 538 (Pt 3):985-994, 2002.

C. L. Sutherland, N. J. Chalupny, K. Schooley, T. VandenBos, M. Kubin, and D. Cosman. UL16-binding proteins, novel MHC class I-related proteins, bind to NKG2D and activate multiple signaling pathways in primary NK cells. *J.Immunol.* 168 (2):671-679, 2002.

N. A. Swanson, A. J. Mitchell, M. S. Leahy, J. T. Headington, and L. A. Diaz. Topical treatment of alopecia areata. *Arch.Dermatol.* 117 (7):384-387, 1981.

M. Tanaka, K. Murakami, S. Ozaki, Y. Imura, X. P. Tong, T. Watanabe, T. Sawaki, T. Kawanami, D. Kawabata, T. Fujii, T. Usui, Y. Masaki, T. Fukushima, Z. X. Jin, H. Umehara, and T. Mimori. DIP2 disco-interacting protein 2 homolog A [Drosophila] is a candidate receptor for follistatin-related protein/follistatin-like 1-analysis of their binding with TGF-beta superfamily proteins. *FEBS J.* 277 (20):4278-4289, 2010.

U. Tepass, K. Truong, D. Godt, M. Ikura, and M. Peifer. Cadherins in embryonic and neural morphogenesis. *Nat.Rev.Mol.Cell Biol.* 1 (2):91-100, 2000.

Y. Teraki, K. Imanishi, and T. Shiohara. Cytokines in alopecia areata: contrasting cytokine profiles in localized form and extensive form (alopecia universalis). *Acta Derm.Venereol.* 76 (6):421-423, 1996.

A. Tichopad, A. Didier, and M. W. Pfaffl. Inhibition of real-time RT-PCR quantification due to tissue-specific contaminants. *Mol.Cell Probes* 18 (1):45-50, 2004.

N. Todes-Taylor, R. Turner, G. S. Wood, P. T. Stratte, and V. B. Morhenn. T cell subpopulations in alopecia areata. *J.Am.Acad.Dermatol.* 11 (2 Pt 1):216-223, 1984.

X. Tong and P. A. Coulombe. Keratin 17 modulates hair follicle cycling in a TNFalpha-dependent fashion. *Genes Dev.* 20 (10):1353-1364, 2006.

E. Toulza, M. F. Galliano, N. Jonca, H. Gallinaro, M. C. Mechin, A. Ishida-Yamamoto, G. Serre, and M. Guerrin. The human dermokine gene: description of novel isoforms with different tissue-specific expression and subcellular location. *J.Invest Dermatol.* 126 (2):503-506, 2006.

S. M. Troyanovsky, R. B. Troyanovsky, L. G. Eshkind, R. E. Leube, and W. W. Franke. Identification of amino acid sequence motifs in desmocollin, a desmosomal glycoprotein, that are required for plakoglobin binding and plaque formation. *Proc.Natl.Acad.Sci.U.S.A* 91 (23):10790-10794, 1994.

S. Tsuchida, M. Bonkobara, J. R. McMillan, M. Akiyama, T. Yodate, Y. Aragane, T. Tezuka, H. Shimizu, P. D. Cruz, Jr., and K. Ariizumi. Characterization of Kdap, a protein secreted by keratinocytes. *J.Invest Dermatol.* 122 (5):1225-1234, 2004.

- E. J. VAN SCOTT. Morphologic changes in pilosebaceous units and anagen hairs in alopecia areata. *J.Invest Dermatol.* 31 (1):35-43, 1958.
- E. J. VAN SCOTT. Keratinization and hair growth. *Annu.Rev.Med.* 19:337-350, 1968.
- J. Vandesompele, Preter K. De, F. Pattyn, B. Poppe, Roy N. Van, Paepe A. De, and F. Speleman. Accurate normalization of real-time quantitative RT-PCR data by geometric averaging of multiple internal control genes. *Genome Biol.* 3 (7):RESEARCH0034, 2002.
- J. K. Wahl, J. E. Nieset, P. A. Sacco-Bubulya, T. M. Sadler, K. R. Johnson, and M. J. Wheelock. The amino- and carboxyl-terminal tails of [beta]-catenin reduce its affinity for desmoglein 2. *J.Cell Sci.* 113 (Pt 10):1737-1745, 2000.
- Y. Wang, C. Barbacioru, F. Hyland, W. Xiao, K. L. Hunkapiller, J. Blake, F. Chan, C. Gonzalez, L. Zhang, and R. R. Samaha. Large scale real-time PCR validation on gene expression measurements from two commercial long-oligonucleotide microarrays. *BMC.Genomics* 7:59, 2006.
- J. Waschke. The desmosome and pemphigus. *Histochem.Cell Biol.* 130 (1):21-54, 2008.
- G. E. Westgate, R. I. Craggs, and W. T. Gibson. Immune privilege in hair growth. *J.Invest Dermatol.* 97 (3):417-420, 1991.
- M. J. Wheelock and P. J. Jensen. Regulation of keratinocyte intercellular junction organization and epidermal morphogenesis by E-cadherin. *J.Cell Biol.* 117 (2):415-425, 1992.
- B. Winpenninckx, K. Debacker, J. Ramsay, D. Smeets, A. Smits, D. R. FitzPatrick, and R. F. Kooy. CGG-repeat expansion in the DIP2B gene is associated with the fragile site FRA12A on chromosome 12q13.1. *Am.J.Hum.Genet.* 80 (2):221-231, 2007.
- A. Wodarz and R. Nusse. Mechanisms of Wnt signaling in development. *Annu.Rev.Cell Dev.Biol.* 14:59-88, 1998.
- S. A. Wolfe, L. Nekludova, and C. O. Pabo. DNA recognition by Cys2His2 zinc finger proteins. *Annu.Rev.Biophys.Biomol.Struct.* 29:183-212, 2000.
- M. L. Wong and J. F. Medrano. Real-time PCR for mRNA quantitation. *Biotechniques* 39 (1):75-85, 2005.
- K. M. Yamada and B. Geiger. Molecular interactions in cell adhesion complexes. *Curr.Opin.Cell Biol.* 9 (1):76-85, 1997.
- A. S. Yap, W. M. Brieher, M. Pruschy, and B. M. Gumbiner. Lateral clustering of the adhesive ectodomain: a fundamental determinant of cadherin function. *Curr.Biol.* 7 (5):308-315, 1997.
- K. Zatloukal, C. Stumptner, M. Lehner, H. Denk, H. Baribault, L. G. Eshkind, and W. W. Franke. Cytokeratin 8 protects from hepatotoxicity, and its ratio to cytokeratin 18 determines the ability of hepatocytes to form Mallory bodies. *Am.J.Pathol.* 156 (4):1263-1274, 2000.
- W. Zeng, C. Corcoran, L. A. Collins-Racie, E. R. Lavallie, E. A. Morris, and C. R. Flannery. Glycosaminoglycan-binding properties and aggrecanase activities of truncated ADAMTSs: comparative analyses with ADAMTS-5, -9, -16 and -18. *Biochim.Biophys.Acta* 1760 (3):517-524, 2006.
- M. Zoledziewska, G. Costa, M. Pitzalis, E. Cocco, C. Melis, L. Moi, P. Zavattari, R. Murrù, R. Lampis, L. Morelli, F. Poddie, P. Frongia, P. Pusceddu, M. Bajorek, A. Marras, A. M. Satta, A. Chessa, M. Pugliatti, S. Sotgiu, M. B. Whalen, G. Rosati, F. Cucca, and M. G. Marrosu. Variation within the CLEC16A gene shows consistent disease association with both multiple sclerosis and type 1 diabetes in Sardinia. *Genes Immun.* 10 (1):15-17, 2009.

J Appendix

1. Primer Sequences

For Sanger-Sequencing of rat samples:

Acd_e1F	AGTGGGCATAGGTCTTTAGGTG	Arhgap10_e20R	ACCTGAACTCTGGAAGTCAC
Acd_e1R	GGTGGTCCCTAGAGAAACAGTG	Arhgap10_e21F	CTGTCCCAGTGGTTTGAAG
Acd_e2F	GAAAAAGCTCAATAAATGCCTTG	Arhgap10_e21R	ACAATACCCAGGAGTGACTG
Acd_e2R	TTACAGCGACTTACTGAAGAACG	Arhgap10_e22F	GGAAACCCACCACCTTACTTG
Acd_e3F	GCGCTTTTCTTAGGAGGTGTC	Arhgap10_e22R	CATCTCTACAAGCCGGTGT
Acd_e3R	CTGGAGTTCTGGAGAGAATCATC	Arhgap10_e23F	AATCCCTCGGCATGGTAAG
Acd_e4.1F	GGGTGGCTAATGGACTGTTTAG	Arhgap10_e2-3F	GCTCTTCTACCCCTCCTAAC
Acd_e4.1R	TAGTCTCACCCAGACAGAGTGG	Arhgap10_e23R	AAGTTCCATCCCCCTCCCTA
Acd_e4.2F	ACATGCCCTACTTCATACCAG	Arhgap10_e2-3R	TCAGGCTTGGCTAAACAG
Acd_e4.2R	TGTCATACAAGCCTACCCTTCC	Arhgap10_e4F	GTGCAGCCTTTTGTAGTACGT
Acd_e5F	GAGAGGGAAGGGTAGGCTTG	Arhgap10_e4R	CAGAGGTAAGCCACGTGTA
Acd_e5R	AGGAGAGAGCCTGGAAAGAAAC	Arhgap10_e5F	GCATTGCCTCAGAAGCTC
Acd_e6F	ATAAATATGGGACACCCTCTGC	Arhgap10_e5R	CCCCAATCCACTGAAGAA
Acd_e6R	AACCAAGCCTCTTCTCCATAC	Arhgap10_e6F	GACCTCTGGTTTGATGGTC
Agrp_e1F	GGATCAACAAGCAAAGGTAAGC	Arhgap10_e6R	CCTCCCAACAGTTTGATG
Agrp_e1R	GGACTAGGGAAGGAGGGTTTAG	Arhgap10_e7F	TTGCTTGCTTCCATGCAC
Agrp_e2F	CTTCCCTAGTCCCAAGCTTAAC	Arhgap10_e7R	GCTACAGTGCAGCTTGTTAC
Agrp_e2R	ATAGGATGGCAGTGGAGTGTG	Arhgap10_e8F	CGTCGTCTCATCTCTCTAT
Agrp_e3F	AACTGCAGACCATCCCTGAC	Arhgap10_e8R	CAGAGCACTTTCCTCTTG
Agrp_e3R	ATGACAAAGATGATGCGGTAGC	Arhgap10_e9F	CGAACTCCTAGAGATAGTCCTG
Arhgap10_e10F	CTGTAATCCTTCTGTCAGTC	Arhgap10_e9R	ACAGCGACAAGTTCTACTCC
Arhgap10_e10R	CAACTACACAGTGACCAACG	Atp6vOd1_e1F	GTTGTTGGGCTCACCAAAGT
Arhgap10_e11F	CTGGAGGCAAATCATGAGG	Atp6vOd1_e1R	AGGGTTTTGGAGCCAAATGT
Arhgap10_e11R	GAATACCAGCTCCAGCAAG	Atp6vOd1_e2.1F	GCCTAACCCGGGAAAACATA
Arhgap10_e12F	GTAAGCAGGGACGAAGAC	Atp6vOd1_e2.1R	ATAAAGCTCCGGGAAGAACG
Arhgap10_e12R	CTAGGGGACAAACAATGAGG	Atp6vOd1_e2.2F	GTCACCTGACGCACTTGACA
Arhgap10_e13F	GCATCACGAAGCCTCTTCT	Atp6vOd1_e2.2R	TTTCTGACATGCCACGAT
Arhgap10_e13R	GCGTGCTGCGTATAAAGTTC	Atp6vOd1_e3F	CATGGGAGGAGGTGGTCTTAG
Arhgap10_e14F	TAGTGGAGATCTTGGAGTGC	Atp6vOd1_e3R	AGAGCTGCCATCTGATCACC
Arhgap10_e14R	GGACACAACCAACCCAAGTA	Atp6vOd1_e4F	GACAGTCCCTCTGGAGCCTA
Arhgap10_e15F	GAAACTGTGCTTTGGCCACT	Atp6vOd1_e4R	GCCGCCTACAATCCATAAAA
Arhgap10_e15R	AGACTTCTCGGGCCAGTAA	Atp6vOd1_e5F	TCAGGGATCTCCAGTACTTAGCTT
Arhgap10_e16F	GTTAGCCTCAGAGTGCACAAG	Atp6vOd1_e5R	CCATAGACCCACCCACTGAC
Arhgap10_e16R	TGGGCTCAGGTCAATACTAC	Atp6vOd1_e6F	TGAAGAGGGGAGATCAAACGAC
Arhgap10_e17F	AAGGTGGAGGGACAGTTTAG	Atp6vOd1_e6R	TAGCCAGTCAGTTGGCAGAG
Arhgap10_e17R	GTCTAATACGCAGCCTGGTC	Atp6vOd1_e7F	CTGCCAACTGACTGGCTATG
Arhgap10_e18F	CTGCTGTTTGGTTTCCAGACAC	Atp6vOd1_e7R	CTCCAGGGTCTTGTCTCCAG
Arhgap10_e18R	GGAATAAGTCCACAGCAAGC	Atp6vOd1_e8F	TGAGTGCCCTAGCTGACAAG
Arhgap10_e19F	TGTATCCTGGCTACCTTCC	Atp6vOd1_e8R	CAGAATCAGGCCCAAGTCAC
Arhgap10_e19R	GTCACCCTCCCTGTTAATC	Atp6vOd1_e9.1F	GTTGTGACTTGGGCTGATT
Arhgap10_e1F	GATCAGCAGACATCAGCAC	Atp6vOd1_e9.1R	GGGGATCTTGGTCCATTCTT
Arhgap10_e1R	GGGTGCAGTAAACCTGAC	Atp6vOd1_e9.2F	ATTGCCCTGGGATTGGTT
Arhgap10_e20F	CAGAAGTATCTGCGTGCTC	Atp6vOd1_e9.2R	GTAGAACTGCCACCCTCCA

C16orf48_e1F	GTCATTTGACCCCTGACCTC	Cdh1_e17.5R	AGAGAACAGTTCGGATTGCTTG
C16orf48_e1R	AGCTCTGTAGCCCCGTGGT	Cdh1_e17.6F	GATAGCGTGCCCTTTGTATGTAG
C16orf48_e2F	GGTACCACGGGGCTACAGAG	Cdh1_e17.6R	GAGGCTTCCAACCTCCATAACC
C16orf48_e2R	CTTGGGCTGAAGAGCAAGAC	Cdh1_e1F	ATTTACAGACGGGTGGAGGAAG
C16orf48_e3F	CCTACTCTCTGCCCGGACTA	Cdh1_e1R	AGGGAAGTGAACCACAGAAG
C16orf48_e3R	TCAAGGCGGTTAAGAAGCAC	Cdh1_e2F	GGGAAGGGTTACTCTTGTTTC
C16orf48_e4F	GGGTAGGGTGTGAATCTGTATG	Cdh1_e2R	TCCATCCTACCGACAAAGTAGC
C16orf48_e4R	TCTTTGTGAACACACCACACAC	Cdh1_e3F	GGGTCTGGAATGAACAGTTAGTC
C16orf48_e5F	AAGGGGAATGGTCTTGTGGT	Cdh1_e3R	AAGAGGACCCAACATTGTAAGC
C16orf48_e5R	GCAGAGACATGGCAAGCAT	Cdh1_e4F	TGCATCTTGTATGATGAACGTG
C16orf48_e6F	GAGGATTTAAAGGCCATCTTCC	Cdh1_e4R	ACAGGTATTTGTTCTGGGCATC
C16orf48_e6R	CTTTGAGCTTCAGCTTCCTT	Cdh1_e5F	GACGTCCATGGGATAGATGAAC
C16orf48_e7F	AGTGCAGTGAGGGAATCCTG	Cdh1_e5R	TGGAAGGCAAGATCTCCAC
C16orf48_e7R	CATGGGAAGTGTGAGTGTGG	Cdh1_e6F	GAAGGCACTCCTGAGAGAAGAG
C16orf48_e8.1F	TCAGAGTGAGTACATGGGCAAG	Cdh1_e6R	GTCCAGGACATCCAACTGG
C16orf48_e8.1R	CTACGAAAGTGTTCGATTCTG	Cdh1_e7f	TTCATTAAGTAGCAACACACAGC
C16orf86_e1F	AACAGGATCCTTACCTCTCAACC	Cdh1_e7R	GTGGCTTTCAAAGAGCGTGTG
C16orf86_e1R	ACTTGGCCTGGCAGTTAGAAG	Cdh1_e8F	GTGACAAAGTGTGCTTGTCTCC
C16orf86_e2F	TTCCTATTCTGTGGCCAATATG	Cdh1_e8R	AAAGCTGGGCCACTTACACTAC
C16orf86_e2R	TTCTAGAGAAACAGGAGCTGGAG	Cdh1_e9F	GCCCAGCTTTACGTCTAATTCC
C16orf86_e3F	AAGCCCTAGGTTCAAGACACAG	Cdh1_e9R	GGGAAGAGGTTCTAAAGGGTTC
C16orf86_e3R	TTCCTGCAAGAACCCAAGG	Cdh3_e10F	GCCTTGTTCCTTACTGTGAGC
C16orf86_e4.1F	GCATCTGCACCCACAGAGAC	Cdh3_e10R	AACAAACTTTATGGAGAAGAGCAAG
C16orf86_e4.1R	CTTGGGTTGTCTTATCCACCTC	Cdh3_e11F	ACTTGATCTGAGGAGGCTCTG
C16orf86_e4.2F	CTGCCCTAATCCATTACACCAC	Cdh3_e11R	CCACCATTCCCTGCTAAGG
C16orf86_e4.2R	AAAGACTAAATCCCTTCTCCATC	Cdh3_e12F	GAAGCTGATCGAGTAGTCTTAGGG
Cdh1_e10F	TGACATCACTCATCCCACCTAC	Cdh3_e12R	GGGAGGTGTGTGAGTCTATTG
Cdh1_e10R	GTTGATCCACTCATGGGAAGAC	Cdh3_e13F	GTGCTGAGGCTGTTCTCAAAC
Cdh1_e11F	TATTTGTTCTGTGGGAGTGGTG	Cdh3_e13R	AACGGATGAACAATATGGATGC
Cdh1_e11R	AGGACGACCTAGTGAGAACCTG	Cdh3_e14F	ATCAATCATCAATGCTCTGTGC
Cdh1_e12F	CTGTAACAAGTGAAGAGGACCTG	Cdh3_e14R	ATGAAGACTGATGGGCTTGC
Cdh1_e12R	AAGGAATGAAATCCCACCCCTAC	Cdh3_e15F	CAGAGGAGTAAGATGTGACTGGTG
Cdh1_e13F	ACCTGCTGAGGGATCACAGATA	Cdh3_e15R	AGAAAGCCAGTGTGTTGTTCTCC
Cdh1_e13R	TGTAAGGAACTAGGGCCGAATA	Cdh3_e16.1F	GATGGGTATAGAGGCTCAGCAG
Cdh1_e14F	GCACCTTGGTTCCCTAAACATT	Cdh3_e16.1R	GTCACATCCTCCCATTTGAAAG
Cdh1_e14R	TGTAAGGAACTAGGGCCGAATA	Cdh3_e16.2F	CTCCTGAGGACTCTGAAGCTC
Cdh1_e15F	GATGGCTGCTTCCCTCTGC	Cdh3_e16.2R	CCTGGAGATCAGAGAAATGTACC
Cdh1_e15R	TACAGCAGGGTGAATGAAGTAG	Cdh3_e16.3F	GGGCAGGGTGCAGACATC
Cdh1_e16F	ACAGTCTGTGATGCCATGAAGC	Cdh3_e16.3R	CAGAGTCTAAAGCCCACCAAAC
Cdh1_e16R	AAGGCAACATTCCCTCACTGG	Cdh3_e1F	GTTTGACCAATCAGCAGCTACC
Cdh1_e17.1F	GATTTGTGCTAGGGTGTGTCTG	Cdh3_e1R	AAGGAGCACAGCCCTAAGATTC
Cdh1_e17.1R	CTGGTAGGTAGAGTGGGACCAG	Cdh3_e2F	CAAGGATGGGTGTACAGAACC
Cdh1_e17.2F	ATGATGTCAGTGGTCTTTCAGC	Cdh3_e2R	CCAGCTCTGGTCTAGACAACCTC
Cdh1_e17.2R	ACACTATCCAGCTCAGTTGCAC	Cdh3_e3F	AGTAAGCCAAGGCCCTGAGTG
Cdh1_e17.3F	CACTAAGTTCCTGAATTCTGTTGC	Cdh3_e3R	AGACTCTGGCCAGCAGAAATC
Cdh1_e17.3R	ACTCATGACAGTGGTCAGGTTTC	Cdh3_e4F	TCTCCTGAGAGCTGGGAGTATG
Cdh1_e17.4F	TTTCTTGCCTTCTTTCAAACC	Cdh3_e4R	GATACCCAGCAGCAAGAAGC
Cdh1_e17.4R	ATACCAGGCTGACCTTGAACCTC	Cdh3_e5F	AAAGGCCTAAGAACAAGGCTTC
Cdh1_e17.5F	AACTGAGACTATGCTGGGTGTG	Cdh3_e5R	CGCACCATTTCTCAGATACAGC

Cdh3_e6F	TTCAGCACCCAACGTAGATATG	Ctcf_e10.4R	ATCACCTGCCAGGATCATCT
Cdh3_e6R	GTTTCAAATGTGAATGCCAGAG	Ctcf_e2F	TCCTCAAGAGAAGTAAAAGTGTGAA
Cdh3_e7F	ACTTCACAGGGTTCCAAGGTAG	Ctcf_e2R	TCAACTTCCTATTGAAGTAATCTTGG
Cdh3_e7R	CTCTAGCCCCAAAGAAGTTGTGG	Ctcf_e3F	TCCAGGGCTCCCTGTAACATA
Cdh3_e8F	GCAGTTTCTCATTACCCAGGTG	Ctcf_e3R	TGGAATAGGTGTCCCCCTAAA
Cdh3_e8R	GTGGGTTGGTTTGAGAGAAGC	Ctcf_e4F	ACCCCATCTCCTTAGACTG
Cdh3_e9F	CAGCTGCTGGAGAGTGGTG	Ctcf_e4R	GTAAGCCCTGGGTGCACAT
Cdh3_e9R	AGTACCTGGAGCCACTGTCTTG	Ctcf_e5F	ATGTCTGCCACTCCGCTATT
Cenpt_e1.1F	ATGGCCTACATTTGCAACG	Ctcf_e5R	GAGAGGGGGAGCTAAGCAAT
Cenpt_e1.1R	GAAAAGCATGGAGCCAGTTC	Ctcf_e6F	ACTCAGGCTCTCACATTGCTT
Cenpt_e1.2F	AAATCAATTTATGATCATGTCCAGACC	Ctcf_e6R	CACACAGAAAACCGTATCTCAATTT
Cenpt_e1.2R	CTAGGAAAGTGCTCTACCACTGAG	Ctcf_e7F	GAAAGTCATAGGGTGTGTGTGC
Cenpt_e10F	AGGCCCTTAGCAATTAGGAGAG	Ctcf_e7R	GTGGCAAAAACTGCATTCTG
Cenpt_e10R	CTGTGCTTGGCAGTCATCTG	Ctcf_e8F	CCCCACTCTCTCACACACCT
Cenpt_e11F	GGCTTGAAGGTGTTGTACCC	Ctcf_e8R	TGCTAACTTCTGGGGTCAT
Cenpt_e11R	CTGCCAAGAAGGTTGCAATAG	Ctcf_e9F	GCCCAGBACTTTTCTTAGGG
Cenpt_e12F	CTAGCATGTGAGTGGGTACAGG	Ctcf_e9R	TGAGCATCTGTGCTGAGACC
Cenpt_e12R	GGAAAAGAGGATCAAACAGAATTAAC	Ctrl_e1F	TCTCAGGCCCAAGACTTCTG
Cenpt_e13F	AGACTGTGAAGCCAAAGGACTTAGAG	Ctrl_e1R	AACCAGGCTGGCCTCTTATC
Cenpt_e13R	ATACTCCAATGTTGCTAACCTTCTTC	Ctrl_e2-3F	GCACCTTGAGGAAGACATTAGG
Cenpt_e2F	ACTCTTAACCACAACCCCTTG	Ctrl_e2-3R	AGGGGAAGTGGGAAGAGATG
Cenpt_e2R	CCCTCAAGTTAGGCTTCAAAAC	Ctrl_e4F	CCAATCCATCTCTTCCCACT
Cenpt_e3F	CCGTGACTGACTTGTTAGAACC	Ctrl_e4R	AATTCCCATGTCCAAAGCAG
Cenpt_e3R	GGGCTGACAAAGAAAGGAATC	Ctrl_e5F	TCTGCTTTGGACATGGGAAT
Cenpt_e4F	GGGTATCAGCCTGCAGTTAAAG	Ctrl_e5R	CTGGTGTACGCTTGCCTGT
Cenpt_e4R	GACATATCAGAAAGCCCAATTTAG	Ctrl_e6F	TGGTGTGGGTAAGGACTTGG
Cenpt_e5F	AAGCCAGCACAAGTACCAGAAG	Ctrl_e6R	GGAAGCAAAGGGGAAAAGTC
Cenpt_e5R	TACTCAAGCCCAAGAAAGCTC	Ctrl_e7F	CTGTCCCGTGGTACACTTCC
Cenpt_e6F	TCCTCTTGGGAGTAGAAAAGACC	Ctrl_e7R	CCAATAGAACCCCAAGAGC
Cenpt_e6R	TGTTAGGACGGAAGCAGATACC	Ddx28_e1.1F	TCTTAAGGATCCTCCCTCCTTC
Cenpt_e7F	TCCTGGGGTTTATACAATCTGG	Ddx28_e1.1R	GCTCTATGGAAAAATGGTCCTG
Cenpt_e7R	AGCAGCCCTGAGTTAGTAGAGC	Ddx28_e1.2F	GGTGCTAGTGCAACCTGGTC
Cenpt_e8F	TTTCGCTGCCTCTACCTTTTAG	Ddx28_e1.2R	ATTCTCGGGAAGGTACCAGAAC
Cenpt_e8R	CAGAAAAGGAGGGAGTCCCTGAG	Ddx28_e1.3F	ATCTACTGCCCTATTTCAACG
Cenpt_e9F	AGGACTCCCTCCTTTTCTGAAG	Ddx28_e1.3R	GTTTAGGCCTTCTGGAAATGTG
Cenpt_e9R	CAGTGGTAGAGCGCTTGCTTAG	Ddx28_e1.4F	AGATGAAAGCTTCGTGGAAGT
Ctcf_e1.1F	CACCTGCCACCCAAAAGT	Ddx28_e1.4R	AGTATGTTTTGGGAGCCCTTCT
Ctcf_e1.1R	TGCAGGGTTATGATTTGGGTA	Ddx28_e1.5F	CTGTCCTGGTATTCTGCAACAG
Ctcf_e1.2F	AGGTGGTCCAGGATGTCAAC	Ddx28_e1.5R	CCTGGAAGGCTTCTCCTTCTAC
Ctcf_e1.2R	CCCCTGCTCTAGTGTCTCCA	Ddx28_e1.6F	CGGGGACTGTTACCAAGTTTTG
Ctcf_e1.3F	TTGCAGAAAGTGAACCGATG	Ddx28_e1.6R	TGACCCAATGTCATCAAAGAC
Ctcf_e1.3R	CCCCAAATGGGTTTACGAGT	Dpep2_e10F	TGGCTCACAACCATCTATCTGT
Ctcf_e10.1F	CATCTGAAGCCGTGCCTATC	Dpep2_e10R	CAGTGGTCAGCAGCTCTCTCT
Ctcf_e10.1R	AGCACTTCACAGTAAACCCCTCA	Dpep2_e11F	TAAGGGCCTGACAGGTAAGTCA
Ctcf_e10.2F	CGAAAACCTCAAGGATGATGTTAG	Dpep2_e11R	AATGCCTAGTTCACAAACCAC
Ctcf_e10.2R	TGCTGGGTTTTCTTACACTGC	Dpep2_e1F	GGCCTACAAGGACAGGAACATA
Ctcf_e10.3F	GGTCAAGCCTGTAAATAACCTTTT	Dpep2_e1R	GGAGAGATGGACGGAAATGAAT
Ctcf_e10.3R	ACAATTCATGTGCAAGAATCAC	Dpep2_e2F	TGAATCGATGACCTCAAACATC
Ctcf_e10.4F	CTGGGCCAAAACATTTCACT	Dpep2_e2R	ATTAGTCCAGCAGGCTCAGAAC

Dpep2_e3F	CGAGTACTGGGATCACAAGCAG	Dus2l_e16.1R	CATTTCTTGGCACTTGTTTCAG
Dpep2_e3R	GTCATTTTCAGGAGCACCAATTT	Dus2l_e1F	CCGGCTAAAGCCATATTTCTC
Dpep2_e4F	CCACAAGTCTGTCCGTTGTAAA	Dus2l_e1R	ACTCCTTCTTCCACCGAGTACC
Dpep2_e4R	TCAGAGCTGTAGGCATAGGTCA	Dus2l_e2F	CTTATGCAGCAAGCCCTTTTC
Dpep2_e5F	CCTATTCAGGGTATTGGGGAAT	Dus2l_e2R	AAACACTGCCATACCCAAAGAT
Dpep2_e5R	AGTCTCAAATTCGAGGGCAAAT	Dus2l_e3F	AAGCCATGAGTCGTTGTAGTA
Dpep2_e6F	TGAATTAGCTCTATGGGATTGC	Dus2l_e3R	CAACAAGAAAGGACCCTGGAG
Dpep2_e6R	AGTTTAGGAGAAGGGTGTCCAGG	Dus2l_e4F	TAGAATCCACCCTTTTCCCTCT
Dpep2_e7F	TGAGGGATACTTCACACAAACG	Dus2l_e4R	ATACAGCATAGCACAGGCATTC
Dpep2_e7R	TTAGAGGCCATGGTTTATGGTT	Dus2l_e5F	ACCAAACAAACAAGCAAACCT
Dpep2_e8F	GCTTTCTCACAGGGGTTATAGG	Dus2l_e5R	AGCCTCCAGATACCACAGAGAA
Dpep2_e8R	CAGAAAGCCTAGGAGGAATTTG	Dus2l_e6F	CAGGAGCTCAGAATCCTTTACC
Dpep2_e9F	ACTGTGAACAAAGGAGGAGTGG	Dus2l_e6R	TCTTTCTAGCCAGCAAATGTT
Dpep2_e9R	AGAGAGGTTGAATGGGCAAAG	Dus2l_e7F	AGGGACTTAGCTACCTTGTTCG
Dpep3_e1.1F	CAGTGGCGCCCTCTAGCG	Dus2l_e7R	GGCCCCAAATAGAGAATCTAGG
Dpep3_e1.1R	TTGTGTCATTAGGAATGCCTGGAG	Dus2l_e8F	CATGGGCCCTTGTAGATGTGTTA
Dpep3_e1.2F	GTAACCTGCAACCAGACTACTCC	Dus2l_e8R	TTCTGACTCCTAAACCTGCTCA
Dpep3_e1.2R	GTGTATAGTGGTGGTGGTGGTG	Dus2l_e9F	GAGCTGAGCAGGTTTAGGAGTC
Dpep3_e10F	CAGGTTTGTAAAGCTACAATCAGA	Dus2l_e9R	AGCTGTTTGTACGTAGGGTCT
Dpep3_e10R	TGTTCTATGCGCTCTGTGAGTT	Edc4_e10F	GTGGTGGTACATTGGAAAGAGC
Dpep3_e2F	GTACCTCCCCTCCCTTTGAC	Edc4_e10R	CATGGGAACTCTCTGAAAGGAC
Dpep3_e2R	TGCATGCTCTAAATGCCTAGTT	Edc4_e11-12F	GAGGAGGAGAGTGACAGTCTGG
Dpep3_e3F	CTGTGGGCGCTAAGGAAG	Edc4_e11-12R	GTGAGACTCTCCAAATGCTG
Dpep3_e3R	GACCTAGAAAAGGTTGGCAGGAG	Edc4_e13F	ACACTGCTCATGAGGACTTCAG
Dpep3_e4F	GAGTTGGAGCTTGTGACCTCAG	Edc4_e13R	ATGCAGAGATCTGGGAAGAGC
Dpep3_e4R	CAAAAAGGTCGCTTTAACTTCA	Edc4_e14F	ATGCTTTCATGACACCTACCG
Dpep3_e5F	GATGTAGGATGGAAAAACAGAGC	Edc4_e14R	TTATAGTCAGGCTGCCATCTAGC
Dpep3_e5R	AAGAGTGTGTCAGGGAGCAAAG	Edc4_e15F	GCTCTCTAACAGCTGTGTCTGC
Dpep3_e6F	CTAGCATGTCCCCTCTCCTCTA	Edc4_e15R	TTCCATTGCCCTCTACCAC
Dpep3_e6R	TCTCGATCCAAGGTTGAGAGTT	Edc4_e16.1F	TTCTGTTAGATGATGTCTAACCACTAC
Dpep3_e7F	CCCAAGAGAAAAGGTTCTTTCA	Edc4_e16.1R	GTGCTGTAGGCCAGACTTGAC
Dpep3_e7R	GACATCTTCTGTCCTGGAGACC	Edc4_e16.2-17F	TGCCTCAGCACTACACCTACTG
Dpep3_e8F	AGCTGCCACAGCCAGGAG	Edc4_e16.2-17R	GAAGGCTGAGTGTCTGCTCAC
Dpep3_e8R	GGCTGGAAGACCAGAACTTGTA	Edc4_e18-19F	GTGAGCACAATCTTGTTCCTTG
Dpep3_e9F	CAGCAGGTTCTAGACCAGGATT	Edc4_e18-19R	GCCAGAAGCACTGACACTTAC
Dpep3_e9R	GACCTCTGCCAGTTAACTCTCC	Edc4_e1F	TGTAGTCTCTGTGCTCTCCTG
Dus2l_e10F	GCTTGAGGTTCAGTAGGAAGGA	Edc4_e1R	TCCTGAATCTGGCTAAAGGAAC
Dus2l_e10R	GCCATCCCAGTTTTCTATGCTA	Edc4_e20F	AAGGGAGCACCTTTCTACCC
Dus2l_e11F	CTCCGTCACCACTTAGAGTCCCT	Edc4_e20R	AGTCGCGGTTCTGTGGTA
Dus2l_e11R	TTAGGGAGTAGAGGCAGGAGAA	Edc4_e21F	ATGAGCAAGAGCGTATCCTTG
Dus2l_e12F	CTCTAAGAGGGCCGTTCCCTT	Edc4_e21R	GGAGACAC CTAGGAGAGACAGG
Dus2l_e12R	CATACACATCTCTGGTCCCTCA	Edc4_e22F	CTATCCCAGGCTTTGTCTTCAG
Dus2l_e13F	CCAGCTCCGAAAAAAGAACC	Edc4_e22R	GGCAATGGCATCTGTAAAGTTC
Dus2l_e13R	GCTTGACAATATTCATATAAAACAGC	Edc4_e23F	GCTACTCAAGTCCAAAGGTGATG
Dus2l_e14F	GTGGCTGATTGGTGGTTCTT	Edc4_e23R	CAGCTGCTGCAAATCTAAAGG
Dus2l_e14R	GCTGCGAGTGTACTACAGAGAGG	Edc4_e24F	CTCAGGAATGTGAGTGTGTGCC
Dus2l_e15F	GGTGGGAGTGGGAGAAGTC	Edc4_e24R	GCTAAGATTGATTCTCTGCAAGC
Dus2l_e15R	CACAACACACCCAAGTCTTGTAG	Edc4_e25F	GCCACTGTGTCTAGCAGTGTTC
Dus2l_e16.1F	GTATTTGTAGGCTCAGGGCTTC	Edc4_e25R	AAAGTATCAACGAGCCTGATGG

Edc4_e26F	GAATCCAACCTTTGGTCTTCTGG	FAM65A_e13.1R	TCTGGATATACAAGTGGGCTAGG
Edc4_e26R	GGGAGCAGGTAAGAGTGAGTTG	FAM65A_e13.2F	GGACTCTCAGCCACATCAGTG
Edc4_e27F	CCAGTTCCCATATGAGGCTTAG	FAM65A_e13.2R	GAGTTGGGCTTGTGGTAGTCTG
Edc4_e27R	TCACAAGGCCGTGTAACATTAG	FAM65A_e13.3F	GCCTAACTTCCACCACTGTAGG
Edc4_e28F	CTGATCCACACAACCTCACTTG	FAM65A_e13.3R	TAGGGAGTAGAGGTTGGGTGAC
Edc4_e28R	AGGACCCAAGAAGGCACAATAC	FAM65A_e13.4F	CAGACCACTACAAGTCCCATTTG
Edc4_e29F	TTTCTTGCTCCTCTGCCTATTC	FAM65A_e13.4R	CCTCCTTACCATGAGCAGACTC
Edc4_e29R	TAGAGCCCTCAAAGCTGATCTC	FAM65A_e13.5F	GGACAGAAGGCTCGAAGAGG
Edc4_e2F	CTGGACATAACAAATGCTCCTG	FAM65A_e13.5R	TAAGGAGAATCAGGGCTACTGC
Edc4_e2R	GATCATCCAGAAGAGAGGAAGC	FAM65A_e14F	GGAGAGTCTGCTCATGGTAAGG
Edc4_e30F	GGGCAGTATCAGGTAACAAGG	FAM65A_e14R	ACAAGCCCATCCTCATGTATTC
Edc4_e30R	CAAAGATTTGGACTGGGAAGAG	FAM65A_e15F	TGTTACTCATTGCTGGTTACCG
Edc4_e31F	ACCCAATCTGTGCTTACCATTG	FAM65A_e15R	GAGGTTTAGAAGGTTGGATTGG
Edc4_e31R	ATATTCTGCAGAGCTCACATGG	FAM65A_e16F	GCATGCTGGGATCTGTACTCC
Edc4_e3F	ATTAACCTCATTGCCAGAAGG	FAM65A_e16R	TGAGTCCCTCTGTACACTGGTC
Edc4_e3R	AAAGTGGTCCCATAGGAATTG	FAM65A_e17F	ACATCTGCCAGGAAGTAAAG
Edc4_e4F	ATGTCAAGTGGGTGTTAGGTTTG	FAM65A_e17R	TTTCTTCAGTCTCGATTGTGTC
Edc4_e4R	GGGACAAACCTCTACTGTACGC	FAM65A_e18F	ACTGACAAATCGAGCACTGAAG
Edc4_e5F	CTGAGGGAGCTGGTCAGG	FAM65A_e18R	GGTGCCTTGTCTCATCATCTC
Edc4_e5R	AAGGCTACATAGGTAGATGATGATG	FAM65A_e19F	ATTCTGGTCTCATGGGTGGTC
Edc4_e6F	CAGTATCCATCCCAGGCAAG	FAM65A_e19R	ATCCTCATCCTCAAGCTGGTC
Edc4_e6R	ATATCCAAGTCCCACACCTCAG	FAM65A_e1F	GTTATACGAGCCAAACCTGCAC
Edc4_e7F	ATGAAGACCGGGTGAGAGG	FAM65A_e1R	GTTCCAGTCTTGGCAGTCTCAG
Edc4_e7R	GAGCCAGGTTGTCTTCAACATC	FAM65A_e20F	CGGGAAAGGGTGAGTTTG
Edc4_e8F	GTTGGTTGGCCCTGTTCACTAC	FAM65A_e20R	ATTGAGGCATTGAGACAGGTTG
Edc4_e8R	GACACCTGCAGGCAGACAG	FAM65A_e21F	GGGCTGTATCAAGGTGATTCC
Edc4_e9F	GCAAACCATTCGGTAAACTAGAG	FAM65A_e21R	CTTCCCTTCCCTGGCATTAC
Edc4_e9R	AGGCTGTAAGGGCTGTGACTAC	FAM65A_e22.1F	ATTTGGGATCTTGGCTATTGG
Ednra_e1F	GGGTTGGGAGATTTCTTG	FAM65A_e22.1R	AAACCAAGGGATGTGGTGAG
Ednra_e1R	CTCTTAAACCGTCTGAGCTG	FAM65A_e2F	ATGAGGCTGAGACTGCCAAG
Ednra_e2F	CTGGTCACAAGTTCACACTG	FAM65A_e2R	CTGAAGAAGAAAGCGCCTTTAG
Ednra_e2R	AGGAGGCTAGTTGTGTCTCA	FAM65A_e3F	TACGCGACAAGGGTATTAATGG
Ednra_e3F	GGAAGGCATTTTCCAGTC	FAM65A_e3R	AGTCAACTTATCCAGCCTCTCG
Ednra_e3R	AGTCAGCACAGTAGCCTTGT	FAM65A_e4F	CCCAAGATTCCACATAGGTTTC
Ednra_e4F	CAGGTCTTCACTGCTGACA	FAM65A_e4R	GGATAGAAACACCTACTAGCTCACC
Ednra_e4R	GCATTGTTGGATGGTACG	FAM65A_e5-6F	GGAAGAGGACTGTCAAAGAAGG
Ednra_e5F	GGTTAATGGCTCCTCCAT	FAM65A_e5-6R	CTCACCACTGAGAACCACAGAG
Ednra_e5R	CTCAGGAAGGAAGTGACAAG	FAM65A_e7F	GAGATCATGGAGAAGAGGGGAAG
Ednra_e6F	TCCCTGCAGTGCTTCTTA	FAM65A_e7R	AGAAGACACATGCTCTGGGAAG
Ednra_e6R	GTGCCTGATCAAAGCAGTAG	FAM65A_e8-9F	TGTGACAGAGCCACAAGGTG
Ednra_e7F	GGCATCTCTCACTGGATG	FAM65A_e8-9R	ATTGGGCTCGTAACTTCCAG
Ednra_e7R	GGACAGTACTCAGGAAAGACC	Gfod2_e1F	ATGCGCAGCTCTCTATCCTG
FAM65A_e10F	GCGATCAATATGAGGTATGAGG	Gfod2_e1R	GTATACTCGCTTCCAACCTCAG
FAM65A_e10R	TGGGAGAATGACACAAGGAATC	Gfod2_e2F	TCCAAATTGCCTTAGAATCTCG
FAM65A_e11F	CTCAAAGTAACCTGCATGTCCTC	Gfod2_e2F	TCCAAATTGCCTTAGAATCTCG
FAM65A_e11R	TGACTGTAGAAGCAGCTGAAGG	Gfod2_e2R	CTAGGAGAGGGCAGTGAGCTG
FAM65A_e12F	GTTGTGGCTGTGGATATCAATG	Gfod2_e2R	CTAGGAGAGGGCAGTGAGCTG
FAM65A_e12R	TCCCATTCTCTAACTCCTCCTG	Gfod2_e3.1F	TTCTAGGACAGCCAAAGCTACC
FAM65A_e13.1F	AGTCCACCAGATACACCCTCAC	Gfod2_e3.1R	ATTCTGCCTCACAAAGGTCTTG

Gfod2_e3.2F	CTATGGCTGGATTTGTGATGAG	Kctd19_e7R	TTTAGCTCATGGGAGAGGCTTA
Gfod2_e3.2R	GCAAGGCCTGAACCATATAGAC	Kctd19_e8-9F	TTATTCTGGTGCCACATTTGAT
Gfod2_e3.3F	GGAGGAGCTGCTAGTGAGAGAC	Kctd19_e8-9R	TCCTTCCCTCCCTAGTCTACAA
Gfod2_e3.3R	ACCTTCAGTTGGCTCCTAACC	Lcat_e1F	AAGACGGAACTGAACCCAAGT
Hsd11b2_2_e1.1R	GGCACAGCCAGTCGAGAG	Lcat_e1R	TATCTGCTGCTGTCTGGCTTAG
Hsd11b2_2_e1.2F	CAGCAAAGAAAGCGAGTATCC	Lcat_e2F	AGAACCTGGAAGGTGTACGAGA
Hsd11b2_e2F	CAGGTGCCTAGATTCCACCT	Lcat_e2R	GTAGACAAACCTGGGGACAGT
Hsd11b2_e2R	CCTGACAGCAAACATGTAATCC	Lcat_e3F	GTATGTCCCATGTGGTCTACCC
Hsd11b2_e3F	GGCTGGAGAGTGTGAAGGAG	Lcat_e3R	GTAGCCTGTGGGGAGAAAAA
Hsd11b2_e3R	GATAGAATGGGGACGCTCAG	Lcat_e4F	GGGCTCTTTTTGGCCTTC
Hsd11b2_e4F	CAAGGGGACGTATTGTGACC	Lcat_e4R	ATGGGTCGATAGGTCAGGGTAG
Hsd11b2_e4R	AGCCAAAGGCCACTCATCTA	Lcat_e5F	CCGTAAGTGTTCGACGGTGAT
Hsd11b2_e5.1F	GAGCATGTAGTGTGGCTTGG	Lcat_e5R	GACAGCTAGCTCTGTGATCTGC
Hsd11b2_e5.1R	CTCAGTGCTCGGGTAGAAG	Lcat_e6.1F	CTTGAATAAAGGTCAGGATGG
Hsd11b2_e5.2F	GGGGCTCATGTATTTTCATCC	Lcat_e6.1R	CTACGTGTGGCTACAGTGTCTG
Hsd11b2_e5.2R	GGTCGTGCCTGGTAGGGTAT	Lcat_e6.2F	GCGCCTGGTGTAGAAGTATATTG
Hsd11b2_e5.3F	GGAGGTGGAATTTGCTAGTGA	Lcat_e6.2R	AGAGACCTTACCAGAGCCCATT
Hsd11b2_e5.3R	CCCAGGATCTCCCAAGAAGT	Lin10_2_e16.2F	AGCTGCCCTAAGGACTTCCAC
Kctd19_2_e18F	CTGATAAGGGAACCCACCTCATA	Lin10_2_e16.2R	CCACAGCCAGCTCATCAAG
Kctd19_2_e18R	TTATCATTTGGCTGGGGATGT	Lin10_2_e5F	GCAATCCCAATGCCTAAGAG
Kctd19_e10F	TGTA AACATTACCCACCAAAGC	Lin10_2_e5R	CCAAGGACCTGAGATGAGGAG
Kctd19_e10R	ATGTGACAAGTCCCAAAGATGC	Lin10_2_e6F	TCTCAGGTCCTTGGATAGGTG
Kctd19_e11F	ATAAAAATCTCCAGCCCTGCTC	Lin10_2_e6R	TCTACCCATTCTCTCTTTGACC
Kctd19_e11R	TACAACCAAGGGTTCTCTTTGC	Lin10_e10F	GCTTACACAATTAAGGCACACG
Kctd19_e12F	GTTATTGCTCGAGGCAGCTT	Lin10_e10R	CTCCCGAAGGTCACACAGG
Kctd19_e12R	TGGCAGATGAAAACATCTGTAAG	Lin10_e11F	TCTGATCGAAGACTCCAAGTAGG
Kctd19_e13F	GCCTGACCAATTAATGGATGG	Lin10_e11R	CACTCAAAGCACTGGGTTCA
Kctd19_e13R	CCCTTGAACCCTGTGGTG	Lin10_e12F	GCAGGTACGTAAGGCTCTGG
Kctd19_e14.1F	GGCTGTCTTAAAGCCTAGCTGA	Lin10_e12R	CCGGCTCAAGAACTACACTCT
Kctd19_e14.1R	TCCCACTCCCTTACCAAAGATA	Lin10_e13F	CCACATTTTTCGAACCAACC
Kctd19_e14.2F	CCAAGAAGAAGTGCACCACTATAA	Lin10_e13R	GTCCCTAGACATGCCACCTG
Kctd19_e14.2R	CCCCTGCTCTGCTACTAACTCT	Lin10_e14F	AGTACCAGGTGGGCATGTCT
Kctd19_e15F	CCAAAAAGTGGGAGGATGACT	Lin10_e14R	GGATCCCTAGCCCAGAAACT
Kctd19_e15R	TAGGGCAGGGAGAAGTGTAGAG	Lin10_e15F	GTAACCCGCATCCCCAAAAG
Kctd19_e16F	CTCTACACTTCTCCCTGCCCTA	Lin10_e15R	TGTTAACCCACAATTCCCTAATCA
Kctd19_e16R	CTTATCCCTGCCTTTTAGCTA	Lin10_e16.1F	CACGCCATGTGTGTACCTTC
Kctd19_e17F	TGAAAAGGCAGGGATAAGAGTGC	Lin10_e16.1R	AGCCTTCCAAACCCAAAGTC
Kctd19_e17R	CTGGCCTGGCCCAACAGTA	Lin10_e16.3F	GAAGACGGGGCTCTTTCTCT
Kctd19_e1F	TGTGATTTCCCTAGGATGTTGT	Lin10_e16.3R	GAGGCAAACAAGATGGAGACA
Kctd19_e1R	CCTCAGAACCCAACATAGAAAA	Lin10_e1F	CCGCCTCTGTGATTTAGCTC
Kctd19_e2F	CCTTGCCATTTTGTATTTGTG	Lin10_e1R	GAGGGTAGGAAAAGGCCAAG
Kctd19_e2R	AGCTCAGATGAGGCTAACGTCT	Lin10_e2F	AGGCTTCAGGGAACAATGCT
Kctd19_e3F	AGAAACTGATGCCTAGGTGGTC	Lin10_e2R	ACACAGCAACTCCTCCCAAC
Kctd19_e3R	GTAACCAACAAATGGACCTTGC	Lin10_e3F	CTGTGTGTTGCAGCCTTGTT
Kctd19_e4-5F	GATGAAGAATCTGCCAGGACAT	Lin10_e3R	AACAGCACATTAGTCAGCTCCA
Kctd19_e4-5R	AGAGGACATGCAGGGTTTTAAG	Lin10_e4F	CCCAGCCTTGAACTCTTGAT
Kctd19_e6F	AACAAACATCTCCCCCTTACAG	Lin10_e4R	TGAAGGCAGTAGATAAAGCTGGT
Kctd19_e6R	AGACAGCATATGCCTAGGAAGC	Lin10_e7F	ACCGTGAGTGCCAGGGAATA
Kctd19_e7F	CACATAAGTCCTAAGCGGGGTA	Lin10_e7R	CAGAAGGAACAAGGCATGG

Lin10_e8F	GCCTCCAGGATACCAAGTGA	Nfatc3_e7R	CTCTTAACCACTGAGCCATTC
Lin10_e8R	AACACGCCTACAAACCAGGA	Nfatc3_e8F	TCATGAATTGCTTTGAATTTGA
Lin10_e9F	GCTAGCTTTTCAGAACCTCTGG	Nfatc3_e8R	CAACAAAAATAGTATGTTGGCATT
Lin10_e9R	GAACAGACTCTCTGTGGAAACCT	Nfatc3_e9.1F	TGAGTTCATCCCCATTGTGTTA
Lypla3_e1F	CGTTTCGTAGCGGAGAGTTACA	Nfatc3_e9.1R	AGGCAGGATTCATAGGAAGACA
Lypla3_e1R	TTTAGAGGGTGCCAGACCAC	Nfatc3_e9.2F	CTGGCAAAGAACAGCACATAAT
Lypla3_e2F	TCCTGGCATTGTGGGATT	Nfatc3_e9.2R	TAGGCTGTAATGGGAAGAAGG
Lypla3_e2R	AAGAAGATGAACAGCAAGAAGAAA	Nfatc3_e9.3F	CCCACCTCATCTGCAGTCAA
Lypla3_e3F	CCTTTAGACCTCAGACCAAACC	Nfatc3_e9.3R	ACCAGGTGGAAACGATGCT
Lypla3_e3R	ACACCACACCCACAGAGACAAT	Nfatc3_e9.4F	CATTCTGGACAGCACTCAACTC
Lypla3_e4F	CCACTTCAGGGAGACAGATG	Nfatc3_e9.4R	CAAGGCCAGCTTAACTCAAAT
Lypla3_e4R	TCAGAGAGAGCCCCAAGGAC	Nol3_e1.1F	TTCTGTGCCCTGGTCTC
Lypla3_e5F	TCTTGGCAGAGGTAGAGACTAAG	Nol3_e1.1R	GCACAGCGCAGTAGTTCCT
Lypla3_e5R	CAGGGAGGAGTTATGAAGGATG	Nol3_e1.2F	CCTGAGTATGAAGCCTTGGATG
Lypla3_e6.1F	TCCACATACAGAAAGACGGAAA	Nol3_e1.2R	CTCTCCCTTACCCTTTGCTTC
Lypla3_e6.1R	GGTCACGATCAGGAAAGTTCTC	Nol3_e2.1F	GGGAGAGCAGAGAATGTAGAGG
Lypla3_e6.2F	GTACCGCCTGGTGTAGAGCTG	Nol3_e2.1R	TCTTGGAAATCAGGCTCTGC
Lypla3_e6.2R	AGACTTAGGACCTTGGATGACG	Nol3_e2.2F	AAGAAATGGAACCAGAACCAGA
Lypla3_e6.3F	CTTGGCTTATCTGAAACGTGTG	Nol3_e2.2R	AGTGGGATTCAGACCATTCTTG
Lypla3_e6.3R	TGTGGAACCTTCTATGACAGGA	Nol3_e2.3F	CAATGCAGCAAGACTCCATTTA
Lypla3_e6.4F	GCCATGCAATCCTCTTATCTTC	Nol3_e2.3R	AGGCCAGACAATTAAGAGCAG
Lypla3_e6.4R	TCAGTACTGGAACCTGCATCAC	Nol3_e2.4F	GTCCATCCACACACAGAGAGAA
Lypla3_e6.5F	ACCTCTCATTTAGTGGCATCCT	Nol3_e2.4R	ATTCAGGCCAGAAGTACAGACC
Lypla3_e6.5R	TCCCTGTGTGCAGAGACTAT	Nr2c3_e1.1F	AATGGTCACAGGTCTCCAC
Lypla3_e6.6F	GGGAAACAGTCCAGAGATTTGA	Nr2c3_e1.2F	CCGGCAAATCTCAACAACCTC
Lypla3_e6.6R	AAGTTCAGGCAGAGGGATAATG	Nr2c3_e1.3F	AGCAAGCACTCATGTTCCAGG
Nfatc3_e10F	AAAACAGTACTGGGCAGTGGAT	Nr2c3_e1F	GCAGCTCCATAGATGCAA
Nfatc3_e10R	TCCTTTGTAGCACATGCAAATC	Nr2c3_e1F	GCAGCTCCATAGATGCAA
Nfatc3_e11.1F	AAGAGAGGAAAAGAAACCCTCA	Nr2c3_e1F2	CCTTGCAATTCAGCAAGACAA
Nfatc3_e11.1R	AGCTCATTTCCACAGCTTAAA	Nr2c3_e1F3	TCATTCATGCCTGACTCTGC
Nfatc3_e1F	CTTTCTAGTCGGAACGGAACAC	Nr2c3_e1F4	GCAGCATGAAATCTCCAATC
Nfatc3_e1R	GCCTCCTCCTCAAATTAATCA	Nr2c3_e1F5	CACGACGTTCTTTCCCTAA
Nfatc3_e2.1F	GCATTTTGGTGTCCAGATTTTT	Nr2c3_e1F6	GAATCTTAGGACCACCTGTGC
Nfatc3_e2.1R	GCCTTTCCAAATATTCCTTTTC	Nr2c3_e1F7	CAATATCTTTATCACGGTCACCT
Nfatc3_e2.2F	GTGGTCTCTAAACCTTTGAATG	Nr2c3_e1R	ATGACTTTTGCGGGTCAG
Nfatc3_e2.2R	CTGGATCTAGGAGAGTGGCAAG	Nr2c3_e1R	ATGACTTTTGCGGGTCAG
Nfatc3_e2.3F	CTCACCTCTGACTTCTCCAGGT	Nr2c3_e1R1	GTTCCCTGGATTCCAGCTCA
Nfatc3_e2.3R	CCCTTGATCATCTGAACAGACC	Nr2c3_e1R2	AGCGGGCTGCTAACAGAAG
Nfatc3_e2.4F	CCGTTTCCATTTCACTACTGTGT	Nr2c3_e1R3	GCAGAGGGACGTTATTTGGA
Nfatc3_e2.4R	GGAGAGGGGAGAGAGAAAAGAA	Nr2c3_e1R4	ATGTACTGGACAATGTTGAGC
Nfatc3_e3F	ACATTGAACCTGGCAAAGAGAT	Nr2c3_e1R5	CCCATCATCTGGTTCTTGCT
Nfatc3_e3R	CCAAGAAAATACAGCCACATCA	Nr2c3_e1R6	ACAGGTCACCGTGTGGTTTC
Nfatc3_e4.2F	TGGGTTACTTCTACTGTCTGTTTTG	Nr2c3_e2F	GCCAAGACTGTGCAAGAT
Nfatc3_e4.2R	TCATTTACAAAGGTTTTAAGTTACCTG	Nr2c3_e2R	GAACTGGAGCAAGAGACAAC
Nfatc3_e5F	CTGGGATTATAGGTGTGCATGA	Nr2c3_e3F	CCTGTTTGCTCTACTGTGT
Nfatc3_e5R	CCAGCAACTCACACTCAATAGC	Nr2C3_e3R	GGAGTTTTGCTCCTGGTTAG
Nfatc3_e6F	TCCAGTGTTTTATTTATAGTTTTGG	Nr2c3_e4F	GTACTCCTTTTGGCACAGAG
Nfatc3_e6R	TTTTCAATAAAACCCAGTGCTT	Nr2c3_e4R	AGTCTTCCGTACTTGAGCAG
Nfatc3_e7F	CTCCCTGCCAGTAATTTGTGAT	Nr2c3_e5F	CGTAGGTGTCTGTGGAATTG

Nr2c3_e5R	GGGCTCGTTTCAGTAGACTC	Prmt7_e2R	GAAAGGTGGCTTCTCTGAACTG
Nr2c3_e6F	GCCCTGACTTAGCATCTCTA	Prmt7_e3F	GGTTCCTGTCTTAAACTGTGCTG
Nr2c3_e6R	GGGTAAGCGTAGGCAGTAA	Prmt7_e3R	GGAACCCGTGTCTGACTCATCTC
NTF2_e1F	CGTTCTAGCCAAGTTCACTAACG	Prmt7_e4F	GACCTGAGATGGGTATTATCTTGC
NTF2_e1R	AGGGCCTCGAAGCAGAAG	Prmt7_e4R	GACTGACTGCTGTGACACTCG
NTF2_e2F	TGAGGAGGCTAGGAAAAGACAG	Prmt7_e5F	GAGTTAACGGGTTCTGAGCTG
NTF2_e2R	AAAGAAAGCCCAAACCTTCTATC	Prmt7_e5R	CGGGAGTATGGAGATTCTGAAG
NTF2_e3F	CTCCCTAAGCAAGATCCTTTTG	Prmt7_e6F	TGACAGGAAGGCCTTAGAGTTAC
NTF2_e3R	GGCTCTGCAAGAGGAAGAATAG	Prmt7_e6R	AAGTTTCCACAGAAAACCTGTCC
NTF2_e4F	TAAGTAAAGGCCAGACATGAGG	Prmt7_e7F	AGCTGAGTCCCTTCCACATCAG
NTF2_e4R	TGACTGTTCCCAACAATAAGCAG	Prmt7_e7R	TCTTCTTTGCCCTTGACTGAATC
NTF2_e5.1F	GTACCTGATCCCAAAGTTGAATACC	Prmt7_e8F	TCTCTTTGCATCTGATTGTTGG
NTF2_e5.1R	GCTGGTACAACAAAACTTTCTCTGT	Prmt7_e8R	CTTGCTACAAGCACCTTTACC
Pard6a_2_e3.1F	CCAGGGCTCTCAGACTTTACAT	Prmt7_e9F	GGATTTGAACTCAGGACCTCTG
Pard6a_2_e3.1R	GGAGCCACACGAACACTCAT	Prmt7_e9R	CTAGCATCTGCTCCAGAGGAAG
Pard6a_3.2bF	AACCTCATTGTCAGTGTCAAGC	Pskh1_e1F	AAGCTCCGCCCTCTCTTCCCTC
Pard6a_e1aF	TCTCTGTAGTGTTTAGCCTTTGGA	Pskh1_e1R	GGGCCGAAGGCTCAGAGTC
Pard6a_e1aR	TACGTCATTACGCTATGGTTCCG	Pskh1_e2.1F	AGGAAAAGGGAAGACGACTTTT
Pard6a_e1bF	ATTTCCGGTTCTGTGTGAGACCT	Pskh1_e2.1R	GTCAAATTTGGCCCTGTACTTT
Pard6a_e1bR	CTCTTCACCTCGACGATGCTAT	Pskh1_e2.2F	CCCTGGTGCTCCCACTACT
Pard6a_e1F	TAGACTCCGCGTTTCTTGGT	Pskh1_e2.2R	AGTGAAAGAACCCTTGGAATA
Pard6a_e1R	GAAGTGGAGGATGGAGGACA	Pskh1_e2.3F	TTTGAGACACAGGAACGGGTAT
Pard6a_e2F	CCTCACCTGACAGCCTCAGT	Pskh1_e2.3R	GGTGCCACTGAGCAGGAT
Pard6a_e2R	GTCTGAGAGCCCTGGGTATG	Pskh1_e2.4F	AGTACATTGCTCCTGAGGTTCT
Pard6a_e3.2aF	CGTGGACCTACTACCTGAGACC	Pskh1_e2.4R	CCTTCTGACCAGGAGCTTCA
Pard6a_e3.2aR	TACAGAAGAAGGCCCTGTGAGA	Pskh1_e3.1F	CTAATTCTGTGGTGGTCTGTGGC
Pard6a_e3.2R	CAAGGAGGGCAGAGAGCTG	Pskh1_e3.1R	GCTGTTGATAGCCGAGGTTAAG
Pard6a_e3.2R	CAAGGAGGGCAGAGAGCTG	Pskh1_e3.2F	AGAGCACCAAATCTTCCCAGT
Pard6a_e3.3F	GCCACCCTCCCTGTTCTAAT	Pskh1_e3.2R	GACTCAGTCCCTGCACCTTTTTC
Pard6a_e3.3R	AGGAAGGTCTCTCCCATGCT	Psemb10_2_e1F	ACCTGGGACTAGAAGCAAAGG
Prmt7_e10F	AGCCACATGAAGACAAACACC	Psemb10_2_e1R	CCTCTACTTGGTCACCCAACAT
Prmt7_e10R	TATCTGCTTTGGCACAGTATCC	Psemb10_2_e7F	GAATGGAGGGAAGAGAAAGGAT
Prmt7_e11F	GTCCCAGGAAGGGAGTAAGG	Psemb10_2_e7R	GACCGACCGACAGACAGC
Prmt7_e11R	CTCCTGGTTGTGATGCTTCTG	Psemb10_2-3F	TAGAGGCTTAACCCAGGAGATG
Prmt7_e12F	AGCCAGGCCTCAAGCATAAC	Psemb10_2-3R	ACTGGCCCGGTAGATACTGAC
Prmt7_e12R	GACATCACAGCATTAGCCAAG	Psemb10_e4F	ACATAAGTTGCACTGTGCTCAC
Prmt7_e13F	TGAATGAATGAATGAACGAACG	Psemb10_e4R	GGTCTCACCTCCTGTCTATCCC
Prmt7_e13R	CTGTTTCCTCTGCACACAAGAG	Psemb10_e5F	GGACTCAGACCAAAAAGCAATA
Prmt7_e14F	TACCTTTACCTCCCAAGCACTG	Psemb10_e5R	GCTGCAGCTGCTGAGGTATAA
Prmt7_e14R	GGCAGTCTTCCAAGTATCCTG	Psemb10_e6F	AAATGAATCTTGCTCCTGCAAC
Prmt7_e15F	TGACAATATGTTGCTCCATGTG	Psemb10_e6R	CTTTACCCCTACAAGCCTTCTCT
Prmt7_e15R	TTGACCCAGGAGTTAAGAGTCC	Psemb10_e7F	AGCAACTTGTCTAGGCTTCGAG
Prmt7_e16F	GATGGGACTGGTTGAGGTTTC	Psemb10_e7R	CTTTAGATCGCAGCCTGTCTCT
Prmt7_e16R	AGGGCATTACAGCACAAAG	Psemb10_e8F	GTGTGTGCTGCTGTCTGTCTG
Prmt7_e17.1F	CCTGTTTCAGGGCAGATAGCTC	Psemb10_e8R	CCAGGAACTGAGAATGAAGTCC
Prmt7_e17.1R	CATTCTCAGGATCACAAACTGTTC	Ranbp10_e1.1F	GCTACAGAACTGAGGCAGGAG
Prmt7_e1F	CCCAGAACTGAGATTGAAGGTC	Ranbp10_e1.1R	GTTCTGCTCTCCAGGTGAC
Prmt7_e1R	GCAGGAACCACTCACTATCCTC	Ranbp10_e1.2F	CAATAGCAGCTCCCTCCAAG
Prmt7_e2F	AGCATTATAGGTGGGAACCTCG	Ranbp10_e1.2R	ACCCCTCTACTCCGGATGAT

Ranbp10_e10F	CTAGATTGGGTGGAAGGGAAAG	Rbm35b_e6-7R	CTGTGGAGCCAGTGTGTTAGT
Ranbp10_e10R	ACAACAGAGGGGAAGGTAAAGG	Rbm35b_e8-9F	GATTCTTCAAAGGGCTCAACAT
Ranbp10_e11F	AGGACCCATTATGGTCTCTCAG	Rbm35b_e8-9R	AGGAATCCCTTGCTGGTTTAAAT
Ranbp10_e11R	AGAGGAAGTGGGCATTAGGACT	RGD_e10F	CCTTAGTCTGTCTCCTGAGC
Ranbp10_e12F	GGTAGACTTAGGCTTCCCCACT	RGD_e10R	CTGACACGTTCCCTTACTCC
Ranbp10_e12R	TGCAGACACGACTAGAGTCCAT	RGD_e11F	GAAAGCAGTGTGAGAAGGAG
Ranbp10_e13F	GTGCTGTGTTCTGTCCCTCCTCT	RGD_e11R	CCTCAGAGGAAATGATAGCC
Ranbp10_e13R	ATGAGTCCTAAAAGCCCAGGAG	RGD_e12.1F	TCCAAGTACAAGCAGGAGAG
Ranbp10_e14.1F	TGGCTAGGACACTCAAACATTG	RGD_e12F	ACGGGCTATCATTTCCCTC
Ranbp10_e14.1R	AACCAGCCAATACTGAGTCACA	RGD_e12R	CACGAGGTGACCCTTTTT
Ranbp10_e2F	GGAGGGTTTGAAGTTATCATGG	RGD_e1F	AACCTAGTGCTCCCAGAAC
Ranbp10_e2R	TCATCCGTTAATACTAGCTCTGGA	RGD_e1R	GAGCCCAGTATGGAATGAC
Ranbp10_e3F	GAGTCTCATCATGGCCTCTCAGAT	RGD_e2F	AGTTCCTACTTGCTGGAGTC
Ranbp10_e3R	ACCCTCCCAAGTCTCTGAGCTG	RGD_e2R	GACATAAGCCCACGAGTTC
Ranbp10_e4F	TCCTGAGTGCTGGCTAAGGT	RGD_e3F	TTTGCAGAGGAGGTAGAGAG
Ranbp10_e4R	GTGCAGAGGCTCCATGATTC	RGD_e3R	ATGACTGGCAATGAGGTG
Ranbp10_e5F	AAGGCCCAGGCCTAAAATA	RGD_e4F	TAGCCATCTTGCTAGTCCTC
Ranbp10_e5R	ACACCCTGCACTTGAGAGTA	RGD_e4R	GTGGACTGTTAGCACCTTTG
Ranbp10_e6F	GCAGAGCCATGGAAGTGAAGAG	RGD_e5F	TCTTCTCGCAGCTTTGAC
Ranbp10_e6R	AGCATGCCACCACCTACAACCTG	RGD_e5R	CTTACCGCTACAGGCAAC
Ranbp10_e7F	ATATGTGTAGTCTGTCCCTCCAG	RGD_e6F	ACTGCTAGGCTCCCATT
Ranbp10_e7R	CTCCAGGATGGTGTGGATAAGGT	RGD_e6R	TGGCTCTGATCCTGGAAT
Ranbp10_e8F	GTCTGGTCCCTGCCTTCAGT	RGD_e7F	GCGCTTAACCACTAACCA
Ranbp10_e8R	AAGGGAGCAGAGCATTGGT	RGD_e7R	AGGAATAGCCAGGCAGTAGT
Ranbp10_e9F	GCCTCAGCTTGATCCAGAGC	RGD_e8F	CTGTGGTGTGGCATTGAG
Ranbp10_e9R	TTCTAAGCCCACCAGGAAAGGTATG	RGD_e8R	TGTGGGTATCAAGTGTCTCTC
Rbm35b_e10F	ATATTCCATTCCCACACTGTC	RGD_e9.1F	AATCCAGGGGATCAGTATC
Rbm35b_e10R	ACAGGTTTATCAGGCTAATTGGAG	RGD_e9.2F	GGAGAAAGACCAGCACTGTA
Rbm35b_e11F	CCCCAATATGCTGCTTCTTC	RGD_e9F	CCGCCAGTGTACTCTTGAT
Rbm35b_e11R	GCACCTTGTAAGCAGTTTGTCA	RGD_e9R	CCACAGTCTAACCTGGGAAC
Rbm35b_e12F	GGCATCTACATGGTAGGAAAGG	Slc12a4_2_e1F	CTCTCGCCACCTCCTCAAC
Rbm35b_e12R	GTCCGTAGTTACCCTGGTTAGG	Slc12a4_2_e1R	AAGTGGAGTCCCGCATGG
Rbm35b_e13F	GTGGGAACCAAGCTGTTCTAAG	Slc12a4_2_e2F	GGGTTGGCTTTCTGGATTG
Rbm35b_e13R	GGCCAGAAATGAGTCAGGATCT	Slc12a4_2_e2R	CTGGATGGCTGCAAAGAGG
Rbm35b_e14F	GTACAGGAGAGGATGGTCTTGG	Slc12a4_2_e3F	AAGCAAGAACAGGGATCAGG
Rbm35b_e14R	CCACTCTTTAGGGGCTTGTAAAC	Slc12a4_e10F	TAAGATCTCCATGCCACAC
Rbm35b_e15F	TCAGTGTCTTTCAAGCCTACCA	Slc12a4_e10R	CCAGCACCTAGTGGTCTTC
Rbm35b_e15R	AGAAGCCACTGGGTTGAGAGTA	Slc12a4_e11F	CATGCAAACCTGGAGACCTAAC
Rbm35b_e1F	CAAGCTCGTCTGTCTGCTGTC	Slc12a4_e11R	GGCTAGAGTGAGGGCAAAAAAAG
Rbm35b_e1R	ACCTAAAAGCACCAGGGTAAT	Slc12a4_e12F	TTTTTCTGACCCCTGACAC
Rbm35b_e2F	ACAGGTAGGTTGAAAGAGGTG	Slc12a4_e12R	AACCTCACCGCATCTGAATC
Rbm35b_e2R	CCCTCCCACAAGGGGGTA	Slc12a4_e13F	GTGACTTGTGGCTGCAAATG
Rbm35b_e3F	CTGAGTCCCTCCCTCCTCCTAC	Slc12a4_e13R	GAGGAGCTGGGGTACTCAGG
Rbm35b_e3R	GAGTGGGGATGAACAGGTAACATA	Slc12a4_e14F	AGGAGTGGGTTCCCTGGAGTT
Rbm35b_e4F	CCAAGGCCCTGTTGTAAA	Slc12a4_e14R	TCCCCTGTGGTAACCTGTA
Rbm35b_e4R	CATCGTGACATGCTTGG	Slc12a4_e15F	CAGCTTCTGACTTGGGACCT
Rbm35b_e5F	AGGATTCTGCGGGTGTTTAG	Slc12a4_e15R	CCACTGCCAACCTAACCAAT
Rbm35b_e5R	GCAAGAGGACTCTGAGGAAGTC	Slc12a4_e16F	GAGAGAGGGAGGGAGGGAAGGAGTC
Rbm35b_e6-7F	ATCCCCTCACCTGTCCATTTTT	Slc12a4_e16R	CTATGATCTCCTGGGGGACACTAC

Slc12a4_e17F	TTGGGAAAAGGCCAGACC	Slc7a6os_e1F	CTGTGGGAAGCACTCCACTC
Slc12a4_e17R	CCCTTATATGCCTGTTGCAC	Slc7a6os_e1R	CTGCTGGATTGGCTCCTC
Slc12a4_e18F	TCCAAGGTCTCCCTGTGAAC	Slc7a6os_e2F	GTGCGATCTCAGGTATGAGAAG
Slc12a4_e18R	CCTGTGACCCTCTGGTCTCT	Slc7a6os_e2R	AGGTAGAATGAGGTCAACCTTTAG
Slc12a4_e19F	GTTAAAGTGAGGTGGCAGAGACCAG	Slc7a6os_e3F	CTAGCCAGGGCTACATAGAATG
Slc12a4_e19R	TGCCCAGCCAGCTGGAGCACCTTA	Slc7a6os_e3R	TTATGCCCTTCTCCTCTTAGACC
Slc12a4_e20F	GGTGTGATGAACCAGTCACG	Slc7a6os_e4F	GGGTCTGGGCCCTAAATTAC
Slc12a4_e20R	GGTGTGAGTACTGGGATGC	Slc7a6os_e4R	AAGAACAGCCAGTGCTCTTAGC
Slc12a4_e21F	GGTGGTAGAGATGGTGAGCTG	Slc7a6os_e5.1F	AAGAACTGACTCCTGGAGGTTG
Slc12a4_e21R	TTTACCAAACCCGAACCAAG	Slc7a6os_e5.1R	CATGCTTGGCTTCACTTATCAC
Slc12a4_e22F	GACAGGCAGGATAGCCATGT	Slc9a5_2_e6F	ACCCCCACTGGCTGTTTAC
Slc12a4_e22R	CTGGCCCATCTACACAGCAT	Slc9a5_2_e6R	TTGGACTGAGGGATGGGTAG
Slc12a4_e23F	GTAGATGGGCCAGGGACAG	Slc9a5_e1.1F	AGGGGATCCCAACTGCTAGA
Slc12a4_e23R	CACAGGGCCAAGACAACCTTT	Slc9a5_e1.1R	CACACACTCACCGATTTTGG
Slc12a4_e24.1F	CCCTCTCCTTGAGTGAAAAG	Slc9a5_e1.2F	CCGTTAGGTGAGCCTCCAG
Slc12a4_e24.1R	CACCAGTCATCTCGAGTCAGG	Slc9a5_e1.2R	ACAATGCAAGACGCAGGACT
Slc12a4_e24.2F	CCTTGCAATGGGAATGGAT	Slc9a5_e10F	TGGCTGAGACTCATACCAAGAA
Slc12a4_e24.2R	TGGGTTCAAGTTCCTGCTTTC	Slc9a5_e10R	AGCCCCCTCGCTAACCAAGTCT
Slc12a4_e3R	TGTTCAACACCACAAAGGAAA	Slc9a5_e11F	GGCTCTGGCTCAAAACAAAG
Slc12a4_e4-5F	GACTIONGGCCTCCTTCCTGT	Slc9a5_e11R	GAGGCAGGGATATGTGTGCT
Slc12a4_e4-5R	TGCCTGAGGAGGAAAGACAA	Slc9a5_e12F	GGAAGGATCCACCAACACC
Slc12a4_e6F	TGTGGAGGTTTGCTACAAGAGA	Slc9a5_e12R	ACGCCTGTTGAGTCCATGAT
Slc12a4_e6R	TGCTGGCTAGGCATGATAGA	Slc9a5_e13F	GAGGAACATGTTGGGGTTGT
Slc12a4_e7F	CCAAAATGACAGGTTTCACTCC	Slc9a5_e13R	AACCCCTGACGGTGAATAAA
Slc12a4_e7R	CCCAAGCAATCTGAGGGATA	Slc9a5_e14F	GAGTGGTGGACCCCTTGTGAT
Slc12a4_e8F	GATGCTCCGTATCCCTCAGA	Slc9a5_e14R	GAGGAGAGGAACCCAGCTCT
Slc12a4_e8R	GCTCTGTGCTCTGCTTTCCT	Slc9a5_e15F	AGAGAGCTGGGTTCTCTCC
Slc12a4_e9F	CTTCCCTGGGBACATCAGT	Slc9a5_e15R	AACATGCAGCTCACAAGGAA
Slc12a4_e9R	TGCCTCCAAAACAGACAAG	Slc9a5_e16F	TGGTATCAAGAAGCAGCCACT
Slc7a6_e1.1F	TCCTGCTGTGTTGTATGTGTTG	Slc9a5_e16R	ACTGGCCTCCTAAGGCAGA
Slc7a6_e1.1R	CCCTGACTTGGTGATAGTGGTC	Slc9a5_e17.1F	CTTGGTGCATTTGAGGATTC
Slc7a6_e1.2F	ACTGCTTCCTATGGGTTGTACAC	Slc9a5_e17.1R	GGGGGAAAGCAAAGCTAGAG
Slc7a6_e1.2R	ACGCTCACATCTTCTTCTCCTC	Slc9a5_e17.2aF	CTGGAACCAGAGCATCTCATC
Slc7a6_e2F	TGCTGTTTACCTGTTCCAGTTC	Slc9a5_e17.2aR	CCAGGAAACCCCTTCTGACC
Slc7a6_e2R	AAATGTGCTGAGAGATGAAGC	Slc9a5_e17.2F	GTTCTCAACATGGGCAGAG
Slc7a6_e3F	GGGAGGTTCTGGTTATTGTTCC	Slc9a5_e17.2R	AAAGCAAGATGTGGGGACAC
Slc7a6_e3R	CCTCCTAACTGGAGAAGGGAAG	Slc9a5_e17.3F	AGGATCAGTGCACAGGCAAT
Slc7a6_e4F	AGAGGAGCCTGTCTCAAAGACC	Slc9a5_e17.3R	CCTGGGTTTAAGGTACAAAGCA
Slc7a6_e4R	AAACGCCTACCGTCTACCCTAC	Slc9a5_e17.4F	CCCAGAGTCACTGCACCATT
Slc7a6_e5F	GGGATGGGTCTAGGTAGGGTAG	Slc9a5_e17.4R	CCATTTGTGGATTCCCAGTT
Slc7a6_e5R	AATGCCATTGTTAAGAGGATGC	Slc9a5_e17.5F	TTCCAGTATTGTCCCACTAGCA
Slc7a6_e6F	AGCGTGAGTAATGGGCTAGG	Slc9a5_e17.5R	CCCTGGAGCTTGAATTCCTA
Slc7a6_e6R	ACTACGCTTCAACAAACCTTGG	Slc9a5_e17.6F	GCTCCACATGTAGCACCAC
Slc7a6_e7F	TTTCAGCTCTGACAGACCACTG	Slc9a5_e17.6R	AGACCACAATGGCCTTGAAC
Slc7a6_e7R	CTGCTAGTGTGCATGAGTTGTG	Slc9a5_e2.1F	TATTACAGGTCAGGCTGTGG
Slc7a6_e8F	AGTCTCTGGAAGAGCCATCTC	Slc9a5_e2.1R	CGGCATGAAATAGCCAGAGT
Slc7a6_e8R	GCCATAAGGAAGGTGGAAGAG	Slc9a5_e2.2F	GTGGCCAAGAAGGCTGAGTA
Slc7a6_e9.1F	GTGTGCCTATGGGACAGGTG	Slc9a5_e2.2R	AGATGCCCCGAGTTAGGG
Slc7a6_e9.2R	GCTCCTTTAATTCAGACGGTTTAG	Slc9a5_e3F	GGAAGTGTTCAGAGGCAGA

Slc9a5_e3R	TCTAAGCCTGGTCAGATAGCC	Thap11_e1.4F	CGACCACTCATACTCTTTGTCCG
Slc9a5_e4F	TGGGGAGGAAATAGGATCTG	Thap11_e1.4R	AGTTC AACATCTGCCTGAGGAT
Slc9a5_e4R	GGTCGCAACAATCCAGAAAA	Tmem34_e10F	GGAGGGGAAGCTACTTTTAG
Slc9a5_e5F	GGTGGGTGCCCTTCTCTATT	Tmem34_e10R	AGACCCTTGAGTTTGAGGTC
Slc9a5_e5R	TTTAAGACCTTGCAATTTGGCTA	Tmem34_e1F	CCGTAGCTGACCAATCAT
Slc9a5_e7F	GCCAGACCTTAGCCCAGATA	Tmem34_e1R	GTTTTGCAGACCTCAAGC
Slc9a5_e7R	CCTCAACCCATCACACTCAA	Tmem34_e2 3F	CTGCCTCCAAGGAATCTAGT
Slc9a5_e8-9F	GTGATGGGTTGAGGCCAAAAC	Tmem34_e2 3R	AGAGTGAGCTCCAAAGACAG
Slc9a5_e8-9R	TTCTCAGAAGGGTGGCATATC	Tmem34_e4F	GTGACAAGATCCCCGATT
Smpd3_e1F	GCCTCTCCATTGGCTAGG	Tmem34_e4R	ACTAGCTGTGGATCACGAAC
Smpd3_e1R	AGGACACGTCCCATCAACTC	Tmem34_e5F	GTTCCCTCCTGTTTTAGAGG
Smpd3_e2.1F	CCAAACACTCCGTGTGAAAC	Tmem34_e5R	CTGTCAGAGGGGTGTGAATCT
Smpd3_e2.1R	TGAAGAGTACGGTGCAGAACAG	Tmem34_e6F	CACCCATAGGCTCTCTAA
Smpd3_e2.2F	CCCTCATCTTCCCATGTTACTG	Tmem34_e6R	CTTCTCTGTCTGAGGGTCT
Smpd3_e2.2R	CACTGATGGAGGTGTTGGTG	Tmem34_e7F	GAGTGCCAGGGAAAATGT
Smpd3_e2.3F	CAAAGAGATTGGGCAGAGAATC	Tmem34_e7R	CTGGCACAGGACTAGCTTT
Smpd3_e2.3R	TGCCACCACTGTCTTGTC	Tmem34_e8F	CCAGCATATCCATGTTGC
Smpd3_e2.4F	AGATGCCCAACCACAATCAG	Tmem34_e8R	ACTGTTGGCACGTTGTTC
Smpd3_e2.4R	ACGCCTACCTTGAGAAACAGAG	Tmem34_e9F	GCTACCTTTCAGTCCCTGG
Smpd3_e3F	TAGCCAGAGTCTAGCCAGGAG	Tmem34_e9R	CCAATCTGACAGCTCCTG
Smpd3_e3R	GACAGAGACCAGACTGTGAAGC	Tradd_e1F	TTCTTGCAAAGCGAGTGGAG
Smpd3_e4F	GGTTCAATACCTGGGACCTG	Tradd_e1R	GAGCCTAAACCACAAAGCAAAG
Smpd3_e4R	CTGTGACCATGCCTGGAG	Tradd_e2F	GACTACGGGCTTAGCTTCCCTC
Smpd3_e5-6F	AACTGACAGGAACCAGCTGATAG	Tradd_e2R	GTTTGCAGAACTCATCCTCCAG
Smpd3_e5-6R	CAGGGTTCCACTCCTTGTTAAG	Tradd_e3F	GGTGCTGGTGTCTGTAGTTAGG
Smpd3_e7F	TCTGGTCTCCTCCTTACTG	Tradd_e3R	GAGGTAAGTAAGCATCGGTTCC
Smpd3_e7R	GGGTTGTACAGAGGATTTCAAG	Tradd_e4.1F	GTCACCAGCAGGTAGATCTGAG
Smpd3_e8.1F	CCAGAACTTCCCTTCACAGAAC	Tradd_e4.1R	AAACACTGGCTGAACTGGTTG
Smpd3_e8.1R	TACGAACCTTGGGTTACAAAAC	Tradd_e4.2F	TGGAGGAGAACGAGCTCAC
Smpd3_e8.2F	CATCTCTGCGGACAGAGGAC	Tradd_e4.2R	GGGCTAGACCTCAGTATTTCCAC
Smpd3_e8.2R	AAATGTAATCGCCCTTGAATG	Tradd_e4.3F	ACTGTCACGAGCAGGATGC
Smpd3_e8.3F	AAACAATCAGAACCAGCCAAAG	Tradd_e4.3R	TGTCCTGGAATCACTCGGTAG
Smpd3_e8.3R	CAGGCAAGTGTTCCTGAGC	Tsnaxip1_e10F	AGCCATCTAGAGCTCATCATCC
Smpd3_e8.4F	CGACAGGTTTGTAGCTTCTTCC	Tsnaxip1_e10R	CACCCTACTCCCTACCATCTTG
Smpd3_e8.4R	CCTCAAATCAGTAGCTCAGCAG	Tsnaxip1_e11F	ACTTCAGCTCCAGTTTGAGGAG
Smpd3_e8.5F	CTGCTAGAAGCCCACTGCTC	Tsnaxip1_e11R	CCAAAGTCTATAAGAGGGGAAGCAG
Smpd3_e8.5R	TCCTAGCTCTGGACACTCAAAC	Tsnaxip1_e12F	GTCCCCGGCACAAAATGG
Smpd3_e8.6F	CTTCAGAGTATGGCAGCTTGG	Tsnaxip1_e12R	CCCTTTCCTGAATCTGACC
Smpd3_e8.6R	GGCTTCAGAACCCTGACTGTGTAG	Tsnaxip1_e13F	TGTTGAAATAATAATGGGGATGG
Smpd3_e8.7F	ATCCTTCTCTCCTTCCCAACTC	Tsnaxip1_e13R	GCAAGGTGAGGCCATTTG
Smpd3_e8.7R	AAAGATGAACTGAATGGTCTTTCC	Tsnaxip1_e14F	AAGACACAAAACCTTGCCAGTCC
Smpd3_e8.8F	CAGGGACCACTTGAATCCTAAC	Tsnaxip1_e14R	GTTGCCTGGGGAGACTCAG
Smpd3_e8.8R	AAATAAGTACAGACAAGATGCCAGTC	Tsnaxip1_e15F	CCCCAGGCAACAGGTAATG
Thap11_e1.1F	GGCGTAGTCCTCCTTTCCAG	Tsnaxip1_e15R	TAGGGCCTGCCAGATCAC
Thap11_e1.1R	GAAGTGAACGCTGCAGAGAC	Tsnaxip1_e1F	GAGAGCACACTCTGTGAGGAAG
Thap11_e1.2F	CTTCTACACGTTTCCCAAGGAC	Tsnaxip1_e1R	TTATGCTTTGGGGTTGTAGGTG
Thap11_e1.2R	ACATCATCTCCCAGGAAGTAG	Tsnaxip1_e2F	TGGGTTCAATCCTCAACAATAC
Thap11_e1.3F	GCCGTGCTTCTTACTCTTCAG	Tsnaxip1_e2R	GCCGCAAACTCCACTAAGTTC
Thap11_e1.3R	TTTCATCTTCACTCCATCAGG	Tsnaxip1_e3F	ACGAAAGCCCTGTTCCAGATG

Tsnaxip1_e3R	TCCCCGTGAAGGTCTATTATTC	Zfp90_e2R	TAAGGATCTTCCATGCTCAAAG
Tsnaxip1_e4F	GGCCAGACATAGGCAGTCTC	Zfp90_e3F	TGCTAGTGTGTCTCCTTAAGTTGC
Tsnaxip1_e4R	GGCAAGCAAAACAAGTAGAAAG	Zfp90_e3R	GGAACACCTGACTGGAGAAGAG
Tsnaxip1_e5F	AGAGATCTGCCTCCTCTCTGC	Zfp90_e4.1F	TGACATGACAGACACTCTGGTG
Tsnaxip1_e5R	AATGTGATAGCTCCTCCATTCC	Zfp90_e4.1R	CTTACATTCGCTGGGCCATTATG
Tsnaxip1_e6F	GATCGGTTTGCCTTCTCTTTTC	Zfp90_e4.2F	GAGAGTTGGAGAAGACATCTTGG
Tsnaxip1_e6R	ATCTCCCACCATGTATGGACAC	Zfp90_e4.2R	GACCAAGGGATGAGCTGTG
Tsnaxip1_e8F	AGGAGAGACTTCGAAATGCAAG	Zfp90_e4.3F	ACTTTCCTGTGGAGAACACAGC
Tsnaxip1_e8R	GCTATGACACCTGCAAGTTGG	Zfp90_e4.3R	TTGTTACTTTGGTAAGGTTTGTCTC
Tsnaxip1_e9F	CCAAATGCGAAAGTAATGATTG	Zfp90_e4.4F	CCCTTGTTCAACATGAGAGG
Tsnaxip1_e9R	CCTGTTTGTAAATGGGATGATG	Zfp90_e4.4R	AGTGACGAGAGTCGACTGAAGG
Zfp90_e1F	GGCCGAAGTGGCTACAGAG	Zfp90_e4.5F	GTCAGCAGTCCCTGTCTCATC
Zfp90_e1R	CAAAGCGATCCAGACTAAGAATC	Zfp90_e4.5R	ACAGTGTTCCTACCCATCCTG
Zfp90_e2F	CTTGAGCAGCAAACACAAG		

For qRT-PCR of rat samples:

Arhgap10_F	tgaccattccccctctc	Dsg2R	cagtggcacatcaacaacaa
Arhgap10_R	gccttgcggttgataagg	Dsg3F	cggatgaggacactgtaag
C19orf57_2F	caaacctcagcccagacc	Dsg3R	accatcattacgacccagga
C19orf57_2R	tctgttgctctctgcatc	Dsg4_2F	ggaatccgattgccagaat
C19orf57_F	tcccaggatcaccaaaagag	Dsg4_2R	ccgctccagagattcgataa
C19orf57_R	acaaacctccccactgagc	Dsg4F	gcctctaacaccaagatcg
Cdh1_2F	gatcctggccctctctgat	Dsg4R	tgctcctcaccagcataagt
Cdh1_2R	tctttgaccaccgttctcct	House-ActbF	ccaacctgaaaagatgacc
Cdh15F	ctatacggaccaccaagacca	House-ActbR	accagaggcatacagggaca
Cdh15R	gctcagcgctctcataatcc	House-Mrp2F	atcgcacagctcagctcac
Cdh1F	gatcctggccctctctgat	House-Mrp2R	cgccatggccaactctta
Cdh1R	tctttgaccaccgttctcct	House-Prdx2F	gactctcagttcaccacctg
Cdh2F	ccatcatcgcgatactctg	House-Prdx2R	tattcagtgggccaagc
Cdh2R	ccataccacgaacatgagga	House-R5piaF	tgctgagctcaatctcatcaag
Cdh3F	gttccggaggggtaag	House-R5piaR	ggcataaccagccacaatct
Cdh3R	agtattgatggctgctcct	House-Rpl4F	tttgggtgtaagataaagtga
Cdh4F	tgcatcgtgatcctgctaac	House-Rpl4R	ttctctgggagcatagacc
Cdh4R	ctttccctccgcttcatc	House-Rps18F	cagaaggacgtgaaggatgg
Ctnna1F	tcagaatacatgggcaatgct	House-Rps18R	tctatgggctcggattttctt
Ctnna1R	tttatctatggcagagttgagtgc	House-TbpF	cccaccagcagttcagtagc
Ctnnb1F	gtccatgggtggaacacag	House-TbpR	caattctgggtttgatcattctg
Ctnnb1R	cccagtgacccttaac	House-YwhazF	agatcagggacagagtctcagc
Ctnnd1F	ggagtcagtgctcaccaaca	House-YwhazR	gcaccagctcattttatcca
Ctnnd1R	tcactcctctccgagcttaca	JupF	atthccagagacgcgatt
Dsg1b_2F	gctcatcatggggttcttagt	JupR	aggttcatcacctccatcgt
Dsg1b_2R	aatccagctccaccacca	Krt25F	cgcagggttctggatgaa
Dsg1bF	gggggcctcaatatgaattt	Krt25R	gcagagcctgcatttctc
Dsg1bR	ggacgtccttcatcttcatcc	Krt26F	caatccatcacggctatgaa
Dsg2_2F	gaaatcacgcaccaagaaag	Krt26R	cagccaatctgctcctg
Dsg2_2R	tcggagatgaggaaggaat	Krt27F	cctgggtccaagagaagagc
Dsg2F	cctcatgattctgctctcc	Krt27R	ggtttgagagtcctttca

Krt28_2F	tgaacaacatgagagccgagt	Nol3F	gcctgccaggaactactgc
Krt28_2R	agtcattggagatctgctgct	Nol3R	gcatggagggtcatagctg
Krt28F	cacggctgctaacgctaata	RGD1308358F	caaactgcatagctggctga
Krt28R	tgaagggtgagttcgttttca	RGD1308358R	cccgtgtgtgtttctgat
Krt73F	gaggacattgccctgaagag	Rltpr_2F	ccactcagagcaggtcagtg
Krt73R	tggtgtgcttgaggtcatct	Rltpr_2R	cctggtgcacagcaacct
Mmp12_2F	tggtcgaattccaagagtt	Rltpr_F	acacttgcctcccctgag
Mmp12_2R	aggttttggttggtgcaaa	Rltpr_R	aaaggtgacccgaggaggt
Mmp12F	gctgtcacaacagtgaggaga	TcchF	gcagctgagggacagaaaa
Mmp12R	gaagtaatggttggtgctgga	TcchR	cggaaacttctctctcttctt

For microsatellite analysis:

D19Mit7_F	6'FAM-AGGGCTTTGCTGAATGCTTA	D19Rat33_R	CTCACAGCGGCAATAGCATA
D19Mit7_R	AGAGTGGTGGTAAAAGTGGG	D19Rat7_F	HEX-CTAGTCATCCATTGGTCGGG
D19Rat11_F	6'FAM-GGAAACTCACTTTGCAGGGT	D19Rat7_R	TAGAAAGCCATGCTCACGTG
D19Rat11_R	TCAGAGTTTTCAACTGGCTGG	D19Rat70_F	6'FAM-GTGTAGGTCAGAGGACAACCT
D19Rat14_F	HEX-CACTGGCATAACAGATGCAGG	D19Rat70_R	AAGCTGGACAACCTGCTTTG
D19Rat14_R	TTCAGGGTCAGTCTGAGCAA	D19Rat72_F	6'FAM-AGGAAGCATTGTCTGCCTT
D19Rat22_F	6'FAM-CCTGCAATGGGATGAATACA	D19Rat72_R	TCAATGCAAAAATGAATCACCA
D19Rat22_R	CAAGGACAGAACTGAACTGGC	D19Rat88_F	6'FAM-CCCATTACCATGTCTTGT
D19Rat23_F	6'FAM-TCTGATCAGGCATGGAACCTCT	D19Rat88_R	CGAGTCCCAGTGGGAAGTTA
D19Rat23_R	CCTTCTTGGTCCCTTGTCTCCT	D19Rat90_F	6'FAM-CAGAGGGGAAGGACACTCAG
D19Rat24_F	6'FAM-GTCCATGTGATGGGATGTGA	D19Rat90_R	TGTCCCAAACATGTATGAGTAACA
D19Rat24_R	TGGGTGTTTCAGAATTCATTTTT	D19Rat91_F	6'FAM-CTTCTCTCTCACACAAAATACG
D19Rat25_F	HEX-CCAGCCCTTAGATGCAACTG	D19Rat91_R	GTAGCAGCAGCAGCAGCA
D19Rat25_R	GAAAAACCTGGCATTTCAGG	D19Rat98_F	6'FAM-ATACATGGGTGTGTGTGCC
D19Rat33_F	6'FAM-CCTGAAAACCTAAGTTCAATCCC	D19Rat98_R	CATACACACAGAAAGGTCAACTT

For qRT-PCR of human samples:

hACTB_F	ccaaccgagagaagatga	SBSN_F	tcaacaacgctgctggac
hACTB_R	ccagaggcgtacagggatag	SBSN_R	cccagtggtgaaccttg
DMKN_F	tgacagcggcagtgagtc	ZNF383_F	gggaaagagccctggatg
DMKN_R	accgggtttatgtccattt	ZNF383_R	ggtttcacacatcgattcca
KRTDAP_F	agatcccggctcctcctg	ZNF567_F	aagaggctaacatgactgataccac
KRTDAP_R	cgcataattctcaatggtgct	ZNF567_R	ttctgagcatgatccagggtg
LOC100289218_F	cctgtctgcacggtattctg	ZNF568_F	aatgtttgggaggcactgtc
LOC100289218_R	tcacttcagacgcacagca	ZNF568_R	atcacttcagacgcacagca
RPL31P61_F	cacaaggtggtgacctgaga	ZNF829_F	gacccttagatctggaggaa
RPL31P61_R	cccctctcctcatgcaaat	ZNF829_R	tcaggggaaaggtgtgttc

For high resolution melting curve analysis of human samples:

ZNF567_e1F	TGGAAGCCTGAAATGTGAAAG	ZNF568_e7.7R	TGGTATTTCTTTCCATTTATTCCA
ZNF567_e1R	AGGTCCAAGCAGCAGGTTCC	ZNF568_e7.8R	AAAGCCAGGATCTTTATGGAAA
ZNF567_e2-3F	AAGCTATTCTCCTGCCTCAGC	ZNF568_e7.8R	TTCATGAATCTGCTTCTGGATATT
ZNF567_e2-3R	AGGCACTTTGAGAGGAAGTG	ZNF568_e7.9F	AGTGTATGAATTGCTGCGACA
ZNF567_e4F	CTTACCCAGTGCAAGGTGCT	ZNF568_e7.9_4R	AAAGCAGAGGCTGCAGTGAG
ZNF567_e4R	GAGCCACCATACCTAGCCTAAA	ZNF568_e7.9_3F	GGGAAATGATGACCTAGTCAATAAA
ZNF567_e5.1F	GGCCAGTGGTCATTTGTTCT	ZNF568_e7.9_3R	TCAAGACTACCCTGGCCAAC
ZNF567_e5.1R	TGAAAGCTCTGGCACTTTGAT	ZNF568_e7.10F	GGAGTACGGTGGTGAATCT
ZNF567_e5.2F	GGATATGGGAAATCACTCCTGA	ZNF568_e7.10_2R	CAGGTGCAGTGGCTCAAG
ZNF567_e5.2R	TCAGTGAGGGCTGTCTTGAG	ZNF568_e7.10_2F	CATGTTGGCCAGGGTAGTCT
ZNF567_e5.3R	TGTCATCAATGTGGAAATGC	ZNF568_e7.10R	ATCAGCCTCCCAAGTAGCTG
ZNF567_e5.3R	TCATGAAGAGCAAGGGTTGTC	ZNF568_e7.11_2F	GTTGAGGCCAAGGAGCTTT
ZNF567_e5.4F	CACACCTCATTGTCATCAG	ZNF568_e7.11_2R	TGGATCTGGTTCAGTCTTT
ZNF567_e5.4R	TGATGTGCTACAAGGGTTGTCT	ZNF568_e7.12_2F	AAACAACCTAAATATTCATCAGTGG
ZNF567_e5.5F	AAGACAACCCCTTGCTCTTCA	ZNF568_e7.12_2R	TCAATAATTGGGTGTGTATCCTTC
ZNF567_e5.5R	TAGGATTTCTGGCCGGTATG	ZNF568_e7.13F	TGGAATGAAATCATTATAAAGAACAA
ZNF567_e5.6F	TTTCGCCAGAAAGCAACC	ZNF568_e7.13R	TGGCCTGTTGTGAGAAAGAA
ZNF567_e5.6R	TGTTTCAGCATGCTTTTCTTTT	ZNF568_e8.1F	GCACCCACCTCTGGACTACA
ZNF568_e1F	ACCCTCACACAGGAAAGCAG	ZNF568_e8.1R	CTGACACCCCTTCTCCCATCC
ZNF568_e1R	ACACAACCACACACCCACAC	ZNF568_e8.2F	AGGTGGCTCTCGGAGATGT
ZNF568_e2F	GAGGGTGTGAGGAATTGGAC	ZNF568_e8.2_2R	CCGCGATACCCTAGACCTC
ZNF568_e2R	AAAGGGATAAGGTGAATTTGC	ZNF568_e8.2_2F	GGAGTGGGTGTGGTGTGAG
ZNF568_e3R	TTGGAAGCTGGTTATCACAGG	ZNF568_e8.2R	AATGTACAGCGAGGGTGTCC
ZNF568_e3F	CCCAATGTAGAGCCTTTCTC	ZNF568_e9F	AGGGATTCAGGATGGCTTCT
ZNF568_e4F	GAGGGTCTTCTAGCCACCTG	ZNF568_e9R	CCTTTGTCCAAATCATGAATGTAA
ZNF568_e4R	AGAACCACCGTAACCTGCAC	ZNF568_e10F	AGTCTCATGGTTCGCTTG
ZNF568_e5F	GCTAAACAAGTCTTGTATGTTGTG	ZNF568_e10R	GCGGTGGTTCACACCTGTA
ZNF568_e5R	AAGAATTCTCTGTTAAATTGCAAGG	ZNF568_e11F	ACTCCCGACCTCAGGTGAT
ZNF568_e6F	TGGTGTCTCCAGCATTGAC	ZNF568_e11_2R	GATACCTCTGACAGCTAAAGAAGG
ZNF568_e6R	CTCATGTGGCTTTCTCATTGAG	ZNF568_e12_2F	GGGACTGAACACCCATGTTA
ZNF568_e7.1F	TTGGTTGACTAGGCCAACATC	ZNF568_e12_2R	GGAGTTCAAGAATGTTCACTGG
ZNF568_e7.1R	TGGTTTCCCAAATCATTACTC	ZNF568_e13_2F	CCTCCAACGAGTGTCAAGAG
ZNF568_e7.2F	TGACTCACTTGATAAGGGTTTGG	ZNF568_e13_2R	GGGCTCAACCTCATTTAGTACC
ZNF568_e7.2R	GTCTAATGAGGTCAAATTTATGACTG	ZNF568_e14F	ACCTGCTCCTCTTTCTTGGT
ZNF568_e7.3F	TTGTGCATCCTATGTTGTAACC	ZNF568_e14R	CTGCCTTCTCACAGATGAGC
ZNF568_e7.3R	AGCGTAACAGATGACATTGCGAG	ZNF568_e15.1F	TTTCTTTGCTGCAATGTGA
ZNF568_e7.4F	ATCCTTCAGCCAGAAGCAAA	ZNF568_e15.1R	CATTCTCCACATTCAGGTTCTTT
ZNF568_e7.4R	TTCGCATATGTACGGTTAGGG	ZNF568_e15.2F	TCCTGTGAATGCAGGAAATG
ZNF568_e7.5F	CATCTGTTACGCTACATATGAGAA	ZNF568_e15.2R	AGGTGTGAGGGACGGGTAA
ZNF568_e7.5R	TGAGGGATGAGATTCGAGAGA	ZNF568_e15.3F	TCCATCCACTGCACAGCTTA
ZNF568_e7.6F	TGCCAAATCATACAGCTGAG	ZNF568_e15.3R	GAGCTCTCTGATGTCGGGTAA
ZNF568_e7.6R	AGAAAGGGATGCTCTTTGAGA	ZNF568_e15.4F	TGTGCCTCACAGCTGAGTCT
ZNF568_e7.7F	TCTCTCGAATCTCATCCCTCA	ZNF568_e15.4R	GGCCTTTCCACACTGCTG

2. Detailed Expression Analysis Data from Rat Samples

Table 11: 50 highest fold changes in skin expression data. Highlighted in blue: genes affecting hair structure. Highlighted in mauve: genes affecting the immune system. Highlighted in grey: p-values above 0.05.

Probeset_id	Chr.	Variation coefficient DEB_skin	Variation coefficient Wi_skin	Significance (p.ttest)	False discovery rate (q.ttest)	Fold change	Gene
10747051	chr10	0.0771	0.3397	0.0004	0.0545	1.6866	Krt25
10866195	chr4	0.1589	0.2029	0.0004	0.0545	1.6639	[cDNA]
10747067	chr10	0.0898	0.3187	0.0008	0.0545	1.6133	Krt27
10907448	chr7	0.1124	0.2969	0.0015	0.0545	1.5567	Krt73
10755135	chr11	0.1117	0.2331	0.0009	0.0545	1.4988	Kng111
10750958	chr11	0.1254	0.1999	0.0010	0.0545	1.4773	Trat1
10875985	chr5	0.0816	0.2740	0.0016	0.0545	1.4740	[cDNA]
10756147	chr12	0.1963	0.2015	0.0064	0.0663	1.4722	Cd209d
10747058	chr10	0.1328	0.2268	0.0020	0.0559	1.4687	Krt26
10824711	chr2	0.0759	0.2289	0.0006	0.0545	1.4643	[cDNA]
10801978	chr18	0.1030	0.1931	0.0005	0.0545	1.4635	RGD1305184
10784054	chr15	0.0987	0.2739	0.0025	0.0576	1.4618	Gzmb
10859174	chr4	0.1492	0.2213	0.0033	0.0581	1.4539	Klre1
10866193	chr4	0.1571	0.2576	0.0063	0.0659	1.4530	[cDNA]
10907869	chr8	0.1073	0.2530	0.0030	0.0581	1.4309	Mmp12
10866197	chr4	0.1428	0.2469	0.0055	0.0634	1.4307	[cDNA]
10817168	chr2	0.0991	0.2401	0.0022	0.0566	1.4240	Tchh
10771649	chr14	0.1067	0.1574	0.0005	0.0545	1.4213	Cxcl11
10866061	chr4	0.1198	0.1860	0.0014	0.0545	1.4177	Klrc1
10747075	chr10	0.0912	0.2219	0.0015	0.0545	1.4117	Krt28
10866167	chr4	0.1192	0.1561	0.0009	0.0545	1.4091	Ly49i4
10765497	chr13	0.0940	0.1259	0.0001	0.0545	1.4068	Fcgr3a
10771655	chr14	0.0768	0.1955	0.0008	0.0545	1.3923	Cxcl10
10751793	chr11	0.0683	0.2018	0.0008	0.0545	1.3896	Lrrc15
10866056	chr4	0.1017	0.1636	0.0009	0.0545	1.3765	Klrc2
10751988	chr11	0.0663	0.1965	0.0009	0.0545	1.3695	Kng1
10863051	chr4	0.3506	0.1336	0.0985	0.1635	1.3667	[cDNA]
10866163	chr4	0.2101	0.1559	0.0195	0.0907	1.3579	Ly49s4
10866146	chr4	0.0943	0.1651	0.0011	0.0545	1.3533	Ly49s6
10771660	chr14	0.0548	0.1750	0.0006	0.0545	1.3420	Cxcl9
10907858	chr8	0.1773	0.1261	0.0099	0.0744	1.3369	Mmp13
10845784	chr3	0.1343	0.0500	0.0010	0.0545	1.3368	Slc38a11
10718954	chr1	0.0882	0.1119	0.0003	0.0545	1.3340	Lilrb4
10747228	chr10	0.1174	0.2353	0.0115	0.0774	1.3305	Krt35
10863038	chr4	0.4440	0.0623	0.2037	0.2279	1.3292	[cDNA]
10859164	chr4	0.0974	0.1335	0.0009	0.0545	1.3288	Klrd1
10821370	chr2	0.1213	0.1373	0.0025	0.0576	1.3258	Gzma
10772522	chr14	0.0771	0.1459	0.0006	0.0545	1.3246	Gabra4
10800368	chr18	0.1424	0.2128	0.0141	0.0822	1.3240	Dsg4
10780175	chr15	0.1324	0.1528	0.0049	0.0615	1.3230	[cDNA]
10866182	chr4	0.1178	0.0991	0.0012	0.0545	1.3194	[cDNA]
10752990	chr11	0.1602	0.2268	0.0240	0.0960	1.3179	[cDNA]
10830267	chr20	0.1715	0.2015	0.0227	0.0937	1.3168	Fam26d
10747292	chr10	0.1295	0.2870	0.0317	0.1054	1.3159	Krt16
10745631	chr10	0.0699	0.1673	0.0013	0.0545	1.3151	Ccl5
10869527	chr5	0.0534	0.1705	0.0010	0.0545	1.3113	[cDNA]

Continuation of table 11: 50 highest fold changes in skin expression data.

Probeset_id	Chr.	Variation coefficient DEB_skin	Variation coefficient Wi_skin	Significance (p.ttest)	False discovery rate (q.ttest)	Fold change	Gene
10866413	chr4	0.1852	0.1983	0.0296	0.1035	1.3110	Gprc5d
10907375	chr7	0.1179	0.2083	0.0104	0.0755	1.3101	Krt85
10716704	chr1	0.1026	0.1539	0.0026	0.0576	1.3097	Samd5
10866052	chr4	0.0745	0.1572	0.0013	0.0545	1.3055	Klrc3

Table 12: 50 lowest fold changes in skin expression data. Highlighted in blue: genes involved in milk synthesis. Highlighted in grey: p-values above 0.05.

Probeset_id	Chr.	Variation coefficient DEB_skin	Variation coefficient Wi_skin	Significance (p.ttest)	False discovery rate (q.ttest)	Fold change	Gene
10888777	chr6	0.2089	0.3756	0.0174	0.0879	0.5822	cDNA
10776190	chr14	0.7512	0.3829	0.1025	0.1662	0.5878	Csn1s1
10827201	chr2	0.3786	0.4038	0.0569	0.1293	0.6184	Clca3
10776133	chr14	0.6283	0.3590	0.1017	0.1655	0.6247	Csn3
10776160	chr14	0.4980	0.3886	0.1005	0.1649	0.6470	RGD1310384
10886994	chr6	0.2225	0.3207	0.0254	0.0979	0.6528	snoRNA
10886880	chr6	0.2144	0.2858	0.0188	0.0898	0.6639	snoRNA
10886886	chr6	0.1761	0.3059	0.0206	0.0921	0.6639	–
10886870	chr6	0.0928	0.2596	0.0070	0.0681	0.6675	ncRNA
10887010	chr6	0.2818	0.3982	0.0765	0.1464	0.6709	ncRNA
10771893	chr14	0.5183	0.3367	0.1181	0.1771	0.6755	Csn2
10886930	chr6	0.1902	0.2773	0.0191	0.0903	0.6797	ncRNA
10906857	chr7	0.4845	0.3341	0.1146	0.1747	0.6831	Lalba
10844331	chr3	0.2578	0.2648	0.0259	0.0987	0.6837	Lcn2
10886874	chr6	0.1229	0.2447	0.0082	0.0709	0.6845	ncRNA
10776175	chr14	0.6213	0.4108	0.2060	0.2292	0.6864	Csn1s2a
10796418	chr17	0.4274	0.3482	0.1073	0.1693	0.6880	Olah
10886896	chr6	0.1916	0.2898	0.0276	0.1011	0.6916	ncRNA
10886850	chr6	0.2156	0.2477	0.0195	0.0907	0.6955	ncRNA
10907749	chr7	0.4727	0.4246	0.1739	0.2107	0.6962	Glycam1
10886898	chr6	0.2140	0.2971	0.0366	0.1097	0.6975	ncRNA
10886938	chr6	0.2318	0.2541	0.0268	0.0999	0.7025	ncRNA
10886856	chr6	0.1652	0.2509	0.0178	0.0883	0.7059	ncRNA
10886876	chr6	0.2285	0.2470	0.0267	0.0997	0.7084	ncRNA
10795245	chr17	0.3714	0.3268	0.1263	0.1830	0.7266	Btn1a1
10887014	chr6	0.0938	0.2671	0.0243	0.0962	0.7286	ncRNA
10886868	chr6	0.1602	0.2193	0.0170	0.0873	0.7322	ncRNA
10886862	chr6	0.1615	0.2304	0.0207	0.0925	0.7325	ncRNA
10886848	chr6	0.1943	0.2312	0.0291	0.1028	0.7372	ncRNA
10886888	chr6	0.1641	0.2206	0.0209	0.0929	0.7398	ncRNA
10886890	chr6	0.1128	0.2891	0.0432	0.1168	0.7402	ncRNA
10887008	chr6	0.1521	0.2951	0.0550	0.1279	0.7424	ncRNA
10886964	chr6	0.1590	0.2190	0.0211	0.0930	0.7434	ncRNA
10886986	chr6	0.1644	0.2080	0.0209	0.0929	0.7496	ncRNA
10887004	chr6	0.1644	0.2080	0.0209	0.0929	0.7496	ncRNA
10886864	chr6	0.1548	0.2140	0.0221	0.0934	0.7514	ncRNA
10886884	chr6	0.2162	0.2708	0.0655	0.1366	0.7514	ncRNA
10781962	chr15	0.1006	0.3074	0.0622	0.1341	0.7522	cDNA

Continuation of table 12: 50 lowest fold changes in skin expression data.

Probeset_id	Chr.	Variation coefficient DEB_skin	Variation coefficient Wi_skin	Significance (p.ttest)	False discovery rate (q.ttest)	Fold change	Gene
10864711	chr4	0.1006	0.3074	0.0622	0.1341	0.7522	cDNA
10851577	chr3	0.0805	0.1183	0.0005	0.0545	0.7545	Slpil3
10886882	chr6	0.1525	0.2092	0.0221	0.0934	0.7561	ncRNA
10886942	chr6	0.1552	0.2063	0.0221	0.0934	0.7571	ncRNA
10886902	chr6	0.1549	0.2053	0.0224	0.0934	0.7587	ncRNA
10886978	chr6	0.1549	0.2053	0.0224	0.0934	0.7587	ncRNA
10886944	chr6	0.1506	0.2085	0.0228	0.0939	0.7588	ncRNA
10886974	chr6	0.1882	0.2128	0.0338	0.1072	0.7597	snoRNA
10886976	chr6	0.1556	0.2026	0.0224	0.0934	0.7606	ncRNA
10886982	chr6	0.1556	0.2026	0.0224	0.0934	0.7606	ncRNA
10886998	chr6	0.1556	0.2026	0.0224	0.0934	0.7606	ncRNA
10886982	chr6	0.1556	0.2026	0.0224	0.0934	0.7606	ncRNA

Table 13: Skin expression data in candidate region Chr19:32.986.041..36.535.127

Highlighted in grey: p-values above 0.05.

Probeset_id	Chr.	Variation coefficient DEB_skin	Variation coefficient Wi_skin	Significance (p.ttest)	False discovery rate (q.ttest)	Fold change	Gene
10807083	chr19	0.0618	0.1120	0.0130	0.0801	1.1515	RGD1308358
10807525	chr19	0.0369	0.0641	0.0014	0.0545	1.1254	Cdh3
10810556	chr19	0.0426	0.0649	0.0116	0.0776	1.0936	Tradd
10810727	chr19	0.0392	0.0651	0.0107	0.0757	1.0924	Psmb10
10810703	chr19	0.0393	0.0511	0.0072	0.0685	1.0856	Cenpt
10807071	chr19	0.0467	0.0515	0.0173	0.0878	1.0793	RGD1308358
10807464	chr19	0.0508	0.0313	0.0135	0.0807	1.0743	Pla2g15
10810795	chr19	0.0340	0.0616	0.0394	0.1132	1.0642	Rbm35b
10810717	chr19	0.0382	0.0433	0.0198	0.0907	1.0634	cDNA
10807272	chr19	0.0549	0.0390	0.1044	0.1673	1.0493	Hsd11b2
10807177	chr19	0.0266	0.0190	0.0044	0.0604	1.0482	cDNA
10807542	chr19	0.0348	0.0642	0.1363	0.1891	1.0455	Cdh1
10807131	chr19	0.0233	0.0277	0.0314	0.1051	1.0354	Cbfb
10810689	chr19	0.0333	0.0220	0.0625	0.1343	1.0339	Ranbp10
10807085	chr19	0.0257	0.0229	0.0342	0.1077	1.0336	LOC498940
10807188	chr19	0.0401	0.0340	0.1784	0.2136	1.0305	Elmo3
10807473	chr19	0.0379	0.0281	0.1771	0.2127	1.0276	Slc7a6
10810811	chr19	0.0246	0.0161	0.0448	0.1186	1.0272	Slc7a6os
10807211	chr19	0.0343	0.0213	0.1416	0.1917	1.0262	Tmem208
10807384	chr19	0.0350	0.0222	0.1664	0.2065	1.0251	Thap11
10807114	chr19	0.0566	0.1831	0.7426	0.4531	1.0245	RGD1307418
10810614	chr19	0.0113	0.0427	0.2478	0.2517	1.0204	Kctd19
10810649	chr19	0.0103	0.0119	0.0075	0.0691	1.0203	Atp6vod1
10810662	chr19	0.0220	0.0192	0.1191	0.1777	1.0198	Acd
10807391	chr19	0.0251	0.0141	0.1372	0.1896	1.0189	Edc4
10810791	chr19	0.0295	0.0187	0.2123	0.2329	1.0188	Ddx28
10807504	chr19	0.0426	0.0247	0.4444	0.3443	1.0159	Zfp90
10807140	chr19	0.0244	0.0132	0.1923	0.2220	1.0157	RGD621098
10810553	chr19	0.0313	0.0508	0.5212	0.3749	1.0153	B3gnt9
10810685	chr19	0.0380	0.0416	0.5218	0.3752	1.0147	Gfod2

Continuation of table 13: Skin expression data in candidate region Chr19:32,986,041..36,535,127

Probeset_id	Chr.	Variation coefficient DEB_skin	Variation coefficient Wi_skin	Significance (p.ttest)	False discovery rate (q.ttest)	Fold change	Gene
10810778	chr19	0.0609	0.0398	0.6412	0.4194	1.0141	Dpep2
10807300	chr19	0.0128	0.0187	0.1995	0.2259	1.0120	Ctcf
10807560	chr19	0.0277	0.0228	0.4938	0.3639	1.0101	RGD1559841
10807435	chr19	0.0098	0.0049	0.0585	0.1310	1.0094	Dus2l
10807311	chr19	0.0283	0.0207	0.5695	0.3935	1.0082	RGD1562390
10807157	chr19	0.0267	0.0167	0.5917	0.4021	1.0070	Fbxl8
10810585	chr19	0.0456	0.0358	0.7866	0.4671	1.0064	LOC502201
10810743	chr19	0.0363	0.0181	0.8108	0.4737	1.0040	Slc12a4
10807514	chr19	0.0195	0.0061	0.6939	0.4374	1.0034	Rps12
10807452	chr19	0.0233	0.0134	0.8339	0.4804	1.0023	Nfatc3
10807098	chr19	0.0310	0.0186	0.9738	0.5184	1.0005	LOC689754
10810549	chr19	0.0195	0.0677	0.9128	0.5027	0.9970	RGD1564421
10810562	chr19	0.0201	0.0302	0.8002	0.4709	0.9964	MGC116202
10807353	chr19	0.0198	0.0410	0.7786	0.4649	0.9950	Pard6a
10810570	chr19	0.0214	0.0037	0.4730	0.3560	0.9934	Exoc3l
10807386	chr19	0.0133	0.0236	0.4938	0.3639	0.9927	Nutf2
10807484	chr19	0.0317	0.0157	0.6104	0.4090	0.9925	Prmt7
10807430	chr19	0.0256	0.0188	0.5490	0.3857	0.9922	Pskh1
10807235	chr19	0.0295	0.0425	0.6734	0.4313	0.9914	Plekhg4
10810677	chr19	0.0164	0.0279	0.4602	0.3506	0.9905	RGD1307357
10810631	chr19	0.0344	0.0517	0.6639	0.4278	0.9893	Tppp3
10810736	chr19	0.0524	0.0287	0.5981	0.4044	0.9871	Lcat
10807367	chr19	0.0772	0.0555	0.7154	0.4442	0.9859	Tsnaxip1
10807517	chr19	0.0359	0.0190	0.3020	0.2798	0.9825	cDNA
10810768	chr19	0.0399	0.0517	0.4375	0.3414	0.9797	Dpep3
10810817	chr19	0.0631	0.0586	0.5477	0.3853	0.9792	Smpd3
10810635	chr19	0.0229	0.0247	0.1025	0.1662	0.9768	Zdhhc1
10807278	chr19	0.0217	0.0201	0.0483	0.1221	0.9744	Fam65a
10810828	chr19	0.0189	0.0435	0.1667	0.2065	0.9733	cDNA
10810551	chr19	0.0335	0.0176	0.0799	0.1490	0.9712	Slc25a36
10810719	chr19	0.0194	0.0223	0.0161	0.0861	0.9677	Ctrl
10807360	chr19	0.0305	0.0422	0.1066	0.1688	0.9650	RGD1561415
10810583	chr19	0.0263	0.0327	0.0401	0.1139	0.9626	rno-mir-328
10807217	chr19	0.0443	0.0537	0.1818	0.2158	0.9619	Slc9a5
10807256	chr19	0.0453	0.0358	0.1127	0.1732	0.9614	Lrrc36
10810658	chr19	0.0417	0.0426	0.0920	0.1586	0.9577	Agrp
10807160	chr19	0.0395	0.0574	0.0966	0.1621	0.9519	Hsf4
10807068	chr19	0.0470	0.0599	0.0802	0.1493	0.9442	LOC688462
10810591	chr19	0.0201	0.0410	0.0076	0.0691	0.9439	Fhod1
10807520	chr19	0.0281	0.0306	0.0033	0.0581	0.9411	—
10810793	chr19	0.0303	0.0958	0.1033	0.1665	0.9329	ncRNA
10807174	chr19	0.0593	0.0441	0.0250	0.0973	0.9274	Nol3

Table 14: 50 highest and lowest heart expression fold changes. Highlighted in mauve: genes affecting the immune system. Highlighted in grey: p-values above 0.05.

50 highest fold changes heart expression					50 lowest fold changes heart expression				
Probeset_id	Chr.	Fold change	Significance (p.ttest)	Gene	Probeset_id	Chr.	Fold change	Significance (p.ttest)	Gene
10817071	chr2	1.4408	0.3317	S100a8	10776519	chr14	0.8528	0.1476	Spata18
10907913	chr8	1.4389	0.3050	Mmp8	10771893	chr14	0.8520	0.3964	Csn2
10824695	chr2	1.4380	0.2881	S100a9	10766910	chr13	0.8500	0.0607	–
10924245	chr9	1.4226	0.1983	Il8rb	10805092	chr18	0.8485	0.0194	LOC680077
10751434	chr11	1.3773	0.0062	Stfa2i3	10752266	chr11	0.8478	0.0519	–
10863410	chr4	1.3772	0.3713	Reg3g	10748193	chr10	0.8472	0.2079	–
10702716	chr1	1.3658	0.0042	–	10856082	chr4	0.8462	0.0043	–
10915103	chr8	1.3658	0.0042	–	10939791	chrX	0.8459	0.0557	–
10902859	chr7	1.3419	0.0623	–	10854417	chr4	0.8452	0.0049	Akr1b10
10749818	chr11	1.3245	0.0334	–	10820494	chr2	0.8448	0.0356	Bhmt
10791602	chr16	1.3210	0.0548	–	10817331	chr2	0.8428	0.0031	Tmod4
10833416	chr20	1.3210	0.0548	–	10791552	chr16	0.8414	0.0281	–
10881659	chr5	1.3171	0.0115	Cort	10862978	chr4	0.8403	0.0305	–
10746588	chr10	1.3095	0.0083	Calcoco2	10824742	chr2	0.8392	0.4894	Smcp
10869527	chr5	1.2930	0.0149	–	10726346	chr1	0.8392	0.0001	Uros
10718954	chr1	1.2804	0.2035	Lilrb4	10846740	chr3	0.8384	0.0006	Frzb
10746914	chr10	1.2756	0.3849	–	10883595	chr6	0.8377	0.2587	Nt5c1b
10794866	chr17	1.2722	0.3614	Serpib1a	10931678	chrUn	0.8371	0.0128	Sctr
10858599	chr4	1.2699	0.1751	Clec4d	10928337	chr9	0.8368	0.3310	Als2cr11
10850208	chr3	1.2685	0.0532	Pak7	10778247	chr14	0.8360	0.0004	Myl7
10886210	chr6	1.2651	0.2391	–	10859162	chr4	0.8357	0.0187	Lkre1
10852682	chr4	1.2632	0.2108	–	10920741	chr8	0.8342	0.1345	–
10856474	chr4	1.2588	0.4847	Reg3b	10892493	chr6	0.8339	0.1040	–
10842660	chr3	1.2586	0.0297	–	10909307	chr8	0.8321	0.0379	–
10866195	chr4	1.2566	0.1301	–	10751988	chr11	0.8308	0.0603	Kng1
10842663	chr3	1.2565	0.0079	–	10871413	chr5	0.8239	0.1231	–
10831099	chr20	1.2534	0.0019	RT1-CE5	10910047	chr8	0.8223	0.0001	Sln
10806198	chr19	1.2511	0.0215	LOC679726	10779790	chr15	0.8192	0.2102	Olr1627
10765195	chr13	1.2487	0.2693	Selp	10888777	chr6	0.8181	0.2964	–
10750624	chr11	1.2485	0.2391	Olr1541	10903290	chr7	0.8123	0.2964	RGD1565493
10762254	chr12	1.2470	0.1255	Oas1k	10922027	chr9	0.8116	0.4417	Crisp2
10718944	chr1	1.2460	0.0366	Kir3dl1	10704115	chr1	0.8113	0.1381	–
10733849	chr10	1.2455	0.2749	LOC24906	10857541	chr4	0.8071	0.0251	Lrrn1
10781630	chr15	1.2433	0.0727	–	10740496	chr10	0.8070	0.0207	LOC497860
10839307	chr3	1.2420	0.0857	MGC105649	10903292	chr7	0.8060	0.2436	RGD1565493
10939699	chrX	1.2411	0.0804	–	10746040	chr10	0.8051	0.0078	–
10740331	chr10	1.2409	0.0196	–	10771002	chr14	0.7978	0.2849	–
10886870	chr6	1.2395	0.2121	–	10937179	chrX	0.7974	0.2217	Akap4
10722481	chr1	1.2384	0.0402	–	10891491	chr6	0.7956	0.0587	–
10712090	chr1	1.2369	0.1396	Cyp2e1	10776190	chr14	0.7925	0.1949	Csn1s1
10722451	chr1	1.2358	0.0681	–	10889213	chr6	0.7862	0.0037	Vsn1
10847174	chr3	1.2343	0.0432	Olr687	10823819	chr2	0.7835	0.0054	Rxfp1
10710338	chr1	1.2322	0.0343	–	10866576	chr4	0.7833	0.0419	RGD1561357
10837604	chr3	1.2310	0.1789	Olr648	10829888	chr20	0.7776	0.0065	Pbld
10847076	chr3	1.2293	0.0015	Olr587	10830962	chr20	0.7503	0.1569	–
10722419	chr1	1.2267	0.0017	–	10875983	chr5	0.7503	0.1569	–
10806012	chr19	1.2263	0.0081	–	10727806	chr1	0.7390	0.1833	–
10847156	chr3	1.2252	0.0185	Olr673	10775968	chr14	0.7167	0.0275	Alb

Continuation of table 14: 50 highest and lowest heart expression fold changes

50 highest fold changes heart expression					50 lowest fold changes heart expression				
Probeset_id	Chr.	Fold change	Significance (p.ttest)	Gene	Probeset_id	Chr.	Fold change	Significance (p.ttest)	Gene
10913664	chr8	1.2246	0.4211	Ngp	10714106	chr1	0.6784	2.88E-05	Fam111a
10924441	chr9	1.2244	1.50E-06	–	10765850	chr13	0.6622	0.0058	Spta1

Table 15: Heart expression data in candidate region Chr19:32.986.041..36.535.127

Highlighted in grey: p-values above 0.05.

Probeset_id	Chr.	Fold change	Significance (p.ttest)	Gene	Probeset_id	Chr.	Fold change	Significance (p.ttest)	Gene
10810717	chr19	1.1527	0.1492	–	10807360	chr19	0.9915	0.6995	RGD1561415
10807083	chr19	1.1280	0.1796	RGD1308358	10810743	chr19	0.9914	0.2880	Slc12a4
10807071	chr19	1.1228	0.0302	RGD1308358	10807140	chr19	0.9903	0.2717	RGD621098
10807367	chr19	1.0632	0.2684	Tsnaxip1	10807235	chr19	0.9881	0.4494	Plekhg4
10810727	chr19	1.0481	0.0229	Psemb10	10807174	chr19	0.9881	0.2541	Nol3
10810556	chr19	1.0389	0.2052	Tradd	10810631	chr19	0.9875	0.1511	Tppp3
10810793	chr19	1.0313	0.4296	–	10807256	chr19	0.9872	0.3512	Lrrc36
10807217	chr19	1.0228	0.5513	Slc9a5	10810562	chr19	0.9866	0.5300	MGC116202
10807514	chr19	1.0193	0.4253	Rps12	10807160	chr19	0.9864	0.6175	Hsf4
10810553	chr19	1.0187	0.0955	B3gnt9	10810551	chr19	0.9859	0.1064	Slc25a36
10810689	chr19	1.0179	0.4510	Ranbp10	10807177	chr19	0.9843	0.4683	–
10807157	chr19	1.0167	0.6522	Fbxl8	10807386	chr19	0.9843	0.1052	Nutf2
10810549	chr19	1.0149	0.4196	RGD1564421	10807384	chr19	0.9836	0.2061	Thap11
10807473	chr19	1.0134	0.5511	Slc7a6	10810791	chr19	0.9805	0.0311	Ddx28
10807278	chr19	1.0105	0.3806	Fam65a	10807560	chr19	0.9792	0.4784	RGD1559841
10807300	chr19	1.0095	0.4916	Ctcf	10807452	chr19	0.9784	0.1016	Nfatc3
10810658	chr19	1.0083	0.7791	Agrp	10810635	chr19	0.9778	0.1256	Zdhc1
10807430	chr19	1.0073	0.5682	Pskh1	10807068	chr19	0.9775	0.1180	LOC688462
10810817	chr19	1.0072	0.8192	Smpd3	10810591	chr19	0.9774	0.2730	Fhod1
10810736	chr19	1.0052	0.8365	Lcat	10810570	chr19	0.9763	0.0455	Exoc3l
10807211	chr19	1.0044	0.8856	Tmem208	10810778	chr19	0.9746	0.6598	Dpep2
10807391	chr19	1.0038	0.7839	Edc4	10807272	chr19	0.9737	0.1760	Hsd11b2
10807517	chr19	1.0031	0.9305	–	10810677	chr19	0.9713	0.0493	RGD1307357
10807435	chr19	1.0028	0.8198	Dus2l	10810585	chr19	0.9699	0.1527	LOC502201
10807504	chr19	1.0013	0.9446	Zfp90	10807464	chr19	0.9697	0.1027	Pla2g15
10807188	chr19	1.0012	0.9601	Elmo3	10807525	chr19	0.9677	0.2132	Cdh3
10810703	chr19	0.9999	0.9971	Cenpt	10810583	chr19	0.9649	0.0864	–
10807520	chr19	0.9997	0.9952	–	10810768	chr19	0.9642	0.3571	Dpep3
10807098	chr19	0.9996	0.9899	LOC689754	10807311	chr19	0.9629	0.2362	RGD1562390
10810811	chr19	0.9991	0.9597	Slc7a6os	10810685	chr19	0.9627	0.2349	Gfod2
10807484	chr19	0.9988	0.9389	Prmt7	10810614	chr19	0.9590	0.2527	Kctd19
10810828	chr19	0.9986	0.9712	–	10810795	chr19	0.9563	0.5894	Rbm35b
10807085	chr19	0.9973	0.9639	LOC498940	10810719	chr19	0.9489	0.1100	Ctrl
10807131	chr19	0.9971	0.7111	Cbfb	10807353	chr19	0.9476	0.1217	Pard6a
10810662	chr19	0.9920	0.5247	Acd	10807542	chr19	0.9175	0.1636	Cdh1
10810649	chr19	0.9917	0.2527	Atp6vOd1	10807114	chr19	0.9160	0.1045	RGD1307418

3. Detailed Association and Linkage Analysis Data from Human Samples

Table 17: P-values for each SNP in a case control analysis using PLINK.

P value für dominant and recessive model p_DOM/p_REC; data not available NA

SNP_ID	CHR	POSITION	p_DOM	p_REC	SNP_ID	CHR	POSITION	p_DOM	p_REC
rs541169	19	40410860	0.3356	0.7556	rs1035441	19	42045631	0.6142	0.9720
rs12975589	19	40531570	0.5540	0.4095	rs10403306	19	42067119	0.0253	0.2697
rs8107905	19	40613537	0.4379	0.7058	rs543518	19	42078051	NA	NA
rs409093	19	40633088	NA	NA	rs7250197	19	42081310	0.4812	0.7589
rs926026	19	40659264	NA	NA	rs547483	19	42133205	0.1061	0.3142
rs11880530	19	40660984	0.8735	0.9267	rs496730	19	42143279	0.8797	0.0155
rs8102875	19	40661629	0.1739	0.6505	rs569371	19	42145837	0.9071	0.1510
rs6510490	19	40669149	NA	NA	rs565721	19	42147671	0.8728	0.0090
rs7976	19	40670139	0.5842	0.5134	rs7251087	19	42147743	0.8912	0.0081
rs10407971	19	40671304	0.1213	0.8614	rs7254717	19	42149242	0.4328	0.7871
rs11880364	19	40680634	NA	NA	rs472226	19	42150553	NA	NA
rs4254439	19	40690202	0.2143	0.9764	rs17639910	19	42158969	0.7965	0.0145
rs7254211	19	40695561	0.1599	0.6284	rs1667354	19	42173991	0.3162	0.7904
rs4806163	19	40695946	0.5348	0.2055	rs8102196	19	42274044	0.9165	0.2701
rs17705633	19	40707492	0.1021	0.9691	rs1533736	19	42346816	NA	NA
rs12151182	19	40715572	NA	NA	rs11084878	19	42362309	0.5133	0.2386
rs17705657	19	40716582	0.2988	0.4396	rs12459637	19	42381838	0.1096	0.4842
rs2239945	19	40725300	0.2876	0.7732	rs320890	19	42395940	0.0373	0.3394
rs7599	19	40730230	0.4468	0.9720	rs172786	19	42404824	0.5329	0.8808
rs2301617	19	40734047	0.3895	0.4269	rs2460950	19	42445079	0.9559	0.4283
rs17776451	19	40736289	0.5538	0.8358	rs1530500	19	42515651	NA	NA
rs2733743	19	40742809	NA	NA	rs3745765	19	42546075	0.7150	0.8805
rs2285421	19	40860754	NA	NA	rs10422527	19	42586308	NA	NA
rs437168	19	41026259	0.4475	0.6890	rs12461941	19	42676490	0.7754	0.3080
rs2285424	19	41191013	NA	NA	rs12977460	19	42716111	0.0465	0.8221
rs1008328	19	41287276	0.5126	0.9692	rs10500277	19	42749242	0.0532	0.7884
rs3108186	19	41876810	0.3459	0.8828	rs4803277	19	42764767	NA	NA
rs1830031	19	41895089	0.7945	0.8119	rs2927743	19	42824174	NA	NA
rs1673082	19	41932981	0.7648	0.8982	rs35153242	19	42843582	0.1866	0.8623
rs1227820	19	41949357	NA	NA	rs2909109	19	42861195	0.0451	0.1280
rs2245366	19	41956174	0.2460	0.4044	rs17246792	19	42876102	NA	NA
rs8107274	19	41977233	0.4435	0.5899	rs1469698	19	43685396	0.2460	0.3390
rs1148399	19	42021145	0.0119	0.1706	rs8103362	19	44452031	NA	NA
rs1144540	19	42022453	0.2368	0.4015					

Table 18: P-values for each SNP in a TDT analysis using PLINK.

CHR	SNP	Position	P-Value	CHR	SNP	Position	P-Value
19	rs11672876	34923945	0.2087	19	rs1144540	42022453	0.4579
19	rs541169	40410860	0.5583	19	rs1035441	42045631	0.9387
19	rs12975589	40531570	0.5715	19	rs10403306	42067119	0.5472
19	rs8107905	40613537	0.6473	19	rs543518	42078051	0.1003
19	rs409093	40633088	0.4658	19	rs7250197	42081310	0.9183
19	rs926026	40659264	0.6494	19	rs547483	42133205	0.5108
19	rs11880530	40660984	0.3008	19	rs496730	42143279	0.6144
19	rs8102875	40661629	0.0660	19	rs569371	42145837	0.9368
19	rs6510490	40669149	0.9379	19	rs565721	42147671	0.8131
19	rs7976	40670139	0.7216	19	rs7251087	42147743	0.5637
19	rs10407971	40671304	0.8575	19	rs7254717	42149242	0.0955
19	rs11880364	40680634	0.8597	19	rs472226	42150553	0.9376
19	rs4254439	40690202	0.6737	19	rs17639910	42158969	0.1530
19	rs7254211	40695561	0.5076	19	rs1667354	42173991	1.0000
19	rs4806163	40695946	0.7216	19	rs8102196	42274044	0.8864
19	rs17705633	40707492	0.5445	19	rs1533736	42346816	0.5469
19	rs12151182	40715572	0.8551	19	rs11084878	42362309	0.7371
19	rs17705657	40716582	0.9270	19	rs12459637	42381838	1.0000
19	rs2239945	40725300	0.2752	19	rs320890	42395940	0.5900
19	rs7599	40730230	0.9334	19	rs172786	42404824	0.9376
19	rs2301617	40734047	0.4726	19	rs2460950	42445079	0.2273
19	rs17776451	40736289	1.0000	19	rs1530500	42515651	0.8460
19	rs2733743	40742809	0.7098	19	rs3745765	42546075	0.6799
19	rs2285421	40860754	0.3202	19	rs10422527	42586308	0.2170
19	rs437168	41026259	0.6949	19	rs12461941	42676490	0.3843
19	rs2285424	41191013	0.0955	19	rs12977460	42716111	0.8981
19	rs1008328	41287276	0.1508	19	rs10500277	42749242	0.7518
19	rs3108186	41876810	0.8774	19	rs4803277	42764767	1.0000
19	rs1830031	41895089	0.6394	19	rs2927743	42824174	0.4083
19	rs1673082	41932981	0.2643	19	rs35153242	42843582	0.7389
19	rs1227820	41949357	0.5839	19	rs2909109	42861195	0.2636
19	rs2245366	41956174	0.8608	19	rs17246792	42876102	0.9404
19	rs8107274	41977233	0.8501	19	rs1469698	43685396	0.0294
19	rs1148399	42021145	1.0000	19	rs8103362	44452031	0.7216

Table 19: HLOD and npLOD values for each SNP in an ASP linkage analysis using MERLIN.
 Positions in Build36.3. Highest LOD scores exceeding significance threshold of 2.6 highlighted in red.

SNP_ID	CHR	POSITION	HLOD	npLOD	SNP_ID	CHR	POSITION	HLOD	npLOD
rs11672876	19	34923945	0.652	0.570	rs1144540	19	42022453	2.584	3.100
rs541169	19	40410860	1.488	1.480	rs1035441	19	42045631	2.587	3.100
rs12975589	19	40531570	1.765	1.680	rs10403306	19	42067119	2.649	3.160
rs8107905	19	40613537	1.762	1.680	rs543518	19	42078051	2.839	3.390
rs409093	19	40633088	1.762	1.680	rs7250197	19	42081310	2.847	3.400
rs926026	19	40659264	1.762	1.680	rs547483	19	42133205	2.953	3.500
rs11880530	19	40660984	1.762	1.680	rs496730	19	42143279	2.971	3.510
rs8102875	19	40661629	1.762	1.680	rs569371	19	42145837	2.884	3.400
rs6510490	19	40669149	1.762	1.680	rs565721	19	42147671	2.810	3.430
rs7976	19	40670139	1.762	1.680	rs7251087	19	42147743	2.807	3.420
rs10407971	19	40671304	1.790	1.710	rs7254717	19	42149242	2.807	3.420
rs11880364	19	40680634	1.971	1.950	rs472226	19	42150553	2.807	3.420
rs4254439	19	40690202	2.006	1.990	rs17639910	19	42158969	2.808	3.430
rs7254211	19	40695561	2.025	2.010	rs1667354	19	42173991	2.810	3.430
rs4806163	19	40695946	2.027	2.010	rs8102196	19	42274044	2.670	3.280
rs17705633	19	40707492	2.067	2.050	rs1533736	19	42346816	2.547	3.120
rs12151182	19	40715572	1.878	1.790	rs11084878	19	42362309	2.724	3.270
rs17705657	19	40716582	1.881	1.800	rs12459637	19	42381838	2.714	3.250
rs2239945	19	40725300	1.924	1.850	rs320890	19	42395940	2.705	3.230
rs7599	19	40730230	1.935	1.860	rs172786	19	42404824	2.695	3.220
rs2301617	19	40734047	1.943	1.870	rs2460950	19	42445079	2.650	3.140
rs17776451	19	40736289	1.948	1.880	rs1530500	19	42515651	2.562	3.000
rs2733743	19	40742809	1.961	1.890	rs3745765	19	42546075	2.408	2.810
rs2285421	19	40860754	2.225	2.170	rs10422527	19	42586308	2.180	2.560
rs437168	19	41026259	2.360	2.340	rs12461941	19	42676490	1.995	2.240
rs2285424	19	41191013	2.482	2.540	rs12977460	19	42716111	1.947	2.140
rs1008328	19	41287276	2.542	2.650	rs10500277	19	42749242	1.902	2.050
rs3108186	19	41876810	2.812	3.120	rs4803277	19	42764767	1.880	2.010
rs1830031	19	41895089	2.886	3.240	rs2927743	19	42824174	1.786	1.810
rs1673082	19	41932981	2.373	2.840	rs35153242	19	42843582	1.770	1.790
rs1227820	19	41949357	2.415	2.860	rs2909109	19	42861195	1.978	2.080
rs2245366	19	41956174	2.416	2.870	rs17246792	19	42876102	1.972	2.070
rs8107274	19	41977233	2.418	2.870	rs1469698	19	43685396	1.349	1.450
rs1148399	19	42021145	2.424	2.890	rs8103362	19	44452031	1.122	1.140

Table 20: HLOD and npLOD values for each SNP in a family based linkage analysis using MERLIN.
 Positions in Build36.3. Highest LOD scores exceeding significance threshold of 3.6 highlighted in red.

SNP_ID	CHR	POSITION	HLOD	npLOD	SNP_ID	CHR	POSITION	HLOD	npLOD
rs11672876	19	34923945	1.939	1.430	rs1144540	19	42022453	3.798	3.980
rs541169	19	40410860	2.846	2.570	rs1035441	19	42045631	3.915	4.170
rs12975589	19	40531570	3.252	2.870	rs10403306	19	42067119	4.019	4.310
rs8107905	19	40613537	3.333	2.930	rs543518	19	42078051	4.207	4.550
rs409093	19	40633088	3.352	2.940	rs7250197	19	42081310	4.220	4.570
rs926026	19	40659264	3.377	2.960	rs547483	19	42133205	4.357	4.730
rs11880530	19	40660984	3.379	2.960	rs496730	19	42143279	4.374	4.740
rs8102875	19	40661629	3.379	2.960	rs569371	19	42145837	4.298	4.650
rs6510490	19	40669149	3.386	2.970	rs565721	19	42147671	4.234	4.670
rs7976	19	40670139	3.386	2.970	rs7251087	19	42147743	4.231	4.670
rs10407971	19	40671304	3.410	3.000	rs7254717	19	42149242	4.231	4.670
rs11880364	19	40680634	3.571	3.210	rs472226	19	42150553	4.231	4.670
rs4254439	19	40690202	3.570	3.220	rs17639910	19	42158969	4.228	4.660
rs7254211	19	40695561	3.571	3.230	rs1667354	19	42173991	4.222	4.650
rs4806163	19	40695946	3.572	3.230	rs8102196	19	42274044	3.967	4.370
rs17705633	19	40707492	3.592	3.280	rs1533736	19	42346816	3.726	4.090
rs12151182	19	40715572	3.123	3.010	rs11084878	19	42362309	3.837	4.160
rs17705657	19	40716582	3.122	3.020	rs12459637	19	42381838	3.831	4.140
rs2239945	19	40725300	3.044	2.960	rs320890	19	42395940	3.826	4.130
rs7599	19	40730230	2.993	2.910	rs172786	19	42404824	3.817	4.110
rs2301617	19	40734047	2.961	2.890	rs2460950	19	42445079	3.889	4.170
rs17776451	19	40736289	2.936	2.880	rs1530500	19	42515651	3.950	4.190
rs2733743	19	40742809	2.852	2.830	rs3745765	19	42546075	3.809	4.040
rs2285421	19	40860754	2.932	2.990	rs10422527	19	42586308	3.614	3.850
rs437168	19	41026259	3.024	3.040	rs12461941	19	42676490	3.438	3.600
rs2285424	19	41191013	3.166	3.170	rs12977460	19	42716111	3.386	3.530
rs1008328	19	41287276	3.244	3.240	rs10500277	19	42749242	3.336	3.460
rs3108186	19	41876810	3.719	3.640	rs4803277	19	42764767	3.310	3.430
rs1830031	19	41895089	3.739	3.730	rs2927743	19	42824174	3.190	3.280
rs1673082	19	41932981	3.274	3.400	rs35153242	19	42843582	3.144	3.250
rs1227820	19	41949357	3.289	3.410	rs2909109	19	42861195	3.148	3.370
rs2245366	19	41956174	3.291	3.410	rs17246792	19	42876102	3.140	3.360
rs8107274	19	41977233	3.397	3.480	rs1469698	19	43685396	2.270	2.300
rs1148399	19	42021145	3.657	3.800	rs8103362	19	44452031	1.891	1.820

Table 22: P-values for clustered SNPs in a case control analysis with a dominant model using PLINK for chr 5 only. Positions in Build36.3. Lowest p-value in SNP cluster highlighted in red.

SNP_ID	CHR	POSITION	P - VALUE
rs10512779	5	5334408	2.34E-05
rs6555346	5	5351102	1.19E-05
rs6555347	5	5351142	1.13E-05
rs6555348	5	5351767	1.36E-05
rs7720820	5	5352206	5.55E-06
rs6555349	5	5352686	0.002773
rs6555350	5	5352740	1.36E-05
rs11134108	5	5353735	1.77E-05
rs4473739	5	5361229	3.71E-05

Table 23: P-values for clustered SNPs in a case control analysis with a dominant model using PLINK for chr 5 only. Positions in Build36.3. Lowest p-value in SNP cluster highlighted in red.

SNP_ID	CHR	POSITION	P - VALUE	SNP_ID	CHR	POSITION	P - VALUE
rs6596007	5	130616449	5.89E-06	rs3776007	5	130902984	3.38E-06
rs6890410	5	130622646	2.84E-05	rs250888	5	131043245	2.25E-05
rs3756295	5	130720739	0.002284	rs251015	5	131057582	9.46E-06
rs798413	5	130724485	1.00E-05	rs251012	5	131058194	9.69E-06
rs27421	5	130771670	8.76E-07	rs32115	5	131079227	3.29E-06
rs6596024	5	130797684	2.95E-06	rs548635	5	131083445	1.24E-05
rs1422081	5	130803952	1.65E-06	rs4705894	5	131107187	1.44E-06
rs3776030	5	130804637	2.11E-06	rs11242095	5	131180474	2.23E-05
rs10463887	5	130804753	1.70E-06	rs2896961	5	131192905	2.25E-06
rs31239	5	130841276	6.17E-06	rs1875176	5	131230356	1.49E-05
rs40400	5	130859264	6.78E-05	rs10045303	5	131230700	1.24E-05
rs10067982	5	130863839	1.38E-06	rs13174462	5	131245887	5.10E-06
rs13163091	5	130863940	1.88E-06	rs12653237	5	131269677	6.18E-06
rs4705890	5	130882899	7.91E-06				

Table 24: P-values for clustered SNPs in a case control analysis with a dominant model using PLINK for chr 6 only. Positions in Build36.3. Lowest p-value in SNP cluster highlighted in red.

SNP_ID	CHR	POSITION	P - VALUE
rs1233367	6	29730199	0.002285
rs29228	6	29731718	4.87E-06
rs3129063	6	29753592	0.0001571
rs387642	6	29753613	0.006505
rs3129045	6	29760555	0.036
rs3129046	6	29778631	7.19E-05
rs1610742	6	29785931	6.50E-05
rs2523405	6	29803284	0.06543

Table 25: P-values for clustered SNPs in a case control analysis with a dominant model using PLINK for chr 6 only. Positions in Build36.3. Lowest p-value in SNP cluster highlighted in red.

SNP_ID	CHR	POSITION	P - VALUE
rs3135363	6	32497626	0.0006048
rs3129847	6	32504484	1.59E-06
rs3135342	6	32504593	3.60E-07
rs5000563	6	32512113	6.68E-07
rs3129872	6	32515131	9.08E-07
rs3129877	6	32516575	9.72E-08
rs7194	6	32520458	0.0007573
rs9268856	6	32537697	4.34E-09
rs9268877	6	32539125	0.007743
rs615672	6	32682149	0.004358
rs41269947	6	32716055	0.01457
rs9469220	6	32766288	5.54E-08
rs6457617	6	32771829	5.07E-06
rs3892710	6	32790840	1.16E-04

Table 26: P-values for clustered SNPs in a case control analysis with a dominant model using PLINK for chr 6 only. Positions in Build36.3. Lowest p-value in SNP cluster highlighted in red.

SNP_ID	CHR	POSITION	P - VALUE
rs6557200	6	150314225	0.04341
rs5017316	6	150375182	3.14E-07
rs9479403	6	150379439	2.10E-07
rs494825	6	150395716	0.001051
rs3860823	6	150398219	1.39E-06
rs2181923	6	150403682	2.90E-05

Table 27: P-values for clustered SNPs in a case control analysis with a dominant model using PLINK for chr 16 only. Positions in Build36.3. Lowest p-value in SNP cluster highlighted in red.

SNP_ID	CHR	POSITION	P - VALUE
rs6498146	16	11014208	0.005808
rs3893660	16	11101431	7.40E-07
rs9941107	16	11103542	2.65E-07
rs17806299	16	11107481	0.0004071
rs7198004	16	11115118	1.93E-06
rs7203150	16	11115223	9.41E-08
rs9746695	16	11115395	0.005313

Table 28: P-values for clustered SNPs in a case control analysis with a trend model using PLINK for chr 5 only. Positions in Build36.3. Lowest p-value in SNP cluster highlighted in red.

SNP_ID	CHR	POSITION	p_TREND
rs2913657	5	5316152	0.03871
rs10512779	5	5334408	1.31E-06
rs6555342	5	5346260	0.08207
rs6555346	5	5351102	2.61E-06
rs6555347	5	5351142	2.63E-06
rs6555348	5	5351767	3.16E-06
rs7720820	5	5352206	1.81E-07
rs6555349	5	5352686	0.000316
rs6555350	5	5352740	3.42E-06
rs11134108	5	5353735	3.77E-06
rs4473739	5	5361229	2.77E-05

Table 29: P-values for clustered SNPs in a case control analysis with a trend model using PLINK for chr 5 only. Positions in Build36.3. Lowest p-value in SNP cluster highlighted in red.

SNP_ID	CHR	POSITION	p_TREND	SNP_ID	CHR	POSITION	p_TREND
rs17165964	5	130557021	0.003323	rs251012	5	131058194	4.02E-06
rs6596007	5	130616449	5.66E-06	rs32115	5	131079227	2.31E-06
rs6890410	5	130622646	1.30E-05	rs548635	5	131083445	4.84E-06
rs3756295	5	130720739	0.0004998	rs4705894	5	131107187	1.37E-06
rs798413	5	130724485	4.17E-06	rs11242095	5	131180474	6.59E-06
rs27421	5	130771670	2.55E-06	rs2896961	5	131192905	4.59E-06
rs6596024	5	130797684	1.77E-06	rs1875176	5	131230356	6.26E-06
rs1422081	5	130803952	4.93E-06	rs10045303	5	131230700	5.23E-06
rs3776030	5	130804637	6.70E-06	rs13174462	5	131245887	2.14E-06
rs10463887	5	130804753	5.50E-06	rs12653237	5	131269677	2.94E-06
rs31239	5	130841276	3.31E-06	rs667437	5	131303408	1.21E-05
rs40400	5	130859264	9.50E-05	rs667419	5	131309963	7.79E-06
rs10067982	5	130863839	4.14E-06	rs477086	5	131312509	2.97E-06
rs13163091	5	130863940	5.91E-06	rs676944	5	131316367	3.17E-05
rs4705890	5	130882899	4.05E-06	rs2240525	5	131343783	0.02957
rs3776007	5	130902984	9.21E-06	rs559971	5	131344063	2.11E-05
rs17671387	5	130911895	0.0005832	rs173812	5	131347359	2.64E-05
rs250888	5	131043245	9.63E-06	rs253943	5	131348629	6.91E-05
rs251015	5	131057582	3.30E-06				

Table 30: P-values for clustered SNPs in a case control analysis with a trend model using PLINK for chr 6 only. Positions in Build36.3. Lowest p-value in SNP cluster highlighted in red.

SNP_ID	CHR	POSITION	p_TREND	SNP_ID	CHR	POSITION	p_TREND
rs1611699	6	29935732	0.01103	rs2517672	6	30045241	0.01215
rs1611703	6	29936414	4.53E-06	rs4947244	6	30062343	0.08682
rs1611711	6	29937087	0.01108	rs3115631	6	30094303	0.0008066
rs1611714	6	29937386	1.99E-06	rs259940	6	30119913	0.008756
rs2734970	6	29942451	3.18E-05	rs3869070	6	30131847	0.002092
rs3094159	6	29943813	0.01385	rs9261301	6	30149538	0.02827
rs3132718	6	29944556	0.0124	rs3132682	6	30152367	0.03356
rs1611637	6	29944720	0.006318	rs9261317	6	30156284	0.08271
rs3132712	6	29949000	0.008305	rs6457144	6	30171347	0.05627
rs2523807	6	29958253	0.07597	rs9261394	6	30172541	0.04527
rs1632882	6	30024347	0.0007669	rs1264704	6	30173298	0.03399
rs417162	6	30024484	0.003631	rs1264703	6	30173395	5.29E-06
rs1655900	6	30024597	1.66E-06	rs1264702	6	30173554	7.69E-06
rs2508037	6	30026415	0.003011	rs2517595	6	30192528	0.02589

Table 31: P-values for clustered SNPs in a case control analysis with a trend model using PLINK for chr 6 only. Positions in Build36.3. Lowest p-value in SNP cluster highlighted in red.

SNP_ID	CHR	POSITION	p_TREND	SNP_ID	CHR	POSITION	p_TREND
rs9268429	6	32453030	0.003674	rs9268877	6	32539125	0.05446
rs3129953	6	32469799	1.35E-07	rs615672	6	32682149	0.0001881
rs2076530	6	32471794	0.03144	rs9272346	6	32712350	0.01135
rs9268480	6	32471822	0.00215	rs41269947	6	32716055	0.03702
rs10947261	6	32481210	0.01789	rs3129716	6	32765414	4.35E-05
rs3763307	6	32482600	0.004194	rs9469220	6	32766288	5.35E-12
rs2001097	6	32491836	1.42E-09	rs6457617	6	32771829	6.40E-08
rs3135378	6	32493077	2.37E-09	rs2858308	6	32777978	0.02038
rs2395161	6	32495730	2.81E-09	rs3892710	6	32790840	4.79E-05
rs2395164	6	32495838	6.68E-09	rs9275618	6	32792365	0.04749
rs2395167	6	32496286	5.72E-10	rs5024432	6	32792446	0.06377
rs3135366	6	32496687	4.02E-09	rs3916765	6	32793528	0.07974
rs9268557	6	32497283	0.05422	rs9461799	6	32797507	1.08E-05
rs3135363	6	32497626	0.0001255	rs2227127	6	32819760	7.56E-05
rs3129847	6	32504484	8.49E-08	rs9276429	6	32820082	2.61E-06
rs3135342	6	32504593	1.84E-08	rs9276431	6	32820225	3.86E-07
rs5000563	6	32512113	1.83E-08	rs9276432	6	32820362	2.90E-07
rs3129872	6	32515131	2.38E-08	rs28420297	6	32822738	1.94E-05
rs3129877	6	32516575	4.13E-09	rs9276440	6	32822761	2.26E-07
rs3135393	6	32516820	2.76E-09	rs7768538	6	32837799	7.33E-07
rs7194	6	32520458	8.81E-06	rs2051549	6	32838064	1.86E-06
rs9268831	6	32535726	0.03867	rs6902723	6	32839938	2.58E-06
rs9268856	6	32537697	1.05E-10	rs9296044	6	32844122	3.83E-05

Table 32: P-values for clustered SNPs in a case control analysis with a trend model using PLINK for chr 6 only. Positions in Build36.3. Lowest p-value in SNP cluster highlighted in red.

SNP_ID	CHR	POSITION	p_TREND
rs4870174	6	150345094	0.01517
rs5017316	6	150375182	3.31E-08
rs9479403	6	150379439	2.67E-08
rs494825	6	150395716	4.33E-05
rs3860823	6	150398219	1.07E-07
rs6935051	6	150398646	0.03236
rs2181923	6	150403682	3.98E-06
rs644866	6	150405702	1.39E-06
rs9479513	6	150409013	3.60E-07
rs11155699	6	150409590	0.07373

Table 33: npLOD values for clustered SNPs in a family based non parametric linkage analysis using PLINK for chr 10 only. Positions in Build36.3. Highest npLOD score in SNP cluster highlighted in red.

SNP_ID	CHR	POSITION	npLOD	SNP_ID	CHR	POSITION	npLOD
rs12246970	10	414200	3.62	rs10466270	10	546129	3.95
rs10904083	10	419977	3.63	rs4881399	10	557325	3.89
rs11594718	10	422103	3.63	rs12252141	10	579228	3.63
rs4488125	10	427940	3.64	rs11253096	10	580418	3.62
rs3935081	10	459349	3.78	rs7076375	10	582926	3.62
rs7077209	10	474159	3.85	rs7914425	10	585877	3.61
rs4881313	10	477973	3.86	rs2605905	10	596908	3.6
rs2050970	10	505870	3.95	rs816627	10	608409	3.58
rs1539231	10	520644	3.99	rs17221323	10	608685	3.58
rs11252693	10	522139	3.99	rs816628	10	609170	3.57
rs2096134	10	523331	3.99	rs816620	10	635916	3.36
rs11252756	10	528811	3.98	rs816570	10	670475	3.26
rs885593	10	530161	3.98	rs17136375	10	698293	3.11
rs11252842	10	542355	3.97				

Table 34: npLOD values for clustered SNPs in a family based non parametric linkage analysis using PLINK for chr 10 only. Positions in Build36.3. Highest npLOD score in SNP cluster highlighted in red.

SNP_ID	CHR	POSITION	npLOD	SNP_ID	CHR	POSITION	npLOD
rs17294166	10	1866813	3.31	rs2492866	10	1912296	3.75
rs10903569	10	1887722	3.74	rs962762	10	1913115	3.75
rs7084728	10	1888169	3.75	rs962760	10	1913557	3.75
rs11250832	10	1888716	3.75	rs962759	10	1913602	3.75
rs7921481	10	1888756	3.75	rs11250876	10	1913685	3.75
rs7082514	10	1890661	3.77	rs11250877	10	1913821	3.75
rs11250838	10	1892085	3.77	rs10128507	10	1925529	3.71

SNP_ID	CHR	POSITION	npLOD	SNP_ID	CHR	POSITION	npLOD
rs4077784	10	1892429	3.77	rs10903593	10	1935296	3.68
rs9919410	10	1892486	3.77	rs2039568	10	1943525	3.65
rs10794793	10	1892639	3.77	rs12413921	10	1948188	3.63
rs10794794	10	1892670	3.77	rs7079003	10	1967135	3.65
rs10903579	10	1899520	3.76	rs11250965	10	1998811	3.37
rs7098110	10	1906190	3.76				

Table 35: npLOD values for clustered SNPs in a family based non parametric linkage analysis using PLINK for chr 10 only. Positions in Build36.3. Highest npLOD score in SNP cluster highlighted in red.

SNP_ID	CHR	POSITION	npLOD	SNP_ID	CHR	POSITION	npLOD	SNP_ID	CHR	POSITION	npLOD
rs10751884	10	2728447	3.38	rs7922626	10	2772413	3.84	rs1577249	10	2826854	3.76
rs2050343	10	2733897	3.64	rs1537616	10	2772787	3.84	rs11251521	10	2839913	3.59
rs2050342	10	2734009	3.65	rs7093144	10	2773069	3.84	rs7080882	10	2854447	3.56
rs10903846	10	2736750	3.67	rs7093433	10	2773225	3.84	rs10794949	10	2855170	3.56
rs1931865	10	2743676	3.72	rs7094332	10	2774947	3.84	rs10736962	10	2859096	3.53
rs11251447	10	2747337	3.74	rs2065683	10	2794898	3.88	rs9633756	10	2865792	3.49
rs11251448	10	2747555	3.74	rs2184413	10	2794997	3.88	rs7098771	10	2866202	3.49
rs11593477	10	2748071	3.74	rs2065685	10	2795185	3.88	rs11593983	10	2867503	3.5
rs11251468	10	2756759	3.78	rs11251502	10	2800427	3.88	rs1909692	10	2881279	3.61
rs11251469	10	2756921	3.78	rs7895748	10	2807535	3.87	rs6601988	10	2891165	3.61
rs17158961	10	2770813	3.83	rs11251504	10	2808244	3.87	rs7093545	10	2891275	3.61
rs11599371	10	2771027	3.83	rs11251505	10	2808320	3.87	rs6601989	10	2891320	3.61
rs11593350	10	2771146	3.83	rs11251508	10	2818596	3.82	rs1909690	10	2900624	3.45
rs1106272	10	2772045	3.84	rs10736960	10	2821743	3.81				

Table 36: npLOD values for clustered SNPs in a family based non parametric linkage analysis using PLINK for chr 19 only. Positions in Build36.3. Highest npLOD score in SNP cluster highlighted in red.

SNP_ID	CHR	POSITION	npLOD	SNP_ID	CHR	POSITION	npLOD
rs2432055	19	41413208	3.49	rs10417204	19	42726562	5.9
rs2271844	19	41592850	3.78	rs11083428	19	42775807	5.89
rs2945989	19	41595102	3.8	rs16958863	19	42816075	5.87
rs17206393	19	41630434	4.2	rs2927740	19	42832806	5.86
rs10421461	19	41707727	4.63	rs2909105	19	42859746	5.85
rs2967449	19	41708165	4.64	rs11083433	19	42901141	5.81
rs17707014	19	41709636	4.64	rs2972437	19	42902351	5.81
rs2912438	19	41718283	4.66	rs856300	19	42942664	5.75
rs3108548	19	41742622	4.69	rs241960	19	42976129	5.68
rs3096620	19	41762083	4.7	rs10409487	19	42976951	5.68
rs2162296	19	41792090	4.7	rs3910952	19	42984209	5.66
rs10419469	19	41826577	4.69	rs8101752	19	42985327	5.66
rs3108559	19	41874511	4.88	rs241935	19	42985803	5.66

SNP_ID	CHR	POSITION	npLOD	SNP_ID	CHR	POSITION	npLOD
rs3108181	19	41879580	4.88	rs11878269	19	42997553	5.65
rs3108214	19	41894154	4.89	rs241937	19	43002500	5.65
rs826969	19	41939312	4.89	rs8110293	19	43004942	5.65
rs1673086	19	41955857	4.89	rs10420891	19	43012379	5.65
rs1673087	19	41956030	4.89	rs10402530	19	43013478	5.65
rs2245366	19	41956174	4.89	rs17249138	19	43047720	5.64
rs2431776	19	42018124	5.28	rs7250821	19	43065318	5.62
rs1144540	19	42022453	5.29	rs3894129	19	43076261	5.62
rs486221	19	42030704	5.26	rs4802150	19	43107654	5.59
rs493482	19	42057888	5.45	rs705495	19	43118825	5.57
rs477725	19	42066106	5.49	rs705496	19	43118937	5.57
rs9304878	19	42089141	5.6	rs17249336	19	43132976	5.51
rs484001	19	42114062	5.71	rs705500	19	43138890	5.46
rs547483	19	42133205	5.75	rs1725494	19	43138950	5.46
rs528504	19	42139188	5.75	rs941038	19	43156628	5.23
rs569371	19	42145837	5.76	rs6508755	19	43164562	5.04
rs523979	19	42148245	5.76	rs1725468	19	43165769	4.99
rs472226	19	42150553	5.76	rs833915	19	43165900	4.98
rs1375476	19	42157015	5.76	rs1643459	19	43168013	4.64
rs1667337	19	42159352	5.76	rs833911	19	43168897	4.63
rs1644666	19	42167326	5.75	rs833904	19	43177305	4.55
rs1612652	19	42169480	5.75	rs860627	19	43178032	4.55
rs1644673	19	42170551	5.75	rs17309382	19	43196877	4.45
rs1667353	19	42172993	5.75	rs705503	19	43206158	4.38
rs8106386	19	42195739	5.75	rs6508757	19	43214032	4.24
rs2562587	19	42202099	5.75	rs8110656	19	43218023	4.24
rs2562599	19	42208214	5.78	rs1628394	19	43226848	4.25
rs7248948	19	42239059	5.83	rs1620082	19	43233843	4.24
rs2385374	19	42274857	5.85	rs1618385	19	43234734	4.24
rs6510588	19	42289235	5.85	rs1725510	19	43247682	4.22
rs1402468	19	42312088	5.85	rs1614979	19	43269277	4.16
rs11084878	19	42362309	5.84	rs855640	19	43272184	4.15
rs320891	19	42397185	5.83	rs941039	19	43296954	4.03
rs7246657	19	42438948	5.83	rs3852911	19	43297276	4.03
rs12709812	19	42486690	5.82	rs855614	19	43311582	4.01
rs7408736	19	42488151	5.82	rs332860	19	43348970	3.92
rs1530500	19	42515651	6.09	rs10420506	19	43362295	3.87
rs713256	19	42557205	6.13	rs3745945	19	43365138	3.86
rs256733	19	42567471	6.13	rs2278431	19	43398829	3.67
rs8106839	19	42650315	6.12	rs10993	19	43435431	3.61
rs1236810	19	42658501	6.12	rs7250689	19	43445465	3.6
rs12461941	19	42676490	6.08	rs7253245	19	43445626	3.6
rs8109038	19	42707549	5.98	rs41465446	19	43454980	3.57

Table 37: npLOD values for clustered SNPs in a family based non parametric linkage analysis using PLINK for chr 19 only. Positions in Build36.3. Highest npLOD score in SNP cluster highlighted in red.

SNP_ID	CHR	POSITION	npLOD	SNP_ID	CHR	POSITION	npLOD
rs16970276	19	40562188	3.55	rs528504	19	42139188	4.05
rs10420543	19	40589758	3.62	rs1667337	19	42159352	4.06
rs756971	19	40635609	3.72	rs8106386	19	42195739	4.07
rs17705450	19	40667407	3.75	rs7248948	19	42239059	4.10
rs4806163	19	40695946	3.76	rs2385374	19	42274857	4.11
rs17705657	19	40716582	3.80	rs1402468	19	42312088	4.11
rs1033330	19	40761472	3.88	rs11084878	19	42362309	4.11
rs4805131	19	40789137	3.73	rs320891	19	42397185	4.11
rs8106576	19	40816016	3.73	rs256733	19	42567471	4.15
rs107068	19	40896530	3.74	rs10417204	19	42726562	4.13
rs179570	19	40943166	3.72	rs11083428	19	42775807	4.12
rs10409299	19	41016164	3.66	rs11083433	19	42901141	4.07
rs12462868	19	41163676	3.54	rs241960	19	42976129	4.03
rs17639286	19	41212605	3.50	rs241937	19	43002500	4.01
rs7257383	19	41255260	3.48	rs17249138	19	43047720	4.00
rs4555271	19	41302030	3.50	rs3894129	19	43076261	3.99
rs2438517	19	41412230	3.64	rs4802150	19	43107654	3.98
rs2271844	19	41592850	3.78	rs17249336	19	43132976	3.97
rs17206393	19	41630434	3.80	rs941038	19	43156628	3.94
rs2967449	19	41708165	3.83	rs833904	19	43177305	3.90
rs3108548	19	41742622	3.84	rs705503	19	43206158	3.87
rs3108559	19	41874511	3.80	rs1628394	19	43226848	3.85
rs826969	19	41939312	3.79	rs3852911	19	43297276	3.69
rs2431776	19	42018124	3.87	rs332860	19	43348970	3.61
rs484001	19	42114062	4.03	rs2278431	19	43398829	3.50

Table 38: npLOD values for clustered SNPs in a family based non parametric linkage analysis using PLINK for chr 19 only. Positions in Build36.3. Highest npLOD score in SNP cluster highlighted in red.

SNP_ID	CHR	POSITION	npLOD	SNP_ID	CHR	POSITION	npLOD
rs16970293	19	40590481	3.49	rs12973004	19	40750614	3.85
rs17304632	19	40620406	3.75	rs1033330	19	40761472	3.86
rs8108454	19	40634973	3.85	rs4805131	19	40789137	3.70
rs756971	19	40635609	3.86	rs8106576	19	40816016	3.70
rs17705450	19	40667407	3.85	rs12459634	19	40922014	3.72
rs7254211	19	40695561	3.84	rs179570	19	40943166	3.71
rs4806163	19	40695946	3.84	rs41426049	19	41001358	3.65
rs7254744	19	40702499	3.83	rs10409299	19	41016164	3.64
rs17705657	19	40716582	3.86	rs12462868	19	41163676	3.48
rs2239945	19	40725300	3.87				

**Alles Wissen und alles Vermehren unseres Wissens
endet nicht mit einem Schlusspunkt, sondern mit einem Fragezeichen.**

Hermann Hesse (1877-1962), dt. Dichter, 1946 Nobelpr. f. Lit.

Erklärung I

Ich versichere, dass ich die von mir vorgelegte Dissertation selbständig angefertigt, die benutzten Quellen und Hilfsmittel vollständig angegeben und die Stellen der Arbeit – einschließlich Tabellen, Karten und Abbildungen –, die anderen Werken im Wortlaut oder dem Sinn nach entnommen sind, in jedem Einzelfall als Entlehnung kenntlich gemacht habe; dass diese Dissertation noch keiner anderen Fakultät oder Universität zur Prüfung vorgelegen hat; dass sie noch nicht veröffentlicht worden ist sowie, dass ich eine solche Veröffentlichung vor Abschluss des Promotionsverfahrens nicht vornehmen werde.

Die Bestimmungen dieser Promotionsordnung sind mir bekannt.

Die von mir vorgelegte Dissertation ist von Prof. Dr. Peter Nürnberg betreut worden.

Teilpublikationen liegen nicht vor.

Ich versichere, dass ich alle Angaben wahrheitsgemäß nach bestem Wissen und Gewissen gemacht habe und verpflichte mich, jedmögliche, die obigen Angaben betreffenden Veränderungen, dem Dekanat unverzüglich mitzuteilen.

Datum

Unterschrift

Lebenslauf

Persönliche Angaben:

Name: Jennifer Kristina Kuhn
Adresse: Moltkestr. 35
50859 Köln

Geboren am/ in: 19.11.1981/ Heilbronn Neckargartach
Staatsangehörigkeit: Deutsch
Familienstand: ledig

Berufserfahrung:

08/ 2007 - 01/2008 Zwei Projektarbeiten für Prof. Dr Dr. h.c. Blin
(Molekulargenetik, Tübingen) am Cologne Center for
Genomics, Universität zu Köln

03/ 2005 - 12/ 2006 Firma KB Biosystem Clédon, Tübingen
(aktueller Sitz in Ulm)

Ausbildung:

10/ 2009 – Herbst 2011 Ausbau des Kompaktstudiums zum MBA,
Wissenschaftliche Hochschule Lahr (WHL)

02/ 2008 – 06/ 2011 Doktorarbeit zum Thema „Molecular Genetics of Alopecia
Areata in Dundee Experimental Bald Rats and in Humans“
am Cologne Center for Genomics, Universität zu Köln

06/ 2008 – 08/ 2009 Kompaktstudium Management, WHL

10/ 2002 – 08/ 2007 Biologiestudium, Universität Hohenheim (Vordiplom) und
Eberhard Karls Universität Tübingen (Diplom)
Hauptfach: Humangenetik, 1. Nebenfach Tierphysiologie,
2. Nebenfach Medizinische Mikrobiologie und Hygiene

08/1998 – 06/1999 Fremont High School, Indiana, USA

1992 - 1998 u.1999 - 2002 Albert-Schweitzer-Gymnasium, Neckarsulm
Leistungskurse: Mathematik und Englisch
Grundkurse: Biologie und Ethik